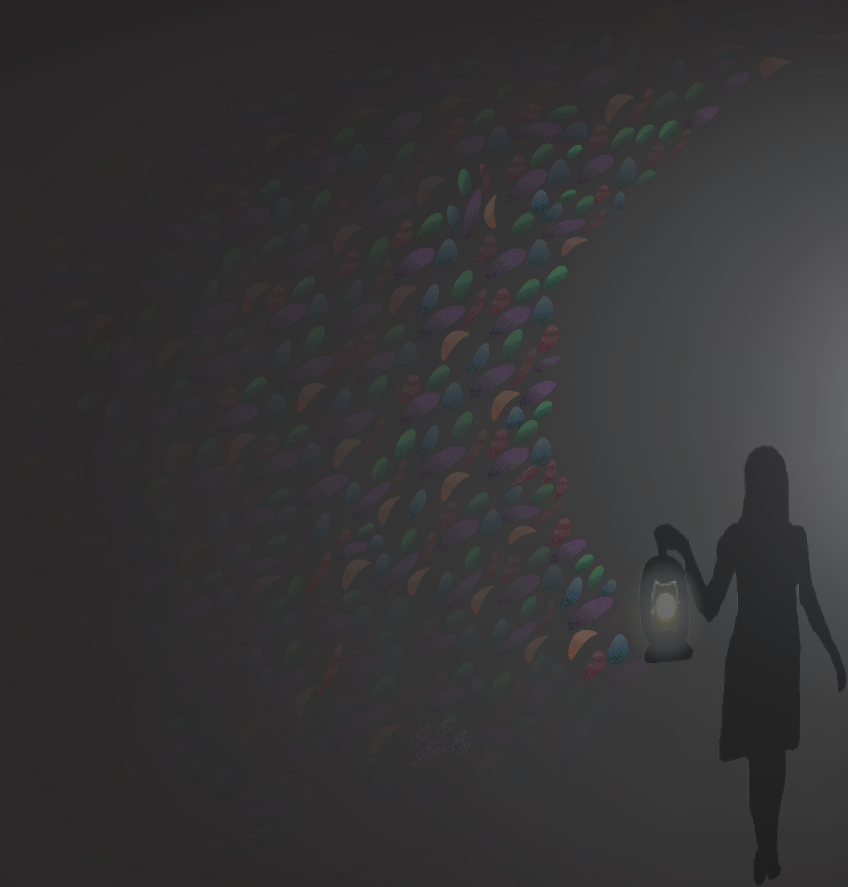


The role of intestinal microbial and mammalian co-metabolism in the toxicity of (modified) zearalenone



Diana Marisol Mendez Catala

Propositions

1. Physiologically-based kinetic modelling is a suitable tool to assess the role of intestinal microbial metabolism in toxicology.
(this thesis)
2. In spite of the high estrogenic potency of α -zearalenol, the contribution of this metabolite to the toxicity of zearalenone is negligible.
(this thesis)
3. Self-avoiding random walks (SAWs) are a powerful tool to study protein-folding configurations.
4. Promising scientific developments result from scientific co-operation instead of competition.
5. The introduction of a universal basic income will increase the number of (young) professionals satisfied with their jobs.
6. Learning that a change in direction during a PhD represents growth and not failure is part of the journey.
7. Creativity is a spontaneous process, it must not be enforced.

Propositions belonging to the thesis, entitled

“The role of intestinal microbial and mammalian co-metabolism in the toxicity of (modified) zearalenone”.

Diana Marisol Mendez Catala
Wageningen, 11 June 2021

**The role of intestinal microbial and
mammalian co-metabolism in the toxicity of
(modified) zearalenone**

Diana Marisol Mendez Catala

Thesis committee

Promotor

Prof. Dr I.M.C.M. Rietjens
Professor of Toxicology
Wageningen University & Research

Co-promotor

Dr K. Beekmann
Scientist, Toxicology
Wageningen University & Research

Other members

Prof. Dr A.H. Kersten, Wageningen University & Research
Dr J. Louisse, WFSR, Wageningen University & Research
Prof. Dr C. Dall'Asta, University of Parma, Italy
Dr M. Mengelers, National Institute of Public Health and Environment (RIVM), Bilthoven

This research was conducted under the auspices of the Graduate School VLAG (Advanced studies in Food Technology, Agrobiotechnology, Nutrition and Health Sciences)

The role of intestinal microbial and mammalian co-metabolism in the toxicity of (modified) zearalenone

Diana Marisol Mendez Catala

Thesis

submitted in fulfilment of the requirements for the degree of doctor
at Wageningen University

by the authority of the Rector Magnificus,

Prof. Dr A.P.J. Mol,

in the presence of the

Thesis Committee appointed by the Academic Board

to be defended in public

on Friday 11 June 2021

at 11 a.m. in the Aula.

Diana Marisol Mendez Catala

The role of intestinal microbial and mammalian co-metabolism in the toxicity of
(modified) zearalenone, 208 pages.

PhD thesis, Wageningen University, Wageningen, the Netherlands (2021)

With references, with summary in English

ISBN 978-94-6395-728-1

DOI <https://doi.org/10.18174/542328>

Contents

Chapter 1	7
<i>General Introduction</i>	
Chapter 2	27
<i>An in vitro model to quantify interspecies differences in kinetics for intestinal microbial bioactivation and detoxification of zearalenone</i>	
Chapter 3	59
<i>PBK model-based prediction of intestinal microbial and host metabolism of zearalenone and consequences for its estrogenicity</i>	
Chapter 4	121
<i>Interindividual differences in the hepatic and intestinal microbial metabolism of zearalenone characterized by physiologically-based kinetic (PBK) modelling linked to Monte Carlo simulation</i>	
Chapter 5	149
<i>Interspecies and human inter-individual differences in the intestinal microbial metabolism of zearalenone-14-glucoside (ZEN-14-G)</i>	
Chapter 6	169
<i>General Discussion</i>	
Chapter 7	199
<i>Summary</i>	
Annex	203
<i>Acknowledgements, Curriculum Vitae, Overview of completed training activities</i>	



Chapter 1

General

Introduction

1.1 Background information

An endocrine disrupting-chemical (EDC) is defined by the European Union (EU) as an “exogenous substance that can cause adverse health effect in an intact organism, or its progeny, secondary to changes in endocrine function” (European Commission, 2001). EDCs include substances from natural sources (hormones, plant and fungal constituents) and artificial origin (drugs and pesticides) (Karrow *et al.*, 2011). The main concern rises from continued chronic exposure to these kind of compounds. EDCs can affect the endocrine function of an organism in different ways, including influences on hormone biosynthesis, metabolism, transport, and effects at receptor and post-receptor level. Some EDCs can act as the endogenous estrogen 17 β -estradiol (E2) through the binding to estrogen receptors (ERs) (La Merrill *et al.*, 2020). Critical effects related to this mode of action can be noticed on reproductive organs, causing hyperestrogenism, stillbirth, infertility, disturbance of the menstrual cycle, miscarriages, decreased sperm count and quality and swallowed uterus (Balabanić *et al.*, 2011; Fink-Gremmels and Malekinejad, 2007; Metzler *et al.*, 2010; Yang *et al.*, 2018). The mycotoxin zearalenone (ZEN) is a well-known example of a contaminant of food and feed that causes reproductive disorders in young gilts (Döll *et al.*, 2004; Minervini *et al.*, 2005). Metabolites of ZEN may add to this effect (Metzler *et al.*, 2010). This observation has led to a broader study of the metabolism of ZEN and the endocrine activity of its metabolites; due to the endocrine-disrupting nature of ZEN, data from humans are still limited. Therefore the aim of this PhD project was to gain further insight into the metabolism of ZEN, including its metabolism in liver and intestinal microbiota of not only experimental animals but also human, and to include this information in physiologically-based kinetic (PBK) models to enable evaluation of the role of metabolism of ZEN in its estrogenic activity. The next sections present an overview of the metabolism and toxicity of ZEN and of the methods used in the present thesis to study the role of this metabolism, including the metabolism by the intestinal microbiota, in the estrogenicity of ZEN.

1.2 Zearalenone

Zearalenone (ZEN; C₁₈H₂₂O₅), a non-steroidal phenolic resorcylic acid lactone (3,4,5,6,9,10-hexahydro-14, 16-dihydroxy-3-methyl-1*H*-2-benzoxacyclotetradecin-1,7(8*H*)-dione) (Figure 1.1) (EFSA, 2011), is a mycotoxin resulting from the secondary metabolism of fungi growing on crops intended for food and feed. Although ZEN is best known to commonly contaminate maize crops, it can also

contaminate other cereal crops such as oats, barley, wheat, rice and sorghum (Lawley *et al.*, 2012). ZEN is produced by several species of the genus *Fusarium* such as *F. graminearum*, *F. cerealis*, *F. culmorum* and *F. equiseti*, of which growth is favored by humid, pre-harvest and storage conditions (Gromadzka *et al.*, 2008).

1.2.1 Metabolism of ZEN

In animals, following the ingestion and absorption of ZEN in the upper part of the intestinal tract (Kowalska *et al.*, 2016), two major pathways for ZEN biotransformation have been described (Olsen *et al.*, 1981). The first pathway is the reduction of the keto group at the 7 position of ZEN resulting in the hydroxylated metabolites α -zearalenol (α -ZEL) and β -zearalenol (β -ZEL) (Figure 1.1). These reactions are catalyzed by 3α - and 3β -hydroxysteroid dehydrogenases (HSDs) in liver, while similar biotransformation by the intestinal microbiota has also been reported (Gratz *et al.*, 2017; Rogowska *et al.*, 2019). Malekinejad *et al.* (2006) described significant interspecies differences in the formation of α -ZEL and β -ZEL in incubations with liver fractions, where pigs have a higher preference for the formation of α -ZEL over β -ZEL, and rats vice a higher preference for the formation of β -ZEL over α -ZEL. The second pathway of metabolism for ZEN, which is also relevant for its metabolites α -ZEL and β -ZEL, is the conjugation with glucuronic acid catalyzed by uridine diphosphate glucuronosyltransferases (UGTs), which are active in liver and intestinal tissue (Kutsukake *et al.*, 2019; Pfeiffer *et al.*, 2010). This conjugation of ZEN and its metabolites facilitate the excretion of the compounds through urine and/or feces (Fitzpatrick *et al.*, 1988; Mirocha *et al.*, 1981).

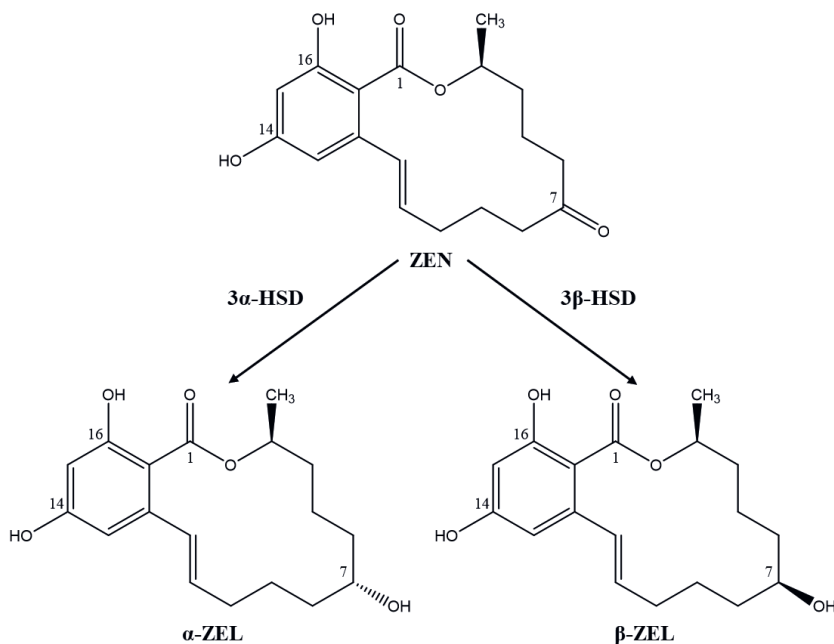


Figure 1.1. Metabolism of ZEN by hydroxysteroid dehydrogenases in mammals

1.2.2 Toxicity of ZEN

The exposure to ZEN is associated with reproductive disorders generally due to its ability to bind to estrogen receptors (ERs) and exert estrogenic effects. The European Food Safety Authority (EFSA, 2011) reviewed all data available and concluded young gilts to be most sensitive to ZEN exposure. Due to limited data on the effects of ZEN in humans, the risk assessment for humans is based on the estrogenic effects in young gilts. A tolerable daily intake (TDI) for humans of 0.25 $\mu\text{g/kg bw}$ for ZEN was established based on a No-observed effect level (NOEL) for ZEN of 10.4 $\mu\text{g/kg bw}$ (Döll *et al.*, 2003; EFSA, 2011), and an uncertainty factor of 40 accounting for interspecies differences in kinetics and human interindividual variability. Due to the higher sensitivity of pigs, the uncertainty factor for the differences in toxicodynamics between pigs and humans was reduced from 2.5 to 1.0. Interspecies differences in sensitivity may also be to some extent related to differences in toxicokinetics, with a higher preference for the formation of more estrogenic metabolites, such as α -ZEL, observed in pigs relative to other species such as rat and chicken (Malekinejad *et al.*, 2006).

The structural similarity of ZEN and its metabolites with the natural estrogen E2 explains their ability to bind and activate ERs (Kuiper *et al.*, 1998). In mammalian tissues, subtypes for ER, i.e. ER α and ER β , are described. It is commonly assumed

that ZEN has higher binding affinity for ER α than ER β (EFSA, 2016; Kuiper *et al.*, 1998). The estrogenic potencies of ZEN and its metabolites, α -ZEL and β -ZEL, have been characterized *in vitro* using assays with endpoints including the binding affinity to ERs, activation of ER-regulated reporter genes or proliferation of estrogen-sensitive cells (Ehrlich *et al.*, 2015; Frizzell *et al.*, 2011; Le Guevel and Pakdel, 2001; Malekinejad *et al.*, 2005; Metzler *et al.*, 2010; Minervini *et al.*, 2005; Molina-Molina *et al.*, 2014). Some of the estrogenic activities observed *in vitro* are summarized in Table 1.1. This Table focuses on interactions and activation of ER α , because this ER is generally assumed to be involved in the adverse estrogenic health effects induced by EDCs including ZEN (Shier *et al.*, 2001). Though differences in the estrogenic potency are observed, all the studies rank the potency of ZEN and its major metabolites as follows: α -ZEL > ZEN > β -ZEL. This ranking is in line with the *in vivo* uterotrophic assay in rats where the activity of the metabolite α -ZEL was 60-times higher than that of ZEN, while β -ZEL was 5 times less potent than ZEN (Everett *et al.*, 1987). The formation of α -ZEL is not only of relevance because the compound is more potent as an estrogen than ZEN itself but also because its estrogenic potency was shown to be only 10-fold lower than that of E2 (Everett *et al.*, 1987). Together, these results support the notion that the formation of α -ZEL represents a bioactivation pathway while β -ZEL formation represents a detoxification pathway. Therefore, as observed for pigs, a higher preference for α -ZEL formation may play a role in the higher sensitivity of this species to ZEN exposure. To what extent this α -ZEL formation actually plays a role in the toxicity of ZEN in not only pigs but also in human remains to be elucidated. Glucuronidation of ZEN and also of its metabolites α -ZEL and β -ZEL hinders the binding of the molecules to the ER, providing a detoxification pathway (Frizzell *et al.*, 2015)

Table 1.1. EC₅₀ values and relative potencies for ERα agonist activity of ZEN, α-ZEL and β-ZEL obtained from literature.

	EC ₅₀ (nM)			Relative potency ^a		Reference
	ZEN	α-ZEL	β-ZEL	α-ZEL	β-ZEL	
Activation of reporter gene (ERα-CALUX)	0.49	0.01	2.50	51	0.20	Ehrlich <i>et al.</i> (2015)
Activation of reporter gene (MMV-Luc)	1.60	0.02	3.90	73	0.41	Frizzell <i>et al.</i> (2011)
MCF7 cell proliferation	3.81	0.06	8.49	64	0.45	Molina-Molina <i>et al.</i> (2014)
MCF7 cell proliferation	0.31	0.0014	5.20	221	0.06	Minervini <i>et al.</i> (2005)
MCF7 cell proliferation	1.64	0.05	20.01	33	0.08	Malekinejad <i>et al.</i> (2005)
Ishikawa cell proliferation	0.06	0.01	25	8.79	0.002	Le Guevel and Pakdel (2001)
Average (± SD)	1.3 (± 1.2)	0.03 (± 0.02)	15.2 (± 14.4)	72.3 (± 69.0)	0.18 (± 0.18)	

^a EC₅₀ ZEN/EC₅₀ metabolite

1.2.3 ZEN-14-glucoside, a modified form of ZEN

ZEN-14-glucoside (ZEN-14-G) is a modified form of ZEN resulting from the metabolism of ZEN in plants for its storage in the vacuoles (Broekaert *et al.*, 2015). ZEN-14-G has been reported to be present in food commodities at levels similar to or higher than those of ZEN. Similar to the glucuronide forms of ZEN, ZEN-14-G has a lower affinity for activation of ERs as shown in a combined *in vitro/in silico* study (Dellafiora *et al.*, 2017). The efficient release of the parent compound ZEN from ZEN-14-G via hydrolysis by the action of intestinal microbiota (Dall’Erta *et al.*, 2013; Gratz *et al.*, 2017) indicates the importance of the inclusion of ZEN-14-G in a group health-based guidance value (HBGV), i.e. the TDI of 0.25 µg/kg bw expressed in ZEN equivalents under the assumption that ZEN-14-G will be fully hydrolyzed, absorbed and therefore contributing with the same potency as ZEN (EFSA, 2016). This further indicates the importance of including metabolism by the intestinal microbiota in the hazard and risk assessment of ZEN and its modified forms.

1.3 Intestinal microbiota

The mammalian gastro-intestinal tract consists of 100 trillions of microbes including bacteria, viruses, archaea, fungi and protozoa (Lu *et al.*, 2015). Bacteria have been the main focus of studies on intestinal microbiota, with *Firmicutes* and *Bacteroides* representing the most dominant phyla in most laboratory animals and humans (Qin *et al.*, 2010; Turner, 2018). The highest bacterial density is found in the large intestine with estimates of 10^{13} bacterial cells present in the human colon (Sender *et al.*, 2016a; Sender *et al.*, 2016b), which makes it an important site for microbial metabolism. The intestinal microbiome alone has 150-fold higher genetic content than the human genome, providing a large source of complementary metabolic activity to that of the liver and gut mucosa (Qin *et al.*, 2010). The complimentary activity provided by the intestinal microbiota plays primary roles in the production of metabolites, such as short chain fatty acids, resulting from the fermentation of non-digestible carbohydrates and protein, and the production of bile acids (Sousa *et al.*, 2008). The activity of the intestinal microbiota may also include metabolism of drugs and xenobiotics, and in some cases the metabolic activity provided by the intestinal microbiota may be even as extensive as, for example, that of the liver (Clarke *et al.*, 2019; Scheline, 1973). Despite the fact that the presence and metabolic capacity of the intestinal microbiome is well known for already a long time, the

inclusion of the metabolic potential of the intestinal microbiota in toxicology has not been fully considered.

1.3.1 The intestinal microbial metabolic capacity of xenobiotics in toxicology

The liver is considered to act as the main site for the metabolism of dietary components and xenobiotics, but the large capacity for metabolic activity of the gut microbiome makes the intestinal microbiota of interest for research considering co-metabolism (Clarke *et al.*, 2019). High interspecies and interindividual variations in intestinal microbiota related to diverse factors like diet, host genetics and environmental conditions are described in literature (Nguyen *et al.*, 2015). The variability reported is mainly related to taxonomic profiling, with the major phyla *Firmicutes* and *Bacteroides* being shared in all species, but quantitative differences occurring at genera and species levels (Turner, 2018). In spite of the microbial diversity, the microbial metabolic pathways are shared between individuals of the same species, as reported widely for humans (Huttenhower *et al.*, 2012; Visconti *et al.*, 2019). The metabolic capacity of the intestinal microbiota for drugs and xenobiotics includes reduction and hydrolysis as two main chemical modifications. Other transformations by the intestinal microbiota include decarboxylation, dihydroxylation, (de-) acetylation, proteolysis and denitration (Claus *et al.*, 2016). These modifications are in line with the demand of energy required by the bacteria, because the reductive activity provides the bacteria with an electron acceptor for anaerobic respiration, while the hydrolytic activity, e.g. deglycosylation, provides carbon sources required as substrate for microbial growth (Spanogiannopoulos *et al.*, 2016). The metabolites derived from the intestinal microbial metabolism can result in an altered bioactivity, bioavailability and toxicity of the xenobiotics (Koppel *et al.*, 2017). Such is the case for ZEN-14-G when converted to ZEN; the intestinal microbial hydrolysis of ZEN-14-G to ZEN results in an increase in its bioavailability, and an increased estrogenic potential, while the subsequent reduction of ZEN to α -ZEL and β -ZEL represents bioactivation and detoxification pathways of ZEN, respectively.

1.3.2 Methods in toxicology to study the intestinal microbial metabolism

The study of the intestinal microbial metabolism poses several challenges. *In vivo* studies with experimental animals provide an approach for such studies, but raises ethical issues arising from the use of experimental animals, while taking difference in *in vivo* intestinal microbial composition into account when comparing different species can also pose technical challenges (McCabe *et al.*, 2015). *In vitro* methods

such as the (anaerobic) incubation of isolated strains, synthetic communities or fecal samples have been developed as alternative testing strategies. The use of fecal samples, as used in the present thesis, is widely discussed as they might not represent the microbial composition present in the whole gastro-intestinal tract. However, as stated above, the main site for intestinal microbial metabolism is the colon, which harbors 70% of the bacterial community. Additionally, the communities in feces and colon have been reported to be highly comparable (Behr *et al.*, 2018; Yang *et al.*, 2019). The use of fecal samples provides advantages such as the fact that it represents a non-invasive and high yield sampling method compared to the collection of samples from different parts of the intestine in individual subjects (Zoetendal *et al.*, 2002). Another advantage provided by the use of *in vitro* incubations with fecal samples is that it facilitates studies on interspecies and interindividual differences in the intestinal microbial metabolism. When using *in vitro* technologies it has to be kept in mind that results obtained still need translation to the *in vivo* situation. This is where so-called physiologically-based kinetic modelling may be of use, since it allows modeling of *in vivo* kinetics based on kinetic parameters defined in *in vitro* studies. This approach was also used in the present thesis.

1.4 Physiologically-based kinetic (PBK) models

PBK models offer an alternative approach for non-animal based testing strategies. They describe the absorption, distribution, metabolism, and excretion (ADME) characteristics of a specific chemical in the whole body in time via a series of mathematical equations, and enable translation of *in vitro* data to the *in vivo* situation (Louisse *et al.*, 2017; Rietjens *et al.*, 2011). The development of a PBK model to be used for so-called quantitative *in vitro* to *in vivo* extrapolation (QIVIVE) includes six steps: (1) definition of the conceptual model, (2) translation into a mathematical model, (3) definition of the parameters, (4) solving the model equations, (5) evaluation of the model performance and (6) making predictions (Rietjens *et al.*, 2011). In the first step, it is necessary to define the compartments necessary to describe the organs that are important for the ADME of the compound. Figure 1.2 presents the conceptual model developed in the present thesis for ZEN, with a sub-model for the metabolite α -ZEL, including compartments for liver, blood, fat tissue, small intestine, and also a compartment for the colon enabling inclusion of intestinal microbial metabolism. The rest of the tissues are grouped together in compartments for either rapidly or slowly perfused tissues. The compartments are connected via the systemic circulation. In the second step the

mathematical equations for each compartment are defined using physiological, physico-chemical and kinetic parameters. These parameters have to be defined in the third step. The physiological parameters such as tissue volumes and tissue blood flows can usually be obtained from literature. The physico-chemical parameters, such as for example tissue/blood partition coefficients, can be obtained from *in silico* approaches while the kinetic parameters (absorption and metabolism) are defined in *in vitro* experiments. In the fourth step, the mathematical model is solved to predict the concentrations of the compound and its metabolites in each compartment using software such as Berkeley Madonna or MATLAB. The model outcomes are subsequently compared with *in vivo* data as part of the evaluation in the fifth step. Additionally, a sensitivity analysis is generally performed to identify the most influential parameters for the predictions. In the last step, the model can be used for making predictions, such as concentrations of the compound or its relevant metabolite(s) in relevant tissues or in blood over time at any dose level. Once evaluated, the PBK models can be used to study dose- and species-dependent effects by changing the relevant parameters. In this PhD thesis, the PBK model approach facilitated the study of the contribution of the intestinal microbial metabolism of ZEN, defining the relevant kinetic parameters in *in vitro* assays with fecal samples, to the blood concentration of ZEN and its metabolite α -ZEL in rats and humans.

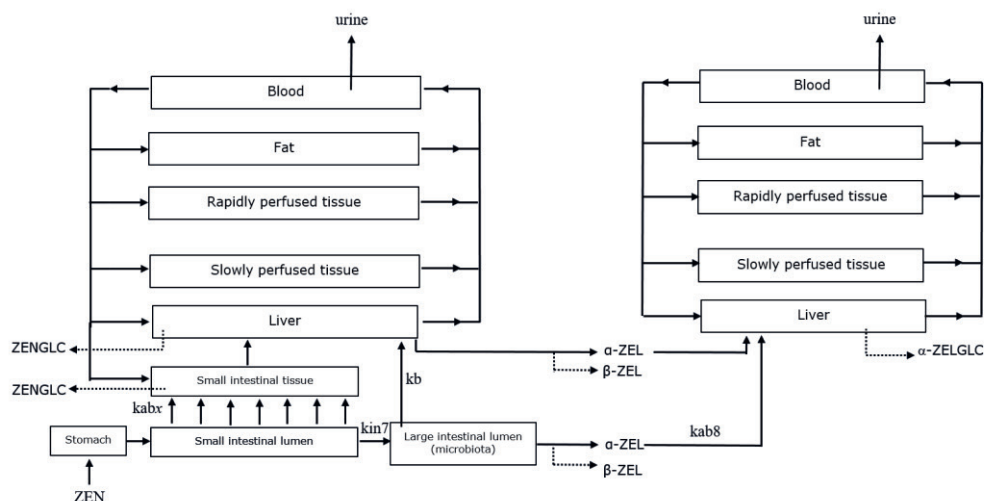


Figure 1.2. Schematic representation of the conceptual PBK model for ZEN with a sub-model for the metabolite α -ZEL

1.5 Combining PBK models and Monte Carlo simulation

The PBK model developed along the lines described above predicts the outcome for an average population since the parameters defining the model are selected to represent the average of the respective population or species. It may be of interest however to not only consider interspecies but also intraspecies variability. The PBK model approach can facilitate this as well.

This can be done by defining parameters for the PBK model using tissue or fecal samples from individual donors instead of pooled samples, enabling definition of individual PBK models that can be used to predict the endpoint of interest, for example the dose-dependent maximum blood concentrations (C_{\max}) of ZEN or α -ZEL. This will provide insight in the interindividual variability for the endpoint of interest. The data obtained for the various parameters using individual tissue samples can also be used to define the distributions for the respective parameters in the population as a whole which can subsequently be used as input for so-called Monte Carlo modeling combined with PBK modeling to define the interindividual variability in the population as a whole. A Monte Carlo simulation is a computer-based method of analysis enabling combination of a large number of sets of randomly generated values for input variables to assess their impact on the model output (Tan *et al.*, 2011). The distribution of the input variables can be defined based on the results obtained with individual tissue or fecal samples in *in vitro* assays. Then, the Monte Carlo algorithm randomly samples from the distributions of the input variables to run the PBK model and generate the output parameter of interest (e.g. blood or tissue concentrations of ZEN or α -ZEL). Each run or simulation will represent one randomly selected individual. In general, a ‘virtual population’ of 1,000 or more individuals is generated to obtain a stable output distribution from which central tendencies (geometric mean) and percentiles (95th and 99th) for the population as a whole can be derived (Figure 1.3). The distributions obtained from the method described, can subsequently be used to derive a so-called chemical-specific adjustment factors (CSAF) for interindividual differences in kinetics, a value that can substitute the default uncertainty factor for interindividual variability in kinetics (IPCS, 2005). For the interindividual variability, the CSAF is defined from the comparison of the percentiles obtained from the output distribution to the geometric mean (IPCS, 2005).

In the present thesis, the distribution in the kinetic parameters obtained for hepatic and intestinal microbial metabolism of ZEN and α -ZEL *in vitro* were the input variables for a Monte Carlo simulation.

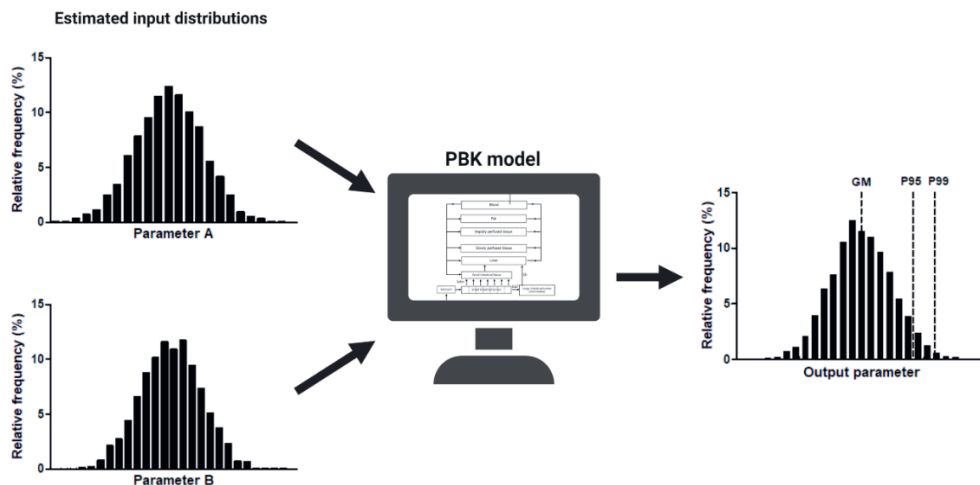


Figure 1.3. Schematic representation of PBK modeling linked to Monte Carlo simulation to predict interindividual variability.

1.6 Thesis overview

As mentioned above, the aim of this PhD project was to acquire further knowledge of the intestinal microbial and the liver metabolism of ZEN in three different species, i.e. rats, pigs and humans. For rats and humans the information obtained *in vitro* for intestinal microbial and hepatic metabolism was integrated in PBK models enabling assessment of the contribution of metabolism by the intestinal microbiota and liver to the predicted C_{\max} of ZEN and its bioactive metabolite α -ZEL. The PBK model also enabled conversion of estimated daily intake values to C_{\max} levels that could be compared to concentrations actually causing estrogenic responses in *in vitro* bioassays in order to elucidate whether at realistic dietary exposure levels ZEN or α -ZEL induced estrogenicity is to be expected. The effects on the predicted C_{\max} of ZEN and α -ZEL due to the human interindividual differences in the metabolism of ZEN were assessed with the PBK model coupled to Monte Carlo simulations and this also provided a CSAF for interindividual differences in kinetics of ZEN. Finally, the *in vitro* model for intestinal microbial metabolism was used to assess the metabolism of ZEN-14-glucoside.

In **Chapter 1**, the current chapter, the background information, outline and aims of this PhD thesis are provided.

In **Chapter 2**, an *in vitro* model with fecal samples for the study of intestinal microbial formation of α -ZEL and β -ZEL from ZEN was developed, optimized to allow quantification of kinetic parameters and used to assess and quantify

interspecies differences. Furthermore the relative contribution of intestinal microbial metabolism, as compared to that of hepatic metabolism, to the bioactivation and detoxification of ZEN was assessed.

In **Chapter 3**, PBK models for rat and human for ZEN with sub-models for the metabolite α -ZEL were developed that included the intestinal microbial bioactivation and detoxification of ZEN. The models allowed quantification of the role of intestinal microbiota in the overall metabolism of ZEN and the influence of intestinal metabolism on the blood concentrations (C_{\max}) of ZEN and α -ZEL. The PBK model for humans was further used to compare the predicted internal concentrations of ZEN and α -ZEL to the concentration able to induce estrogenicity *in vitro*.

In **Chapter 4**, the PBK model for human was coupled to Monte Carlo simulation to assess interindividual variation in the formation of α -ZEL and β -ZEL from ZEN by the intestinal microbiota and liver in a simulated human population. The results were used to define a CSAF for the interindividual variability in kinetics of ZEN.

In **Chapter 5**, interspecies and interindividual variation of the hydrolysis of ZEN-14-G to ZEN was studied using the *in vitro* model with fecal samples developed in Chapter 2. The time for full hydrolysis of a relevant dose was estimated and compared to the total colonic residence time in order to elucidate the potential contribution of ZEN-14-G to ZEN exposure as a result of intestinal microbial metabolism.

Finally in **Chapter 6**, the main findings from the chapters in this thesis are discussed. This chapter includes a discussion on the strengths and limitations of the methods applied and results obtained, to further define the characteristics of metabolism of ZEN by humans and the consequences of this metabolism for the hazards posed upon exposure to this EDC with estrogenic potential. Furthermore, the chapter presents future perspectives defining potential data gaps and future studies when considering the use of alternative *in silico* and *in vitro* approaches when studying the role of intestinal microbial metabolism in human hazard and risk assessment, in line with the 3R framework (Berg *et al.*, 2011).

1.7 References

- Balabanič, D., Rupnik, M., Klemenčič, A.K. Negative impact of endocrine-disrupting compounds on human reproductive health. *Reprod. Fert. Develop.*, 23 (2011), 403-416. doi: 10.1071/RD09300
- Behr, C., Ramirez-Hincapie, S., Cameron, H.J., Strauss, V., Walk, T., Herold, M., Beekmann, K., Rietjens, I., van Ravenzwaay, B. Impact of lincosamides antibiotics on the composition of the rat gut microbiota and the metabolite profile of plasma and feces. *Toxicol. Lett.*, 296 (2018), 139-151. doi: 10.1016/j.toxlet.2018.08.002
- Berg, N., De Wever, B., Fuchs, H.W., Gaca, M., Krul, C., Roggen, E.L. Toxicology in the 21st century – Working our way towards a visionary reality. *Toxicol. In Vitro*, 25 (2011), 874-881. doi: 10.1016/j.tiv.2011.02.008
- Broekaert, N., Devreese, M., De Baere, S., De Backer, P., Croubels, S. Modified *Fusarium* mycotoxins unmasked: From occurrence in cereals to animal and human excretion. *Food Chem. Toxicol.*, 80 (2015), 17-31. doi: 10.1016/j.fct.2015.02.015
- Clarke, G., Sandhu, K.V., Griffin, B.T., Dinan, T.G., Cryan, J.F., Hyland, N.P. Gut Reactions: Breaking Down Xenobiotic–Microbiome Interactions. *Pharmacol. Rev.*, 71 (2019), 198-224. doi: 10.1124/pr.118.015768
- Claus, S.P., Guillou, H., Ellero-Simatos, S. The gut microbiota: a major player in the toxicity of environmental pollutants? *NPJ Biofilms And Microbiomes*, 2 (2016), 16003. doi: 10.1038/npjbiofilms.2016.3
- Dall’Erta, A., Cirlini, M., Dall’Asta, M., Del Rio, D., Galaverna, G., Dall’Asta, C. Masked Mycotoxins Are Efficiently Hydrolyzed by Human Colonic Microbiota Releasing Their Aglycones. *Chem. Res. Toxicol.*, 26 (2013), 305-312. doi: 10.1021/tx300438c
- Dellafiora, L., Ruotolo, R., Perotti, A., Cirlini, M., Galaverna, G., Cozzini, P., Buschini, A., Dall’Asta, C. Molecular insights on xenoestrogenic potential of zearalenone-14-glucoside through a mixed in vitro/in silico approach. *Food Chem. Toxicol.*, 108 (2017), 257-266. doi: 10.1016/j.fct.2017.07.062
- Döll, S., Dänicke, S., Schnurrbusch, U. The effect of increasing concentrations of *Fusarium* toxins in piglet diets on histological parameters of the uterus and vagina. *Arch. Anim. Nutr.*, 58 (2004), 413-417. doi: 10.1080/00039420400004987
- Döll, S., Dänicke, S., Ueberschär, K.H., Valenta, H., Schnurrbusch, U., Ganter, M., Klobasa, F., Flachowsky, G. Effects of graded levels of *Fusarium* toxin

- contaminated maize in diets for female weaned piglets. *Arch. Anim. Nutr.*, 57 (2003), 311-334. doi: 10.1080/00039420310001607680
- EFSA. Scientific Opinion on the risks for public health related to the presence of zearalenone in food. *EFSA J.*, 9 (2011), 2197. doi: 10.2903/j.efsa.2011.2197
- EFSA. Appropriateness to set a group health-based guidance value for zearalenone and its modified forms. *EFSA J.*, 14 (2016), e04425. doi: 10.2903/j.efsa.2016.4425
- Ehrlich, V.A., Dellafiora, L., Mollergues, J., Dall'Asta, C., Serrant, P., Marin-Kuan, M., Lo Piparo, E., Schilter, B., Cozzini, P. Hazard assessment through hybrid in vitro / in silico approach: The case of zearalenone. *Altex*, 32 (2015), 275-286. doi: 10.14573/altex.1412232
- European Commission, 2001. Communication from the Commission to the Council and the European Parliament on the implementation of the Community Strategy for Endocrine Disrupters - a range of substances suspected of interfering with the hormone systems of humans and wildlife (COM (1999) 706), Brussels, pp.
- Everett, D.J., Perry, C.J., Scott, K.A., Martin, B.W., Terry, M.K. Estrogenic potencies of resorcylic acid lactones and 17 β -estradiol in female rats. *J. Toxicol. Environ. Health*, 20 (1987), 435-443. doi: 10.1080/15287398709530995
- Fink-Gremmels, J., Malekinejad, H. Clinical effects and biochemical mechanisms associated with exposure to the mycoestrogen zearalenone. *Anim. Feed Sci. Technol.*, 137 (2007), 326-341. doi: 10.1016/j.anifeedsci.2007.06.008
- Fitzpatrick, D.W., Arbuckle, L.D., Hassen, A.M. Zearalenone metabolism and excretion in the rat: effect of different doses. *J. Environ. Sci. Health B*, 23 (1988), 343-354. doi: 10.1080/03601238809372610
- Frizzell, C., Ndossi, D., Verhaegen, S., Dahl, E., Eriksen, G., et al. Endocrine disrupting effects of zearalenone, alpha- and beta-zearalenol at the level of nuclear receptor binding and steroidogenesis. *Toxicol. Lett.*, 206 (2011), 210-217. doi: 10.1016/j.toxlet.2011.07.015
- Frizzell, C., Uhlig, S., Miles, C.O., Verhaegen, S., Elliott, C.T., Eriksen, G.S., Sørli, M., Ropstad, E., Connolly, L. Biotransformation of zearalenone and zearalenols to their major glucuronide metabolites reduces estrogenic activity. *Toxicol. In Vitro*, 29 (2015), 575-581. doi: 10.1016/j.tiv.2015.01.006
- Gratz, S.W., Dinesh, R., Yoshinari, T., Holtrop, G., Richardson, A.J., Duncan, G., MacDonald, S., Lloyd, A., Tarbin, J. Masked trichothecene and zearalenone

- mycotoxins withstand digestion and absorption in the upper GI tract but are efficiently hydrolyzed by human gut microbiota in vitro. *Mol. Nutr. Food Res.*, 61 (2017), E1600680. doi: 10.1002/mnfr.201600680
- Gromadzka, K., Waskiewicz, A., Chelkowski, J., Golinski, P. Zearalenone and its metabolites: occurrence, detection, toxicity and guidelines. *World Mycotoxin J.*, 1 (2008), 209-220. doi: 10.3920/WMJ2008.x015
- Huttenhower, C., Gevers, D., Knight, R., Abubucker, S., Badger, J.H., et al. Structure, function and diversity of the healthy human microbiome. *Nature*, 486 (2012), 207-214. doi: 10.1038/nature11234
- IPCS, 2005. Chemical-specific adjustment factors for interspecies differences and human variability : guidance document for use of data in dose/concentration-response assessment. World Health Organization, Geneva, pp.
- Karrow, N.A., Sharma, B.S., Fisher, R.E., Mallard, B.A., 2011. 4.33 - Epigenetics and Animal Health. In Moo-Young, M., (Ed.), *Comprehensive Biotechnology* (Third Edition). Pergamon, Oxford, pp. 390-403.
- Koppel, N., Maini Rekdal, V., Balskus, E.P. Chemical transformation of xenobiotics by the human gut microbiota. *Science*, 356 (2017), eaag2770. doi: 10.1126/science.aag2770
- Kowalska, K., Habrowska-Górczyńska, D.E., Piastowska-Ciesielska, A.W. Zearalenone as an endocrine disruptor in humans. *Environ. Toxicol. Pharmacol.*, 48 (2016), 141-149. doi: 10.1016/j.etap.2016.10.015
- Kuiper, G.G.J.M., Lemmen, J.G., Carlsson, B., Corton, J.C., Safe, S.H., van der Saag, P.T., van der Burg, B., Gustafsson, J.-A.k. Interaction of Estrogenic Chemicals and Phytoestrogens with Estrogen Receptor β . *Endocrinology*, 139 (1998), 4252-4263. doi: 10.1210/endo.139.10.6216
- Kutsukake, T., Furukawa, Y., Ondo, K., Gotoh, S., Fukami, T., Nakajima, M. Quantitative Analysis of UDP-Glucuronosyltransferase Ugt1a and Ugt2b mRNA Expression in the Rat Liver and Small Intestine: Sex and Strain Differences. *Drug Metab. Dispos.*, 47 (2019), 38-44. doi: 10.1124/dmd.118.083287
- La Merrill, M.A., Vandenberg, L.N., Smith, M.T., Goodson, W., Browne, P., et al. Consensus on the key characteristics of endocrine-disrupting chemicals as a basis for hazard identification. *Nat. Rev. Endocrinol.*, 16 (2020), 45-57. doi: 10.1038/s41574-019-0273-8
- Lawley, R.A., Curtis, L., Davis, J., 2012. *The food safety hazard guidebook*. RSC Pub., Cambridge, UK.

- Le Guevel, R., Pakdel, F. Assessment of oestrogenic potency of chemicals used as growth promoter by in-vitro methods. *Hum. Reprod.*, 16 (2001), 1030-1036. doi: 10.1093/humrep/16.5.1030
- Lu, K., Mahbub, R., Fox, J.G. Xenobiotics: Interaction with the Intestinal Microflora. *ILAR J.*, 56 (2015), 218-227. doi: 10.1093/ilar/ilv018
- Malekinejad, H., Maas-Bakker, R., Fink-Gremmels, J. Species differences in the hepatic biotransformation of zearalenone. *Veterinary journal*, 172 (2006), 96-102. doi: 10.1016/j.tvjl.2005.03.004
- Malekinejad, H., Maas-Bakker, R.F., Fink-Gremmels, J. Bioactivation of zearalenone by porcine hepatic biotransformation. *Vet. Res.*, 36 (2005), 799-810. doi: 10.1051/vetres:2005034
- McCabe, M., Sane, R.S., Keith-Luzzi, M., Xu, J., King, I., Whitcher-Johnstone, A., Johnstone, N., Tweedie, D.J., Li, Y. Defining the Role of Gut Bacteria in the Metabolism of Deleobuvir: In Vitro and In Vivo Studies. *Drug Metab. Dispos.*, 43 (2015), 1612-1618. doi: 10.1124/dmd.115.064477
- Metzler, M., Pfeiffer, E., Hildebrand, A. Zearalenone and its metabolites as endocrine disrupting chemicals. *World Mycotoxin J.*, 3 (2010), 385-401. doi: 10.3920/WMJ2010.1244
- Minervini, F., Giannoccaro, A., Cavallini, A., Visconti, A. Investigations on cellular proliferation induced by zearalenone and its derivatives in relation to the estrogenic parameters. *Toxicol. Lett.*, 159 (2005), 272-283. doi: 10.1016/j.toxlet.2005.05.017
- Mirocha, C.J., Pathre, S.V., Robison, T.S. Comparative metabolism of zearalenone and transmission into bovine milk. *Food and Cosmet. Toxicol.*, 19 (1981), 25-30. doi: 10.1016/0015-6264(81)90299-6
- Molina-Molina, J.-M., Real, M., Jimenez-Diaz, I., Belhassen, H., Hedhili, A., Torné, P., Fernández, M.F., Olea, N. Assessment of estrogenic and anti-androgenic activities of the mycotoxin zearalenone and its metabolites using in vitro receptor-specific bioassays. *Food Chem. Toxicol.*, 74 (2014), 233-239. doi: 10.1016/j.fct.2014.10.008
- Nguyen, T.L.A., Vieira-Silva, S., Liston, A., Raes, J. How informative is the mouse for human gut microbiota research? *Dis. Model Mech.*, 8 (2015), 1-16. doi: 10.1242/dmm.017400
- Olsen, M., Pettersson, H., Kiessling, K.-H. Reduction of Zearalenone to Zearalenol in Female Rat Liver by 3 α -Hydroxysteroid Dehydrogenase. *Acta Pharmacologica et Toxicologica*, 48 (1981), 157-161. doi: 10.1111/j.1600-0773.1981.tb01602.x

- Pfeiffer, E., Hildebrand, A., Mikula, H., Metzler, M. Glucuronidation of zearalenone, zeranol and four metabolites in vitro: formation of glucuronides by various microsomes and human UDP-glucuronosyltransferase isoforms. *Mol. Nutr. Food Res.*, 54 (2010), 1468-1476. doi: 10.1002/mnfr.200900524
- Qin, J., Li, R., Raes, J., Arumugam, M., Burgdorf, K.S., et al. A human gut microbial gene catalogue established by metagenomic sequencing. *Nature*, 464 (2010), 59-65. doi: 10.1038/nature08821
- Rietjens, I.M., Louisse, J., Punt, A. Tutorial on physiologically based kinetic modeling in molecular nutrition and food research. *Mol. Nutr. Food Res.*, 55 (2011), 941-956. doi: 10.1002/mnfr.201000655
- Rogowska, A., Pomastowski, P., Sagandykova, G., Buszewski, B. Zearalenone and its metabolites: Effect on human health, metabolism and neutralisation methods. *Toxicon*, 162 (2019), 46-56. doi: 10.1016/j.toxicon.2019.03.004
- Scheline, R.R. Metabolism of Foreign Compounds by Gastrointestinal Microorganisms. *Pharmacol. Res.*, 25 (1973), 451-523. doi:
- Sender, R., Fuchs, S., Milo, R. Are We Really Vastly Outnumbered? Revisiting the Ratio of Bacterial to Host Cells in Humans. *Cell*, 164 (2016a), 337-340. doi: 10.1016/j.cell.2016.01.013
- Sender, R., Fuchs, S., Milo, R. Revised Estimates for the Number of Human and Bacteria Cells in the Body. *PLoS Biol.*, 14 (2016b), e1002533. doi: 10.1371/journal.pbio.1002533
- Shier, W.T., Shier, A.C., Xie, W., Mirocha, C.J. Structure-activity relationships for human estrogenic activity in zearalenone mycotoxins. *Toxicon*, 39 (2001), 1435-1438. doi:
- Sousa, T., Paterson, R., Moore, V., Carlsson, A., Abrahamsson, B., Basit, A.W. The gastrointestinal microbiota as a site for the biotransformation of drugs. *Int. J. Pharm.*, 363 (2008), 1-25. doi: 10.1016/j.ijpharm.2008.07.009
- Spanogiannopoulos, P., Bess, E.N., Carmody, R.N., Turnbaugh, P.J. The microbial pharmacists within us: a metagenomic view of xenobiotic metabolism. *Nat. Rev. Microbiol.*, 14 (2016), 273-287. doi: 10.1038/nrmicro.2016.17
- Tan, Y.M., Yang, Y.C., Andersen, M.E., Clewell, H.J., 2011. Exposure Science: Pharmacokinetic Modeling. In Nriagu, J.O., (Ed.), *Encyclopedia of Environmental Health*. Elsevier, Burlington, pp. 681-692.
- Turner, P.V. The role of the gut microbiota on animal model reproducibility. *Anim. models Exp. Med.*, 1 (2018), 109-115. doi: 10.1002/ame2.12022

- Visconti, A., Le Roy, C.I., Rosa, F., Rossi, N., Martin, T.C., et al. Interplay between the human gut microbiome and host metabolism. *Nat. Commun.*, 10 (2019), 4505. doi: 10.1038/s41467-019-12476-z
- Yang, N., Yan, W., Sun, C., Zheng, J., Wen, C., Ji, C., Zhang, D., Chen, Y., Hou, Z. Efficacy of fecal sampling as a gut proxy in the study of chicken gut microbiota. *Front. Microbiol.*, 10 (2019), 2126. doi: 10.3389/fmicb.2019.02126
- Yang, S., Zhang, H., Zhang, J., Li, Y., Jin, Y., et al. Deglucosylation of zearalenone-14-glucoside in animals and human liver leads to underestimation of exposure to zearalenone in humans. *Arch. Toxicol.*, 92 (2018), 2779-2791. doi: 10.1007/s00204-018-2267-z
- Zoetendal, E.G., von Wright, A., Vilpponen-Salmela, T., Ben-Amor, K., Akkermans, A.D., de Vos, W.M. Mucosa-associated bacteria in the human gastrointestinal tract are uniformly distributed along the colon and differ from the community recovered from feces. *Appl. Environ. Microbiol.*, 68 (2002), 3401-3407. doi: 10.1128/AEM.68.7.3401-3407.2002

Chapter 2

An *in vitro* model to quantify interspecies differences in kinetics for intestinal microbial bioactivation and detoxification of zearalenone

*Diana M. Mendez-Catala, Albertus Spengelink,
Ivonne M.C.M. Rietjens & Karsten Beekmann*

Toxicology reports, 7 (2020): 938-946
DOI: [10.1016/j.toxrep.2020.07.010](https://doi.org/10.1016/j.toxrep.2020.07.010)

Abstract

Zearalenone (ZEN) is a mycotoxin known for its estrogenic activities. The metabolism of ZEN plays a role in the interspecies differences in sensitivity to ZEN, and is known to occur in the liver and via the intestinal microbiota, although the relative contribution of these two pathways remains to be characterized. In the present study a fecal *in vitro* model was optimized and used to quantify the interspecies differences in kinetics of the intestinal microbial metabolism of ZEN in rat, pig and human. V_{\max} , K_m , and catalytic efficiencies (k_{cat}) were determined, and results obtained reveal that the k_{cat} values for formation of α -ZEL and β -ZEL amounted to 0.73 and 0.12 ml/h/kg bw for human microbiota, 2.6 and 1.3 ml/h/kg bw for rat microbiota and 9.4 and 6.3 ml/h/kg bw for pig microbiota showing that overall ZEN metabolism increased in the order human < rat < pig microbiota. Expressed per kg bw the k_{cat} for ZEN metabolism by the liver surpassed that of the intestinal microbiota in all three species. In conclusion, it is estimated that the activity of the intestinal colon microbiome may be up to 36% of the activity of the liver, and that it can additionally contribute to the species differences in bioactivation and detoxification and thus the toxicity of ZEN in pigs and rats but not in humans. The results highlight the importance of the development of human specific models for the assessment of the metabolism of ZEN.

Keywords: Intestinal microbiota; bioactivation; detoxification; zearalenone; interspecies differences

Abbreviations: α -ZEL: α -zearalenol; β -ZEL: β -zearalenol; ER: estrogen receptor; k_{cat} : catalytic efficiency; RP: relative potency; UPLC-PDA: ultra-performance liquid chromatography method with diode array detection; LC-MS/MS: Liquid chromatography tandem mass spectrometry; ZEN: zearalenone

2.1 Introduction

Zearalenone (ZEN) is a mycotoxin produced by *Fusarium* species contaminating grains and cereals, particularly wheat and corn. ZEN is known to act as an endocrine disruptor, and exposure to ZEN is known to cause reproductive-toxicity, mediated via estrogen receptor agonism (EFSA, 2016). Upon ingestion, ZEN is metabolized to α -zearalenone (α -ZEL) and β -zearalenone (β -ZEL). Conversion to α -ZEL represents bioactivation because α -ZEL has been shown in different *in vitro* and *in vivo* studies to be on average 60 times more potent as an ER α agonist than ZEN. In contrast, β -ZEL is 5 times less potent than ZEN so that conversion of ZEN to β -ZEL is considered a detoxification (EFSA, 2016). Differences in the reduction of ZEN to α -ZEL and β -ZEL between species is considered a key factor contributing to differences in the sensitivity to ZEN exposure. Interspecies differences in bioactivation and detoxification of ZEN to α -ZEL and β -ZEL have been well-described for liver tissue (Mukherjee *et al.*, 2014). Pigs, whose liver appears to be more efficient in α -ZEL production than that of other species are also most sensitive towards ZEN toxicity observed in reproductive organs (Malekinejad *et al.*, 2006; EFSA, 2011). However, in addition to the liver also the intestinal microbiota can metabolize ZEN to α -ZEL and β -ZEL (Gratz *et al.*, 2017), although the relative contribution of conversion by the gut microbiota as well as interspecies differences in bioactivation and detoxification of ZEN by the intestinal microbiota remain to be characterized. Mammalian intestinal microbiota is known to modulate many processes essential to maintain host health, including the biotransformation of xenobiotics (Nicholson *et al.*, 2012). The overall metabolic capacity of the intestinal microbiome has been described to complement the metabolic capacity of the host by encoding for enzymes that the host does not possess itself, with an overall broader substrate specificity (Koppel *et al.*, 2017). While there is a significant body of literature showing interspecies differences in microbiome composition (Ley *et al.*, 2008; Krych *et al.*, 2013; Nguyen *et al.*, 2015) due to lifestyles and diets (Sousa *et al.*, 2008; Hörmannspurger *et al.*, 2015), little is known about the potentially resulting differences in functionality. Typical microbial reactions include the reduction of chemicals (Sousa *et al.*, 2008), an important reaction for the bioactivation and/or detoxification of ZEN, so that differences in metabolic capacity of the intestinal microbiota might contribute to the interspecies differences in sensitivity to ZEN exposure.

The aim of the present study was to develop an *in vitro* model system to assess and quantify the contribution of the intestinal microbial metabolism to the bioactivation and detoxification of ZEN. The model to be developed should enable the

quantification of kinetics for the conversion of ZEN in incubations with fecal samples from different host species, facilitating the quantitative characterization of species differences in bioactivation and detoxification and thus the contribution of gut microbial metabolism to species differences in sensitivity to ZEN exposure. The development of an *in vitro* model that enables quantification of kinetic parameters for intestinal metabolism is essential for future incorporation of conversion by the intestinal microbiota in alternative testing strategies within the 3R the framework for alternatives for animal testing (Berg *et al.*, 2011).

In the present study an *in vitro* model with fecal slurries was optimized and successfully applied for i) the assessment of interspecies differences in the intestinal microbial metabolism of ZEN in rats, pigs, and humans, and ii) comparison of the relative intestinal and hepatic bioactivation and detoxification of ZEN to α -ZEL and β -ZEL.

2.2 Materials and methods

2.2.1 Materials

ZEN (CAS registry number 17924-92-4; $\geq 99.0\%$), α -ZEL (CAS registry number 36455-72-8; $>98\%$), β -ZEL (CAS registry number 71030-11-0; $>98\%$) and 17 β -estradiol (E2; CAS registry number 50-28-2) were purchased from Sigma-Aldrich (Schnellendorf, Germany). Stock solutions of the test chemicals were prepared in dimethyl sulfoxide (DMSO; CAS registry number 67-68-5) purchased from Merck (Darmstadt, Germany). Cryopreserved UltraPoolTM human microsomes (150 mixed gender donors) and pooled human liver S9 (20 mixed gender donors) were obtained from Corning (Woburn, MA, USA). β -Nicotinamide adenine dinucleotide phosphate, reduced form (NADPH; CAS registry number 2646-71-1) was purchased from Carbosynth (Berkshire, UK). Trizma[®] base (Tris, CAS registry number 77-86-1) and glycerol (CAS registry number 56-81-5) were obtained from Sigma-Aldrich (Steinheim, Germany). Magnesium chloride hexahydrate ($\text{MgCl}_2 \cdot 6\text{H}_2\text{O}$; CAS registry number 7791-18-6) and formic acid (FA; CAS registry number 64-18-6) were obtained from VWR International (Amsterdam, The Netherlands). Methanol (MeOH, UPLC/MS grade; CAS registry number 67-56-1) and acetonitrile (ACN, UPLC/MS grade; CAS registry number 75-05-8) were purchased from Biosolve (Valkenswaard, The Netherlands). Phosphate-buffered saline (PBS, pH 7.4), Dulbecco's modified Eagle's medium nutrient mixture F12 (DMEM/F12), phenol red-free DMEM/F12, fetal bovine serum (FBS), non-essential amino acids (NEAA),

dextran coated charcoal-filtered fetal calf serum (DCC-FBS) and geneticin (G418; CAS registry number 108321-42-2) were obtained from Gibco (Paisley, UK).

2.2.2 Estrogenicity of ZEN, α -ZEL and β -ZEL studied in an estrogen receptor-mediated reporter gene (ER α -CALUX) assay

U2OS ER α reporter gene cells, derived from a stably transfected human osteosarcoma cell line expressing ER α were kindly provided by BioDetection Systems (Amsterdam, The Netherlands) (Sonneveld *et al.*, 2004), were cultured in DMEM/F12 supplemented with 10% FCS, 0.5% NEAA and 4 μ g/ml of geneticin. The cells were routinely subcultured every 3 to 4 days.

For the CALUX assay, cells were seeded in 96-well view plates at a density of 1×10^5 cells/ml in 100 μ l of assay medium (phenol red-free DMEM/F-12 supplemented with 5% DCC-FCS and 0.5% NEAA) and allowed to attach for 48 hours with a renewal of assay medium after the first 24 hours. 48 Hours after seeding, the medium was aspirated and replaced with 100 μ l assay medium containing ZEN (0.1 pM-10 nM), α -ZEL (0.01-1000 pM), or β -ZEL (0.01 pM-10 nM) added from 200 times concentrated stock solutions in DMSO (0.5% DMSO maximum final concentration). For each assay, the concentrations were tested in triplicate. 100 pM E2 was used as positive control and 0.5% DMSO as solvent control. After 24 hours, the cells were washed with 100 μ l 0.5 PBS, and lysed with 30 μ l of low salt buffer (LSB; pH 7.8) containing 10 mM Tris, 2 mM dithiothreitol (DTT), and 2 mM 1, 2-diaminocyclohexanete triacetic acid monohydrate. The plates were placed on ice for 15 minutes and frozen at -80°C for at least 2 hours. Plates were thawed while being shaken and luciferase activity was measured using a luminometer (Glomax-Multi Detection System, Promega, California) upon adding 100 μ l of FLASH mix (pH 7.8) containing 20 mM tricine, 1.07 mM (MgCO₃)₄Mg(OH)₂·5H₂O, 2.67 mM MgSO₄, 0.1 mM ethylenedinitrilotetraacetic acid disodium salt dihydrate, 2 mM DTT, 0.47 mM D-luciferin and 5 mM adenosine-5-triphosphate.

The luciferase activity was measured in relative light units and used to calculate the fold increases of luminescence relative to the solvent control in MS Excel (2016). The obtained values were normalized to the maximum response of E₂ (100 pM) set at 100% and the concentration-response curves were fitted in GraphPad Prism 5.04 (GraphPad software, San Diego California, U.S.A.) by using a non-linear regression model (four parameter sigmoidal dose-response) to obtain the half-maximal effect concentrations (EC₅₀).

The EC₅₀ values from other studies using ER activation as endpoint were collected and used to calculate the relative potency factors (EC₅₀ ZEN/EC₅₀ metabolite) that could be compared to the relative potency factors obtained in the present study.

2.2.3 Collection of rat, pig and human fecal samples

Fresh fecal samples from Wistar rats (10 male and 15 female) were kindly provided by BASF (Ludwigshafen, Germany). Feces from each individual were obtained by physical stimulation of the abdomen to trigger defecation, weighed and immediately transferred into an anaerobic solution of 10% (v/v) glycerol in PBS and diluted to a final fecal concentration of 20% (w/v). Samples were manually homogenized using a sterile glass wand, and tubes flushed with N₂ gas before being frozen to -80 °C. Subsequently, individual samples were mixed and filtered using a woven sterile medical gauze dressing (HeltiQ) under anaerobic conditions (85% N₂, 10% CO₂ and 5% H₂, in a Bactron EZ anaerobic chamber). Aliquots of the resulting fecal slurry were prepared and stored at -80 °C until further use.

Fecal samples collected from 10 piglets (5 females and 5 males) were kindly provided by Wageningen Livestock Research (Wageningen, The Netherlands) during dissection of untreated control animals of an animal study for which permission (license number 2016.D0136.003) by the Animal Care and Use Committee of Wageningen University & Research (Wageningen, The Netherlands) was obtained. Samples from each individual were treated and stored separately as described. The colorectal part of the intestines containing feces were closed with artery clamps before being removed. Fecal matter from these sections were transferred to 50 ml centrifuge tubes, immediately flushed with N₂ gas and transported in an airtight container into the anaerobic environment of the anaerobic chamber described below for further processing. Samples were weighed and fecal slurry prepared by diluting the samples with an anaerobic solution of 10% glycerol in PBS to obtain a final concentration of 20% (w/v). Samples were manually homogenized with a sterile serological pipette and filtered using a woven sterile medical gauze dressing (HeltiQ). Aliquots of the fecal slurry were prepared and stored at -80°C until further use. Prior to the experiments a pool of the 10 individuals was prepared.

Human fecal samples were donated by 10 volunteers (7 females and 3 males), aged 24-64 years. Volunteer donors did not consume antibiotics or visit tropical countries for 3 months prior to sample donation and have no history of intestinal diseases. The research protocol for use of these human samples was evaluated by the Medical Ethical Reviewing Committee of Wageningen University (METC-WU) and judged

not to require further evaluation within the scope of the Dutch Medical Research Involving Human Subjects Act. Samples from each individual were treated and stored separately as follows: in specimen tubes, 3-5 gram of fecal samples were collected and subsequently transferred into an anaerobic environment within 2 minutes after donation by the participants. Samples were immediately diluted in an anaerobic solution of 10% glycerol in PBS to obtain the fecal slurry (20% w/v). Samples were manually homogenized with a sterile serological pipette and filtered using SpinCon® (Meridian Bioscience Europe) centrifugal filters at 2,500 rpm for 5 minutes. The filtrate was divided into aliquots and stored at -80°C until further use. Prior to the experiments a pool of fecal samples of 10 individuals was prepared.

2.2.4 *In vitro* incubation of ZEN with rat, pig and human fecal samples

To optimize the incubation conditions, linearity of reaction rates over different fecal concentrations and over time was established for rat, pig and human samples. To this end, 20 µM ZEN was incubated under anaerobic conditions with different concentrations of fecal slurry and for different time points. To assess linearity over different fecal concentrations, incubation mixes of 100 µL containing 1.4 - 20% of fecal slurry from rats, pigs, and humans in anaerobic PBS (pH 7.4) containing 20 µM of ZEN added from a 200x concentrated stock in DMSO (0.5% DMSO final concentration) were prepared under anaerobic conditions and incubated anaerobically at 37 °C for 5 hours. To assess linearity over time, ZEN was incubated with 5% of fecal slurry and sampled every hour for a total of 8 hours. To stop the reactions, 100 µl of ice-cold MeOH were added, the samples were vortexed, and kept on ice for 10 minutes. The samples were centrifuged at 21,500 x g for 15 minutes at 4 °C, and the supernatant was kept for ultra-performance liquid chromatography photodiode array (UPLC-PDA) or liquid chromatography-tandem mass spectrometry (LC-MS/MS) analysis. Blank controls were included to assess the stability of ZEN during incubation.

Using the optimized incubation conditions, a range of substrate concentrations of ZEN was incubated to establish reaction kinetics. Incubation mixes of 100 µL were prepared containing 1 - 250 µM of ZEN added from 200x concentrated stock solutions in DMSO (0.5% DMSO final concentration), 5% of fecal slurry from rats, pigs, or humans, and PBS (pH 7.4). The samples were incubated anaerobically at 37°C for 5 hours. To stop the reaction, 100 µl of ice-cold MeOH were added, the samples were vortexed, and kept on ice for at least 10 minutes. The samples were centrifuged at 21,500 x g for 15 minutes at 4°C and the supernatant was kept on ice

for immediate UPLC-PDA or LC-MS/MS analysis. Three independent experiments for each species were done and data are presented as mean \pm standard deviation (SD).

2.2.5 *In vitro* human hepatic metabolism of ZEN

Human liver microsomal and S9 fraction incubations to characterize the reduction of ZEN by hepatic samples were optimized to establish the linearity over time and protein concentration. To obtain the kinetic parameters, the incubation mixtures with a final volume of 200 μ l contained (final concentrations) 2 mM NADPH, 5 mM $MgCl_2$ and 0.3 mg/ml liver microsomal or S9 fraction proteins in 0.1 M Tris-HCl buffer (pH 7.4). After 1-minute pre-incubation at 37°C, the reactions were started by the addition of 1 - 500 μ M ZEN (from 100 times concentrated stock solutions in DMSO). The incubations were carried out for 10 min for the microsomes and 5 min for the S9 fractions. To stop the reaction 20% (v/v) ice-cold ACN was added. Blank incubations were performed without the addition of NADPH. The samples were centrifuged for 5 min at 15,000 \times g and the supernatant was kept on ice for immediate UPLC-PDA analysis.

2.2.6 Kinetic analysis

To derive the kinetic constants for the formation of α -ZEL and β -ZEL by both the microbial and human hepatic metabolism, the amount of metabolites formed expressed per gram of feces or protein, respectively, and per unit of time (rate of formation) were calculated using Microsoft Excel (version 2016) and plotted against the substrate concentrations used. The curve for each metabolite was fitted in GraphPad Prism 5.04 (GraphPad software, San Diego California, U.S.A.) using a standard Michaelis-Menten regression ($V = V_{max} * [S] / (K_m + [S])$) to obtain the *in vitro* kinetic constants, V_{max} (pmol/min/mg of feces or pmol/min/mg of protein) and K_m (μ M) for the microbial and human hepatic formation of α -ZEL and β -ZEL.

2.2.7 Comparison of microbial and hepatic metabolism of ZEN

Using the reported average defecation masses of 3 g feces/day for rat (Cavigelli *et al.*, 2005), 1,360 g feces/day for pigs (Mariscal-Landin, 2007) and 128 g feces/day for humans (Rose *et al.*, 2015), and correcting for average body masses of 0.25 kg for rats (Brown *et al.*, 1997), 25 kg for pigs (Upton, 2008) and 70 kg for humans (Brown *et al.*, 1997), the *in vitro* V_{max} (in pmol/min/mg of feces) was scaled to an *in vivo* V_{max} (in μ mol/h/kg bw).

The hepatic V_{\max} (pmol/min/mg of protein), K_m (μM) and k_{cat} (defined as V_{\max}/K_m) values obtained in this study for human and as reported in literature (Malekinejad *et al.*, 2006) for rat and pig based on *in vitro* studies with liver microsomes and S9 fractions were used for comparison to the *in vivo* V_{\max} and k_{cat} values for conversion by the intestinal microbiota. In line with the requirements of the 3Rs (reduction, refinement and replacement) for animal experimentation only the data for hepatic metabolism of human, which were not available in literature, were experimentally determined in this study. The *in vitro* V_{\max} values for conversion by liver samples were scaled to an *in vivo* V_{\max} (in $\mu\text{mol/h/kg}$ bw) using protein yields, liver weight and body mass for each species. Microsomal protein yield used for rat liver was 38 mg/g liver (Chiu and Ginsberg, 2011), for pig liver it was 32.6 mg/g liver (Millecam *et al.*, 2018) and for human liver it amounted to 32 mg/g liver (Barter *et al.*, 2007); S9 protein yield used for rat liver was 87 mg/g liver (Chiu and Ginsberg, 2011), and it was 127.9 mg/g liver for pig liver (Lignet *et al.*, 2016) and 143 mg/g liver for human liver (Punt *et al.*, 2009). Liver weights for rats, pigs and humans were calculated using body masses of 0.25, 25 and 70 kg, respectively, and tissue volumes (% of body weight) of 3.4 (Brown *et al.*, 1997), 2.9 (Upton, 2008) and 2.6 (Brown *et al.*, 1997), respectively.

Once the *in vivo* k_{cat} values were obtained, the percentage of contribution for hepatic (microsomes and S9 fractions) and microbial metabolism were calculated.

2.2.8 Quantification of α -ZEL and β -ZEL: UPLC-PDA and LC-MS/MS analyses

A UPLC-PDA system (Waters Acquity) was used for the quantification of ZEN, α -ZEL and β -ZEL formed in incubations with rat fecal slurry. The UPLC system was equipped with an Acquity BEH C18 column 1.7 μm , 50 mm x 2.1 mm (Waters) set at 45 °C and a UV detection system recording wavelengths of 190-400 nm. Nanopure water (A) and ACN (B) were used as eluents at a flow rate of 0.6 ml/min with the following gradient profile: 0-25% B (0 - 0.5 min), 25-50% B (0.5 - 1.2 min), 50-75% B (1.2 - 3 min), 75% B (3 - 3.5 min), 75-100% B (3.5 - 4 min), 100-0% B (4 - 4.25 min) and 0% B (4.25 - 5 min). Per run, 3.5 μl of sample were injected. ZEN, α -ZEL and β -ZEL were identified using commercially available standards. Chromatograms were presented at 235 nm and chemicals were quantified by comparison of the peak areas at 235 nm to those from standard curves (estimated LOD = 0.02 μM ; LOQ = 0.05 μM) prepared using commercially available standards.

ZEN, α -ZEL and β -ZEL formed in pig and human incubations were quantified by LC-MS/MS. The analysis was performed on a Nexera XR LC-20AD SR UPLC

system coupled to a triple quadrupole LCMS 8040 mass spectrometer (Shimadzu Benelux, 's Hertogenbosch, The Netherlands) with electrospray ionization (ESI) interface. The UPLC system was equipped with a Kinetex® C18 column 1.7 μ m, 50 mm x 2.1 mm (Phenomenex) and set at 40 °C with a flow rate of 0.3 ml/min. The mobile phases consisted of nanopure water containing 0.1% (v/v) formic acid (A) and ACN containing 0.1% (v/v) formic acid (B). The total run time was 14 minutes with the following gradient profile: 0-40% B (0 – 1.3 min), 40-50% B (1.3 - 5.7 min), 50-100% B (5.7 - 6 min), 100 % B kept for 2 minutes and 100-0% B (8 - 8.1 min) for equilibration. Per run, 1 μ l of sample was injected. MS/MS analysis was operated in the positive ion mode and the MRM mode with a spray voltage of 4.5 KV. The transitions monitored were (m/z) 319.2 \rightarrow 301.2, 319.2 \rightarrow 283.1, 319.2 \rightarrow 187.1 for ZEN; (m/z) 321.2 \rightarrow 303.1, 321.2 \rightarrow 285.1, 321.2 \rightarrow 131.0 for α -ZEL; and 321.2 \rightarrow 303.2, 321.2 \rightarrow 285.15, 321.2 \rightarrow 267.0 for β -ZEL. The Postrun Analysis function from the LabSolutions software (Shimadzu, Kyoto, Japan) was used to obtain the peak area of the total ion chromatogram (TIC) for each compound. For quantification of the compounds, the areas were compared to standard curves made using commercially available standards (estimated LOD = 0.01 μ M; LOQ = 0.04 μ M).

2.3 Results

2.3.1 Estrogenicity of ZEN, α -ZEL and β -ZEL

The concentration-response curves (Supplementary Figure 2.1) for the induction of ER α -mediated gene expression were used to derive EC₅₀ values of 1.6 nM, 0.03 nM and 41.6 nM for ZEN, α -ZEL and β -ZEL, respectively. EC₅₀ values, from this study and other relevant literature, are listed in Table 2.1 together with the calculated relative potencies (RP) of the metabolites compared to ZEN. The relative potencies (RP) of the metabolites compared to ZEN were calculated and are included in Table 2.1. Substantial variation in RPs between the studies is observed, with, in spite of this, α -ZEL always showing higher potency than ZEN being 12- to 200-fold more potent, while the RP for β -ZEL was always lower amounting to 0.002- to 0.6 times the RP of ZEN. In all cases, the potency ranking of the compounds is α -ZEL > ZEN > β -ZEL, with α -ZEL being on average 72.3 times more potent and β -ZEL on average 5.5 times less potent than ZEN. Therefore, the formation of α -ZEL from ZEN is considered a bioactivation while the formation of β -ZEL a detoxification.

Table 2.1. EC₅₀ values and relative potencies for ERα agonist activity of ZEN, α-ZEL and β-ZEL as derived from the ERα-CALUX assay in the present study or taken from literature.

	EC ₅₀ (nM)			Relative potency ^h	
	ZEN	α-ZEL	β-ZEL	α-ZEL	β-ZEL
Activation of reporter gene (ERα-CALUX) ^a	1.58	0.03	41.59	55	0.04
Activation of reporter gene (ERα-CALUX) ^b	0.49	0.01	2.50	51	0.20
Activation of reporter gene (MMV-Luc) ^c	1.60	0.02	3.90	73	0.41
MCF7 cell proliferation ^d	3.81	0.06	8.49	64	0.45
MCF7 cell proliferation ^e	0.31	1.4x10 ⁻³	5.20	221	0.06
MCF7 cell proliferation ^f	1.64	0.05	20.01	33	0.08
Ishikawa cell proliferation ^g	0.06	0.01	25	8.79	0.002
Average (± SD)	1.3 (± 1.2)	0.03 (± 0.02)	15.2 (± 14.4)	72.3 (± 69.0)	0.18 (± 0.18)

^a this study

^b Ehrlich *et al.* (2015)

^c Frizzell *et al.* (2011)

^d Molina-Molina *et al.* (2014)

^e Minervini *et al.* (2005)

^f Malekinejad *et al.* (2005)

^g Le Guevel and Pakdel (2001)

^h EC₅₀ ZEN/EC₅₀ metabolite

2.3.2 Conversion of ZEN in *in vitro* incubations with rat, pig and human fecal slurries

To study its intestinal microbial metabolism, ZEN was incubated anaerobically with rat, pig and human fecal slurries. This resulted in the formation of two metabolites identified as α -ZEL and β -ZEL (Figure 2.1). Under the conditions applied no other metabolites were formed at a detectable level. Incubation conditions were optimized for subsequent study of reaction kinetics defining the range where metabolite formation was linear with respect to time and fecal slurry concentration. Based on the experimental results obtained (Supplementary Figure 2.2), optimal

conditions for subsequent kinetic experiments were defined as 5-hour incubation time using 5% fecal slurry.

Using the conditions thus established for linear conversion with respect to incubation time and fecal concentration, the ZEN concentration-dependent conversion of ZEN to α -ZEL and β -ZEL was quantified (Figure 2.2). The formation of α -ZEL and β -ZEL followed Michaelis-Menten behavior (Figure 2.2) and allowed determination of the kinetic constants V_{\max} and K_m . The *in vitro* kinetic constants and catalytic efficiencies (k_{cat} ; calculated as V_{\max}/K_m) for the formation of α -ZEL and β -ZEL by fecal samples of the three species are presented in Table 2.2. In all three species, α -ZEL was formed at a higher rate than β -ZEL at all substrate concentrations tested. The k_{cat} values for formation of α -ZEL in incubations with fecal slurries from rats and pigs appeared to be comparable, with the k_{cat} for the pooled fecal samples from rats, being 1.23 times higher than that of the pooled fecal samples from pigs. Among the three species, the highest k_{cat} for the formation of α -ZEL was observed with the pooled human fecal samples, mainly due to a higher V_{\max} . When comparing human with rat and pig fecal samples, the k_{cat} for the formation of α -ZEL by human fecal samples was 1.8 to 2.0 times higher. The k_{cat} for formation of β -ZEL for rat and pig fecal samples was also comparable, with a 1.1 times higher value for pig samples. Human fecal samples showed for β -ZEL formation a k_{cat} that was 1.6 to 2.0 fold lower than that for the other two species, suggesting a less efficient detoxification. As shown in Table 2.2, the resulting ratio between $k_{\text{cat},\alpha\text{ZEL}}$ and $k_{\text{cat},\beta\text{ZEL}}$ is highest for human (6:1) indicating human to be the species with the highest relative level of bioactivation of ZEN to α -ZEL with relatively low detoxification to β -ZEL by the fecal samples.

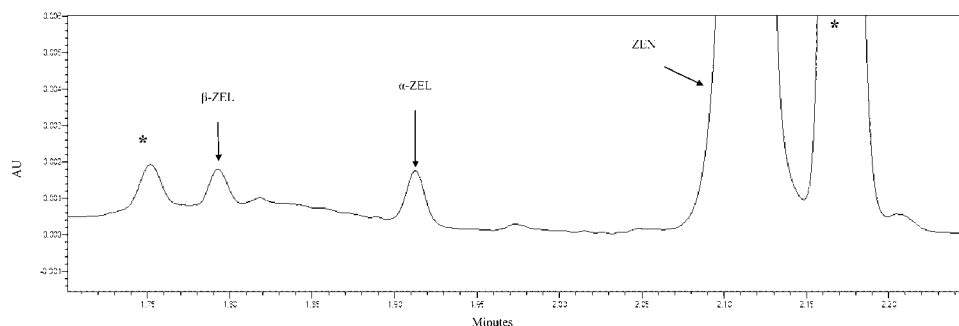


Figure 2.1. Chromatogram of the incubation of 20 μM ZEN with fecal slurries from rats for 5 hours at 37°C under anaerobic conditions. Peaks marked with an * represent peaks also present in blank incubations without ZEN and originating from the fecal slurry.

In a next step the *in vitro* V_{max} and k_{cat} values obtained for the formation of α -ZEL and β -ZEL were scaled to *in vivo* V_{max} and k_{cat} values expressed per kg bw using the defecation volume per day and the respective body masses as scaling factors (Table 2.2). After this conversion, the *in vivo* k_{cat} of pigs for the formation of α -ZEL appeared to be almost 3.6 and 12.8 times higher than that for rats and humans, respectively, revealing that on a per kg basis pigs represent the species with the highest potential of the three investigated species for the formation of α -ZEL. For β -ZEL, the *in vivo* k_{cat} values for pigs were 4.9 and 52.4 times higher than those in rats and humans, respectively. In spite of humans showing the highest *in vitro* k_{cat} α -ZEL and β -ZEL for, they appeared to have the lowest *in vivo* k_{cat} due to a relatively lower defecation volume per kg bw.

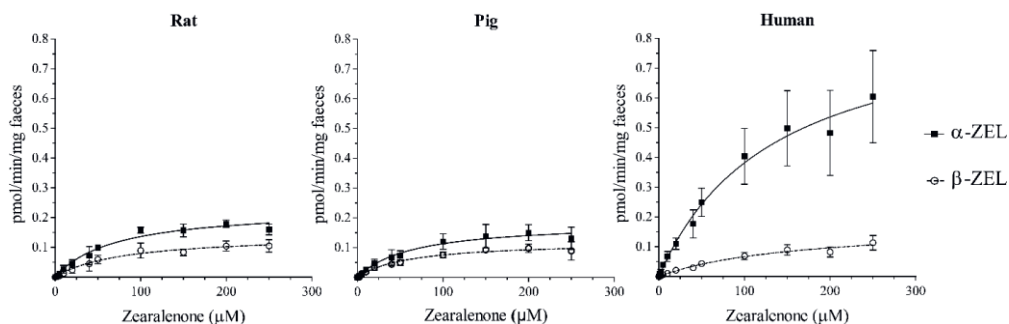


Figure 2.2. ZEN concentration-dependent formation of α -ZEL and β -ZEL in incubations with pooled fecal samples of rat, pig and human. Each data point represents the mean \pm SD of three independent experiments.

Table 2.2. Kinetic parameters for the intestinal microbial formation of α -ZEL and β -ZEL from ZEN scaled to the *in vivo* situation for rat, pig and human.

		V_{\max} <i>in vitro</i> ^a	K_m ^b	k_{cat} <i>in vitro</i> ^c	Scaled V_{\max} <i>in vivo</i> ^d	k_{cat} <i>in vivo</i> ^e	Ratio $k_{cat,\alpha ZEL}/$ $k_{cat,\beta ZEL}$
Rat	α -ZEL	0.23	66	3.5	0.17	2.60	2.0
	β -ZEL	0.14	80	1.8	0.10	1.30	
Pig	α -ZEL	0.19	65	2.9	0.61	9.40	1.5
	β -ZEL	0.12	61	2.0	0.38	6.30	
Human	α -ZEL	0.90	135	6.6	0.10	0.73	6.0
	β -ZEL	0.18	163	1.1	0.02	0.12	

^a pmol/min/mg of feces;

^b μ M

^c (10^{-3}) μ l/min/mg feces

^d Expressed as μ mol/h/kg bw and calculated from $[(V_{\max}, \text{in vitro}) \times (\text{defecation volume in mg}) \times (60 \text{ min/h})] / (10^6 \mu\text{mol/pmol}) / (\text{kg bw})$.

^e ml/h/kg bw

2.3.3 *In vitro* liver conversion of ZEN by microsomal and S9 fractions

To enable comparison of intestinal microbial conversion to conversion by the liver, the *in vitro* kinetic data for hepatic metabolism of ZEN in humans were determined in this study from *in vitro* incubations with liver microsomes and S9 fractions, where the formation of α -ZEL and β -ZEL followed Michaelis-Menten behavior (Figure 2.3). V_{\max} , K_m and k_{cat} values derived from these data are presented in Table 2.3, together with the kinetic constants V_{\max} , K_m and k_{cat} obtained from literature for conversion of ZEN by liver microsomes and S9 from rats and pigs (Malekinejad *et al.*, 2006). Also these V_{\max} and k_{cat} values were scaled to the *in vivo* situation and the values thus obtained are also presented in Table 2.3. The catalytic efficiencies for liver metabolism of ZEN in humans and pigs showed a preference for the formation of α -ZEL over β -ZEL, while in rats β -ZEL was formed more efficiently than α -ZEL. Overall human liver catalyzed the conversion of ZEN to α -ZEL 7 and 75 times more efficiently (based on microsomes and S9 liver fractions, respectively) than liver from pigs. The lowest k_{cat} for the formation of α -ZEL were observed for rat microsomes and S9 fractions with 8 and 899 times lower k_{cat} values than obtained for human liver microsomes and S9 fractions, respectively. The highest k_{cat} for the formation of β -ZEL was observed for rat microsomes and human S9 fractions, pig liver samples showing the lowest preference for β -ZEL formation.

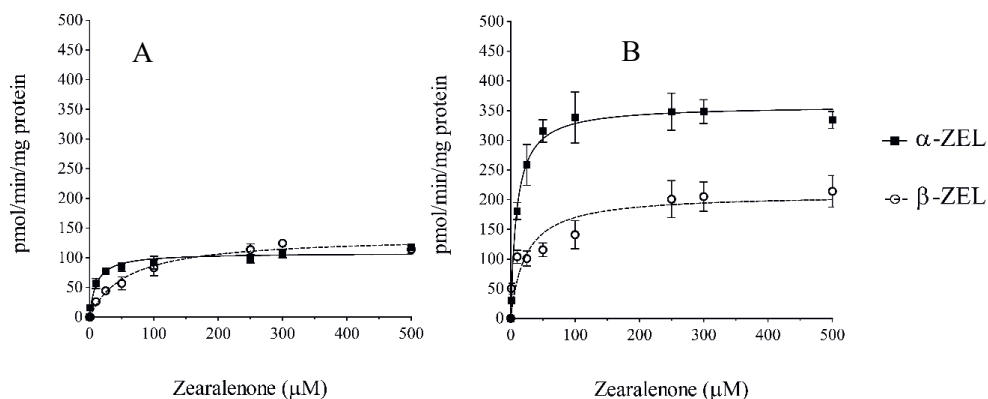


Figure 2.3. Substrate (i.e. ZEN) concentration-dependent formation of α -ZEL and β -ZEL in incubations with pooled human liver microsomes (A) and pooled human S9 fractions (B). Each data point represents the mean \pm SD of three independent experiments.

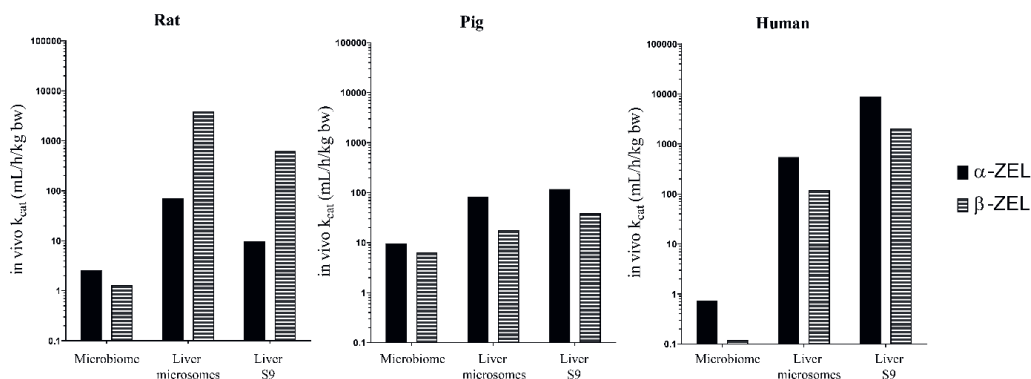


Figure 2.4. Calculated *in vivo* k_{cat} from microbial and hepatic (microsomes and S9 fractions) formation of α -ZEL and β -ZEL from ZEN in rats, pigs and humans

2.3.4 Comparison of intestinal microbial and hepatic metabolism of ZEN

The *in vivo* k_{cat} values derived for the metabolism of ZEN to α -ZEL and β -ZEL from the *in vitro* liver and fecal incubations allow the comparison of the activities of the liver and colonic microbiome, revealing marked species differences (Figure 2.4). When comparing these values, the *in vivo* V_{max} and k_{cat} appear to be higher for liver (microsomes and S9 fractions) than for the intestinal microbiota for all three species. While for pigs and rats the K_m for metabolism of ZEN by the intestinal microbiota was lower than the K_m for liver, for humans the K_m for the intestinal microbiota was higher than that for liver.

For the three species, the relative activity of the colonic microbiome compared to the liver for the formation of α -ZEL ranged from 0.1 (in human) to 8 - 12% (in pigs) to 4 - 27% (in rats), while for β -ZEL the values ranged from 0.1 (in human) to 0.1 - 0.2% (in rats) and 17 - 36% (in pigs) (Table 2.4). In pigs, the relative activity of the intestinal colonic microbiota was the highest for both α -ZEL and β -ZEL formation, followed by rats where the activity of the colonic microbiota to form α -ZEL was a quarter of the activity of liver S9. This comparison suggests that overall the k_{cat} of the liver is higher than of the microbiota for the reduction of ZEN.

Table 2.3. Kinetic parameter for the formation of α-ZEL and β-ZEL via *in vitro* rat, pig and human hepatic metabolism of ZEN

Microsomes		V_{max} , in vitro (pmol/min/mg of protein)	K_m (μM)	k_{cat} , in vitro (μl/min/mg protein)	Scaled V_{max} , in vivo (μmol/h/kg bw) ^a	k_{cat} , in vivo (ml/h/kg bw)	Ratio $k_{cat,\alpha ZEL}/k_{cat,\beta ZEL}$
Rat ^b	α-ZEL	80	89	0.9	6.2	70	0.02
	β-ZEL	495	10	49.5	38.4	3837	
Pig ^b	α-ZEL	796	566	1.4	45.8	81	4.70
	β-ZEL	512	1696	0.3	29.4	17	
Human ^c	α-ZEL	108	10	10.7	5.4	536	4.60
	β-ZEL	136.5	58	2.4	6.8	118	
S9 fractions							
Rat ^b	α-ZEL	32	592	0.05	5.7	10	0.016
	β-ZEL	72	21	3.40	12.8	609	
Pig ^b	α-ZEL	480	936	0.50	108.3	116	3.10
	β-ZEL	208	1243	0.17	47.0	38	
Human ^c	α-ZEL	358.7	9	38.7	80.02	8623	4.30
	β-ZEL	209.3	23	9.02	46.7	2014	

^a Calculated from $[(V_{max}, \text{ in vitro}) \times (\text{mg microsomes or S9/g liver}) \times (60 \text{ min/h})] / (10^6 \text{ μmol/pmol}) / \text{kg bw}$

^b Malekinejad et al. (2006)

^c this study

Table 2.4. Activity (%) of the intestinal colonic microbiome metabolism to the overall conversion of ZEN to α -ZEL and β -ZEL compared to the hepatic metabolism based on *in vivo* k_{cat} values. The liver microsomes or S9 fraction activity represent 100% of the activity.

	% activity of the microbiome vs liver microsomes		% activity of the microbiome vs liver S9 fractions	
	α -ZEL	β -ZEL	α -ZEL	β -ZEL
Rat	4	≤ 0.1	27	≤ 0.2
Pig	12	36	8	17
Human	≤ 0.1	≤ 0.1	≤ 0.1	≤ 0.1

2.4 Discussion

The aim of the present study was to develop an *in vitro* model system to predict and quantify intestinal microbial metabolism, and to apply this model system to study interspecies differences in the intestinal microbial metabolism of ZEN. The level of reduction of ZEN to α -ZEL has been linked to interspecies differences in sensitivity to the estrogenic effects of ZEN (Malekinejad *et al.*, 2006; Pfeiffer *et al.*, 2011) given that α -ZEL has a significantly higher estrogenic potency than ZEN. While kinetics are considered to play a major role in interspecies differences (EFSA, 2011), it should be noted that also other factors, such as differences in the estrogen receptors themselves (Harris, *et al.*, 2002, Matthews, *et al.*, 2000) and differences in estrogen receptor activation sites (O'Lone, *et al.*, 2004) can be involved in the interspecies differences in sensitivity to ZEN exposure. The results from the ER α -CALUX assay used in this study showed that α -ZEL was 55 times more estrogenic than ZEN, while β -ZEL was 25 times less estrogenic than ZEN, an observation in line with other studies comparing the relative potencies of ZEN, α -ZEL and β -ZEL for ER- α -mediated responses although the size of the relative differences varied with the study (Table 2.1). Prior studies have also reported that ZEN and its metabolites can bind to and activate ER- β , but it is not clear if there is a receptor subtype specific preference (Takemura *et al.*, 2007; Cozzini and Dellafiora, 2012). Despite the variation in the size of the differences, all studies corroborate that reduction of ZEN to α -ZEL is a bioactivation pathway, while the reduction to β -ZEL can be considered a detoxification (Metzler *et al.*, 2010).

In the *in vitro* model for intestinal microbial conversion of ZEN developed in this study, the intestinal microbiota were derived from fecal slurries prepared from fecal samples from rat, pigs and humans. Intestinal microbial metabolism has been studied

previously by the use of synthetic communities or isolated microbial strains (Lagier *et al.*, 2016), but one of the main advantages of using fecal samples for metabolic studies is that they allow for studying interspecies differences, as well as interindividual differences. Another advantage of the use of fecal samples is that these can be sampled non-invasively, as opposed to collection of microbial communities from other parts of the intestinal tract, usually involving individuals with compromised health status (Ahmed *et al.*, 2007; Leimena *et al.*, 2013; Zoetendal *et al.*, 2002). When using fecal samples to characterize intestinal microbial metabolism, it is of importance to note that there are differences in bacterial numbers and compositions along the intestinal tract, which might lead to regiospecific differences. However, the colon, harboring 70% of the total bacteria present in the gut, is the main site for bacterial fermentation (Hillman *et al.*, 2017). The bacterial communities in colon and feces have been reported to be highly comparable (Behr *et al.*, 2018; Hold *et al.*, 2002; Yang *et al.*, 2019). Furthermore, proofs of principle that show that anaerobic *in vitro* incubations using fecal communities can be used to predict intestinal microbial metabolic activities have been reported (Wang *et al.*, 2020), supporting the use of anaerobic fecal samples as a representative population of intestinal microbes. Therefore, the use of anaerobic fecal samples for the study of intestinal microbial metabolism represents a first tier approach to estimate its contribution to the total metabolism in the host. An additional advantage of using fecal samples as inoculum is the high yield of material obtained, which, together with the short incubation times and volumes, allows for a high-throughput application required in *in vitro* testing (Bisanz *et al.*, 2018). The effect of freezing, storing and thawing on the metabolic activity of the fecal samples for conversion of ZEN was tested and shown not to affect the metabolism (data not shown).

In the present study, the microbiota obtained from fecal samples enabled characterization and also quantification of the kinetic interspecies differences in the metabolism of ZEN. Fecal samples have previously been used successfully in anaerobic incubations with pharmaceuticals and foodborne chemicals to assess their susceptibility to microbial metabolism (Atkinson *et al.*, 2004; Dall'Asta *et al.*, 2012; Gaya *et al.*, 2016; Rowland *et al.*, 2018). These studies, however, assessed the presence or absence of metabolism in only a qualitative or semi-quantitative manner, which does not allow for the definition of *in vitro* kinetic constants of intestinal microbial metabolism. Optimizing the incubation conditions as done in the present study for linearity in time and with the amount of fecal slurry, allows definition of kinetic constants. Definition of these kinetic constants would be an essential requirement for integration of intestinal microbial metabolism in so-called

physiologically-based kinetic (PBK) models used in *in vitro-in silico* based testing strategies developed to replace *in vivo* testing (Louisse *et al.*, 2017; National Research Council, 2007). To our knowledge, the results of the present study provide the first proof-of-principle to use *in vitro* fecal incubations to quantify kinetic constants for intestinal microbial metabolism, and to use these *in vitro* k_{cat} values obtained for conversion to *in vivo* k_{cat} for interspecies comparisons.

In the current study, it was shown that ZEN was reduced to both α -ZEL and β -ZEL (Figure 2.1) under anaerobic conditions, which corroborates qualitative results from previous studies reporting incubations of ZEN with human fecal material (Gratz *et al.*, 2017). α -ZEL and β -ZEL appeared to be the major metabolites in the incubations (Figure 2.1), which indicates that the results from the *in vitro* fecal incubations are in line with the *in vivo* observation that α -ZEL and β -ZEL are the major metabolites of ZEN observed in different species such as rats, pigs, chickens and humans (Ali and Degen, 2018; Binder *et al.*, 2017; Buranatragool *et al.*, 2015; Dänicke *et al.*, 2005; Fleck *et al.*, 2017; Sun *et al.*, 2019). Conversion of ZEN to α -ZEL and β -ZEL represents a chemical reduction and is in line with the notion of Spanogiannopoulos *et al.* (2016) who suggested that anaerobic respiration of the intestinal microbiota could be facilitated by the use of the broad range of xenobiotics available as terminal electron acceptors, as in anaerobic environments no oxygen is available to fulfill this function.

Our results show species differences in the *in vitro* formation of α -ZEL and β -ZEL by the intestinal microbiota under anaerobic conditions, supporting the idea that the differences in the intestinal microbial composition may affect the metabolic activity (Conlon and Bird, 2014; Sousa *et al.*, 2008). Comparison of the estimated *in vivo* k_{cat} (Table 2.2) of the different species showed that the microbiome of pigs was overall most efficient in metabolizing ZEN, followed by that of rats and humans. Although the relatively high sensitivity of pigs to adverse effects of ZEN has been linked to the higher formation of α -ZEL in the liver (Malekinejad *et al.*, 2006; EFSA, 2011), the results from microbial metabolism now obtained indicate that metabolism by the gut microbiota may contribute to this interspecies difference in sensitivity where the highest α -ZEL formation was observed in pigs (Table 2.4). Additionally, the preference for the detoxification of ZEN together with the lower intestinal microbial metabolism observed for rats compared to pigs is in line with the lower sensitivity to ZEN reported for this species (EFSA, 2011).

The *in vivo* k_{cat} for the formation of α -ZEL by the human intestinal microbiota is lower than that for pigs and rats, but so is the detoxification to β -ZEL. The human intestinal microbiota strongly favors the formation of α -ZEL over β -ZEL, with ratios

of formation for α -ZEL: β -ZEL around 6:1 in humans, an observation in line with what was observed for the hepatic metabolism ratio for α -ZEL: β -ZEL of 4:1. In addition to having a high preference for the formation of α -ZEL, as shown also by Bravin *et al.* (2009), and in contrast to what was observed for the intestinal microbial metabolism, expressed per kg bw human hepatic metabolism appeared to show the highest *in vivo* k_{cat} of the three species. The establishment of safe dose levels of exposure to ZEN for humans has been based on pigs as model species due to similarities in physiological and anatomical characteristics, as well as their efficient formation of α -ZEL (EFSA, 2011; Uchiyama *et al.*, 2019), however, the higher preference for the bioactivation of ZEN shown in the present study together with the low preference for detoxification to β -ZEL, 4-6 times lower than α -ZEL formation, indicate a need for human-specific models to study metabolism and sensitivity to ZEN exposure. There is an urgent need for more human-relevant models in toxicology, as has also been demonstrated by the other researchers highlighting the differences in kinetics as an important contributor to species differences (Islam *et al.*, 2018). A better understanding of human ADME can further aid the development of human biomonitoring strategies to assess exposure to mycotoxins. This is particularly useful for mycotoxins such as ZEN, for which the occurrence of conjugated forms have been reported, but are difficult to quantify due to the lack of commercially available analytical standards (Lorenz *et al.*, 2019).

The comparison of the relative catalytic efficiency of microbial and the hepatic metabolism of ZEN showed that humans compared to pigs and rats, have the lowest microbial activity with less than 0.1% of α -ZEL and β -ZEL formed by the microbiota. Although the use of fecal samples as a source of gut microbiota may represent a first tier approach to estimate and quantify intestinal microbial activity it likely adequately reflects the relative interspecies differences in the intestinal microbial metabolism of ZEN.

Overall, the developed *in vitro* model was able to capture interspecies differences in the formation α -ZEL and β -ZEL by intestinal microbiota, which can also be applied to study interindividual differences in the conversion of other chemicals known to be converted by the intestinal microbiota. The model system enables quantification of kinetic data that can be used to integrate intestinal microbial metabolism in so-called PBK models for quantitative *in vitro* to *in vivo* extrapolations (QIVIVE).

It is concluded that the intestinal colonic microbial activity may be up to 36% of the activity of the liver and that it can additionally contribute to the species differences in bioactivation and detoxification and thus the toxicity of ZEN in pigs and rats but

not in humans. The results highlight the importance of the development of human specific models for the assessment of the metabolism of ZEN.

Acknowledgements

This research was financially supported by the National Council of Science and Technology (CONACYT) through a scholarship awarded to Diana M. Mendez Catala (CVU 619449) for conducting her PhD in The Netherlands.

Conflict of interest

The authors state no conflict of interests.

2.5 References

- Ahmed, S., Macfarlane, G.T., Fite, A., McBain, A.J., Gilbert, P., Macfarlane, S. Mucosa-associated bacterial diversity in relation to human terminal ileum and colonic biopsy samples. *Appl. Environ. Microbiol.*, 73 (2007), 7435-7442. doi: 10.1128/aem.01143-07
- Ali, N., Degen, G.H. Urinary biomarkers of exposure to the mycoestrogen zearalenone and its modified forms in German adults. *Arch. Toxicol.*, 92 (2018), 2691-2700. doi: 10.1007/s00204-018-2261-5
- Atkinson, C., Berman, S., Humbert, O., Lampe, J.W. In Vitro Incubation of Human Feces with Daidzein and Antibiotics Suggests Interindividual Differences in the Bacteria Responsible for Equol Production. *Nutr. J.*, 134 (2004), 596-599. doi: 10.1093/jn/134.3.596
- Barter, Z.E., Bayliss, M.K., Beaune, P.H., Boobis, A.R., Carlile, D.J., et al. Scaling factors for the extrapolation of in vivo metabolic drug clearance from in vitro data: reaching a consensus on values of human microsomal protein and hepatocellularity per gram of liver. *Curr. Drug Metab.*, 8 (2007), 33-45. doi: 10.2174/138920007779315053
- Behr, C., Ramirez-Hincapie, S., Cameron, H.J., Strauss, V., Walk, T., Herold, M., Beekmann, K., Rietjens, I., van Ravenzwaay, B. Impact of lincosamides antibiotics on the composition of the rat gut microbiota and the metabolite profile of plasma and feces. *Toxicol. Lett.*, 296 (2018), 139-151. doi: 10.1016/j.toxlet.2018.08.002
- Berg, N., De Wever, B., Fuchs, H.W., Gaca, M., Krul, C., Roggen, E.L. Toxicology in the 21st century – Working our way towards a visionary reality. *Toxicol. In Vitro*, 25 (2011), 874-881. doi: 10.1016/j.tiv.2011.02.008
- Binder, S.B., Schwartz-Zimmermann, H.E., Varga, E., Bichl, G., Michlmayr, H., Adam, G., Berthiller, F. Metabolism of Zearalenone and Its Major Modified Forms in Pigs. *Toxins*, 9 (2017), 56. doi: 10.3390/toxins9020056
- Bisanz, J.E., Spanogiannopoulos, P., Pieper, L.M., Bustion, A.E., Turnbaugh, P.J. How to Determine the Role of the Microbiome in Drug Disposition. *Drug Metab. Dispos.*, 46 (2018), 1588-1595. doi: 10.1124/dmd.118.083402
- Bravin, F., Duca, R.C., Balaguer, P., Delaforge, M. In vitro cytochrome p450 formation of a mono-hydroxylated metabolite of zearalenone exhibiting estrogenic activities: possible occurrence of this metabolite in vivo. *Int. J. Mol. Sci.*, 10 (2009), 1824-1837. doi: 10.3390/ijms10041824
- Brown, R.P., Delp, M.D., Lindstedt, S.L., Rhomberg, L.R., Beliles, R.P. Physiological parameter values for physiologically based pharmacokinetic

- models. *Toxicol. Ind. Health*, 13 (1997), 407-484. doi: 10.1177/074823379701300401
- Buranatragool, K., Poapolathep, S., Isariyodom, S., Imsilp, K., Klangkaew, N., Poapolathep, A. Dispositions and tissue residue of zearalenone and its metabolites α -zearalenol and β -zearalenol in broilers. *Toxicol. Rep.*, 2 (2015), 351-356. doi: 10.1016/j.toxrep.2014.12.011
- Cavigelli, S.A., Monfort, S.L., Whitney, T.K., Mechref, Y.S., Novotny, M., McClintock, M.K. Frequent serial fecal corticoid measures from rats reflect circadian and ovarian corticosterone rhythms. *J. Endocrinol.*, 184 (2005), 153-163. doi: 10.1677/joe.1.05935
- Chiu, W.A., Ginsberg, G.L. Development and evaluation of a harmonized physiologically based pharmacokinetic (PBPK) model for perchloroethylene toxicokinetics in mice, rats, and humans. *Toxicol. Appl. Pharmacol.*, 253 (2011), 203-234. doi: 10.1016/j.taap.2011.03.020
- Conlon, M.A., Bird, A.R. The impact of diet and lifestyle on gut microbiota and human health. *Nutrients*, 7 (2014), 17-44. doi: 10.3390/nu7010017
- Cozzini, P., Dellaflora, L. In silico approach to evaluate molecular interaction between mycotoxins and the estrogen receptors ligand binding domain: a case study on zearalenone and its metabolites. *Toxicol. Lett.*, 214 (2012), 81-85. doi: 10.1016/j.toxlet.2012.07.023
- Dall'Asta, M., Calani, L., Tedeschi, M., Jechiu, L., Brighenti, F., Del Rio, D. Identification of microbial metabolites derived from in vitro fecal fermentation of different polyphenolic food sources. *Nutrition*, 28 (2012), 197-203. doi: 10.1016/j.nut.2011.06.005
- Dänicke, S., Swiech, E., Buraczewska, L., Ueberschär, K.H. Kinetics and metabolism of zearalenone in young female pigs. *J. Anim. Physiol. Anim. Nutr.*, 89 (2005), 268-276. doi: 10.1111/j.1439-0396.2005.00516.x
- EFSA. Scientific Opinion on the risks for public health related to the presence of zearalenone in food. *EFSA J.*, 9 (2011), 2197. doi: 10.2903/j.efsa.2011.2197
- EFSA. Appropriateness to set a group health-based guidance value for zearalenone and its modified forms. *EFSA J.*, 14 (2016), e04425. doi: 10.2903/j.efsa.2016.4425
- Ehrlich, V.A., Dellaflora, L., Mollergues, J., Dall'Asta, C., Serrant, P., Marin-Kuan, M., Lo Piparo, E., Schilter, B., Cozzini, P. Hazard assessment through hybrid in vitro / in silico approach: The case of zearalenone. *Altex*, 32 (2015), 275-286. doi: 10.14573/altex.1412232

- Fleck, S.C., Churchwell, M.I., Doerge, D.R. Metabolism and pharmacokinetics of zearalenone following oral and intravenous administration in juvenile female pigs. *Food Chem. Toxicol.*, 106 (2017), 193-201. doi: 10.1016/j.fct.2017.05.048
- Frizzell, C., Ndossi, D., Verhaegen, S., Dahl, E., Eriksen, G., et al. Endocrine disrupting effects of zearalenone, alpha- and beta-zearalenol at the level of nuclear receptor binding and steroidogenesis. *Toxicol. Lett.*, 206 (2011), 210-217. doi: 10.1016/j.toxlet.2011.07.015
- Gaya, P., Medina, M., Sanchez-Jimenez, A., Landete, J.M. Phytoestrogen Metabolism by Adult Human Gut Microbiota. *Molecules* (Basel, Switzerland), 21 (2016), E1034. doi: 10.3390/molecules21081034
- Gratz, S.W., Dinesh, R., Yoshinari, T., Holtrop, G., Richardson, A.J., Duncan, G., MacDonald, S., Lloyd, A., Tarbin, J. Masked trichothecene and zearalenone mycotoxins withstand digestion and absorption in the upper GI tract but are efficiently hydrolyzed by human gut microbiota *in vitro*. *Mol. Nutr. Food Res.*, 61 (2017), E1600680. doi: 10.1002/mnfr.201600680
- Harris, H.A., Bapat, A.R., Gonder, D.S., Frail, D.E. The ligand binding profiles of estrogen receptors alpha and beta are species dependent. *Steroids*, 67 (2002), 379-384. doi: 10.1016/s0039-128x(01)00194-5
- Hillman, E.T., Lu, H., Yao, T., Nakatsu, C.H. Microbial Ecology along the Gastrointestinal Tract. *Microbes Environ.*, 32 (2017), 300-313. doi: 10.1264/jsme2.ME17017
- Hold, G.L., Pryde, S.E., Russell, V.J., Furrie, E., Flint, H.J. Assessment of microbial diversity in human colonic samples by 16S rDNA sequence analysis. *FEMS Microbiol. Ecol.*, 39 (2002), 33-39. doi: 10.1111/j.1574-6941.2002.tb00904.x
- Hörmannspurger, G., Schaubeck, M., Haller, D. Intestinal Microbiota in Animal Models of Inflammatory Diseases. *ILAR J.*, 56 (2015), 179-191. doi: 10.1093/ilar/ilv019
- Islam, M.A., Hooiveld, G.J.E.J., van den Berg, J.H.J., van der Velpen, V., Murk, A.J., Rietjens, I.M.C.M., van Leeuwen, F.X.R. Soy supplementation: Impact on gene expression in different tissues of ovariectomized rats and evaluation of the rat model to predict (post) menopausal health effect. *Toxicol. Rep.*, 5 (2018), 1087-1097. doi: 10.1016/j.toxrep.2018.10.012
- Kararli, T.T. Comparison of the gastrointestinal anatomy, physiology, and biochemistry of humans and commonly used laboratory animals. *Biopharm. Drug Dispos.*, 16 (1995), 351-380. doi: 10.1002/bdd.2510160502

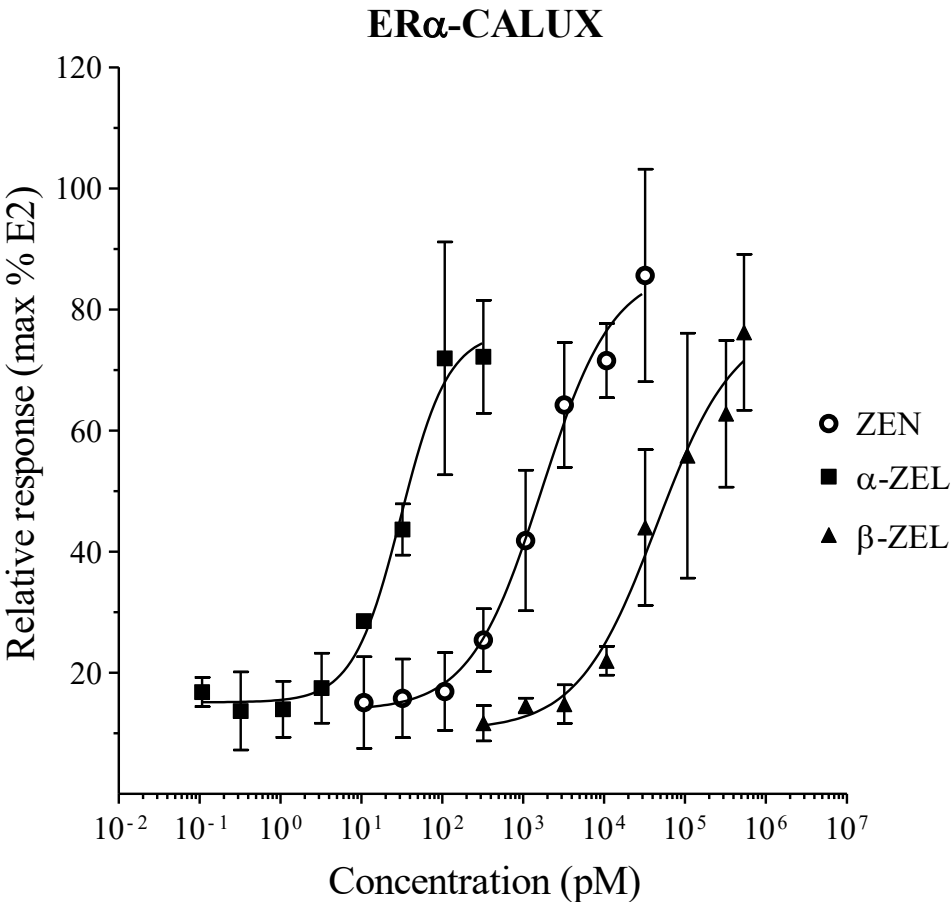
- Koppel, N., Maini Rekdal, V., Balskus, E.P. Chemical transformation of xenobiotics by the human gut microbiota. *Science*, 356 (2017), eaag2770. doi: 10.1126/science.aag2770
- Krych, L., Hansen, C.H.F., Hansen, A.K., van den Berg, F.W.J., Nielsen, D.S. Quantitatively Different, yet Qualitatively Alike: A Meta-Analysis of the Mouse Core Gut Microbiome with a View towards the Human Gut Microbiome. *PLoS One*, 8 (2013), e62578. doi: 10.1371/journal.pone.0062578
- Lagier, J.-C., Khelaifia, S., Alou, M.T., Ndongo, S., Dione, N., et al. Culture of previously uncultured members of the human gut microbiota by culturomics. *Nat. Microbiol.*, 1 (2016), 16203. doi: 10.1038/nmicrobiol.2016.203
- Le Guevel, R., Pakdel, F. Assessment of oestrogenic potency of chemicals used as growth promoter by in-vitro methods. *Hum. Reprod.*, 16 (2001), 1030-1036. doi: 10.1093/humrep/16.5.1030
- Leimena, M.M., Ramiro-Garcia, J., Davids, M., van den Bogert, B., Smidt, H., et al. A comprehensive metatranscriptome analysis pipeline and its validation using human small intestine microbiota datasets. *BMC genomics*, 14 (2013), 530. doi: 10.1186/1471-2164-14-530
- Ley, R.E., Hamady, M., Lozupone, C., Turnbaugh, P., Ramey, R.R., et al. Evolution of mammals and their gut microbes. *Science*, 320 (2008), 1647-1651. doi: 10.1126/science.1155725
- Lignet, F., Sherbetjian, E., Kratochwil, N., Jones, R., Suenderhauf, C., Otteneder, M.B., Singer, T., Parrott, N. Characterization of Pharmacokinetics in the Göttingen Minipig with Reference Human Drugs: An In Vitro and In Vivo Approach. *Pharm. Res.*, 33 (2016), 2565-2579. doi: 10.1007/s11095-016-1982-5
- Lorenz, N., Dänicke, S., Edler, L., Gottschalk, C., Lassek, E., Marko, D., Rychlik, M., Mally, A. A critical evaluation of health risk assessment of modified mycotoxins with a special focus on zearalenone. *Mycotoxin Res.*, 35 (2019), 27-46. doi: 10.1007/s12550-018-0328-z
- Louisse, J., Beekmann, K., Rietjens, I.M. Use of Physiologically Based Kinetic Modeling-Based Reverse Dosimetry to Predict in Vivo Toxicity from in Vitro Data. *Chem. Res. Toxicol.*, 30 (2017), 114-125. doi: 10.1021/acs.chemrestox.6b00302
- Malekinejad, H., Maas-Bakker, R., Fink-Gremmels, J. Species differences in the hepatic biotransformation of zearalenone. *Veterinary journal*, 172 (2006), 96-102. doi: 10.1016/j.tvjl.2005.03.004

- Malekinejad, H., Maas-Bakker, R.F., Fink-Gremmels, J. Bioactivation of zearalenone by porcine hepatic biotransformation. *Vet. Res.*, 36 (2005), 799-810. doi: 10.1051/vetres:2005034
- Mariscal-Landin, G., 2007. Tratamiento excretas cerdos. Capítulo 7, Reporte de la Iniciativa de la Ganadería, el Medio Ambiente y el Desarrollo (LEAD)-Integración por Zonas de la Ganadería y de la Agricultura Especializadas (AWI)-Opciones para el Manejo de Efluentes de Granjas Porcícolas de la Zona Centro de México. FAO, pp.
- Matthews, J., Celius, T., Halgren, R., Zacharewski, T. Differential estrogen receptor binding of estrogenic substances: a species comparison. *J. Steroid Biochem. Mol. Biol.*, 74 (2000), 223-234. doi: 10.1016/s0960-0760(00)00126-6
- Metzler, M., Pfeiffer, E., Hildebrand, A. Zearalenone and its metabolites as endocrine disrupting chemicals. *World Mycotoxin J.*, 3 (2010), 385-401. doi: 10.3920/WMJ2010.1244
- Millecam, J., De Clerck, L., Govaert, E., Devreese, M., Gasthuys, E., et al. The Ontogeny of Cytochrome P450 Enzyme Activity and Protein Abundance in Conventional Pigs in Support of Preclinical Pediatric Drug Research. *Front. Pharmacol.*, 9 (2018), 470. doi: 10.3389/fphar.2018.00470
- Minervini, F., Giannoccaro, A., Cavallini, A., Visconti, A. Investigations on cellular proliferation induced by zearalenone and its derivatives in relation to the estrogenic parameters. *Toxicol. Lett.*, 159 (2005), 272-283. doi: 10.1016/j.toxlet.2005.05.017
- Molina-Molina, J.-M., Real, M., Jimenez-Diaz, I., Belhassen, H., Hedhili, A., Torné, P., Fernández, M.F., Olea, N. Assessment of estrogenic and anti-androgenic activities of the mycotoxin zearalenone and its metabolites using in vitro receptor-specific bioassays. *Food Chem. Toxicol.*, 74 (2014), 233-239. doi: 10.1016/j.fct.2014.10.008
- Mukherjee, D., Royce, S.G., Alexander, J.A., Buckley, B., Isukapalli, S.S., Bandera, E.V., Zarbl, H., Georgopoulos, P.G. Physiologically-based toxicokinetic modeling of zearalenone and its metabolites: application to the Jersey girl study. *PLoS One*, 9 (2014), e113632. doi: 10.1371/journal.pone.0113632
- National Research Council, 2007. Toxicity Testing in the 21st Century: A Vision and a Strategy. The National Academies Press, Washington, DC, pp. 216.
- Nguyen, T.L.A., Vieira-Silva, S., Liston, A., Raes, J. How informative is the mouse for human gut microbiota research? *Dis. Model Mech.*, 8 (2015), 1-16. doi: 10.1242/dmm.017400

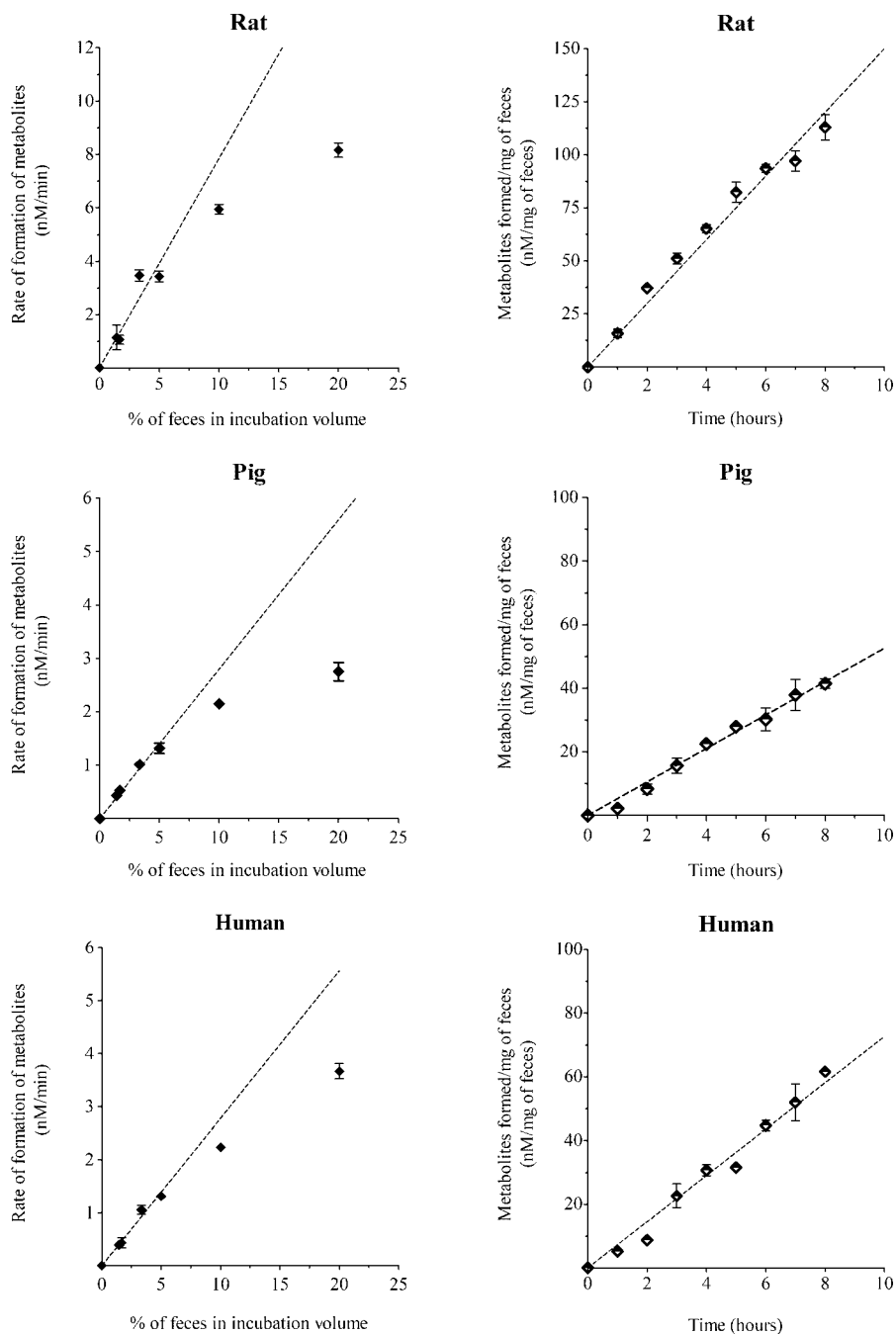
- Nicholson, J.K., Holmes, E., Kinross, J., Burcelin, R., Gibson, G., Jia, W., Pettersson, S. Host-Gut Microbiota Metabolic Interactions. *Science*, 336 (2012), 1262-1267. doi: 10.1126/science.1223813
- O'Lone, R., Frith, M.C., Karlsson, E.K., Hansen, U. Genomic targets of nuclear estrogen receptors. *Mol. Endocrinol.*, 18 (2004), 1859-1875. doi: 10.1210/me.2003-0044
- Pfeiffer, E., Kommer, A., Dempe, J.S., Hildebrand, A.A., Metzler, M. Absorption and metabolism of the mycotoxin zearalenone and the growth promotor zeranol in Caco-2 cells in vitro. *Mol. Nutr. Food Res.*, 55 (2011), 560-567. doi: 10.1002/mnfr.201000381
- Punt, A., Paini, A., Boersma, M.G., Freidig, A.P., Delatour, T., Scholz, G., Schilter, B., van Bladeren, P.J., Rietjens, I.M.C.M. Use of physiologically based biokinetic (PBBK) modeling to study estragole bioactivation and detoxification in humans as compared with male rats. *Toxicol. Sci.*, 110 (2009), 255-269. doi: 10.1093/toxsci/kfp102
- Rose, C., Parker, A., Jefferson, B., Cartmell, E. The Characterization of Feces and Urine: A Review of the Literature to Inform Advanced Treatment Technology. *Crit. Rev. Environ. Sci. Technol.*, 45 (2015), 1827-1879. doi: 10.1080/10643389.2014.1000761
- Rowland, I., Gibson, G., Heinken, A., Scott, K., Swann, J., Thiele, I., Tuohy, K. Gut microbiota functions: metabolism of nutrients and other food components. *Eur. J. Nutr.*, 57 (2018), 1-24. doi: 10.1007/s00394-017-1445-8
- Sonneveld, E., Jansen, H.J., Riteco, J.A.C., Brouwer, A., van der Burg, B. Development of Androgen- and Estrogen-Responsive Bioassays, Members of a Panel of Human Cell Line-Based Highly Selective Steroid-Responsive Bioassays. *Toxicol. Sci.*, 83 (2004), 136-148. doi: 10.1093/toxsci/kfi005
- Sousa, T., Paterson, R., Moore, V., Carlsson, A., Abrahamsson, B., Basit, A.W. The gastrointestinal microbiota as a site for the biotransformation of drugs. *Int. J. Pharm.*, 363 (2008), 1-25. doi: 10.1016/j.ijpharm.2008.07.009
- Spanogiannopoulos, P., Bess, E.N., Carmody, R.N., Turnbaugh, P.J. The microbial pharmacists within us: a metagenomic view of xenobiotic metabolism. *Nat. Rev. Microbiol.*, 14 (2016), 273-287. doi: 10.1038/nrmicro.2016.17
- Sun, F., Tan, H., Li, Y., De Boevre, M., De Saeger, S., et al. Metabolic Profile, Bioavailability and Toxicokinetics of Zearalenone-14-Glucoside in Rats after Oral and Intravenous Administration by Liquid Chromatography High-Resolution Mass Spectrometry and Tandem Mass Spectrometry. *Int. J. Mol. Sci.*, 20 (2019), 5473. doi: 10.3390/ijms20215473

- Takemura, H., Shim, J.Y., Sayama, K., Tsubura, A., Zhu, B.T., Shimoi, K. Characterization of the estrogenic activities of zearalenone and zeranol in vivo and in vitro. *J. Steroid Biochem. Mol. Biol.*, 103 (2007), 170-177. doi: 10.1016/j.jsbmb.2006.08.008
- Uchiyama, Y., Takino, M., Noguchi, M., Shiratori, N., Kobayashi, N., Sugita-Konishi, Y. The In Vivo and In Vitro Toxicokinetics of Citreoviridin Extracted from *Penicillium citreonigrum*. *Toxins*, 11 (2019), 360. doi: 10.3390/toxins11060360
- Upton, R.N. Organ weights and blood flows of sheep and pig for physiological pharmacokinetic modelling. *J. Pharmacol. Toxicol. Methods*, 58 (2008), 198-205. doi: 10.1016/j.vascn.2008.08.001
- Wang, Q., Spenkelink, B., Boonpawa, R., Rietjens, I., Beekmann, K. Use of Physiologically Based Kinetic Modeling to Predict Rat Gut Microbial Metabolism of the Isoflavone Daidzein to S-Equol and Its Consequences for ER α Activation. *Mol. Nutr. Food Res.*, 64 (2020), e1900912. doi: 10.1002/mnfr.201900912
- Yang, N., Yan, W., Sun, C., Zheng, J., Wen, C., Ji, C., Zhang, D., Chen, Y., Hou, Z. Efficacy of fecal sampling as a gut proxy in the study of chicken gut microbiota. *Front. Microbiol.*, 10 (2019), 2126. doi: 10.3389/fmicb.2019.02126
- Zoetendal, E.G., von Wright, A., Vilpponen-Salmela, T., Ben-Amor, K., Akkermans, A.D., de Vos, W.M. Mucosa-associated bacteria in the human gastrointestinal tract are uniformly distributed along the colon and differ from the community recovered from feces. *Appl. Environ. Microbiol.*, 68 (2002), 3401-3407. doi: 10.1128/AEM.68.7.3401-3407.2002

Supplementary Material



Supplementary Figure 2.1. Concentration-response curves in U2OS-ER α CALUX assay determined from the measured luciferase activity. The results are presented as mean \pm -SD from two independent experiments of the induction of luciferase activity relative to the positive control (100pM E2)



Supplementary Figure 2.2. Linearity of the metabolite formation from the microbial metabolism of ZEN in rats, pigs and humans as part of the optimization process.

Chapter 3

PBK model-based prediction of intestinal microbial and host metabolism of zearalenone and consequences for its estrogenicity

*Diana M. Mendez-Catala, Qianrui Wang
& Ivonne M.C.M. Rietjens*

Submitted

Abstract

Zearalenone (ZEN) is a nonsteroidal mycotoxin found mainly in cereals. The toxicity of ZEN is linked to reproductive disorders caused by the ability of ZEN and its metabolites to bind to estrogen receptors. Metabolism of ZEN may occur not only in host tissue but may also be catalysed by the intestinal microbiome. The aim of the present study was to develop PBK models for rats and humans that include intestinal microbial and hepatic metabolism of ZEN in order to obtain insight in the contribution of metabolism by the microbiota to the overall metabolism of ZEN. The models include a sub-model for the metabolite, α -zearalenol (α -ZEL), a metabolite known to be 60-times more potent as an estrogen than ZEN. Integrating intestinal microbial ZEN metabolism into the PBK models revealed that hepatic metabolism drives the formation of α -ZEL. Furthermore, the models predicted that at the TDI of 0.25 $\mu\text{g/kg bw}$ the internal concentration of ZEN and α -ZEL are 3 orders of magnitude below concentrations reported to induce estrogenicity in *in vitro* bioassays. It is concluded that combining kinetic data on liver and intestinal microbial metabolism in a PBK model facilitates a holistic view on the role of the intestinal microbiota in the overall metabolism of ZEN and its bioactivation to α -ZEL.

3.1 Introduction

Zearalenone (ZEN) is a nonsteroidal mycotoxin that is formed by *Fusarium* spp., primarily *F. graminearum*. The fungus is known to infect mainly crops of wheat and maize, and while in the field usually the concentrations of ZEN are still low, they show a tendency to increase under storage conditions with high moisture content (Gupta *et al.*, 2018). In the European Union (EU), the presence of ZEN in food commodities is regulated with maximum permitted levels ranging from 20 to 400 µg/kg for cereals and cereal products (Borzekowski *et al.*, 2018; EFSA, 2011).

The adverse health effects of ZEN have been related to its estrogenicity, originating from its structural similarity to the natural hormone 17β-estradiol (E2) and proceed through binding of ZEN to the estrogen receptors (ERs) (Metzler *et al.*, 2010). Also, ZEN metabolites may play a role in this estrogenicity. ZEN is known to undergo reduction to form the metabolites α-zearalenol (α-ZEL) and β-zearalenol (β-ZEL) (Fitzpatrick *et al.*, 1988), with α-ZEL showing a relative potency that is about 60-fold higher than that of ZEN reflecting bioactivation, while the formation of β-ZEL decreases the potency 5 times representing a detoxification (EFSA, 2016). ZEN as well as α-ZEL and β-ZEL can be further metabolized to glucuronide conjugates, before they are eliminated through urine and/or feces (Fitzpatrick *et al.*, 1988; Mirocha *et al.*, 1981; Warth *et al.*, 2013). ZEN and its metabolites are conjugated at a lower extent to sulfate conjugates as observed *in vitro* (Pfeiffer *et al.*, 2010), but this not confirmed *in vivo* (Warth *et al.*, 2013). This metabolism of ZEN may occur in the liver and intestinal tissue, while anaerobic *in vitro* fecal incubations have shown the intestinal microbiota to also play a role in the conversion of ZEN to α- and β-ZEL (Gratz *et al.*, 2017; Mendez-Catala *et al.*, 2020). *In vitro* studies with liver S9 fractions (Malekinejad *et al.*, 2006) and fecal slurries (Mendez-Catala *et al.*, 2020) have shown interspecies differences in bioactivation and detoxification by both the liver and intestinal microbiota. Due to limited data available on the kinetics and toxicity of ZEN in humans, the risk assessment has been based on the observations in young gilts identified as the most sensitive species (Dänicke *et al.*, 2005; Döll *et al.*, 2003; EFSA, 2011). Based on a no observed effect level (NOEL) of 10.4 µg/kg bw for estrogenic effects of ZEN in young gilts (Döll *et al.*, 2003) a tolerable daily intake (TDI) of 0.25 µg/kg bw/day was defined taking an uncertainty factor of only 40 to account for interspecies differences and human variability (EFSA, 2011).

Given the limited data on the role of the intestinal microbiota in the *in vivo* bioactivation and detoxification of ZEN, the aim of the present study was to develop a physiologically-based kinetic (PBK) model in human that would enable an

integrated description of the metabolism of ZEN, and provide insight in the overall role of the intestinal microbiota in the bioactivation and detoxification of ZEN *in vivo*. This model requires description of a separate compartment in the PBK model for intestinal microbial metabolism describing the formation of α - and β -ZEL by the microbiota. To enable evaluation of the model also a PBK model for rats was developed to allow comparison of model predictions to *in vivo* kinetic data, which for this species are available in literature (Shin *et al.*, 2009). The PBK models obtained allowed evaluation of the role of metabolism of ZEN by the intestinal microbiota in the overall metabolism of ZEN and comparison of dose-dependent internal concentrations with *in vitro* concentrations for ZEN and α -ZEL able to induce estrogenicity.

3.2 Materials and methods

3.2.1 Materials

ZEN (CAS registry number 17924-92-4; $\geq 99.0\%$), α -ZEL (CAS registry number 36455-72-8; $>98\%$), β -ZEL (CAS registry number 71030-11-0; $>98\%$), were purchased from Sigma-Aldrich (Schnelldorf, Germany). Test chemicals were prepared in dimethyl sulfoxide (DMSO; CAS 67-68-5) purchased from Merck (Darmstadt, Germany). Pooled rat and human liver S9 fractions were purchased from Corning (Woburn, MA, USA) and pooled rat and human intestinal S9 fractions were purchased from Xenotech (Kansas City, USA). Uridine 5-diphosphoglucuronide trisodium salt (UDPGA; CAS registry number 63700-19-6) was obtained from Carbosynth (Berkshire, United Kingdom). Trizma® base (Tris, CAS registry number 77-86-1) and alamethicin (from *Trichoderma viride*; CAS 27061-78-5) were obtained from Sigma-Aldrich (Steinheim, Germany). Magnesium chloride hexahydrate ($\text{MgCl}_2 \cdot 6\text{H}_2\text{O}$; CAS registry number 7791-18-6) and formic acid (FA; CAS registry number 64-18-6) were obtained from VWR International (Amsterdam, The Netherlands). Phosphate-buffered saline (PBS, pH 7.4), was obtained from Gibco (Paisley, UK). UPLC/MS grade methanol (MeOH; CAS registry number 67-56-1) and acetonitrile (ACN; CAS registry number 75-05-8) were purchased from Biosolve (Valkenswaard, The Netherlands).

3.2.2 *In vitro* incubations with ZEN and α -ZEL to derive kinetic parameters for the PBK model

The kinetic parameters (V_{\max} and K_m) for the glucuronidation of ZEN and α -ZEL in liver tissue were obtained from *in vitro* incubations of ZEN and α -ZEL with rat and

human liver S9 fractions. The incubation mixtures (final volume 100 μ l) contained (final concentrations) 0.1 M Tris-HCl (pH 7.4), 5 mM $MgCl_2$, 0.025 mg/ml alamethicin, the substrate in concentrations ranging from 0.3-150 μ M (added from 100 times concentrated stock solutions in DMSO) and 0.2 mg/ml of pooled liver S9 fraction from rat or human. After 1-minute preincubation in a shaking water bath at 37°C, the reaction was started by the addition of 3 mM (final concentration) UDPGA. Control incubations were performed without the addition of UDPGA. The incubations were carried out for 7 minutes. Intestinal S9 incubations for the glucuronidation of ZEN were performed in a similar way with only a few modifications. Final incubation mixtures contained 0.01 mg/ml alamethicin and 0.04 mg/ml intestinal S9 fractions. The incubations were carried out for 20 minutes. Under all these conditions the conversion was linear with time and S9 protein concentration (data not shown). All reactions were terminated by the addition of 20% (v/v) ice-cold ACN followed by centrifugation at 15,000 \times g for 5 minutes and the supernatant was immediately analyzed by UPLC-PDA. The formation of glucuronides was confirmed by the incubation of non-terminated samples with β -glucuronidase.

3.2.3 UPLC-PDA analysis

A UPLC-PDA system (Waters Acquity) was used for the quantification of ZEN, α -ZEL and their glucuronides. The UPLC system was equipped with an Acquity BEH C18 column 1.7 μ m, 50 mm \times 2.1 mm (Waters) set at 40 °C and a UV diode array detection system recording wavelengths of 190-400 nm. Nanopure water (A) and ACN (B) were used as eluents at a flow rate of 0.3 ml/min with the following gradient profile: 0-40% B (0 – 1.3 min), 40-50% B (1.3 - 5.7 min), 50-100% B (5.7 - 6 min), 100 % B kept for 2 minutes and 100-0% B (8 - 8.1 min) for equilibration. Per run, 3.5 μ l of sample were injected. ZEN, α -ZEL and β -ZEL were identified using commercially available standards. Chromatograms were analyzed at 235 nm and glucuronides quantified using calibration curves of the respective commercially available non-conjugated analogues. The glucuronides were identified by their conversion to the corresponding non-conjugated analogues upon incubation with β -glucuronidase.

3.2.4 Kinetic analysis

To derive the kinetic constants for the formation of ZEN-glucuronide and α -ZEL-glucuronide, the amount of metabolite formed expressed per mg of protein and per unit of time (rate of formation) was calculated using Microsoft Excel (version 2016)

and plotted against the substrate concentration. The curve for the concentration dependent metabolite formation was fitted in GraphPad Prism 5.04 (GraphPad software, San Diego California, U.S.A.) using a standard Michaelis-Menten equation ($V=V_{\max}*[S]/(K_m+[S])$) to obtain the *in vitro* kinetic constants, V_{\max} in pmol/min/mg S9 protein and K_m in μM .

3.2.5 Development of PBK models for rat and human

A schematic representation of the PBK model of ZEN, including a sub-model for α -ZEL, for rat and human is presented in Figure 3.1. The model is based on a model previously reported and evaluated by Wang *et al.* (2020) for the isoflavone daidzein. The PBK model describes the kinetics upon intravenous (i.v.) injection or oral exposure. The i.v. administration was included to allow comparison of the model predictions to available *in vivo* kinetic data in rats (Shin *et al.*, 2009). The main model for the parent compound ZEN consisted of separate compartments for blood, fat, rapidly perfused tissue (heart, lung and brain), slowly perfused tissue (skin, muscle and bone), liver, intestine and stomach. The intestinal compartment consisted of three separate compartments including the small intestinal lumen, small intestinal tissue and the large intestinal lumen in order to enable description of both metabolism in small intestinal tissue and by the intestinal microbiota. The process of stomach emptying [half-life, rat: 15 min (Reilly *et al.*, 1990); human: 15 min (Sun *et al.*, 1988)] and the small intestinal transition [transition time in rat: 1.5 h; human: 4 h (Davies and Morris, 1993)] were included in the model. The compartment for the small intestinal lumen was divided in 7 sub-compartments enabling the description of the transition through the compartment (Louisse *et al.*, 2015; Li *et al.*, 2017; Zhang *et al.*, 2018; Gilbert-Sandoval *et al.*, 2020). The elimination of ZEN was modeled via its glucuronidation in intestinal and liver tissue assumed to be followed by efficient excretion.

In order to predict the blood concentrations of α -ZEL, a sub-model for α -ZEL was included. In this sub-model α -ZEL is formed in the liver from ZEN and also enters the liver upon its formation by the intestinal microbiota. Glucuronidation of α -ZEL formed by the microbiota was assumed to occur in the liver following its transport from the large intestinal lumen to the liver.

The parameters required for the PBK model of ZEN are (i) physiological parameters, (ii) physicochemical parameters and (iii) kinetic parameters for metabolism and excretion. The values for the physiological parameters (i.e. tissue volumes and blood flows) were taken from literature (Brown *et al.*, 1997) and are presented in Table 3.1. The physicochemical parameters (i.e. tissue/blood partition coefficients) are

presented in Table 3.2 and were estimated as previously described (DeJongh *et al.*, 1997) based on the octanol-water partition coefficients (Log P) of 3.32 and 3.16 for ZEN and α -ZEL, respectively, obtained from ChemDraw version 18 (Perkin Elmer & CambridgeSoft, USA).

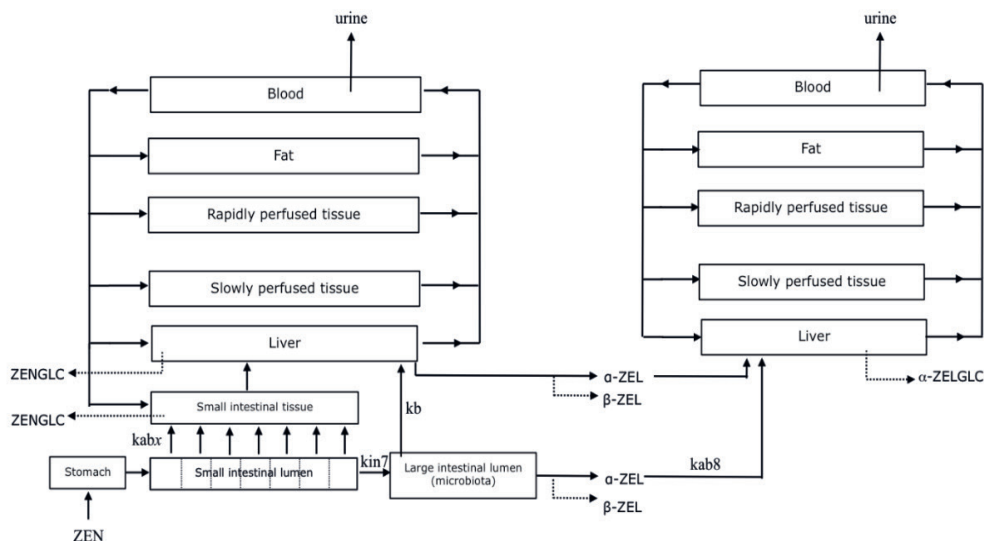


Figure 3.1. Schematic presentation of the main PBK model for ZEN including a sub-model for the bioactive metabolite α -ZEL

The apparent permeability coefficients (P_{app}) obtained from *in vitro* transport studies using Caco-2 cell layers were used to describe the intestinal absorption of ZEN and α -ZEL from the different sub-compartments in the model into the small intestinal tissue or from the large intestinal lumen directly to the liver. The $P_{app, \text{Caco-2}}$ value reported for ZEN was 10.3×10^{-6} (Pfeiffer *et al.*, 2011). The $P_{app, \text{Caco-2}}$ value for ZEN was one of the most influential factors for the prediction of ZEN in blood (see result section), therefore this values was also optimized by curve fitting to the *in vivo* data from Shin *et al.* (2009) using the curve fit option present in Berkeley Madonna, yielding a value of $10.4 \times 10^{-5} \text{ cm s}^{-1}$ ($P_{app, \text{Caco-2}}$ fitted). The latter value was used for predictions and evaluation. Subsequently, *in vivo* P_{app} values ($P_{app, \text{in vivo}}$) were estimated by the following correlation established by Sun *et al.* (2002): $\text{Log}(P_{app, \text{in vivo}}) = 0.6836 \times \text{Log}(P_{app, \text{Caco-2}} \text{ fitted}) - 0.5579$. It was assumed that the estimated $P_{app, \text{in vivo}}$ was the same for both rats and humans. The parameter values for the intestinal absorption rates were derived from the $P_{app, \text{in vivo}}$ by using the following equation (Verwei *et al.*, 2006; Louisse *et al.*, 2015; Li *et al.*, 2017; Zhang *et al.*, 2018; Gilbert-Sandoval *et al.*, 2020): Absorption rate ($\mu\text{mol h}^{-1}$) = apparent

permeability coefficient *in vivo* ($P_{app, in vivo}$; cm h^{-1}) \times surface area of the small intestine (cm^2) \times luminal concentration of the compound (mM). The surface areas of the rat small and large intestine were calculated to be 94 [based on radius of 0.18 cm and small intestinal length of 83 cm (Tsutsumi *et al.*, 2008)] and 157 cm^2 [based on radius of 1 cm and small intestinal length of 25 cm (Vdoviaková *et al.*, 2016)]. For human the surface areas for small and large intestine were calculated to be 72 [based on radius of 2.5 cm (Kararli, 1995) and small intestine length of 460 cm (Hosseinpour and Behdad, 2008)] and 47 dm^2 [based on radius of 5 cm and large intestine length of 150 cm (Vdoviaková *et al.*, 2016)]. The luminal concentration of ZEN in the small intestine was calculated by dividing the amount of ZEN in the tissue by the small intestinal volume. The calculated volumes for rat and human small intestine were 8.4 mL (Tsutsumi *et al.*, 2008) and 9 L (Kararli, 1995; Hosseinpour and Behdad, 2008), respectively, based on radius and small intestinal length. The transport of α -ZEL formed by intestinal microbiota was modeled to go directly from the large intestine to liver with the absorption calculated from $P_{app, caco-2}$ value of $5.4 \times 10^{-6} \text{ cm s}^{-1}$, this value was kept as reported in literature (Pfeiffer *et al.*, 2011), as no kinetic data for fitting is available for α -ZEL.

The kinetic constants (V_{\max} and K_m) for the conversion of ZEN to α -ZEL and β -ZEL by the intestinal microbiota were obtained from anaerobic incubations with fecal samples performed as previously described (Mendez-Catala *et al.*, 2020). The V_{\max} , expressed in pmol/min/g feces , was scaled to the whole body by means of the fecal fraction of body weight of 0.0164 [based on a defecation volume per day of 4.1 g (Hoskins and Zamcheck, 1968)] for rats and 0.0018 for humans [based on a defecation volume per day of 128 g (Rose *et al.*, 2015)]. The V_{\max} values for the formation of α -ZEL and β -ZEL and the subsequent glucuronidation of α -ZEL, obtained from incubations with rat liver S9 (Malekinejad *et al.*, 2006) or human liver S9 (Mendez-Catala *et al.*, 2020), were scaled to the whole tissue assuming an S9 protein concentration of 143 mg S9 protein/g liver for rats (Punt *et al.*, 2008) and 120.7 mg protein/g liver (sum of 40 mg microsomal protein and 80.7 mg of cytosolic protein) for human (Cubitt *et al.*, 2011). The intestinal V_{\max} for glucuronidation of ZEN was scaled to whole tissue using an S9 protein yield of 37.1 and 35.2 mg S9 protein/g intestinal tissue for rat and human, respectively (Peters *et al.*, 2016). The K_m values *in vivo* were assumed to be similar to those obtained *in vitro*.

Due to the absence of studies reporting dose related blood levels of ZEN in humans and because excretion through urine is presented as an adequate biomarker for ZEN biomonitoring (Lorenz *et al.*, 2019), the urinary excretion of ZEN and α -ZEL were modeled to occur from the blood with excretion rates of 0.096 and 0.015 h^{-1} ,

respectively, estimated before in Mukherjee *et al.* (2014). Additionally, the excretion of the ZEN glucuronide in humans was modeled taking under the assumption that with 90% of the glucuronides formed in the liver will be excreted through the urine (Teegarden *et al.*, 2005; Yang *et al.*, 2013).

The PBK model equations were coded and integrated in Berkeley Madonna 8.0.1 (UC Berkeley, CA, USA) using the Rosenbrock's algorithm for stiff systems. The model code for rat and human are presented in Supplementary material.

Table 3.1. Physiological parameters used in the rat and human PBK model for ZEN based on Brown *et al.* (1997)

	Symbol	Values	
		Rat	Human
Physiological parameters			
Body weight (kg)	BW	0.25	70
Tissue volumes (fraction of body weight)			
Small intestine	VS _{Ic}	0.014	0.009
Liver	VL _c	0.034	0.026
Rapidly perfused tissue	VR _c	0.034	0.041
Slowly perfused tissue	VSc	0.667	0.596
Fat	VFc	0.07	0.214
Blood	VB _c	0.074	0.074
Cardiac output (L/h)	Q _c	5.38	347.9
Blood flow to tissue (fraction cardiac output)			
Intestine	QS _{Ic}	0.151	0.181
Liver	QL _c	0.099	0.046
Rapidly perfused tissue	QR _c	0.51	0.473
Slowly perfused tissue	QSc	0.17	0.248
Fat	QFc	0.07	0.052

Table 3.2. Physicochemical parameters used in the rat and human PBK model. Tissue: blood partition coefficients of ZEN and α -ZEL were calculated based on the method by DeJongh *et al.* (1997)

	Rat		Human	
	ZEN	α -ZEL	ZEN	α -ZEL
Intestine	2.64	2.38	6.56	6.11
Liver	2.64	2.38	6.56	6.11
Rapidly perfused tissues	2.64	2.38	6.56	6.11
Slowly perfused tissues	0.76	0.71	4.25	3.99
Fat	106.93	92.79	134.86	131.61

3.2.6 PBK model evaluation

The performance of the model developed for rats was evaluated by comparison of i) the predicted blood concentration time profile of ZEN to the time dependent blood concentrations reported in literature upon single i.v. doses of 1, 2, 4 and 8 mg/kg bw (Shin *et al.*, 2009), and ii) the predicted maximum blood concentration (C_{\max}) of ZEN to the C_{\max} obtained in a rat study following a single oral dose of 8 mg/kg bw (Shin *et al.*, 2009). The study from Mallis *et al.* (2003) was considered unsuitable for the evaluation due to differences in the experimental design, where ZEN was co-administered with 4 other isoflavones. As the PBK model developed predicts ZEN blood concentrations, the serum concentrations of ZEN from *in vivo* studies in rats were converted to blood concentrations assuming that blood concentrations are 0.6 times the serum concentration in rats (Walker *et al.*, 1990; Probst *et al.*, 2006; Yang *et al.*, 2007).

As data on dose-dependent blood levels upon exposure to ZEN in humans suitable for model evaluation were not available, the evaluation of the human PBK model was done by comparison to the cumulative urinary concentration of ZEN and ZEN-glucuronide (total ZEN) reported by Mirocha *et al.* (1981) and Warth *et al.* (2013) at oral doses of 1.43 mg/kg bw and 0.2 μ g/kg bw, respectively.

To further evaluate the PBK models a sensitivity analysis was performed to identify the parameters having the largest impact on the model predictions. The sensitivity coefficients (SC) were determined following the equation (Evans and Andersen, 2000):

$$SC = (C' - C)/(P' - P) \times P/C$$

where C is the initial value of the model output (C_{\max} of ZEN), C' the modified value of the model output resulting from a 5% increase in the parameter value, P is the initial parameter value and P' is the parameter value with a 5% increase. Each parameter change was analyzed individually, while others were kept at the initial values. The analysis was conducted with an oral dose of 8 mg/kg bw for rats and oral doses of 1.43 mg/kg bw and 0.2 µg/kg bw for human representing the dose levels from available *in vivo* studies used for model evaluation (Mirocha *et al.*, 1981; Warth *et al.*, 2013). Larger SC values represent a higher impact of the parameter on the predictions for the C_{\max} of ZEN and α -ZEL.

3.3 Results

3.3.1 *In vitro* kinetic data for rats and humans

Tables 3.3 to 3.5 summarize the kinetic parameters of the metabolism of ZEN and α -ZEL required for the PBK model.

The *in vitro* kinetics for the formation of α -ZEL and β -ZEL in rat and human liver were obtained from literature (Malekinejad *et al.*, 2006; Mendez-Catala *et al.*, 2020) and are presented in Table 3.3 together with the scaled V_{\max} , K_m and k_{cat} values for the formation of α -ZEL and β -ZEL. A substantial interspecies difference is observed in the k_{cat} for formation of α -ZEL and β -ZEL by rat and human liver. A comparison of the k_{cat} values shows humans to have a 563- and 2-fold higher k_{cat} for conversion of ZEN to respectively α -ZEL and β -ZEL than rat.

The kinetics for the formation of α -ZEL and β -ZEL from ZEN by the intestinal microbiota, obtained from anaerobic *in vitro* incubations of ZEN with pooled rat and human feces, were also obtained from literature (Mendez-Catala *et al.*, 2020) and are presented in Table 3.4 along with the scaled V_{\max} and k_{cat} values for the formation of the metabolites based on the 24 h defecation volumes of 4.1 and 128 g for rats and humans, respectively. A comparison of the scaled k_{cat} values for formation of α -ZEL and β -ZEL by the intestinal microbiota shows that the values for rats are 4- and 14-fold higher than those obtained for humans. The ratio of α -ZEL/ β -ZEL was shown to be higher in humans (i.e. 6/1) than in rats (i.e. 2/1). Overall, humans showed a higher preference for the bioactivation of ZEN to α -ZEL in both liver and intestinal microbial metabolism.

The extent of glucuronidation of ZEN and α -ZEL by rat and humans was quantified by UPLC-PDA analysis of formation of the respective glucuronides upon incubation of ZEN with liver (Figure 3.2) and intestinal (Figure 3.3) S9 fractions and of α -ZEL with liver S9 fractions (Figure 3.2). The results obtained show that the concentration dependent rate of glucuronidation followed Michaelis-Menten kinetics. The *in vitro* V_{\max} and K_m values and the catalytic efficiencies (k_{cat} calculated as V_{\max}/K_m) for the glucuronidation of ZEN and α -ZEL derived from these data, as well as the scaled V_{\max} and k_{cat} values are presented in Table 3.5. The *in vivo* k_{cat} for glucuronidation of ZEN by S9 liver fractions showed to be comparable for rats and humans. Larger interspecies differences were observed for the glucuronidation of ZEN by S9 intestinal tissue samples, with the *in vivo* k_{cat} for rats being 2.7-fold higher than for human.

Table 3.1. *In vitro* and scaled *in vivo* kinetic parameters for the conversion of ZEN to α -ZEL and β -ZEL in rat and human liver, as derived from literature data using *in vitro* incubations of ZEN with rat and human liver S9 fractions.

Species Metabolite	V_{\max} , <i>in vitro</i> (pmol/min/mg S9 protein)	K_m (μ M)	k_{cat} , <i>in vitro</i> (μ l/min/mg S9 protein)	Scaled V_{\max} , <i>in vivo</i> (μ mol/h/kg bw) ^a	k_{cat} , <i>in vivo</i> (L/h/kg bw)
Rat ^b					
α -ZEL	32	592	0.05	9.34	0.02
β -ZEL	72	21	3.43	21	1.00
Human ^c					
α -ZEL	358.7	9	38.7	80.02	8.89
β -ZEL	209.3	23	9.02	46.7	2.03

^a Calculated from $[(V_{\max}, \textit{in vitro}) \times (\text{mg S9 protein/g liver}) \times (\text{g liver}) \times (60 \text{ min/h})] / (10^6 \mu\text{mol/pmol}) / \text{kg bw}$. For rat and human the mg S9 protein/g liver were 143 and 120.7, respectively.

^b Malekinejad *et al.* (2006)

^c Mendez-Catala *et al.* (2020)

Table 3.2. *In vitro* and scaled *in vivo* kinetic parameter for the conversion of ZEN to α -ZEL and β -ZEL by the intestinal microbiota as derived from anaerobic *in vitro* incubations of ZEN with rat and human fecal slurries (Mendez-Catala *et al.*, 2020)

Species Metabolite	V_{\max} , <i>in vitro</i> ($\mu\text{mol}/\text{min}/\text{mg}$ feces)	K_m (μM)	k_{cat} , <i>in vitro</i> ($\mu\text{L}/\text{min}/\text{mg}$ feces) ^a	Scaled V_{\max} , <i>in vivo</i> ($\mu\text{mol}/\text{h}/\text{kg}$ bw) ^b	k_{cat} , <i>in vivo</i> ($\text{mL}/\text{h}/\text{kg}$ bw)
Rat					
α -ZEL	0.23	66	3.5	0.23	2.60
β -ZEL	0.14	80	1.8	0.10	1.30
Human					
α -ZEL	0.90	135	6.6	0.10	0.73
β -ZEL	0.18	163	1.1	0.02	0.12

^a (10^{-3}) $\mu\text{L}/\text{min}/\text{mg}$ feces

^b Calculated from $[(V_{\max}, \text{in vitro}) \times (\text{defecation volume in mg}) \times (60 \text{ min}/\text{h})]/(10^6 \mu\text{mol}/\text{pmol})/(\text{kg bw})$. Rat and human defecation volumes were 4.1 and 128 g, respectively

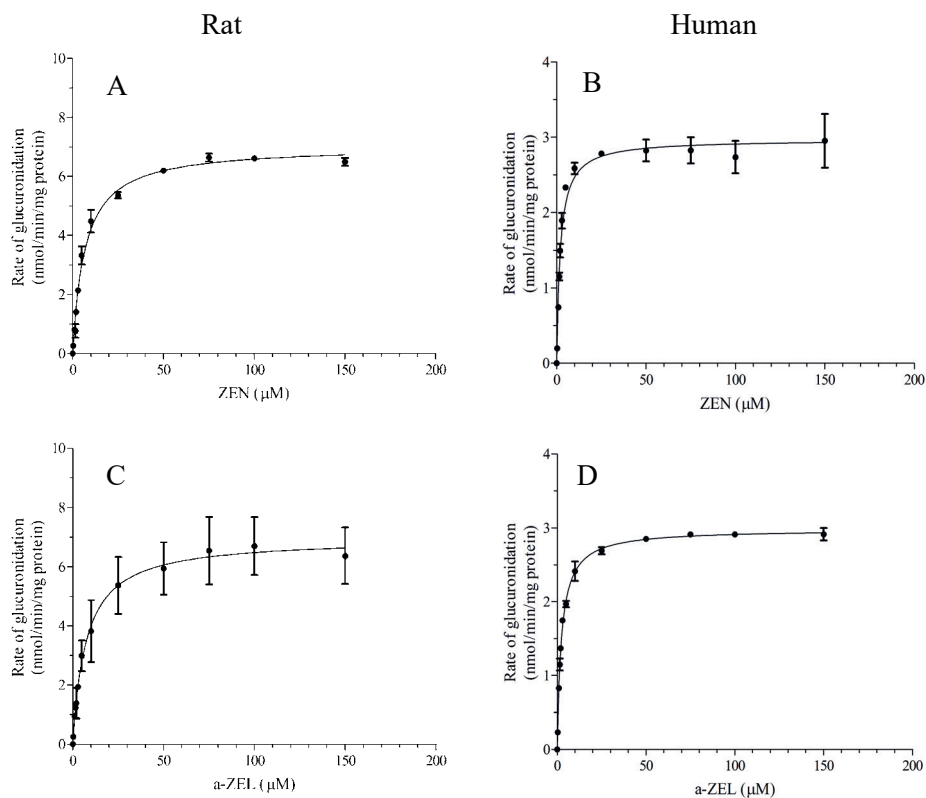


Figure 3.2. Concentration dependent formation of (A-B) ZEN glucuronide and (C-D) α -ZEL glucuronide in incubations with rat and human liver S9

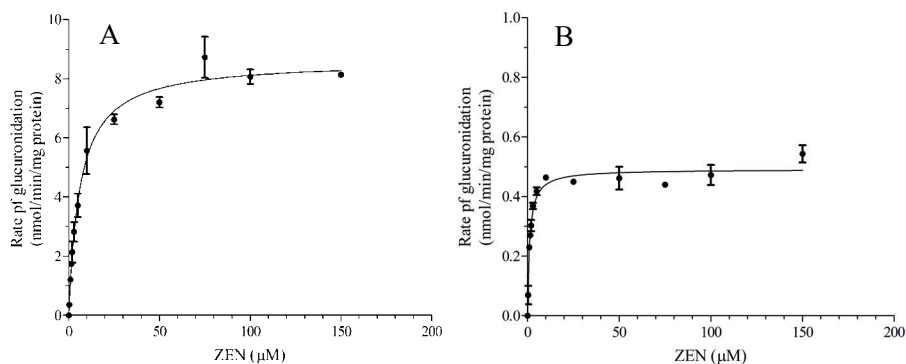


Figure 3.3. Concentration dependent formation of ZEN glucuronide in incubations with (A) rat and (B) human intestinal S9

Table 3.3. *In vitro* and scaled *in vivo* kinetic parameters for the glucuronidation of ZEN and α -ZEL in incubations with rat or human liver S9 obtained from *in vitro* incubations of ZEN or α -ZEL with rat and human liver S9 fractions and UDPGA (Figure 3.2 and 3.3)

Compound	V_{\max} , <i>in vitro</i> (nmol/min/mg of protein)	K_m (μ M)	k_{cat} , <i>in vitro</i> (ml/min/mg protein)	Scaled V_{\max} , <i>in vivo</i> (μ mol/h/kg bw) ^a	k_{cat} , <i>in vivo</i> (L/h/kg bw)
Organ					
Rat					
ZEN					
Liver	7.03	6.75	1.04	2050.50	303.64
Intestine	8.62	6.19	1.39	268.54	43.44
α-ZEL					
Liver	6.96	7.43	0.94	2031.25	273.53
Human					
ZEN					
Liver	2.97	2.04	1.45	559.23	273.73
Intestine	0.49	1.17	0.42	18.67	15.90
α-ZEL					
Liver	2.98	2.42	1.24	561.68	232.58

^a Calculated from $[(V_{\max}, \text{in vitro}) \times (\text{mg S9/g liver}) \times (60 \text{ min/h})] / (10^3 \text{ } \mu\text{mol/nmol}) / \text{kg bw}$.

3.3.2 PBK model development and evaluation

The kinetic constants for the conversion of ZEN to α -ZEL and β -ZEL and for glucuronidation of ZEN and α -ZEL were integrated into the PBK models for rat and human. First, the performance of the model was evaluated based on the comparison of the concentration-time curves of ZEN predicted by the rat PBK model with available *in vivo* kinetic data upon i.v. administration of ZEN at various dose levels to rats (Shin *et al.*, 2009) as shown in Figure 3.4. These results indicate that the model predicts the time dependent blood concentrations and clearance of ZEN well. In a next step literature data from an *in vivo* rat study with oral dosing were used for evaluation of the model. In Figure 3.5 the C_{\max} of unconjugated ZEN predicted upon oral dosing was compared to the C_{\max} reported by Shin *et al.* (2009) upon oral dosing of rats with 8 mg/kg bw ZEN, with resulting values of 6.08 and 8.14 nM, respectively, showing an only 1.3-fold difference.

It was also evaluated to what extent inclusion of the α -ZEL sub-model affected the prediction for the C_{\max} of ZEN. The C_{\max} of ZEN appeared to be minimally affected by the inclusion of its intestinal microbial metabolism to α -ZEL into the model, and the concentration of α -ZEL in blood was predicted to amount to less than 0.1% of the concentration of ZEN when ZEN is dosed at 8 mg/kg bw (Figure 3.5).

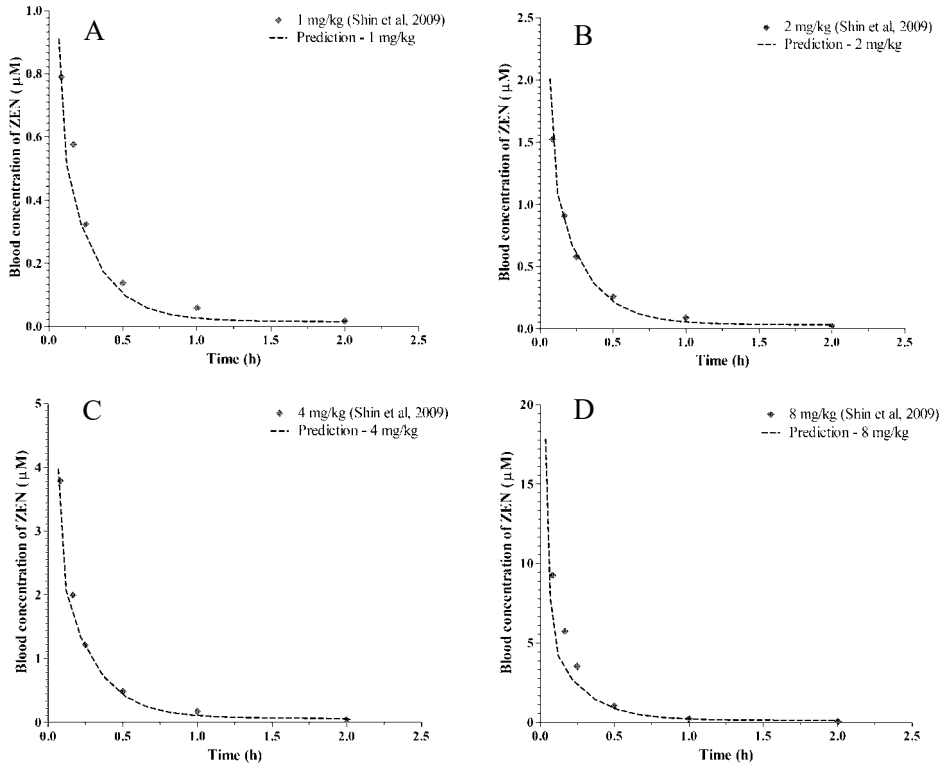


Figure 3.4. Comparison of predicted and reported (Shin *et al.*, 2009) time dependent plasma concentrations of ZEN in rats upon i.v. administration of doses of (A) 1 mg/kg bw, (B) 2 mg/kg bw, (C) 4 mg/kg bw and (D) 8 mg/kg bw

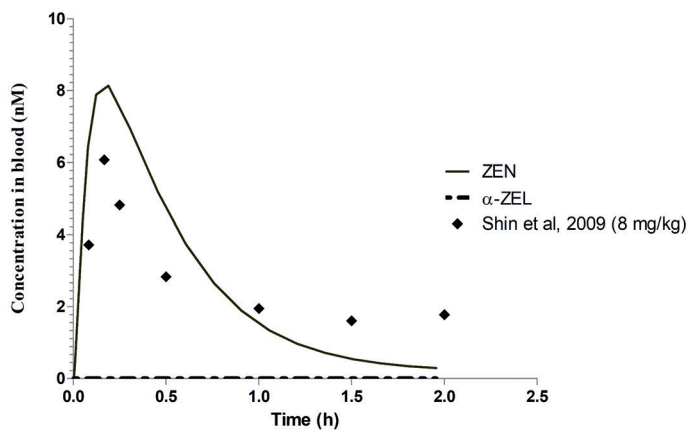


Figure 3.5. PBK model predicted time dependent blood concentration of ZEN and α-ZEL in rat upon an oral dose of 8 mg/kg bw.

The predictions made by the human PBK model were evaluated based on urinary levels of ZEN and its metabolites reported in human studies (Mirocha *et al.*, 1981; Warth *et al.*, 2013). The cumulative 24 hours urinary excretion data reported for humans by Mirocha *et al.* (1981) and Warth *et al.* (2013) after an oral dose of ZEN were compared to the human PBK model predicted values in Table 3.6. The reported *in vivo* cumulative urinary concentrations were calculated based on a mean urinary volume for human of 2.42 L (Warth *et al.*, 2013) to allow comparison with the PBK model based predicted amount of urinary excretion of ZEN metabolites.

The evaluation of the human model by comparison of the cumulative urinary amount (Table 3.6) resulted in an excretion of 15.1- 18.1% of the total oral dose, in line with the reported 7.2 - 32.1% of the dose recovered in urine. The comparison of the predicted excretion in urine with the reported data reveals that the model predicts the reported data reasonably well especially for the study of Mirocha *et al.* (1981). The prediction of C_{\max} of ZEN and α -ZEL showed the concentration of α -ZEL in blood to amount to about 3% of the concentration of ZEN when ZEN is dosed at 0.143 and 1.43 $\mu\text{g/kg}$ bw (Supplementary Figure 3.1). Finally, the contribution of intestinal microbiota to metabolism revealed that the formation of α -ZEL from ZEN was driven by hepatic metabolism (Supplementary Figure 3.2)

Table 3.6. *In vivo* and predicted cumulative urinary excretion of total ZEN in humans 24 hours after oral dosing of ZEN

Dose (mg)	<i>In vivo</i> urine amount (mg) ^a	Predicted urine amount (mg)	Predicted / <i>in vivo</i>	Reference
100	32.1	18.1	0.56	Mirocha <i>et al.</i> (1981)
0.01	0.73×10^{-3}	1.58×10^{-3}	2.08	Warth <i>et al.</i> (2013)

^a based on an average urine volume of 2.42 L per day (Warth *et al.*, 2013)

The performance of the models was further evaluated through a sensitivity analysis to assess the parameters affecting the prediction of the concentration of ZEN in blood to the largest extent. Figure 3.6 presents the results obtained. The sensitivity analysis was performed at an oral dose levels of 8 mg/kg bw in rats and 0.143 $\mu\text{g/kg}$ bw and 1.43 mg/kg bw for humans, representing the dose levels used in the *in vivo* studies used for model evaluation (Mirocha *et al.*, 1981; Shin *et al.*, 2009; Warth *et al.*, 2013). Only the parameters resulting in a normalized sensitivity coefficient higher than 0.1 (absolute value) are shown in Figure 3.6. In all scenarios, the C_{\max} values for

ZEN were greatly affected by the kinetic parameters for glucuronidation of ZEN in the small intestine and liver tissue. Other parameters found to impact the C_{\max} predictions for ZEN included physiological parameters such as body weight, tissue volume and blood flows, especially those of the small intestine and the liver. The parameters describing the absorption from the small intestinal lumen to the small intestinal tissue (Papp Caco-2, V_{in} , A_{in}) also appeared to have a substantial effect on the C_{\max} prediction.

3.3.3 Comparison of EC_{10} values for estrogenicity with predicted C_{\max} values derived from dietary exposure of an adult population

To obtain further insight in the potential of the PBK models, they were applied to evaluate whether at dose levels equal to the TDI of 0.25 $\mu\text{g/kg bw}$ or equal to estimated dietary intakes of ZEN (2.4-29 ng/kg bw) (EFSA, 2011), the C_{\max} values of ZEN and α -ZEL would reach levels that induce estrogenic responses. To this end predicted C_{\max} values were compared to data from the ZEN or α -ZEL concentration-dependent responses in a selection of different *in vitro* model systems for estrogenicity. The predicted concentrations were corrected for the plasma unbound fractions calculated to be 0.089 and 0.103 for ZEN and α -ZEL, respectively (WFSR, 2020). Figure 3.7 reflects that different bioassays for estrogenicity result in somewhat different potencies for ZEN and α -ZEL. Nevertheless, the results presented in Figure 3.7 also reveal that the C_{\max} for both α -ZEL and ZEN predicted by the PBK models, both at levels of normal dietary intake and at the TDI are predicted to be below the EC_{10} values of all bioassays.

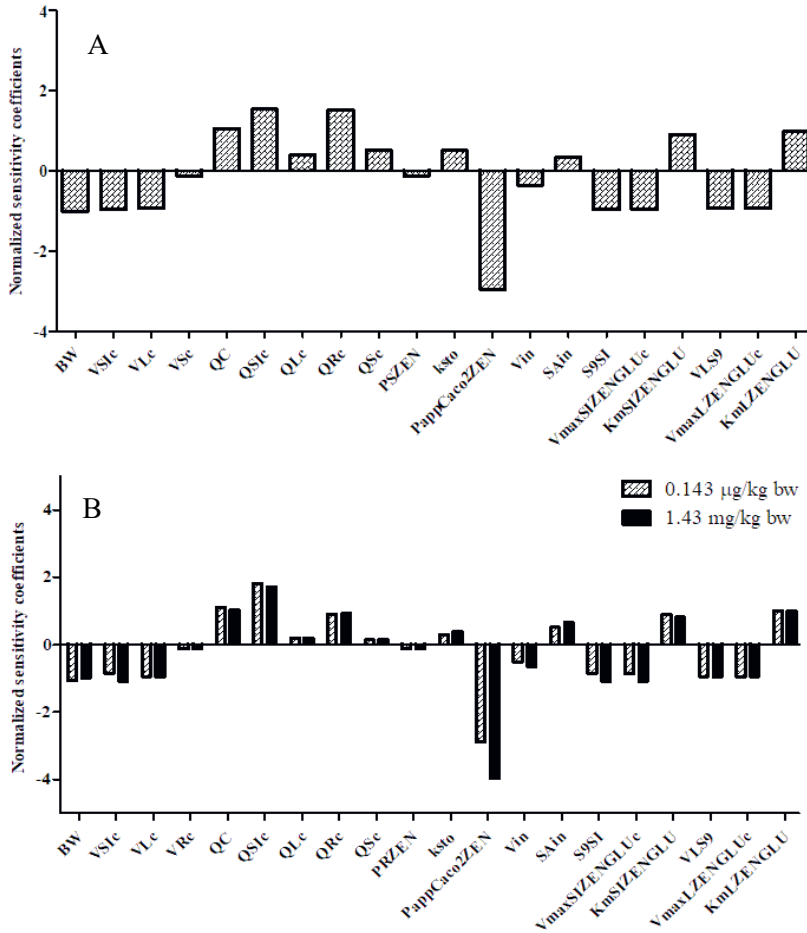


Figure 3.6. Sensitivity coefficients of the PBK model parameters for the predicted C_{\max} of ZEN in (A) rat at an oral dose of 8 mg/kg bw, and (B) human at oral doses of 0.143 µg/kg bw and 1.43 mg/kg bw. The parameters stand for: BW = body weight, VTic = fraction of tissue volume (Ti = SI (small intestine), L (liver), R (rapidly perfused), S (slowly perfused)), Qc = cardiac output, QTic = fraction of blood flow to tissue (Ti = SI (small intestine), L (liver), R (rapidly perfused)), PRZEN = rapidly perfused tissue/blood partition coefficient, ksto = stomach emptying rate, PappCaco2ZEN = Papp valued derived from Caco-2 transport studies, Vin = volume for small intestinal sub-compartment, SAin = surface area for small intestinal subcompartment, S9SI = small intestinal S9 protein yield, VLS9 = liver S9 protein yield, V_{\max} and K_m = maximum rate of formation and the Michaelis-Menten kinetic constant for the formation of ZEN glucuronide (ZENGLU) in SI (small intestine) and L (liver).

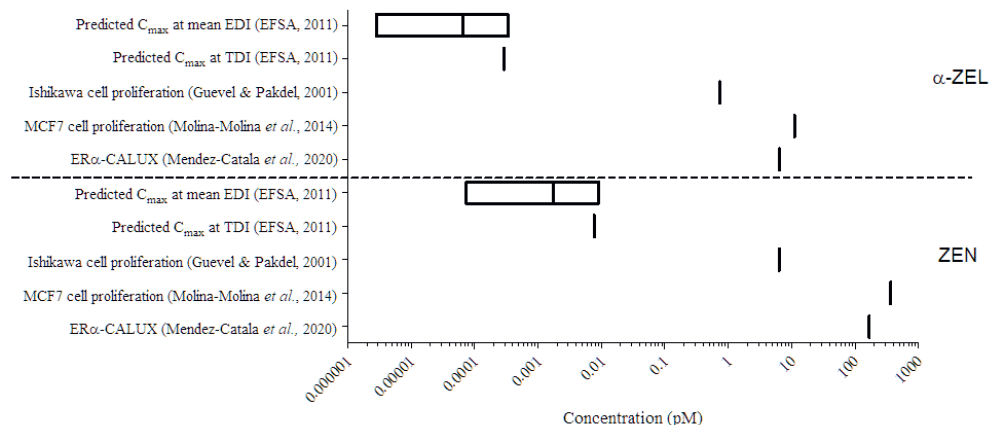


Figure 3.7. Comparison of EC_{10} values derived from estrogenic *in vitro* studies (Le Guevel and Pakdel, 2001; Mendez-Catala *et al.*, 2020; Molina-Molina *et al.*, 2014) to C_{max} values predicted by the human PBK model to occur at a mean estimated daily intake (EDI) of ZEN, ranging from 2.4–29 ng/kg bw and at the TDI of 0.25 μ g/kg bw.

3.4 Discussion

In the present study, PBK models for ZEN in both rat and human were developed that include intestinal microbial metabolism of ZEN. The models include a sub-model for the metabolite, α -ZEL, known to be more active as an estrogen than ZEN itself (Fitzpatrick *et al.*, 1989; Shier *et al.*, 2001). By integrating microbial ZEN metabolism into the models they provide insight into the role of the intestinal microbiota in the metabolism of ZEN and its bioactivation to α -ZEL. The results obtained revealed that, in spite of the conversion of ZEN to α -ZEL by intestinal microbiota, the formation of α -ZEL from ZEN is mainly driven by hepatic metabolism. In the PBK models developed, the intestinal microbial metabolism of ZEN was integrated as a separate compartment by the inclusion of kinetic parameters obtained from *in vitro* anaerobic incubations of ZEN with fecal samples (Mendez-Catala *et al.*, 2020). Previously Wang *et al.* (2020) showed a first proof-of-principle for the inclusion of microbial metabolism in a PBK model based on kinetic parameters obtained in such anaerobic fecal incubations. This earlier PBK study described the metabolism of the isoflavone daidzein including its microbial conversion to *S*-equol in addition to host-based metabolism. In this study it was shown that the inclusion of microbial metabolism allowed prediction of host plasma levels of *S*-equol and its conjugates, and also revealed that in spite of the higher estrogenicity of *S*-equol its role compared to the contribution of daidzein itself was

limited because of its substantially lower systemic concentrations (Wang *et al.*, 2020). The results of the present study show a similar outcome for ZEN and α -ZEL. This followed from the fact that the C_{\max} predicted for α -ZEL amounted to less than 0.1% or about 3% of the C_{\max} for ZEN itself in rats and humans, respectively. This indicates that in despite of the 60-fold higher estrogenicity reported for α -ZEL its contribution to the *in vivo* estrogenicity upon exposure to ZEN may be limited, while in human it may be higher than in rats.

The PBK model for the metabolism of ZEN in rat allowed the comparison to available *in vivo* kinetic data in blood upon i.v. and oral dosing of ZEN. The model prediction of blood concentrations after 4 different i.v. doses of ZEN showed to be in line with the kinetics reported by (Shin *et al.*, 2009). A study dosing ZEN at 8 mg/kg bw orally to rats (Shin *et al.*, 2009) reported a C_{\max} that was also adequately predicted by the model. The evaluation of the human model resulted in differences in the cumulative urinary amount possibly related to the exposure, while Mirocha *et al.* (1981) exposed ZEN directly, Warth *et al.* (2013) did it from naturally contaminated products.

The PBK models developed showed that liver is the main site for the conversion of ZEN to α -ZEL (Supplementary Figure 3.2), a conclusion that holds at dose levels as low as the dose representing daily dietary intake (2.4 ng/kg bw/day) (EFSA, 2011) to dose levels used in rodent bioassays of 8 mg/kg bw (Shin *et al.*, 2009). The model predictions also revealed humans to have on average a 76-times higher concentration of α -ZEL in liver compared to rat. This is in line with previous reports on species differences in the metabolism of ZEN, indicating that humans (Bravin *et al.*, 2009), similar to pigs, form relatively more α -ZEL than rats. The integration of the kinetic parameters for α -ZEL formation in the PBK model for human revealed the predicted blood concentration of α -ZEL to amount to about 3% of the total concentration of ZEN reaching the blood (Supplementary Figure 3.1). The low concentration of α -ZEL reaching the circulation can be ascribed to an efficient glucuronidation of ZEN in the intestinal tissue and liver competing with formation of α -ZEL in these organs, in combination with efficient hepatic glucuronidation of α -ZEL. The glucuronidation of ZEN has previously been reported to represent the main conjugation pathway for ZEN (Kiessling and Pettersson, 1978; Malekinejad *et al.*, 2006; Mikula *et al.*, 2012; Pfeiffer *et al.*, 2010) and results in a decrease in the toxicity of ZEN due to the absence of estrogenic activity of ZEN glucuronide (Frizzell *et al.*, 2015). The kinetic constants in Table 3.5 show rat and human liver to perform the glucuronidation of ZEN with comparable catalytic efficiencies, with rat being 1.1 times more efficient than humans. The glucuronidation of α -ZEL in liver was also comparable with rats

again being 1.1 times more efficient than humans. These results are in line with those of Pfeiffer *et al.* (2010) reporting the percentage of glucuronidation of ZEN and α -ZEL by male rat liver fractions to be 1.6 and 1.5 and times higher than by human liver fractions, respectively. The somewhat higher catalytic efficiency observed for the glucuronidation by rat than human intestinal tissues *in vitro* is in line with results for glucuronidation of other UGT substrates such as flavonoids (Brand *et al.*, 2010; Boonpawa *et al.*, 2015). The glucuronidation of ZEN in human liver is reported to be catalyzed by UGTs, with UGT1A1, 1A3 and 1A8 being the major contributors (Pfeiffer *et al.*, 2010). In the same study, intestinal glucuronidation of ZEN in humans was linked to UGT1A1 and 1A8. A higher mRNA expression of UGT1A1 and 1A3 in rat liver and intestine has been reported offering a possible explanation for the species differences in glucuronidation observed (Kutsukake *et al.*, 2019). Based on studies in a rat everted model Ieko *et al.* (2020) reported the rapid glucuronidation of ZEN immediately after absorption and low transport of ZEN into the serosa portion. The amount of ZEN predicted by the PBK model to reach the liver in rats was lower than the amount reaching the small intestinal tissue, in line with the notion from Ieko *et al.* (2020) that only low amounts of ZEN could reach the liver. The PBK model predicted the glucuronidation of ZEN to mainly occur in the small intestinal tissue (Supplementary Table 3.1).

Furthermore, the outcomes of the human PBK model enabled prediction of the internal concentrations of ZEN and α -ZEL resulting from dietary intake of ZEN or from intake at the level of the TDI, with concentrations of ZEN and α -ZEL known to induce estrogenicity in *in vitro* bioassays. The predicted C_{\max} values were on average 3 orders of magnitude lower than the EC_{10} for ZEN and α -ZEL in bioassays with different estrogenic endpoints, suggesting that at the current levels of dietary intake up to at least the TDI, the concentration of ZEN and α -ZEL in blood will not reach the concentrations known to cause estrogenic effects. This comparison illustrates the potential of the PBK model-based approach to conclude on *in vivo* effects without the need for studies in experimental animals or a human intervention study.

Nevertheless, it is of use to discuss some of the limitations of the current approach. First of all, it is important to note that the study is based on the average adult population and does not (yet) take interindividual differences or possible differences of different age groups in sensitivity to ZEN into account. To take such potential interindividual differences into account remains an interesting topic for further studies especially given a possible correlation between exposure to ZEN and early onset of puberty in young girls as suggested before (Hannon *et al.*, 1987; Szuets *et*

al., 1997; Massart and Saggese, 2010; Bandera *et al.*, 2011). The human PBK model developed in the present study can form a basis to build individual PBK models and study such interindividual differences within the human population. Second, the potential of the use of fecal samples as a source of the intestinal microbiota for the study of intestinal microbial metabolism needs some further considerations. Although differences in the microbial composition along the intestinal tract are known, the colon harbors 70% of total bacteria in the intestinal tract, making it the main site for fermentation (Hillman *et al.*, 2017). Furthermore, Behr *et al.* (2018) reported colon and fecal bacterial communities to be highly comparable, supporting the notion that fecal slurries can be used as a surrogate for intestinal microbiota. Furthermore, in a previous study the *in vitro* anaerobic incubations with fecal slurries were shown to adequately describe the kinetics of the formation of S-equiol from daidzein, a metabolite formed only by intestinal microbiota, allowing description of S-equiol kinetics by PBK modeling in both rat and human (Atkinson *et al.*, 2004; Wang *et al.*, 2020). Therefore, the *in vitro* anaerobic incubations with fecal slurries show a good first tier approach for the estimation of overall intestinal microbial metabolism in the host.

In conclusion, the PBK models developed in this study are able to quantify interspecies differences in metabolism of ZEN taking intestinal microbial metabolism into account. Results obtained reveal that in spite of the capacity of the microbial community in both rat and human to catalyze conversion of ZEN to α -ZEL, the contribution of this intestinal microbial metabolism to systemic concentrations of α -ZEL in the host are limited. Furthermore, it was shown that in spite of the higher estrogenic potency of α -ZEL its contribution to the estrogenic effects occurring upon exposure to ZEN are limited, and that at current levels of intake ZEN and also α -ZEL concentrations remain low enough to not raise a concern. The study also shows a proof of principle on how an *in vitro*- PBK model-based approach can be of use to conclude on *in vivo* effects of compounds studied without the need for studies in experimental animals or a human intervention study.

Acknowledgements

This research was financially supported by the National Council of Science and Technology (CONACYT) through a scholarship awarded to Diana M. Mendez Catala (CVU 619449) for conducting her PhD in The Netherlands. Special thanks go to Karsten Beekmann for critical reading of the manuscript.

3.5 References

- Atkinson, C., Berman, S., Humbert, O., Lampe, J.W. In Vitro Incubation of Human Feces with Daidzein and Antibiotics Suggests Interindividual Differences in the Bacteria Responsible for Equol Production. *Nutr. J.*, 134 (2004), 596-599. doi: 10.1093/jn/134.3.596
- Bandera, E.V., Chandran, U., Buckley, B., Lin, Y., Isukapalli, S., Marshall, I., King, M., Zarbl, H. Urinary mycoestrogens, body size and breast development in New Jersey girls. *Sci. Total Environ.*, 409 (2011), 5221-5227. doi: 10.1016/j.scitotenv.2011.09.029
- Behr, C., Ramirez-Hincapie, S., Cameron, H.J., Strauss, V., Walk, T., Herold, M., Beekmann, K., Rietjens, I., van Ravenzwaay, B. Impact of lincosamides antibiotics on the composition of the rat gut microbiota and the metabolite profile of plasma and feces. *Toxicol. Lett.*, 296 (2018), 139-151. doi: 10.1016/j.toxlet.2018.08.002
- Boonpawa, R., Moradi, N., Spenkelink, A., Rietjens, I.M.C.M., Punt, A. Use of physiologically based kinetic (PBK) modeling to study interindividual human variation and species differences in plasma concentrations of quercetin and its metabolites. *Biochem. Pharmacol.*, 98 (2015), 690-702. doi: 10.1016/j.bcp.2015.09.022
- Borzekowski, A., Drewitz, T., Keller, J., Pfeifer, D., Kunte, H.-J., Koch, M., Rohn, S., Maul, R. Biosynthesis and Characterization of Zearalenone-14-Sulfate, Zearalenone-14-Glucoside and Zearalenone-16-Glucoside Using Common Fungal Strains. *Toxins*, 10 (2018), 104. doi: 10.3390/toxins10030104
- Brand, W., Boersma, M.G., Bik, H., Hoek-van den Hil, E.F., Vervoort, J., et al. Phase II metabolism of hesperetin by individual UDP-glucuronosyltransferases and sulfotransferases and rat and human tissue samples. *Drug Metab. Dispos.*, 38 (2010), 617-625. doi: 10.1124/dmd.109.031047
- Bravin, F., Duca, R.C., Balaguer, P., Delaforge, M. In vitro cytochrome p450 formation of a mono-hydroxylated metabolite of zearalenone exhibiting estrogenic activities: possible occurrence of this metabolite in vivo. *Int. J. Mol. Sci.*, 10 (2009), 1824-1837. doi: 10.3390/ijms10041824
- Brown, R.P., Delp, M.D., Lindstedt, S.L., Rhomberg, L.R., Beliles, R.P. Physiological parameter values for physiologically based pharmacokinetic models. *Toxicol. Ind. Health*, 13 (1997), 407-484. doi: 10.1177/074823379701300401
- Cubitt, H.E., Houston, J.B., Galetin, A. Prediction of human drug clearance by multiple metabolic pathways: integration of hepatic and intestinal

- microsomal and cytosolic data. *Drug Metab. Dispos.*, 39 (2011), 864-873. doi: 10.1124/dmd.110.036566
- Dänicke, S., Swiech, E., Buraczewska, L., Ueberschär, K.H. Kinetics and metabolism of zearalenone in young female pigs. *J. Anim. Physiol. Anim. Nutr.*, 89 (2005), 268-276. doi: 10.1111/j.1439-0396.2005.00516.x
- Davies, B., Morris, T. *Physiological Parameters in Laboratory Animals and Humans*. *Pharm. Res.*, 10 (1993), 1093-1095. doi: 10.1023/A:1018943613122
- DeJongh, J., Verhaar, H.J., Hermens, J.L. A quantitative property-property relationship (QPPR) approach to estimate in vitro tissue-blood partition coefficients of organic chemicals in rats and humans. *Arch. Toxicol.*, 72 (1997), 17-25. doi: 10.1007/s002040050463
- Döll, S., Dänicke, S., Ueberschär, K.H., Valenta, H., Schnurrbusch, U., Ganter, M., Klobasa, F., Flachowsky, G. Effects of graded levels of Fusarium toxin contaminated maize in diets for female weaned piglets. *Arch. Anim. Nutr.*, 57 (2003), 311-334. doi: 10.1080/00039420310001607680
- EFSA. Scientific Opinion on the risks for public health related to the presence of zearalenone in food. *EFSA J.*, 9 (2011), 2197. doi: 10.2903/j.efsa.2011.2197
- EFSA. Appropriateness to set a group health-based guidance value for zearalenone and its modified forms. *EFSA J.*, 14 (2016), e04425. doi: 10.2903/j.efsa.2016.4425
- Evans, M.V., Andersen, M.E. Sensitivity analysis of a physiological model for 2,3,7,8-tetrachlorodibenzo-p-dioxin (TCDD): assessing the impact of specific model parameters on sequestration in liver and fat in the rat. *Toxicol. Sci.*, 54 (2000), 71-80. doi: 10.1093/toxsci/54.1.71
- Fitzpatrick, D.W., Arbuckle, L.D., Hassen, A.M. Zearalenone metabolism and excretion in the rat: effect of different doses. *J. Environ. Sci. Health B*, 23 (1988), 343-354. doi: 10.1080/03601238809372610
- Fitzpatrick, D.W., Picken, C.A., Murphy, L.C., Buhr, M.M. Measurement of the relative binding affinity of zearalenone, α -zearalenol and β -zearalenol for uterine and oviduct estrogen receptors in swine, rats and chickens: An indicator of estrogenic potencies. *Comp. Biochem. Physiol. C Comp. Pharmacol. Toxicol.*, 94 (1989), 691-694. doi: 10.1016/0742-8413(89)90133-3
- Frizzell, C., Uhlig, S., Miles, C.O., Verhaegen, S., Elliott, C.T., Eriksen, G.S., Sørli, M., Ropstad, E., Connolly, L. Biotransformation of zearalenone and zearalenols to their major glucuronide metabolites reduces estrogenic

- activity. *Toxicol. In Vitro*, 29 (2015), 575-581. doi: 10.1016/j.tiv.2015.01.006
- Gilbert-Sandoval, I., Wesseling, S., Rietjens, I.M.C.M. Predicting the Acute Liver Toxicity of Aflatoxin B1 in Rats and Humans by an In Vitro–In Silico Testing Strategy. *Mol. Nutr. Food Res.*, 64 (2020), 2000063. doi: 10.1002/mnfr.202000063
- Gratz, S.W., Dinesh, R., Yoshinari, T., Holtrop, G., Richardson, A.J., Duncan, G., MacDonald, S., Lloyd, A., Tarbin, J. Masked trichothecene and zearalenone mycotoxins withstand digestion and absorption in the upper GI tract but are efficiently hydrolyzed by human gut microbiota in vitro. *Mol. Nutr. Food Res.*, 61 (2017), E1600680. doi: 10.1002/mnfr.201600680
- Gupta, R.C., Mostrom, M.S., Evans, T.J., 2018. Chapter 76 - Zearalenone. In Gupta, R.C., (Ed.), *Veterinary Toxicology (Third Edition)*. Academic Press, pp. 1055-1063.
- Hannon, W.H., Hill, R.H., Bernert, J.T., Haddock, L., Lebron, G., Cordero, J.F. Premature thelarche in Puerto Rico: A search for environmental estrogenic contamination. *Arch. Environ. Contam. Toxicol.*, 16 (1987), 255-262. doi: 10.1007/BF01054942
- Hillman, E.T., Lu, H., Yao, T., Nakatsu, C.H. Microbial Ecology along the Gastrointestinal Tract. *Microbes Environ.*, 32 (2017), 300-313. doi: 10.1264/jsme2.ME17017
- Hoskins, L.C., Zamcheck, N. Bacterial Degradation of Gastrointestinal Mucins: I. Comparison of mucus constituents in the stools of germ-free and conventional rats. *Gastroenterology*, 54 (1968), 210-217. doi: 10.1016/S0016-5085(68)80005-8
- Hosseinpour, M., Behdad, A. Evaluation of small bowel measurement in alive patients. *Surg. Radiol. Anat.*, 30 (2008), 653-655. doi: 10.1007/s00276-008-0398-2
- Ieko, T., Inoue, S., Inomata, Y., Inoue, H., Fujiki, J., Iwano, H. Glucuronidation as a metabolic barrier against zearalenone in rat everted intestine. *J. Vet. Med. Sci.*, 82 (2020), 153-161. doi: 10.1292/jvms.19-0570
- Kararli, T.T. Comparison of the gastrointestinal anatomy, physiology, and biochemistry of humans and commonly used laboratory animals. *Biopharm. Drug Dispos.*, 16 (1995), 351-380. doi: 10.1002/bdd.2510160502
- Kiessling, K.-H., Pettersson, H. Metabolism of Zearalenone in Rat Liver. *Acta Pharmacol. Toxicol.*, 43 (1978), 285-290. doi: 10.1111/j.1600-0773.1978.tb02267.x

- Kutsukake, T., Furukawa, Y., Ondo, K., Gotoh, S., Fukami, T., Nakajima, M. Quantitative Analysis of UDP-Glucuronosyltransferase Ugt1a and Ugt2b mRNA Expression in the Rat Liver and Small Intestine: Sex and Strain Differences. *Drug Metab. Dispos.*, 47 (2019), 38-44. doi: 10.1124/dmd.118.083287
- Le Guevel, R., Pakdel, F. Assessment of oestrogenic potency of chemicals used as growth promoter by in-vitro methods. *Hum. Reprod.*, 16 (2001), 1030-1036. doi: 10.1093/humrep/16.5.1030
- Li, H., Zhang, M., Vervoort, J., Rietjens, I.M., van Ravenzwaay, B., Lousse, J. Use of physiologically based kinetic modeling-facilitated reverse dosimetry of in vitro toxicity data for prediction of in vivo developmental toxicity of tebuconazole in rats. *Toxicol. Lett.*, 266 (2017), 85-93. doi: 10.1016/j.toxlet.2016.11.017
- Lorenz, N., Dänicke, S., Edler, L., Gottschalk, C., Lassek, E., Marko, D., Rychlik, M., Mally, A. A critical evaluation of health risk assessment of modified mycotoxins with a special focus on zearalenone. *Mycotoxin Res.*, 35 (2019), 27-46. doi: 10.1007/s12550-018-0328-z
- Lousse, J., Bosgra, S., Blaauboer, B.J., Rietjens, I.M., Verwei, M. Prediction of in vivo developmental toxicity of all-trans-retinoic acid based on in vitro toxicity data and in silico physiologically based kinetic modeling. *Arch. Toxicol.*, 89 (2015), 1135-1148. doi: 10.1007/s00204-014-1289-4
- Malekinejad, H., Maas-Bakker, R., Fink-Gremmels, J. Species differences in the hepatic biotransformation of zearalenone. *Veterinary journal*, 172 (2006), 96-102. doi: 10.1016/j.tvjl.2005.03.004
- Mallis, L.M., Sarkahian, A.B., Harris, H.A., Zhang, M.-Y., McConnell, O.J. Determination of rat oral bioavailability of soy-derived phytoestrogens using an automated on-column extraction procedure and electrospray tandem mass spectrometry. *J. Chromatogr. B*, 796 (2003), 71-86. doi: 10.1016/j.jchromb.2003.08.003
- Massart, F., Saggese, G. Oestrogenic mycotoxin exposures and precocious pubertal development. *Int. J. Androl.*, 33 (2010), 369-376. doi: 10.1111/j.1365-2605.2009.01009.x
- Mendez-Catala, D.M., Spenkelink, A., Rietjens, I.M.C.M., Beekmann, K. An in vitro model to quantify interspecies differences in kinetics for intestinal microbial bioactivation and detoxification of zearalenone. *Toxicol. Rep.*, 7 (2020), 938-946. doi: 10.1016/j.toxrep.2020.07.010

- Metzler, M., Pfeiffer, E., Hildebrand, A. Zearalenone and its metabolites as endocrine disrupting chemicals. *World Mycotoxin J.*, 3 (2010), 385-401. doi: 10.3920/WMJ2010.1244
- Mikula, H., Hametner, C., Berthiller, F., Warth, B., Krska, R., Adam, G., Fröhlich, J. Fast and reproducible chemical synthesis of zearalenone-14- β ,D-glucuronide. *World Mycotoxin J.*, 5 (2012), 289-296. doi: 10.3920/wmj2012.1404
- Mirocha, C.J., Pathre, S.V., Robison, T.S. Comparative metabolism of zearalenone and transmission into bovine milk. *Food Cosmet. Toxicol.*, 19 (1981), 25-30. doi: 10.1016/0015-6264(81)90299-6
- Molina-Molina, J.-M., Real, M., Jimenez-Diaz, I., Belhassen, H., Hedhili, A., Torné, P., Fernández, M.F., Olea, N. Assessment of estrogenic and anti-androgenic activities of the mycotoxin zearalenone and its metabolites using in vitro receptor-specific bioassays. *Food Chem. Toxicol.*, 74 (2014), 233-239. doi: 10.1016/j.fct.2014.10.008
- Mukherjee, D., Royce, S.G., Alexander, J.A., Buckley, B., Isukapalli, S.S., Bandera, E.V., Zarbl, H., Georgopoulos, P.G. Physiologically-based toxicokinetic modeling of zearalenone and its metabolites: application to the Jersey girl study. *PLoS One*, 9 (2014), e113632. doi: 10.1371/journal.pone.0113632
- Peters, S.A., Jones, C.R., Ungell, A.-L., Hatley, O.J.D. Predicting Drug Extraction in the Human Gut Wall: Assessing Contributions from Drug Metabolizing Enzymes and Transporter Proteins using Preclinical Models. *Chem. Res. Toxicol.*, 55 (2016), 673-696. doi: 10.1007/s40262-015-0351-6
- Pfeiffer, E., Hildebrand, A., Mikula, H., Metzler, M. Glucuronidation of zearalenone, zeranol and four metabolites in vitro: formation of glucuronides by various microsomes and human UDP-glucuronosyltransferase isoforms. *Mol. Nutr. Food Res.*, 54 (2010), 1468-1476. doi: 10.1002/mnfr.200900524
- Pfeiffer, E., Kommer, A., Dempe, J.S., Hildebrand, A.A., Metzler, M. Absorption and metabolism of the mycotoxin zearalenone and the growth promotor zeranol in Caco-2 cells in vitro. *Mol. Nutr. Food Res.*, 55 (2011), 560-567. doi: 10.1002/mnfr.201000381
- Probst, R.J., Lim, J.M., Bird, D.N., Pole, G.L., Sato, A.K., Claybaugh, J.R. Gender differences in the blood volume of conscious Sprague-Dawley rats. *J. Am. Assoc. Lab. Anim. Sci.*, 45 (2006), 49-52. doi:
- Punt, A., Freidig, A.P., Delatour, T., Scholz, G., Boersma, M.G., Schilter, B., van Bladeren, P.J., Rietjens, I.M.C.M. A physiologically based biokinetic

- (PBBK) model for estragole bioactivation and detoxification in rat. *Toxicol. Appl. Pharmacol.*, 231 (2008), 248-259. doi: 10.1016/j.taap.2008.04.011
- Reilly, J.A., Forst, C.F., Quigley, E.M.M., Rikkers, L.F. Gastric emptying of liquids and solids in the portal hypertensive rat. *Dig. Dis. Sci.*, 35 (1990), 781-786. doi: 10.1007/BF01540184
- Rose, C., Parker, A., Jefferson, B., Cartmell, E. The Characterization of Feces and Urine: A Review of the Literature to Inform Advanced Treatment Technology. *Crit. Rev. Environ. Sci. Technol.*, 45 (2015), 1827-1879. doi: 10.1080/10643389.2014.1000761
- Shier, W.T., Shier, A.C., Xie, W., Mirocha, C.J. Structure-activity relationships for human estrogenic activity in zearalenone mycotoxins. *Toxicon*, 39 (2001), 1435-1438. doi:
- Shin, B.S., Hong, S.H., Bulitta, J.B., Hwang, S.W., Kim, H.J., et al. Disposition, oral bioavailability, and tissue distribution of zearalenone in rats at various dose levels. *J. Toxicol. Environ. Health A*, 72 (2009), 1406-1411. doi: 10.1080/15287390903212774
- Sun, D., Lennernas, H., Welage, L.S., Barnett, J.L., Landowski, C.P., Foster, D., Fleisher, D., Lee, K.D., Amidon, G.L. Comparison of human duodenum and Caco-2 gene expression profiles for 12,000 gene sequences tags and correlation with permeability of 26 drugs. *Pharm. Res.*, 19 (2002), 1400-1416. doi: 10.1023/a:1020483911355
- Sun, W.M., Houghton, L.A., Read, N.W., Grundy, D.G., Johnson, A.G. Effect of meal temperature on gastric emptying of liquids in man. *Gut*, 29 (1988), 302-305. doi: 10.1136/gut.29.3.302
- Szuets, P., Mesterhazy, A., Falkay, G.Y., Bartok, T. Early Telarche Symptoms in Children and their Relations to Zearalenon Contamination in Foodstuffs. *Cereal Res. Commun.*, 25 (1997), 429-436. doi: 10.1007/BF03543747
- Teeguarden, J.G., Waechter, J.M., Jr., Clewell, H.J., III, Covington, T.R., Barton, H.A. Evaluation of Oral and Intravenous Route Pharmacokinetics, Plasma Protein Binding, and Uterine Tissue Dose Metrics of Bisphenol A: A Physiologically Based Pharmacokinetic Approach. *Toxicol. Sci.*, 85 (2005), 823-838. doi: 10.1093/toxsci/kfi135
- Tsutsumi, K., Li, S.K., Hymas, R.V., Teng, C.-L., Tillman, L.G., Hardee, G.E., Higuchi, W.I., Ho, N.F.H. Systematic studies on the paracellular permeation of model permeants and oligonucleotides in the rat small intestine with chenodeoxycholate as enhancer. *J. Pharm. Sci.*, 97 (2008), 350-367. doi: 10.1002/jps.21093

- Vdoviaková, K., Petrovová, E., Maloveská, M., Krešáková, L., Teleky, J., Elias, M.Z.J., Petrášová, D. Surgical Anatomy of the Gastrointestinal Tract and Its Vasculature in the Laboratory Rat. *Gastroenterol. Res. Pract.*, 2016 (2016), 2632368. doi: 10.1155/2016/2632368
- Verwei, M., Freidig, A.P., Havenaar, R., Groten, J.P. Predicted serum folate concentrations based on in vitro studies and kinetic modeling are consistent with measured folate concentrations in humans. *J Nutr*, 136 (2006), 3074-3078. doi: 10.1093/jn/136.12.3074
- Walker, H.K., Hall, W.D., Hurst, J.W., 1990. *Clinical Methods: The History, Physical, and Laboratory Examinations*. Butterworths Copyright ©, Boston.
- Wang, Q., Spenkelink, B., Boonpawa, R., Rietjens, I., Beekmann, K. Use of Physiologically Based Kinetic Modeling to Predict Rat Gut Microbial Metabolism of the Isoflavone Daidzein to S-Equol and Its Consequences for ER α Activation. *Mol. Nutr. Food Res.*, 64 (2020), e1900912. doi: 10.1002/mnfr.201900912
- Warth, B., Sulyok, M., Berthiller, F., Schuhmacher, R., Krska, R. New insights into the human metabolism of the Fusarium mycotoxins deoxynivalenol and zearalenone. *Toxicol. Lett.*, 220 (2013), 88-94. doi: 10.1016/j.toxlet.2013.04.012
- WFSR, 2020. QIVIVE tools V 1.0 <https://wfsr.shinyapps.io/wfsrqivivetools/>.
- Yang, J., Jamei, M., Yeo, K.R., Rostami-Hodjegan, A., Tucker, G.T. Misuse of the Well-Stirred Model of Hepatic Drug Clearance. *Drug Metab. Dispos.*, 35 (2007), 501-502. doi: 10.1124/dmd.106.013359
- Yang, X., Doerge, D.R., Fisher, J.W. Prediction and evaluation of route dependent dosimetry of BPA in rats at different life stages using a physiologically based pharmacokinetic model. *Toxicol. Appl. Pharmacol.*, 270 (2013), 45-59. doi: 10.1016/j.taap.2013.03.022
- Zhang, M., van Ravenzwaay, B., Fabian, E., Rietjens, I.M.C.M., Louisse, J. Towards a generic physiologically based kinetic model to predict in vivo uterotrophic responses in rats by reverse dosimetry of in vitro estrogenicity data. *Arch. Toxicol.*, 92 (2018), 1075-1088. doi: 10.1007/s00204-017-2140-5

Supplementary Material**Model Code for Rat**

Physiological parameters

Tissue volumes (reference: Brown et al. (1997))

BW= 0.250	(Kg)	body weight rat
VS _{Ic} = 0.014		fraction of small intestine
VL _c = 0.034		fraction of liver tissue
VR _c = 0.034	0.082-VS _{Ic} -VL _c	fraction of rapidly perfused tissue
VS _c = 0.667	0.737-VF _c	fraction of slowly perfused tissue
VF _c = 0.070		fraction of fat tissue
VB _c = 0.074		fraction of blood

VS _I = VS _{Ic} *BW (calculated)	(L or Kg)	volume of small intestine tissue
VL = VL _c *BW	(L or Kg)	volume of liver tissue (calculated)
VR = VR _c *BW (calculated)	(L or Kg)	volume of rapidly perfused tissue
VS = VS _c *BW (calculated)	(L or Kg)	volume of slowly perfused tissue
VF = VF _c *BW	(L or Kg)	volume of fat tissue (calculated)
VB = VB _c *BW	(L or Kg)	volume of blood (calculated)

Blood flow rates (reference: Brown et al. (1997))

QC = 5.38	(L/h)	cardiac output: $15 \cdot BW^{0.74}$
QS _{Ic} = 0.151		fraction of blood flow to small intestine

Chapter 3

QLc = 0.099	0.25 - QSIc	fraction of blood flow to liver
QRc = 0.51 perfused tissue	0.76 - QSIc - QLc	fraction of blood flow to rapidly
QSc = 0.17 perfused tissue	0.24 - QFc	fraction of blood flow to slowly
QFc = 0.07		fraction of blood flow to fat
QSI = QSIc*QC (calculated)	(L/h)	blood flow to small intestine tissue
QL = QLc*QC	(L/h)	blood flow to liver tissue (calculated)
QR = QRc*QC (calculated)	(L/h)	blood flow to rapidly perfused tissue
QS = QSc*QC (calculated)	(L/h)	blood flow to slowly perfused tissue
QF = QFc*QC	(L/h)	blood flow to fat tissue (calculated)

Physicochemical parameters

partition coefficients, calculated based on QPPR of DeJongh et al. (1997)

ZEN in main model	
PIZEN = 2.64	intestine/blood partition coefficient
PLZEN = 2.64	liver/blood partition coefficient
PRZEN = 2.64	rapidly perfused tissue/blood partition
coefficient	
PSZEN = 0.76	slowly perfused tissue/blood partition
coefficient	
PFZEN = 106.93	fat/blood partition coefficient
α -ZEL in sub-model	
PIaZEL = 2.38	intestine/blood partition coefficient
PLaZEL = 2.38	liver/blood partition coefficient
PRaZEL = 2.38	rapidly perfused tissue/blood partition
coefficient	
PSaZEL = 0.71	slowly perfused tissue/blood partition
coefficient	

PFaZEL = 92.79

fat/blood partition coefficient

absorption/transfer rates

Stomach emptying rate

ksto = 2.8

stomach emptying rate (/h)

reference: Reilly

et al. (1990)

intestinal absorption and transfer rates of ZEN

PappCaco2ZEN=-3.9838

fitted Log Papp, Caco-2 (cm/h) reference: Pfeiffer

et al. (2011)

Log (Papp,*in vivo*) = 0.6836*Log(PappCaco2ZEN)-0.5579

reference:

Sun et al. (2002)

PappZEN=10^{^(0.6836*PappCaco2ZEN-0.5579)}*3600/10

(dm/h)

Vin = 0.0012

volume for each compartment of intestines (L)

SAin = 0.134

surface area (dm²)

kin = 4.17

transfer rate to next compartment within the

intestines (/hr)

kabin1 = PappZEN*SAin

absorption rate constant (L/hr)

Vin1 = Vin

volume of intestine compartment 1 (L)

SAin1 = SAin

surface area of intestine compartment 1 (dm²)

kabin1 = PappZEN*SAin1

absorption rate constant of intestine compartment

1 (L/hr)

kin1 = kin

transfer rate to intestine compartment 2 (/hr)

Vin2 = Vin

volume of intestine compartment 2 (L)

SAin2 = SAin

surface area of intestine compartment 2 (dm²)

kabin2 = PappZEN*SAin2

absorption rate constant of intestine compartment

2 (L/hr)

kin2 = kin

transfer rate to intestine compartment 3 (/hr)

Vin3 = Vin

volume of intestine compartment 3 (L)

SAin3= SAin

surface area of intestine compartment 3 (dm²)

kabin3 = PappZEN*SAin3

absorption rate constant of intestine compartment

3 (L/hr)

kin3 = kin

transfer rate to intestine compartment 4 (/hr)

$V_{in4} = V_{in}$	volume of intestine compartment 4 (L)
$S_{Ain4} = S_{Ain}$	surface area of intestine compartment 4 (dm ²)
$k_{abin4} = P_{appZEN} * S_{Ain4}$	absorption rate constant of intestine compartment 4 (L/hr)
$k_{in4} = k_{in}$	transfer rate to intestine compartment 5 (/hr)
$V_{in5} = V_{in}$	volume of intestine compartment 5 (L)
$S_{Ain5} = S_{Ain}$	surface area of intestine compartment 5 (dm ²)
$k_{abin5} = P_{appZEN} * S_{Ain5}$	absorption rate constant of intestine compartment 5 (L/hr)
$k_{in5} = k_{in}$	transfer rate to intestine compartment 6 (/hr)
$V_{in6} = V_{in}$	volume of intestine compartment 6 (L)
$S_{Ain6} = S_{Ain}$	surface area of intestine compartment 6 (dm ²)
$k_{abin6} = P_{appZEN} * S_{Ain6}$	absorption rate constant of intestine compartment 6 (L/hr)
$k_{in6} = k_{in}$	transfer rate to intestine compartment 7 (hr)
$V_{in7} = V_{in}$	volume of intestine compartment 7 (L)
$S_{Ain7} = S_{Ain}$	surface area of intestine compartment 7 (dm ²)
$k_{abin7} = P_{appZEN} * S_{Ain7}$	absorption rate constant of intestine compartment 7 (L/hr)
$k_{in7} = 0.464$	(/h) transfer rate of ZEN from small intestine to large intestine
reference: Kimura and Higaki (2002)	
$V_{inb} = 0.0338$	volume of large intestine (L) reference: Vdoviaková et al. (2016)
$S_{Ainb} = 1.57$	surface area of large intestine (dm ²) reference: Vdoviaková et al. (2016)
$K_b = P_{appZEN} * S_{Ainb}$	absorption rate constant from the large intestine (L/hr)
$K_b = P_{appZEN} * S_{Ainb}$	absorption rate constant from the large intestine (L/hr)
$\alpha\text{-ZEL}$	
$P_{appCaco2aZEL} = -5.2676$	Log Papp, Caco-2 reference: Pfeiffer et al. (2011)
(cm/h)	

$\text{Log}(\text{Papp}, \text{in vivo}) = 0.6836 * \text{Log}(\text{PappCaco2aZEL}) - 0.5579$ reference: Sun et al. (2002)

$\text{PappaZEL} = 10^{(0.6836 * \text{PappCaco2aZEL} - 0.5579)} * 3600 / 10 \text{ (dm/h)}$

$\text{Vin8} = \text{Vin}$ volume of intestine compartment 7 (L)

$\text{SAin8} = \text{SAinb}$ surface area of intestine compartment 7 (dm²)

$\text{kabin8} = \text{PappaZEL} * \text{SAin8}$ absorption rate constant of α -ZEL from LI to liver (L/hr)

excretion (/h)

$\text{KurZ} = 0.096$ urinary excretion of ZEN reference: Mukherjee et al. (2014)

$\text{KfeZ} = 0.69$ fecal excretion of ZEN reference: Mukherjee et al. (2014)

$\text{KuraZ} = 0.012$ urinary excretion of α -ZEL reference: Mukherjee et al. (2014)

Kinetic parameters

metabolism in small intestine tissue

scaling factors

$\text{S9SI} = 37.1$ small intestinal S9 protein yield (mg S9 protein/gram intestine) reference: (Peters et al., 2016)

$\text{SI} = \text{VSIC} * 1000$ small intestine in body weight (gram/kg BW)

metabolites ZENGLU, unscaled maximum rates of metabolism, (nmol/min/mg S9 protein)

$\text{VmaxSIZENGLUc} = 8.617$ *in vitro*, S9 incubations from this study

metabolites ZENGLU, scaled maximum rates of metabolism, ($\mu\text{mol/h}$)

$\text{VMaxSIZENGLU} = \text{VmaxSIZENGLUc} / 1000 * 60 * \text{S9SI} * \text{SI} * \text{BW}$

metabolites ZENGLU, affinity constants, ($\mu\text{mol/L}$)

$KmSIZENGLU = 6.198$ *in vitro*, S9 incubations from this study

metabolism in large intestine lumen (microbiota compartment)

scaling factors

$VMB = 0.0164$ fraction of feces of BW reference: Hoskins and Zamcheck (1968)

metabolites α -ZEL and β -ZEL, unscaled maximum rates of metabolism, (pmol/h/g faeces)

$V_{maxLIaZELc} = 0.0138$ reference: Mendez-Catala et al. (2020)

$V_{maxLIbZELc} = 0.0084$ reference: Mendez-Catala et al. (2020)

metabolites α -ZEL and β -ZEL, scaled maximum rates of metabolism, (μ mol/h)

$V_{maxLIaZEL} = V_{maxLIaZELc} / 1000000 * 1000 * VMB * BW$

$V_{maxLIbZEL} = V_{maxLIbZELc} / 1000000 * 1000 * VMB * BW$

metabolites α -ZEL and β -ZEL, affinity constants, (μ mol/L)

$KmLIaZEL = 66$ reference: Mendez-Catala et al. (2020)

$KmLIbZEL = 80$ reference: Mendez-Catala et al. (2020)

metabolism in liver

scaling factors

$VLS9 = 143$ liver S9 protein yield (mg S9 protein/gram liver)

reference: Punt et al. (2008)

$L = VLc * 1000$ (gram/kg BW) liver

Part 1: Zearalenone phase I metabolism α -ZEL and β -ZEL formation

metabolites α -ZEL and β -ZEL, unscaled maximum rates of metabolism, (pmol/min/mg S9 protein)

$V_{maxLaZELc} = 32$ reference: Malekinejad et al. (2006)

$V_{maxLbZELc} = 72$ reference: Malekinejad et al. (2006)

metabolites α -ZEL and β -ZEL, scaled maximum rates of metabolism, (μ mol/h)

$V_{maxLaZEL} = V_{maxLaZELc} / 1000000 * 60 * VLS9 * L * BW$

$$V_{\max LbZEL} = V_{\max LbZELc} / 1000000 * 60 * VLS9 * L * BW$$

metabolites α -ZEL and β -ZEL, affinity constants, ($\mu\text{mol/L}$)

$K_{mLaZEL} = 592$ reference: Malekinejad et al. (2006)

$K_{mLbZEL} = 21$ reference: Malekinejad et al. (2006)

Part 2: Zearalenone phase II metabolism-glucuronidation

metabolites ZENGLU, unscaled maximum rates of metabolism, (nmol/min/mg S9 protein)

$V_{\max LZENGLUc} = 7.029$ *in vitro*, S9 incubations from this study

metabolites ZENGLU, scaled maximum rates of metabolism, ($\mu\text{mol/h}$)

$V_{\max LZENGLU} = V_{\max LZENGLUc} / 1000 * 60 * VLS9 * L * BW$

metabolites ZENGLU, affinity constants, ($\mu\text{mol/L}$)

$K_{mLZENGLU} = 6.753$ *in vitro*, S9 incubations from this study

Part 3: α -ZEL phase II metabolism: glucuronidation

metabolites α -ZELGLU, unscaled maximum rates of metabolism, (nmol/min/mg S9 protein)

$V_{\max LaZELGLUc} = 6.963$ *in vitro*, S9 incubations from this study

metabolites α -ZELGLU, scaled maximum rates of metabolism, ($\mu\text{mol/h}$)

$V_{\max LaZELGLU} = V_{\max LaZELGLUc} / 1000 * 60 * VLS9 * L * BW$

metabolites α -ZELGLU, affinity constants, ($\mu\text{mol/L}$)

$K_{mLaZELGLU} = 7.426$ *in vitro*, S9 incubations from this study

=====
Run settings
=====

molecular weight

MWZEN = 318.37

molecular weight ZEN

oral dose

ODOSEmg = 0

(mg/kg bw)

oral

dose, variable

$\text{ODOSEumol} = \text{ODOSEmg} * 1000 / \text{MWZEN} * \text{BW} (\mu\text{mol})$ unit
 change to μmol

IV dose

IVDOSEmg1 = 8 (mg/kg bw) IV dose, variable

$$\text{IVDOSEumol} = \text{IVDOSEmg1} * 1000 / \text{MWZEN} * \text{BW} \quad \text{unit change to } \mu\text{mol}$$

time

$$\text{Starttime} = 0 \quad (\text{h})$$

Stoptime = 24 (h) variable

DTMIN = 1e-6 minimum integration time (DT)

DTMAX = 0.15 maximum integration time (DT)

Main model calculations/dynamics: zearalenone

Stomach

Ast = amount in stomach

$$A_{st}' = -k_{sto} * A_{st}$$

Init Ast = ODOSEumol

small intestine lumen compartment

intestines, divided in 7 compartments

$$A_{in1} = \text{Amount ZEN in intestine compartment 1 } (\mu\text{mol})$$
$$C_{in1} = A_{in1}/V_{in1}$$
$$A_{in1}' = k_{sto} * A_{st} - k_{in1} * A_{in1} - k_{abin1} * C_{in1}$$
$$\text{Init Ain1} = 0$$
$$A_{in2} = \text{Amount ZEN in intestine compartment 2 } (\mu\text{mol})$$
$$C_{in2} = A_{in2}/V_{in2}$$
$$A_{in2'} = k_{in1} * A_{in1} - k_{in2} * A_{in2} - k_{abin2} * C_{in2}$$

Init Ain2 = 0

$$A_{in3} = \text{Amount ZEN in intestine compartment 3 } (\mu\text{mol})$$
$$C_{in3} = A_{in3}/V_{in3}$$
$$A_{in3'} = k_{in2} * A_{in2} - k_{in3} * A_{in3} - k_{abin3} * C_{in3}$$
$$\text{Init Ain3} = 0$$

Ain4 = Amount ZEN in intestine compartment 4 (μmol)

Cin4 = Ain4/Vin4

Ain4' = $\text{kin3} \cdot \text{Ain3} - \text{kin4} \cdot \text{Ain4} - \text{kabin4} \cdot \text{Cin4}$

Init Ain4 = 0

Ain5 = Amount ZEN in intestine compartment 5 (μmol)

Cin5 = Ain5/Vin5

Ain5' = $\text{kin4} \cdot \text{Ain4} - \text{kin5} \cdot \text{Ain5} - \text{kabin5} \cdot \text{Cin5}$

Init Ain5 = 0

Ain6 = Amount ZEN in intestine compartment 6 (μmol)

Cin6 = Ain6/Vin6

Ain6' = $\text{kin5} \cdot \text{Ain5} - \text{kin6} \cdot \text{Ain6} - \text{kabin6} \cdot \text{Cin6}$

Init Ain6 = 0

Ain7 = Amount ZEN in intestine compartment 7 (μmol)

Cin7 = Ain7/Vin7

Ain7' = $\text{kin6} \cdot \text{Ain6} - \text{kin7} \cdot \text{Ain7} - \text{kabin7} \cdot \text{Cin7}$

Init Ain7 = 0

small intestine tissue compartment

ASIZEN: amount of ZEN in small intestinal tissue, (μmol)

ASIZEN' = $\text{kabin1} \cdot \text{Cin1} + \text{kabin2} \cdot \text{Cin2} + \text{kabin3} \cdot \text{Cin3} + \text{kabin4} \cdot \text{Cin4} + \text{kabin5} \cdot \text{Cin5} + \text{kabin6} \cdot \text{Cin6} + \text{kabin7} \cdot \text{Cin7} + \text{QSI} \cdot (\text{CB} - \text{CVSIZEN}) - \text{ASIZENGLU}'$

Init ASIZEN=0

CSIZEN = ASIZEN/VSIZEN

CVSIZEN = CSIZEN/PIZEN

ASIZENGLU: amount of ZEN metabolized to metabolite ZENGLU, (μmol)

ASIZENGLU' = $\frac{\text{VmaxSIZENGLU} \cdot \text{CVSIZEN}}{\text{KmSIZENGLU} + \text{CVSIZEN}}$

Init ASIZENGLU=0

large intestine lumen compartment: microbial activity

ALIZEN: amount of ZEN in large intestine lumen, (μmol)

ALIZEN' = $\text{kin7} \cdot \text{Ain7} - \text{ALIZEL}' - \text{ALIZEL}' - \text{Kb} \cdot \text{CLIZEN} - \text{KfeZ} \cdot \text{ALIZEN}$

Init ALIZEN = 0

$$CLIZEN = ALIZEN / (VMB * BW)$$

AL_{Ia}ZEL: amount of α -ZEL formed due to gut microbial activity, (μ mol)

$$AL_{Ia}ZEL' = V_{maxL_{Ia}ZEL} * CLIZEN / (K_{mL_{Ia}ZEL} + CLIZEN)$$

$$Init\ AL_{Ia}ZEL = 0$$

AL_{Ib}ZEL: amount of β -ZEL formed due to gut microbial activity, (μ mol)

$$AL_{Ib}ZEL' = V_{maxL_{Ib}ZEL} * CLIZEN / (K_{mL_{Ib}ZEL} + CLIZEN)$$

$$Init\ AL_{Ib}ZEL = 0$$

liver compartment

ALZEN: amount of ZEN in liver, (μ mol)

$$ALZEN' = QL * CB + QSI * CVSIZEN - (QL + QSI) * CVLZEN - AL_{aZEL}' - AL_{bZEL}' - ALZENGLU' + K_b * CLIZEN$$

$$Init\ ALZEN = 0$$

$$CLZEN = ALZEN / VL$$

$$CVLZEN = CLZEN / PLZEN$$

AL_aZEL: amount of ZEN metabolized to metabolite α -ZEL in liver, (μ mol)

$$AL_{aZEL}' = V_{maxL_{aZEL}} * CVLZEN / (K_{mL_{aZEL}} + CVLZEN)$$

$$Init\ AL_{aZEL} = 0$$

AL_bZEL: amount of ZEN metabolized to metabolite β -ZEL in liver, (μ mol)

$$AL_{bZEL}' = V_{maxL_{bZEL}} * CVLZEN / (K_{mL_{bZEL}} + CVLZEN)$$

$$Init\ AL_{bZEL} = 0$$

ALZENGLU: amount of ZEN metabolized to metabolite ZENGLU in liver, (μ mol)

$$ALZENGLU' = V_{maxLZENGLU} * CVLZEN / (K_{mLZENGLU} + CVLZEN)$$

$$Init\ ALZENGLU = 0$$

fat compartment

AF = amount of ZEN in fat tissue, (μ mol)

$$AF' = QF * (CB - CVF)$$

$$Init\ AF = 0$$

$$CF = AF / VF$$

$$CVF = CF / PFZEN$$

rapidly perfused tissue

AR = amount of ZEN in rapidly perfused tissue, (μ mol)

$$AR' = QR*(CB-CVR)$$

$$\text{Init } AR = 0$$

$$CR = AR/VR$$

$$CVR = CR/PRZEN$$

slowly perfused tissue

AS = amount of ZEN in slowly perfused tissue, (μmol)

$$AS' = QS*(CB-CVS)$$

$$\text{Init } AS = 0$$

$$CS = AS/VS$$

$$CVS = CS/PSZEN$$

blood compartment

AB: amount of ZEN in blood, (μmol)

$$AB' = (QL+QSI)*CVLZEN + QF*CVF + QS*CVS + QR*CVR - QC*CB - KurZ*AB$$

$$\text{Init } AB = IVDOSEumol$$

$$CB = AB/VB$$

$$AUC' = AB$$

$$\text{Init } AUC = 0$$

urinary excretion

$$AZur' = KurZ*AB$$

$$\text{Init } AZur = 0$$

Main model: mass balance calculation

$$\text{Total} = ODOSEumol + IVDOSEumol$$

$$\begin{aligned} \text{Calculated} = & Ast + Ain1 + Ain2 + Ain3 + Ain4 + Ain5 + Ain6 + Ain7 + ASIZEN \\ & + ASIZENGLU + ALIZEN + ALIaZEL + ALIbZEL + ALZEN + ALaZEL + \\ & ALbZEL + ALZENGLU + AF + AR + AS + AB + AZur + AZfe \end{aligned}$$

$$\text{ERROR} = ((\text{Total} - \text{Calculated}) / \text{Total} + 1E-30) * 100$$

$$\text{MASSBBAL} = \text{Total} - \text{Calculated} + 1$$

Sub-model calculations/dynamics: α -ZEL

large intestine lumen compartment

ARLIaZEL = amount of α -ZEL in large intestine lumen, (μmol)

$$\text{ARLIaZEL}' = \text{ALIaZEL}' - \text{kabin8} * (\text{ARLIaZEL} / \text{VMB} * \text{BW}) - \text{Kfeaz} * \text{ARLIaZEL}$$

$$\text{init ARLIaZEL} = 0$$

liver compartment

ARLaZEL: amount of α -ZEL in liver, (μmol)

$$\text{ARLaZEL}' = \text{ALaZEL}' + \text{kabin8} * (\text{ARLIaZEL} / \text{VMB} * \text{BW}) + (\text{QL} + \text{QSI}) * \text{CBaZEL} - (\text{QL} + \text{QSI}) * \text{CVLaZEL} - \text{ALaZELGLU}'$$

Init ARLaZEL = 0

$$\text{CLaZEL} = \text{ARLaZEL} / \text{VL}$$

$$\text{CVLaZEL} = \text{CLaZEL} / \text{PLaZEL}$$

ALaZELGLU: amount of α -ZEL glucuronide in liver

$$\text{ALaZELGLU}' = \text{VmaxLaZELGLU} * \text{CVLaZEL} / (\text{KmLaZELGLU} + \text{CVLaZEL})$$

Init ALaZELGLU = 0

$$\text{ALaZELGLUmg}' = \text{ALaZELGLU} * \text{MWZEN} / 1000 * \text{BW}$$

Init ALaZELGLUmg = 0

fat compartment

AFaZEL: amount of α -ZEL in fat tissue, (μmol)

$$\text{AFaZEL}' = \text{QF} * (\text{CBaZEL} - \text{CVFaZEL})$$

Init AFaZEL = 0

$$\text{CFaZEL} = \text{AFaZEL} / \text{VF}$$

$$\text{CVFaZEL} = \text{CFaZEL} / \text{PFaZEL}$$

rapidly perfused tissue

ARaZEL: amount of α -ZEL in rapidly perfused tissue, (μmol)

$$\text{ARaZEL}' = \text{QR} * (\text{CBaZEL} - \text{CVRaZEL})$$

Init ARaZEL = 0

$$\text{CRaZEL} = \text{ARaZEL} / \text{VR}$$

$$\text{CVRaZEL} = \text{CRaZEL} / \text{PRaZEL}$$

slowly perfused tissue

ASaZEL: amount of α -ZEL in slowly perfused tissue, (μmol)

$$\text{ASaZEL}' = \text{QS} * (\text{CBaZEL} - \text{CVSaZEL})$$

Init ASaZEL = 0

$$\text{CSaZEL} = \text{ASaZEL} / \text{VS}$$

$$\text{CVSaZEL} = \text{CSaZEL}/\text{PSaZEL}$$

blood compartment

ABaZEL: amount of α -ZEL in blood, (μmol)

$$\text{ABaZEL}' = (\text{QL} + \text{QSI}) * \text{CVLaZEL} + \text{QF} * \text{CVFaZEL} + \text{QR} * \text{CVRaZEL} + \text{QS} * \text{CVSaZEL} - \text{QC} * \text{CBaZEL} - \text{KuraZ} * \text{ABaZEL}$$

$$\text{Init ABaZEL} = 0$$

$$\text{CBaZEL} = \text{ABaZEL}/\text{VB}$$

$$\text{AUCaZEL}' = \text{ABaZEL}$$

$$\text{Init AUCaZEL} = 0$$

urinary excretion

$$\text{AaZur}' = \text{KurZ} * \text{ABaZEL}$$

$$\text{Init AaZur} = 0$$

Model Code for Human

Physiological parameters

Tissue volumes, reference: Brown et al. (1997)

BW= 70	(Kg)	body weight rat
VS _{Ic} = 0.009		fraction of small intestine
VL _c = 0.026		fraction of liver tissue
VR _c = 0.041	;0.076-VS _{Ic} -VL _c	fraction of rapidly perfused tissue
VSc = 0.596	;0.81-VFc	fraction of slowly perfused tissue
VF _c = 0.214		fraction of fat tissue
VB _c = 0.074		fraction of blood

VS _I = VS _{Ic} *BW (calculated)	(L or Kg)	volume of small intestine tissue
VL = VL _c *BW	(L or Kg)	volume of liver tissue (calculated)
VR = VR _c *BW (calculated)	(L or Kg)	volume of rapidly perfused tissue
VS = VSc*BW (calculated)	(L or Kg)	volume of slowly perfused tissue
VF = VF _c *BW	(L or Kg)	volume of fat tissue (calculated)
VB = VB _c *BW	(L or Kg)	volume of blood (calculated)

Blood flow rates, reference: Brown et al. (1997)

QC = 347.9	(L/h)	cardiac output: $15 \cdot BW^{0.74}$
QS _{Ic} = 0.181 intestine		fraction of blood flow to small intestine
QL _c = 0.046	0.227 - QS _{Ic}	fraction of blood flow to liver
QR _c = 0.473 rapidly perfused tissue	0.7 - QS _{Ic} - QL _c	fraction of blood flow to rapidly perfused tissue

Rat and human PBK model of ZEN

QSc = 0.248	0.3 - QFc	fraction of blood flow to slowly perfused tissue
QFc = 0.052		fraction of blood flow to fat
QSI = QSIc*QC (calculated)	(L/h)	blood flow to small intestine tissue
QL = QLc*QC	(L/h)	blood flow to liver tissue (calculated)
QR = QRc*QC (calculated)	(L/h)	blood flow to rapidly perfused tissue
QS = QSc*QC (calculated)	(L/h)	blood flow to slowly perfused tissue
QF = QFc*QC	(L/h)	blood flow to fat tissue (calculated)

Physicochemical parameters

partition coefficients, calculated based on QPPR of DeJongh et al. (1997)

ZEN in main model

PIZEN = 6.56	intestine/blood partition coefficient
PLZEN = 6.56	liver/blood partition coefficient
PRZEN = 6.56	rapidly perfused tissue/blood partition coefficient
PSZEN = 4.25	slowly perfused tissue/blood partition coefficient
PFZEN = 134.86	fat/blood partition coefficient

 α -ZEL in sub-model

PIaZEL = 6.11	intestine/blood partition coefficient
PLaZEL = 6.11	liver/blood partition coefficient
PRaZEL = 6.11	rapidly perfused tissue/blood partition coefficient
PSaZEL = 3.99	slowly perfused tissue/blood partition coefficient
PFaZEL = 131.62	fat/blood partition coefficient

absorption/transfer rates

Stomach emptying rate

Chapter 3

$k_{sto} = 2.8$ stomach emptying rate (/h) reference: Reilly et al. (1990)

intestinal absorption and transfer rates of ZEN

$Papp, \text{Caco-2 ZEN} = 10.3$ ($\times 10^{-5}$ cm/sec) fitted apparent *in vitro*, from Caco-2 reference: Pfeiffer et al. (2011)

$PappCaco2ZEN = -4.9829$ Log $Papp, \text{Caco-2}$

$\text{Log}(Papp, \text{in vivo}) = 0.6836 * \text{Log}(PappCaco2ZEN) - 0.5579$ reference: Sun et al. (2002)

$PappZEN = 10^{(0.6836 * PappCaco2ZEN - 0.5579)} * 3600 / 10$ (dm/h)

$V_{in} = 1.29$ volume for each compartment of intestines (L)
 $SA_{in} = 10.3$ surface area (dm²)
 $k_{in} = 2.19$ transfer rate to next compartment within the intestines (/hr)
 $k_{abin1} = PappZEN * SA_{in}$ absorption rate constant (L/hr)

$V_{in1} = V_{in}$ volume of intestine compartment 1 (L)
 $SA_{in1} = SA_{in}$ surface area of intestine compartment 1 (dm²)
 $k_{abin1} = PappZEN * SA_{in1}$ absorption rate constant of intestine compartment 1 (L/hr)
 $k_{in1} = k_{in}$ transfer rate to intestine compartment 2 (/hr)

$V_{in2} = V_{in}$ volume of intestine compartment 2 (L)
 $SA_{in2} = SA_{in}$ surface area of intestine compartment 2 (dm²)
 $k_{abin2} = PappZEN * SA_{in2}$ absorption rate constant of intestine compartment 2 (L/hr)
 $k_{in2} = k_{in}$ transfer rate to intestine compartment 3 (/hr)

$V_{in3} = V_{in}$ volume of intestine compartment 3 (L)
 $SA_{in3} = SA_{in}$ surface area of intestine compartment 3 (dm²)
 $k_{abin3} = PappZEN * SA_{in3}$ absorption rate constant of intestine compartment 3 (L/hr)
 $k_{in3} = k_{in}$ transfer rate to intestine compartment 4 (/hr)

$V_{in4} = V_{in}$ volume of intestine compartment 4 (L)
 $SA_{in4} = SA_{in}$ surface area of intestine compartment 4 (dm²)

$k_{\text{abin4}} = \text{PappZEN} * \text{SA}_{\text{in4}}$ absorption rate constant of intestine compartment 4 (L/hr)

$k_{\text{in4}} = k_{\text{in}}$ transfer rate to intestine compartment 5 (/hr)

$V_{\text{in5}} = V_{\text{in}}$ volume of intestine compartment 5 (L)

$\text{SA}_{\text{in5}} = \text{SA}_{\text{in}}$ surface area of intestine compartment 5 (dm²)

$k_{\text{abin5}} = \text{PappZEN} * \text{SA}_{\text{in5}}$ absorption rate constant of intestine compartment 5 (L/hr)

$k_{\text{in5}} = k_{\text{in}}$ transfer rate to intestine compartment 6 (/hr)

$V_{\text{in6}} = V_{\text{in}}$ volume of intestine compartment 6 (L)

$\text{SA}_{\text{in6}} = \text{SA}_{\text{in}}$ surface area of intestine compartment 6 (dm²)

$k_{\text{abin6}} = \text{PappZEN} * \text{SA}_{\text{in6}}$ absorption rate constant of intestine compartment 6 (L/hr)

$k_{\text{in6}} = k_{\text{in}}$ transfer rate to intestine compartment 7 (/hr)

$V_{\text{in7}} = V_{\text{in}}$ volume of intestine compartment 7 (L)

$\text{SA}_{\text{in7}} = \text{SA}_{\text{in}}$ surface area of intestine compartment 7 (dm²)

$k_{\text{abin7}} = \text{PappZEN} * \text{SA}_{\text{in7}}$ absorption rate constant of intestine compartment 7 (L/hr)

$k_{\text{in7}} = 0.464$ transfer rate of ZEN from small intestine to large intestine (/h) reference: Kimura and Higaki (2002)

$\text{SA}_{\text{inb}} = 47.12$ surface area of large intestine (dm²) reference: Vdovíaková et al. (2016)

$K_{\text{b}} = \text{PappZEN} * \text{SA}_{\text{inb}}$ absorption rate constant from the large intestine (L/hr)

$\alpha\text{-ZEL}$

$\text{Papp, Caco-2 } \alpha\text{-ZEL} = 5.4$ ($\times 10^{-6}$ cm/sec), apparent *in vitro*, from Caco-2 reference: Pfeiffer et al. (2011)

$\text{PappCaco2aZEL} = -5.2676$ Log Papp, Caco-2

$\text{Log (Papp, in vivo)} = 0.6836 * \text{Log(PappCaco2aZEL)} - 0.5579$ reference: Sun et al. (2002)

$\text{PappaZEL} = 10^{(0.6836 * \text{PappCaco2aZEL} - 0.5579)} * 3600 / 10$ (dm/h)

$\text{SA}_{\text{in8}} = \text{SA}_{\text{inb}}$ surface area of intestine compartment 7 (dm²)

Chapter 3

kabin8 = PappaZEL*SAin8 absorption rate constant of α -ZEL from LI to liver(L/hr)

excretion (/h)

KurZ = 0.096 urinary excretion of ZEN reference: Mukherjee et al. (2014)

KfeZ = 0.024 fecal excretion of ZEN reference: Mukherjee et al. (2014)

KuraZ = 0.015 urinary excretion of α -ZEL reference: Mukherjee et al. (2014)

KfeG = 0.024 urinary excretion of ZENGLU reference: Mukherjee et al. (2014)

Kinetic parameters

metabolism of small intestine tissue

scaling factors

S9SI= 35.2 small intestinal S9 protein yield (mg S9 protein/gram intestine) reference: (Peters et al., 2016)

SI=VSIC*1000 small intestine in body weight (gram/kg BW)

metabolites ZENGLU, unscaled maximum rates of metabolism, (nmol/min/mg S9 protein)

VmaxSIZENGLUc= 0.491 *in vitro*, S9 incubations from this study

metabolites ZENGLU, scaled maximum rates of metabolism, (μ mol/h)

VMaxSIZENGLU = VmaxSIZENGLUc/1000*60*S9SI*SI*BW

metabolites ZENGLU, affinity constants, (μ mol/L)

KmSIZENGLU = 1.174 *in vitro*, S9 incubations from this study

metabolism of large intestine lumen (microbiota compartment)

scaling factors

VMB = 0.0018 fraction of faeces of BW, reference: Rose et al. (2015)

metabolites α -ZEL and β -ZEL, unscaled maximum rates of metabolism, (pmol/h/g faeces)

VmaxLlaZELc=0.054 *in vitro*, anaerobic rat fecal incubations

VmaxLibZELc= 0.0108 *in vitro*, anaerobic rat fecal incubations

metabolites α -ZEL and β -ZEL, scaled maximum rates of metabolism, (μ mol/h)

VmaxLlaZEL= VmaxLlaZELc/1000000*1000 *VMB*BW

VmaxLibZEL= VmaxLibZELc/1000000*1000 *VMB*BW

metabolites α -ZEL and β -ZEL, affinity constants, (μ mol/L)

KmLlaZEL = 135 *in vitro*, anaerobic rat fecal incubations

KmLibZEL = 163 *in vitro*, anaerobic rat fecal incubations

metabolism of liver

scaling factors

VLS9 = 120.7 liver S9 protein yield, (mg S9 protein/gram liver)
reference: Cubitt et al. (2011)

L=VLc*1000 (gram/kg BW) liver

Part 1: Zearalenone phase I metabolism α -ZEL and β -ZEL formation

metabolites α -ZEL and β -ZEL, unscaled maximum rates of metabolism, (pmol/min/mg S9 protein)

VmaxLaZELc= 358.7 reference: Malekinejad et al. (2006)

VmaxLbZELc= 209.3 reference: Malekinejad et al. (2006)

metabolites α -ZEL and β -ZEL, scaled maximum rates of metabolism, (μ mol/h)

VmaxLaZEL= VmaxLaZELc/1000000*60* VLS9 *L*BW

VmaxLbZEL= VmaxLbZELc/1000000*60* VLS9 *L*BW

metabolites α -ZEL and β -ZEL, affinity constants, (μ mol/L)

KmLaZEL = 9 reference: Mendez-Catala et al. (2020)

KmLbZEL = 23 reference: Mendez-Catala et al. (2020)

Part 2: Zearalenone phase II metabolism-glucuronidation

metabolites ZENGLU, unscaled maximum rates of metabolism, (nmol/min/mg S9 protein)

$V_{\max}LZENGLU=2.97$ *in vitro*, S9 incubations from this study

metabolites ZENGLU, scaled maximum rates of metabolism, (μmol/h)

$V_{\max}LZENGLU = V_{\max}LZENGLUc / 1000 * 60 * VLS9 * L * BW$

metabolites ZENGLU, affinity constants, (μmol/L)

$KmLZENGLU = 2.043$ *in vitro*, S9 incubations from this study

Part 3: α-ZEL phase II metabolism: glucuronidation

metabolites α-ZELGLU, unscaled maximum rates of metabolism, (nmol/min/mg S9 protein)

$V_{\max}LaZELGLUc= 2.983$ *in vitro*, S9 incubations from this study

metabolites α-ZELGLU, scaled maximum rates of metabolism, (μmol/h)

$V_{\max}LaZELGLU = V_{\max}LaZELGLUc / 1000 * 60 * VLS9 * L * BW$

metabolites α-ZELGLU, affinity constants, (μmol/L)

$KmLaZELGLU = 2.415$ *in vitro*, S9 incubations from this study

Run settings

molecular weight

$MWZEN = 318.37$

molecular weight ZEN

oral dose

$ODOSEmg = 8$ (mg/kg bw) oral dose, variable

$ODOSEumol= ODOSEmg * 1000 / MWZEN * BW$ (μmol) unit change to μmol

time

$Starttime = 0$ (h) $Stoptime = 24$ (h) variable

DTMIN = 1e-6 minimum integration time (DT)
 DTMAX = 0.15 maximum integration time (DT)

Main model calculations/dynamics: zearalenone

 Stomach

Ast = amount in stomach

Ast' = -ksto*Ast

Init Ast = 0

 small intestine lumen compartment

intestines, divided in 7 compartments

Ain1 = Amount ZEN in intestine compartment 1 (μmol)

Cin1 = Ain1/Vin1

Ain1' = ksto*Ast - kin1*Ain1 - kabin1*Cin1

Init Ain1 = 0

Ain2 = Amount ZEN in intestine compartment 2 (μmol)

Cin2 = Ain2/Vin2

Ain2' = kin1*Ain1 - kin2*Ain2 - kabin2*Cin2

Init Ain2 = 0

Ain3 = Amount ZEN in intestine compartment 3 (μmol)

Cin3 = Ain3/Vin3

Ain3' = kin2*Ain2 - kin3*Ain3 - kabin3*Cin3

Init Ain3 = 0

Ain4 = Amount ZEN in intestine compartment 4 (μmol)

Cin4 = Ain4/Vin4

Ain4' = kin3*Ain3 - kin4*Ain4 - kabin4*Cin4

Init Ain4 = 0

Ain5 = Amount ZEN in intestine compartment 5 (μmol)

Cin5 = Ain5/Vin5

Ain5' = kin4*Ain4 - kin5*Ain5 - kabin5*Cin5

Init Ain5 = 0

Ain6= Amount ZEN in intestine compartment 6 (μmol)

Cin6 = Ain6/Vin6

Ain6' = kin5*Ain5 - kin6*Ain6 - kabin6*Cin6

Init Ain6 = 0

Ain7= Amount ZEN in intestine compartment 7 (μmol)

Cin7 = Ain7/Vin7

Ain7' = kin6*Ain6 - kin7*Ain7 - kabin7*Cin7

Init Ain7 = 0

small intestine tissue compartment

ASIZEN: amount of ZEN in small intestinal tissue, (μmol)

ASIZEN' = kabin1*Cin1+ kabin2*Cin2+ kabin3*Cin3+ kabin4*Cin4+
kabin5*Cin5+ kabin6*Cin6+ kabin7*Cin7+ QSI*(CB- CVSIZEN) - ASIZENGLU'

Init ASIZEN=0

CSIZEN = ASIZEN/VSIZEN

CVSIZEN = CSIZEN/PIZEN

ASIZENGLU: amount of ZEN metabolized to metabolite ZENGLU, (μmol)

ASIZENGLU' = VmaxSIZENGLU*CVSIZEN/(KmSIZENGLU+
CVSIZEN)

Init ASIZENGLU=0

large intestine lumen compartment: microbial activity

ALIZEN: amount of ZEN in large intestine lumen, (μmol)

ALIZEN' = kin7*Ain7 - ALIaZEL' - ALIbZEL' - Kb*CLIZEN -
KfeZ*ALIZEN

Init ALIZEN = 0

CLIZEN = ALIZEN/ (VMB*BW)

ALIaZEL: amount of α-ZEL formed due to gut microbial activity, (μmol)

ALIaZEL' = VmaxLIaZEL*CLIZEN/(KmLIaZEL + CLIZEN)

Init ALIaZEL=0

ALIbZEL: amount of β-ZEL formed due to gut microbial activity, (μmol)

ALIbZEL' = VmaxLIbZEL * CLIZEN/(KmLIbZEL + CLIZEN)

Init ALIbZEL=0

liver compartment

ALZEN: amount of ZEN in liver, (μmol)

$$\text{ALZEN}' = \text{QL} * \text{CB} + \text{QSI} * \text{CVSIZEN} - (\text{QL} + \text{QSI}) * \text{CVLZEN} - \text{ALaZEL}' - \text{ALbZEL}' - \text{ALZENGLU}' + \text{Kb} * \text{CLZEN}$$

$$\text{Init ALZEN} = 0$$

$$\text{CLZEN} = \text{ALZEN} / \text{VL}$$

$$\text{CVLZEN} = \text{CLZEN} / \text{PLZEN}$$

ALaZEL: amount of ZEN metabolized to metabolite α -ZEL in liver, (μmol)

$$\text{ALaZEL}' = \text{VmaxLaZEL} * \text{CVLZEN} / (\text{KmLaZEL} + \text{CVLZEN})$$

$$\text{Init ALaZEL} = 0$$

ALbZEL: amount of ZEN metabolized to metabolite β -ZEL in liver, (μmol)

$$\text{ALbZEL}' = \text{VmaxLbZEL} * \text{CVLZEN} / (\text{KmLbZEL} + \text{CVLZEN})$$

$$\text{Init ALbZEL} = 0$$

ALZENGLU: amount of ZEN metabolized to metabolite ZENGLU in liver, (μmol)

$$\text{ALZENGLU}' = \text{VmaxLZENGLU} * \text{CVLZEN} / (\text{KmLZENGLU} + \text{CVLZEN})$$

$$\text{Init ALZENGLU} = 0$$

fat compartment

AF = amount of ZEN in fat tissue, (μmol)

$$\text{AF}' = \text{QF} * (\text{CB} - \text{CVF})$$

$$\text{Init AF} = 0$$

$$\text{CF} = \text{AF} / \text{VF}$$

$$\text{CVF} = \text{CF} / \text{PFZEN}$$

rapidly perfused tissue

AR = amount of ZEN in rapidly perfused tissue, (μmol)

$$\text{AR}' = \text{QR} * (\text{CB} - \text{CVR})$$

$$\text{Init AR} = 0$$

$$\text{CR} = \text{AR} / \text{VR}$$

$$\text{CVR} = \text{CR} / \text{PRZEN}$$

slowly perfused tissue

AS = amount of ZEN in slowly perfused tissue, (μmol)

$$\text{AS}' = \text{QS} * (\text{CB} - \text{CVS})$$

$$\text{Init AS} = 0$$

$$\text{CS} = \text{AS} / \text{VS}$$

$$\text{CVS} = \text{CS} / \text{PSZEN}$$

Chapter 3

blood compartment

AB: amount of ZEN in blood, (μmol)

$$\text{AB}' = (\text{QL} + \text{QSI}) * \text{CVLZEN} + \text{QF} * \text{CVF} + \text{QS} * \text{CVS} + \text{QR} * \text{CVR} - \text{QC} * \text{CB} - \text{KurZ} * \text{AB}$$

$$\text{Init AB} = 0$$

$$\text{CB} = \text{AB} / \text{VB}$$

$$\text{AUC}' = \text{AB}$$

$$\text{Init AUC} = 0$$

urinary excretion

$$\text{AZur}' = \text{KurZ} * \text{AB}$$

$$\text{Init AZur} = 0$$

=====

Main model: mass balance calculation

=====

$$\text{Total} = \text{ODOSEumol}$$

$$\begin{aligned} \text{Calculated} = & \text{Ast} + \text{Ain1} + \text{Ain2} + \text{Ain3} + \text{Ain4} + \text{Ain5} + \text{Ain6} + \text{Ain7} + \text{ASIZEN} \\ & + \text{ASIZENGLU} + \text{ALIZEN} + \text{ALIaZEL} + \text{ALIbZEL} + \text{ALZEN} + \text{ALaZEL} + \\ & \text{ALbZEL} + \text{ALZENGLU} + \text{AF} + \text{AR} + \text{AS} + \text{AB} + \text{AZur} + \text{AZfe} \end{aligned}$$

$$\text{ERROR} = ((\text{Total} - \text{Calculated}) / \text{Total} + 1\text{E-}30) * 100$$

$$\text{MASSBBAL} = \text{Total} - \text{Calculated} + 1$$

=====

Sub-model calculations/dynamics: α -ZEL

=====

large intestine lumen compartment

ARLIaZEL = amount of α -ZEL in large intestine lumen, (μmol)

$$\text{ARLIaZEL}' = \text{ALIaZEL}' - \text{kabin8} * (\text{ARLIaZEL} / \text{VMB} * \text{BW}) - \text{Kfeaz} * \text{ARLIaZEL}$$

$$\text{init ARLIaZEL} = 0$$

liver compartment

ARLaZEL: amount of α -ZEL in liver, (μmol)

$$\text{ARLaZEL}' = \text{ALaZEL}' + \text{kabin8} * (\text{ARLIaZEL} / \text{VMB} * \text{BW}) + (\text{QL} + \text{QSI}) * \text{CBaZEL} - (\text{QL} + \text{QSI}) * \text{CVLaZEL} - \text{ALaZELGLU}'$$

$$\text{Init ARLaZEL} = 0$$

$$\text{CLaZEL} = \text{ARLaZEL} / \text{VL}$$

$$\text{CVLaZEL} = \text{CLaZEL} / \text{PLaZEL}$$

ALaZELGLU: amount of α -ZEL glucuronide in liver

$$ALaZELGLU' = V_{\max}LaZELGLU * CVLaZEL / (K_mLaZELGLU + CVLaZEL)$$

$$\text{Init } ALaZELGLU = 0$$

$$ALaZELGLUm_g' = ALaZELGLU * MWZEN / 1000 * BW$$

$$\text{Init } ALaZELGLUm_g = 0$$

fat compartment

AFaZEL: amount of α -ZEL in fat tissue, (μmol)

$$AFaZEL' = QF * (CBaZEL - CVFaZEL)$$

$$\text{Init } AFaZEL = 0$$

$$CFaZEL = AFaZEL / VF$$

$$CVFaZEL = CFaZEL / PFaZEL$$

rapidly perfused tissue

ARaZEL: amount of α -ZEL in rapidly perfused tissue, (μmol)

$$ARaZEL' = QR * (CBaZEL - CVRaZEL)$$

$$\text{Init } ARaZEL = 0$$

$$CRaZEL = ARaZEL / VR$$

$$CVRaZEL = CRaZEL / PRaZEL$$

slowly perfused tissue

ASaZEL: amount of α -ZEL in slowly perfused tissue, (μmol)

$$ASaZEL' = QS * (CBaZEL - CVSaZEL)$$

$$\text{Init } ASaZEL = 0$$

$$CSaZEL = ASaZEL / VS$$

$$CVSaZEL = CSaZEL / PSaZEL$$

blood compartment

ABaZEL: amount of α -ZEL in blood, (μmol)

$$ABaZEL' = (QL + QSI) * CVLaZEL + QF * CVFaZEL + QR * CVRaZEL + QS * CVSaZEL - QC * CBaZEL - K_{\text{uraZ}} * ABaZEL$$

$$\text{Init } ABaZEL = 0$$

$$CBaZEL = ABaZEL / VB$$

$$AUCaZEL' = ABaZEL$$

$$\text{Init } AUCaZEL = 0$$

urinary excretion

Chapter 3

$$AaZur' = KurZ * ABaZEL$$

$$Init\ AaZur = 0$$

fecal excretion

$$AaZfe' = KfeaZ * ARLIaZEL$$

$$Init\ AaZfe = 0$$

=====
Sub-model calculations for ZENG excretion
=====

ZEN and α -ZEL-glucuronide available for recirculation and urinary excretion
(Based on model for BPA by Teeguarden et al. (2005) and Yang et al. (2013))

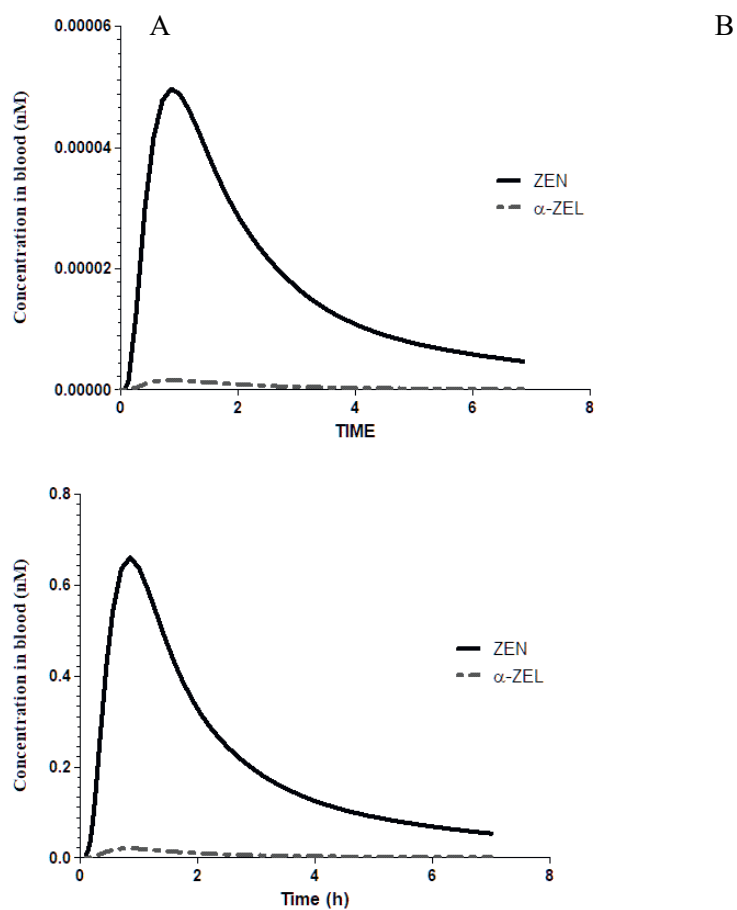
Calculations for urinary excretion of the glucuronides assuming 90% is available for
excretion via urine

$$ADG' = 0.9 * ALZENGLU - KurG * ADG$$

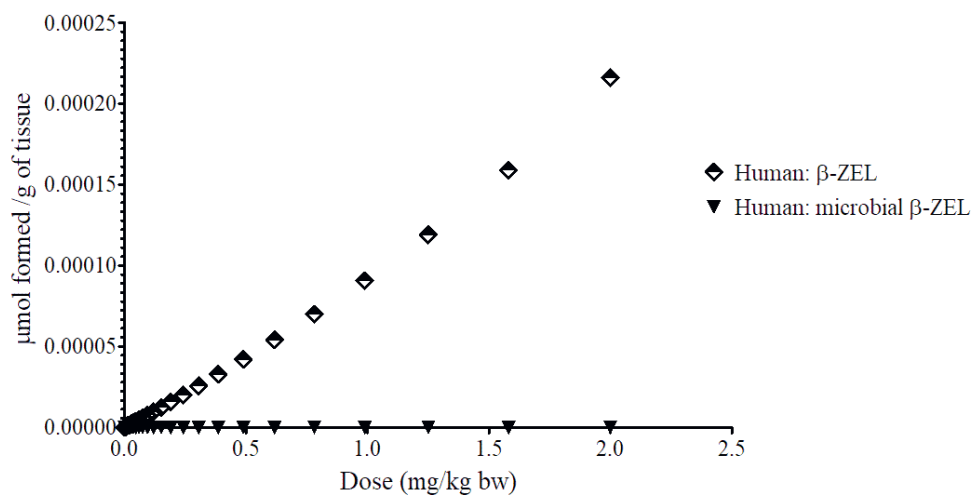
$$Init\ ADG = 0$$

$$AZGur' = KurG * ADG' \quad \text{Amount of ZEN-glucuronide excreted in urine}$$

$$Init\ AZGur = 0$$



Supplementary Figure 3.1. PBK model predicted time dependent blood concentration of ZEN and α -ZEL in human upon oral doses of 1.43×10^{-4} and 1.43 mg/kg bw.



Supplementary Figure 3.2. Predicted formation of α -ZEL in liver and from microbial metabolism at different dose levels in humans.

Supplementary Table 3.1. Glucuronidation of ZEN in small intestinal tissue and liver in rats and humans presented as the percentage of oral dose, after 2 hours after oral dosing

Species	Small intestinal	Liver	Total
Rat	92.3	7.6	99.9
Human	75.8	11.3	87.1

Chapter 4

Interindividual differences in the hepatic and intestinal microbial metabolism of zearalenone characterized by physiologically- based kinetic (PBK) modelling linked to Monte Carlo simulation

*Diana M. Mendez-Catala, Loïs Hiltjesdam &
Ivonne M.C.M. Rietjens*

In preparation

Abstract

Zearalenone (ZEN) is a mycotoxin commonly present in grains such as maize, wheat and oats. ZEN is known to cause reproductive disorders with substantial interspecies and potentially also interindividual differences in sensitivity. These differences may in part be linked to differences in the metabolism of ZEN. In the liver and for the intestinal microbiome, the major biotransformation pathway of ZEN is the reduction to α -zearalenol (α -ZEL), which is a more potent estrogen, and β -zearalenol (β -ZEL) which is less potent. The aim of the present study was to quantify the consequences of interindividual differences in bioactivation and detoxification of ZEN by physiologically-based kinetic (PBK) modelling linked to Monte Carlo simulation. To this end the interindividual variation in V_{\max} and K_m of α -ZEL and β -ZEL formation by intestinal microbiota or liver samples were assessed, each for a group of 20 individuals providing the input parameters for the PBK modeling and Monte Carlo simulation. The results obtained provided a distribution for the blood levels (C_{\max}) of ZEN and its metabolites from which a chemical-specific adjustment factor (CSAF) for human interindividual differences in kinetics was derived. The CSAF thus obtained indicated that use of the default HK_{UF} is adequately protective for a healthy adult population. This study demonstrates the strength of an *in vitro-in silico* approach to characterize inter-individual variation in kinetics of ZEN enabling evaluation of the uncertainty factors for the risk assessment of ZEN.

4.1 Introduction

The mycotoxin zearalenone (ZEN), produced by *Fusarium spp.* is present commonly in grains such as maize, wheat and oats (EFSA, 2011). Oral exposure to high levels of ZEN causes reproductive disorders such as infertility, abnormal lactation and vaginal prolapses in pigs (Mirocha & Christensen, 1974). Species differences observed in the toxicity of ZEN described in literature have been partly linked to differences in the metabolism of ZEN (EFSA, 2011). A major biotransformation pathway of ZEN is the enzymatic reduction of ZEN to α -zearalenol (α -ZEL) and β -zearalenol (β -ZEL) (EFSA, 2011; Fitzpatrick *et al.*, 1988). In the liver, the enzymes 3 α - and 3 β -hydroxysteroid dehydrogenases (HSDs) catalyze the conversion of ZEN to α -ZEL and β -ZEL, respectively, by reducing the keto group at the 7' position, resulting in a hydroxylated metabolite (Figure 4.1).

Upon absorption, ZEN and its metabolites are distributed to various reproductive organs (Liang *et al.*, 2015; Mally *et al.*, 2016). Due to the structural similarity of ZEN and its metabolites to the natural estrogen 17 β -estradiol (E2), they can act as endocrine active chemicals (Takemura *et al.*, 2007). This activity has been linked to binding of ZEN and its metabolites to estrogen receptors (ER), acting as agonist (ER- α) or partial agonist (ER- β) (Metzler *et al.*, 2010). The estrogenic potential of α -ZEL has been reported to be on average 60-times higher than that of ZEN, while for β -ZEL it is on average 5-times lower than that of ZEN (EFSA, 2011). A comparison of the metabolism of ZEN in pigs, rats and humans using *in vitro* incubations with hepatic and intestinal microbial fractions showed pigs and humans to have a preference for the formation of α -ZEL, while rats had a higher preference for β -ZEL formation in incubations with liver samples and comparable preference for the formation of α -ZEL and β -ZEL by intestinal microbiota (Malekinejad *et al.*, 2006; Mendez-Catala *et al.*, 2020). The higher preference for α -ZEL formation together with the *in vivo* observations in young gilts (Dänicke *et al.*, 2005; Döll *et al.*, 2003) has set them as the most susceptible species for ZEN induced adverse effects. Based on data in young gilts, a TDI of 0.25 $\mu\text{g/kg bw}$ has been derived from a No Observed Effect Level (NOEL) of 10.4 $\mu\text{g/kg bw}$ (Döll *et al.*, 2003; EFSA, 2011). To establish the TDI, a default uncertainty factor (UF) of 4 for interspecies differences in kinetics and 10 for human variability were used, with the UF for human variability being divided in 3.16 for toxicokinetics and 3.16 for toxicodynamics (EFSA, 2011; IPCS, 2005). Given the higher sensitivity of pigs and under the assumption that female humans would not be more sensitive than female pigs, the default UF of 2.5 for interspecies differences in dynamics was not included. To further refine the risk assessment, chemical-specific adjustment factors (CSAFs) might also be considered

for interindividual differences in toxicokinetics and toxicodynamics or for interspecies differences in toxicokinetics, to replace the respective default UF values (IPCS, 2005).

The human variability in kinetics or dynamics following ZEN exposure is not yet characterized. The physiologically-based kinetic (PBK) model previously developed for metabolism of ZEN in human, with a sub-model for α -ZEL (Chapter 4 of this thesis, offers a potential novel approach to define a CSAF for the interindividual differences in kinetics for ZEN. The CSAF is based on predictions of the maximum sum of the blood concentrations (C_{\max}) of ZEN and α -ZEL upon exposure to ZEN for different individuals, expressed in ZEN equivalents, calculated from the relative potency factor (RPF) of 1 for ZEN and 60 for α -ZEL (EFSA, 2016). The aim of the present study was to characterize a CSAF for the interindividual human differences in kinetics of ZEN using individual PBK models combined with Monte Carlo simulation, as previously also applied for phenols and lasiocarpine (Ning *et al.*, 2019; Strikwold *et al.*, 2017). To this end, the individual human kinetics for 20 individuals for either hepatic or intestinal microbial metabolism of ZEN and formation of α -ZEL and β -ZEL, were determined to define individual PBK models enabling prediction of the variability in the maximum blood concentration of the sum of ZEN and α -ZEL expressed in ZEN equivalents. Based on the variability parameters thus obtained, Monte Carlo simulations were performed to extend the analysis to a larger number of individuals and define the distribution from which a CSAF for interindividual differences in kinetics within the population as a whole could be derived.

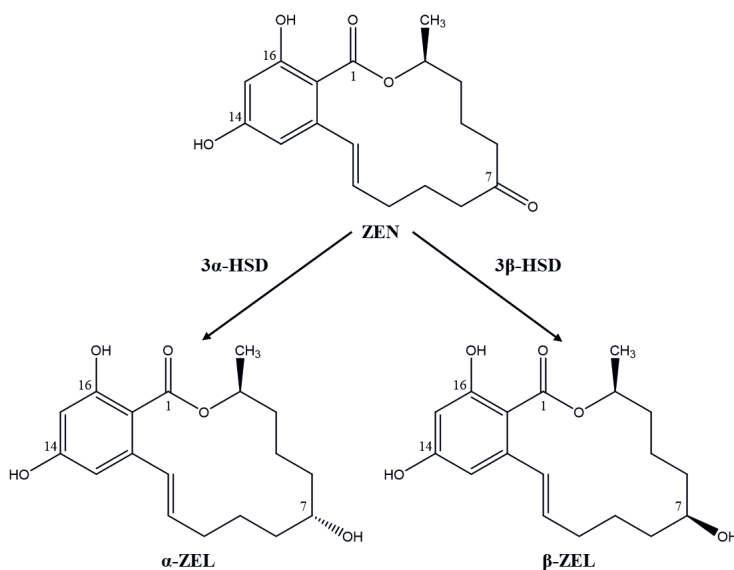


Figure 4.1. Metabolism of ZEN by hydroxysteroid dehydrogenases in mammals

4.2 Materials and Methods

4.2.1 Materials

ZEN (CAS registry number 17924-92-4; $\geq 99.0\%$), α -ZEL (CAS registry number 36455-72-8; $>98\%$), β -ZEL (CAS registry number 71030-11-0; $>98\%$), were purchased from Sigma-Aldrich (Schnelldorf, Germany). Test chemicals were prepared in dimethyl sulfoxide (DMSO; CAS 67-68-5) purchased from Merck (Darmstadt, Germany). Human liver S9 fractions from 20 individuals (10 females and 10 males) were purchased from Corning (Woburn, MA, USA), details on the individuals are found in Supplementary Table 4.1. β -Nicotinamide adenine dinucleotide phosphate, reduced form (NADPH; CAS registry number 2646-71-1) was purchased from Carbosynth (Berkshire, UK). Trizma® base (Tris, CAS registry number 77-86-1) and glycerol (CAS registry number 56-81-5) were obtained from Sigma-Aldrich (Steinheim, Germany). Magnesium chloride hexahydrate ($\text{MgCl}_2 \cdot 6\text{H}_2\text{O}$; CAS registry number 7791-18-6) and formic acid (FA; CAS registry number 64-18-6) were obtained from VWR International (Amsterdam, The Netherlands). UPLC/MS grade methanol (MeOH ; CAS registry number 67-56-1) and acetonitrile (ACN; CAS registry number 75-05-8) were purchased from Biosolve (Valkenswaard, The Netherlands). Phosphate-buffered saline (PBS, pH 7.4), was obtained from Gibco (Paisley, UK).

4.2.2 Collection of human fecal samples

Human fecal samples were donated by 20 volunteers (15 females and 9 males), aged 19-64 years. Individual information can be found in the Supplementary Table 4.2. Volunteer donors did not consume antibiotics or visit tropical countries for 3 months prior to sample donation and have no history of intestinal diseases. The research protocol for use of these human samples was evaluated by the Medical Ethical Reviewing Committee of Wageningen University (METC-WU) and judged not to require further evaluation within the scope of the Dutch Medical Research Involving Human Subjects Act. Samples from each individual were treated and stored separately as follows: in specimen tubes, 3-5 gram of fecal samples were collected and subsequently transferred into an anaerobic environment within 2 minutes after donation by the participants. Samples were immediately diluted in an anaerobic solution of 10% glycerol in PBS to obtain the fecal slurry (20% w/v). Samples were manually homogenized with a sterile serological pipette and filtered using SpinCon® (Meridian Bioscience Europe) centrifugal filters at 2,500 rpm for 5

minutes. Aliquots were prepared from the resulting fecal slurry and stored at -80°C until further use.

4.2.3 Individual *in vitro* human hepatic metabolism of ZEN

Human liver S9 fraction incubations to characterize the reduction of ZEN by hepatic samples were optimized to establish the conditions providing linearity over time and protein concentration. To obtain the kinetic parameters, the incubation mixtures with a final volume of 200 μ l contained (final concentrations) 2 mM NADPH, 5 mM $MgCl_2$ and 0.3 mg/ml liver S9 fraction proteins in 0.1 M Tris-HCl (pH 7.4). After 1-minute pre-incubation at 37°C, the reactions were started by the addition of 1 - 500 μ M ZEN (from 100 times concentrated stock solutions in DMSO). The incubations were carried out for 5 min. To stop the reaction 20% (v/v) ice-cold ACN was added. Blank incubations were performed without the addition of NADPH. The samples were centrifuged for 5 min at 15,000 \times g and the supernatant was kept on ice for immediate UPLC-PDA analysis.

4.2.4 Individual *in vitro* human intestinal microbial metabolism of ZEN

To characterize the formation of α -ZEL and β -ZEL by intestinal microbiota, incubations with individual fecal samples were performed. A range of substrate concentrations of ZEN was incubated to establish reaction kinetics. Incubation mixes of 100 μ L were prepared containing 1 - 250 μ M of ZEN added from 200x concentrated stock solutions in DMSO (0.5% DMSO final concentration), 10 mg feces/mL (final concentration), and PBS (pH 7.4). The samples were incubated anaerobically at 37°C for 5 hours. Under these conditions the reactions were linear time and fecal concentration (data not shown). To stop the reaction, 100 μ l of ice-cold MeOH were added, the samples were vortexed, and kept on ice for at least 10 minutes. The samples were centrifuged at 21,500 \times g for 15 minutes at 4°C and the supernatant was kept on ice for immediate LC-MS/MS analysis. Two independent experiments for each individual were done and data are presented as mean \pm standard deviation (SD).

4.2.5 UPLC-PDA and LC-MS analysis: Quantification of α -ZEL and β -ZEL

The formation of α -ZEL and β -ZEL in incubations with human liver S9 fractions was quantified in an UPLC-PDA system (Waters Acquity). The UPLC system was equipped with an Acquity BEH C18 column 1.7 μ m, 50 mm \times 2.1 mm (Waters) set at 45 °C and a UV detection system recording wavelengths of 190-400 nm. Nanopure

PBK and MC simulation to study interindividual differences in metabolism of ZEN

water (A) and ACN (B) were used as eluents at a flow rate of 0.3 ml/min with the following gradient profile: 0-40% B (0 –1.3 min), 40-50% B (1.3 - 5.7 min), 50-100% B (5.7 - 6 min), 100 % B kept for 2 minutes and 100-0% B (8 - 8.1 min) for equilibration. Per run, 3.5 µl of sample were injected. ZEN, α-ZEL and β-ZEL were identified using commercially available standards. Chromatograms were presented at 235 nm and chemicals were quantified by comparison of the peak areas at 235 nm to those from standard curves prepared using commercially available standards.

α-ZEL and β-ZEL formed in incubations with human fecal samples were quantified by LC-MS/MS to enable quantification without disturbance from matrix-derived peaks. The analysis was performed on a Nexera XR LC-20AD SR UPLC system coupled to a triple quadrupole LCMS 8040 mass spectrometer (Shimadzu Benelux, 's Hertogenbosch, The Netherlands) with electrospray ionization (ESI) interface. The UPLC system was equipped with a Kinetex® C18 column 1.7µm, 50 mm x 2.1 mm (Phenomenex) and set at 40 °C with a flow rate of 0.3 ml/min. The mobile phases consisted of nanopure water containing 0.1% (v/v) formic acid (A) and ACN containing 0.1% (v/v) formic acid (B). The total run time was 14 minutes with the following gradient profile: 0-40% B (0 –1.3 min), 40-50% B (1.3 - 5.7 min), 50-100% B (5.7 - 6 min), 100 % B kept for 2 minutes and 100-0% B (8 - 8.1 min) for equilibration. Per run, 1 µl of sample was injected. MS/MS analysis was operated in the positive ion mode and the MRM mode with a spray voltage of 4.5 KV. The transitions monitored were (*m/z*) 319.2 → 301.2, 319.2 → 283.1, 319.2 → 187.1 for ZEN; (*m/z*) 321.2 → 303.1, 321.2 → 285.1, 321.2 → 131.0 for α-ZEL; and 321.2 → 303.2, 321.2 → 285.15, 321.2 → 267.0 for β-ZEL. The Postrun Analysis function from the LabSolutions software (Shimadzu, Kyoto, Japan) was used to obtain the peak area of the total ion chromatogram (TIC) for each compound. For quantification of the compounds, the areas were compared to standard curves made using commercially available standards.

4.2.6 Kinetic analysis

To derive the kinetic constants for the formation of α-ZEL and β-ZEL by both the microbial and human hepatic metabolism, the amount of metabolites formed expressed per gram of feces or protein, respectively, and per unit of time (rate of formation) were calculated using Microsoft Excel (version 2016) and plotted against the substrate concentrations used. The curve for each metabolite was fitted in GraphPad Prism 5.04 (GraphPad software, San Diego California, U.S.A.) using a standard Michaelis-Menten regression ($V=V_{\max}*[S]/(K_m+[S])$) to obtain the *in vitro*

kinetic constants, V_{\max} (pmol/min/mg feces or pmol/min/mg protein) and K_m (μM) for the microbial and human hepatic formation of α -ZEL and β -ZEL.

4.2.7 PBK modelling and Monte Carlo simulation

In the present study, the PBK model previously developed for ZEN including a sub-model for α -ZEL (Chapter 4 of this thesis) was used for the evaluation of the inter-individual variation in blood concentrations of ZEN and α -ZEL that may result from differences in the kinetics for the metabolism of ZEN in liver and intestinal microbiota.

The interindividual variation in formation of α -ZEL and β -ZEL from ZEN in the liver and by intestinal microbiota was assessed using a population of 20 individuals each. All possible combinations of the kinetic constants V_{\max} and K_m obtained from incubations with 20 individual liver S9 fractions and 20 individual intestinal microbiota samples were used to define 400 different individual PBK models. From the predicted time-dependent concentration profiles for ZEN and α -ZEL obtained from each individual model at a dose equivalent to the current TDI of 0.25 $\mu\text{g}/\text{kg}$ bw (EFSA, 2011) the total time-dependent concentration profile expressed in ZEN equivalents was calculated for each model based on the RPF of 1 for ZEN and 60 for α -ZEL (EFSA, 2016). From this curve the C_{\max} expressed in ZEN equivalents was derived. From the V_{\max} and K_m obtained in the hepatic and fecal incubations, also the mean (μ_x) and coefficient of variation (CV) of the kinetic parameters for α -ZEL and β -ZEL formation were obtained.

Next, the PBK model was linked to Monte Carlo simulations to simulate the consequences of the interindividual variation in V_{\max} and K_m for conversion of ZEN to α -ZEL and β -ZEL in the liver and by the intestinal microbiota for the predicted C_{\max} of ZEN and of α -ZEL (expressed in ZEN equivalents) at an oral dose of 0.25 $\mu\text{g}/\text{kg}$ bw, the current TDI for ZEN (EFSA, 2011), in a larger human population. For the Monte Carlo analysis, a total of 10,000 simulations were performed. In each simulation the V_{\max} and K_m values were taken randomly from a log-normal distribution. The distributions were truncated at ± 3 SD by excluding values that were 3 times higher or lower than the geometric mean (GM) (Ning *et al.*, 2019; Strikwold *et al.*, 2017). The log-normal distribution of V_{\max} and K_m for α -ZEL and β -ZEL formation were defined by the mean (μ_w) and the standard deviation (σ_w) according to (Zhang *et al.*, 2007):

$$\mu_w = \ln \frac{\mu_x}{\sqrt{1 + CV_x^2}}$$

and

$$\sigma_x^2 = \ln(1 + CV_x^2)$$

The model predictions with the Monte Carlo simulation were performed with Berkeley Madonna 8.0.1 (UC Berkeley, CA, USA) using the Rosenbrock's algorithm for stiff systems. The generated population distribution was statically analyzed with GraphPad Prism 5.04 (GraphPad software, San Diego California, U.S.A.) to obtain the GM and different percentiles (P95 and P99) of the C_{\max} values for ZEN equivalents. The population distribution enabled the prediction of the CSAF, obtained by dividing the 95th or 99th percentile of C_{\max} of ZEN plus α -ZEL expressed in ZEN equivalents by the GM (IPCS, 2005).

4.3 Results

4.3.1 Formation of α -ZEL and β -ZEL by individual human liver S9 fractions

Table 4.1 presents the kinetic parameters for the formation of α -ZEL and β -ZEL from ZEN in incubations with liver S9 fractions from 20 individuals. The difference between the highest and the lowest value obtained for k_{cat} for α -ZEL formation is 8-fold with a CV of 40.3%. For β -ZEL formation the difference between the highest and lowest k_{cat} values is 13-fold with a CV of 84.2%. The relatively higher CV for the k_{cat} for β -ZEL formation is caused by the relatively high k_{cat} value for individual H0751. The comparison of the average k_{cat} for α -ZEL and β -ZEL formation, showed the average k_{cat} for β -ZEL to be 3.9-fold lower than the one for α -ZEL indicating an overall preference for conversion of ZEN to α -ZEL over formation of β -ZEL. No significant variations between gender and k_{cat} values were found for the liver metabolism (Supplementary Figure 4.1).

4.3.2 Formation of α -ZEL and β -ZEL by individual human intestinal microbiota

The kinetic parameters for the conversion of ZEN to α -ZEL and β -ZEL in incubations with 20 individual human fecal samples are presented in Table 4.2. Compared to the hepatic metabolism, the intestinal microbiota resulted in a relatively higher interindividual variation in the parameters for α -ZEL and β -ZEL formation. The lowest and the highest k_{cat} values for α -ZEL were 8.5 times different with a CV of 59.1%. The kinetic parameters, V_{\max} and K_m for β -ZEL formation varied greatly with CV values of 133.8% and 150.7%, respectively, which was due to the absence of β -ZEL formation in 11 out of the 20 individuals. No significant variations between gender and k_{cat} values were found for the intestinal microbial metabolism (Supplementary Figure 4.2).

Table 4.1. *In vitro* kinetic parameters for the conversion of ZEN to α -ZEL and β -ZEL in liver, derived from incubations with individual human liver S9 fractions.

Individual	α -ZEL			β -ZEL		
	V_{\max} , <i>in vitro</i> ^a	K_m ^b	k_{cat} , <i>in vitro</i> ^c	V_{\max} , <i>in vitro</i> ^a	K_m ^b	k_{cat} , <i>in vitro</i> ^c
H0033	312.4	13.0	24.1	163.9	20.2	8.1
H0041	360.4	10.5	34.3	218.8	36.0	6.1
H0220	638.9	15.7	40.7	350.6	121.6	2.9
H0208	392.7	14.9	26.4	209.3	77.1	2.7
H0422	349.0	10.1	34.7	253.9	73.5	3.5
H0441	249.7	13.1	19.1	189.8	88.7	2.1
H0751	944.7	26.0	36.3	1116.0	40.0	27.9
H0442	584.4	18.4	31.8	686.5	108.9	6.3
H0487	723.3	21.2	34.1	906.7	81.7	11.1
H0438	329.1	10.9	30.1	246.1	89.0	2.8
H0420	245.2	4.7	52.1	214.4	24.7	8.7
H0251	377.3	13.4	28.1	166.2	9.3	17.9
H0246	425.5	11.5	37.0	256.5	45.5	5.6
H0428	343.6	14.4	23.8	274.2	80.1	3.4
H0164	199.4	14.0	14.3	170.8	50.8	3.4
H0120	391.7	14.3	27.3	342.8	90.3	3.8

^a pmol/min/mg protein

^b μ M

^c μ L/min/mg protein

Table 4.1. (Continued)

	α -ZEL			β -ZEL		
	V_{\max} , <i>in vitro</i> ^a	K_m ^b	k_{cat} , <i>in vitro</i> ^c	V_{\max} , <i>in vitro</i> ^a	K_m ^b	k_{cat} , <i>in vitro</i> ^c
H0177	386.7	17.8	21.8	535.2	153.5	3.5
H0205	397.4	27.2	14.6	550.1	66.2	8.3
H0025	570.5	21.5	26.5	643.2	126.5	5.1
H0463	573.6	90.0	6.4	681.0	58.3	11.7
Mean (μ_x) ^d	439.8	19.1	28.2	408.8	72.1	7.2
SD ^e	177.2	17.1	10.1	267.1	36.8	6.1
CV _x (%) ^f	40.3	89.3	35.7	65.3	51.0	84.2
μ_w ^g	6.0	2.7	3.3	5.8	4.2	1.7
σ_w ^h	0.39	0.77	0.35	0.60	0.48	0.73

^a pmol/min/mg protein

^a pmol/min/mg protein

^b μ M

^c μ L/min/mg protein

^d Mean of the kinetic constants for the formation of α -ZEL and β -ZEL from ZEN derived from 20 individuals

^e Standard deviation of the kinetic constants for the formation of α -ZEL and β -ZEL from ZEN derived from 20 individuals

^f Coefficient of variation % = $SD / \mu_x \times 100$

^g The mean for describing the log-normal distribution $\mu_w = \ln [\mu_x / \sqrt{1 + CV_x^2}]$

^h The standard deviation for describing the log-normal distribution $\sigma_w = \sqrt{\ln(1 + CV_x^2)}$

Table 4.2. *In vitro* kinetic parameters for the conversion of ZEN to α -ZEL and β -ZEL by the intestinal microbiota, derived from incubations with individual human fecal samples.

Individual	α -ZEL			β -ZEL		
	V_{\max} , <i>in vitro</i> ^a	K_m ^b	k_{cat} , <i>in vitro</i> ^c	V_{\max} , <i>in vitro</i> ^a	K_m ^b	k_{cat} , <i>in vitro</i> ^c
1	11.32	103.50	0.109	5.14	249.80	0.021
2	13.05	229.90	0.057	-	-	n.a.
3	11.65	98.59	0.118	-	-	n.a.
4	10.42	157.90	0.066	-	-	n.a.
5	5.39	114.50	0.047	-	-	n.a.
6	14.86	136.50	0.109	-	-	n.a.
7	18.39	136.50	0.135	5.41	111.20	0.049
8	13.69	110.10	0.124	-	-	n.a.
9	10.76	79.13	0.136	2.44	50.58	0.048
10	14.57	102.30	0.142	3.56	33.60	0.106
11	25.21	655.80	0.038	-	-	n.a.
12	13.34	144.30	0.092	-	-	n.a.
13	28.25	130.90	0.216	7.12	92.07	0.077
14	21.31	176.20	0.121	0	0	n.a.
15	37.28	137.70	0.271	12.08	180.70	0.067
16	16.77	73.53	0.228	-	-	n.a.

^a pmol/h/mg feces

^b μ M

^c μ L/h/mg feces

Table 4.2. (Continued)

α -ZEL			β -ZEL		
	V_{\max} , <i>in vitro</i> ^a	K_m ^b	k_{cat} , <i>in vitro</i> ^c	V_{\max} , <i>in vitro</i> ^a	k_{cat} , <i>in vitro</i> ^c
17	6.27	18.18	0.345	2.52	0.294
18	25.44	165.80	0.153	14.03	0.086
19	44.75	135.60	0.330	10.64	0.091
20	26.04	224.70	0.116	-	n.a.
Mean (μ_x) ^d	18.44	156.58	0.148	3.15	n.a.
SD ^e	10.13	127.16	0.087	4.53	n.a.
CV _x (%) ^f	54.96	81.21	59.12	143.84	n.a.
μ_w ^g	2.78	4.80	-2.06	0.59	n.a.
σ_w ^h	0.51	0.71	0.55	1.06	n.a.

^a pmol/h/mg feces

^b μM

^c $\mu\text{L/h/mg feces}$

^d Mean of the kinetic constants for the formation of α -ZEL and β -ZEL from ZEN derived from 20 individuals

^e Standard deviation of the kinetic constants for the formation of α -ZEL and β -ZEL from ZEN derived from 20 individuals

^f Coefficient of variation % = $\text{SD} / \mu_x \times 100$

^g The mean for describing the log-normal distribution $\mu_w = \ln [\mu_x / \sqrt{1 + \text{CV}_x^2}]$

^h The standard deviation for describing the log-normal distribution $\sigma_w = \sqrt{\ln(1 + \text{CV}_x^2)}$

n.a. : not applicable

4.3.3 PBK modeling and Monte Carlo simulation

The influence of the interindividual differences in α -ZEL and β -ZEL formation in liver and intestinal microbiota on the C_{\max} of ZEN plus α -ZEL, expressed in ZEN equivalents, were evaluated by two methods. In the first method, the variation in C_{\max} expressed in ZEN equivalents was determined using the data for the two sets of 20 individuals, one set for liver (Table 4.1) and one set for intestinal microbiota (Table 4.2). The individual kinetic parameters, i.e. V_{\max} and K_m , present in these data sets were combined to result in 400 individual PBK models. Figure 4.2 shows the box and whisker plot for the predicted C_{\max} expressed in ZEN equivalents obtained with these 400 individual PBK models at an oral dose equivalent to the TDI of 0.25 $\mu\text{g/kg}$ bw. Table 4.3 presents the geometric mean (GM), GM CV (%) and fold-variation between the minimum and maximum of the predictions thus obtained. As no gender differences were observed, the current CV for the mixed population was considered adequate for the modelling approach in this study. In the second method, a Monte Carlo simulation was performed at an oral dose of 0.25 $\mu\text{g/kg}$ bw to evaluate the interindividual variation in C_{\max} expressed in ZEN equivalents that could occur in a larger population. The Monte Carlo simulation was performed in order to take the combination of the variability in liver and microbial kinetics into account. The Monte Carlo simulation resulted in the elimination of 1.2% of the 10,000 simulations, so that results obtained relate to 9879 individuals. The box and whisker plot for the predicted C_{\max} expressed in ZEN equivalents obtained from the Monte Carlo simulations is shown in Figure 4.2. The frequency distribution for the predicted C_{\max} obtained from the simulated population is presented in Figure 4.3. The GM, GM CV (%) and the fold variations of the simulated population are presented in Table 4.3. The GM for the C_{\max} expressed in ZEN equivalents obtained from the Monte Carlo simulation appeared to be comparable (1.1-fold higher) to the GM obtained from the 400 individual PBK models. When the 95th and 99th percentile of the population were considered, the fold variation was 4.7 and 8.3, respectively, a variation being higher for the Monte Carlo simulation than what was obtained using the 400 individual PBK models. The chemical specific adjustment factor (CSAF) was defined as the ratio between the 95th and 99th percentile obtained from the distribution of the C_{\max} expressed in ZEN equivalents in the simulated population (Figure 4.3) divided by the GM (IPCS, 2005). The 95th and 99th percentiles of the C_{\max} of ZEN equivalents amounted to 0.55 and 0.84 pM, respectively. The CSAF values obtained were 2.45 for the 95th percentile and 3.97 for the 99th percentile.

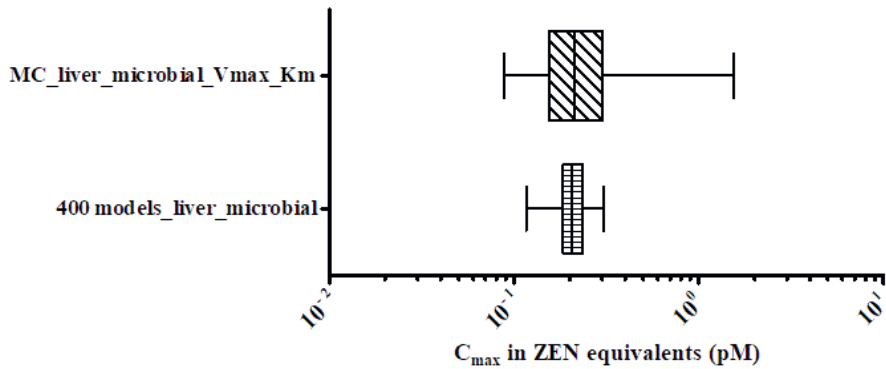


Figure 4.2. Box and whisker plot representing the distribution of the maximum blood concentration (C_{max}) expressed in ZEN equivalents at an oral dose of 0.25 μg ZEN/ kg bw, representing the TDI of ZEN, predicted with the PBK model resulting in 400 individual PBK models from a combination of 20 individuals for liver and 20 individuals for intestinal microbiota. Also, the distribution in C_{max} predicted with the PBK model linked with Monte Carlo (MC) simulation for 9879 individuals including the variation in V_{max} and K_m for α -ZEL and β -ZEL formation from ZEN in liver and intestinal microbial metabolism is presented. The whiskers represent the minimum and maximum C_{max} expressed in ZEN equivalents.

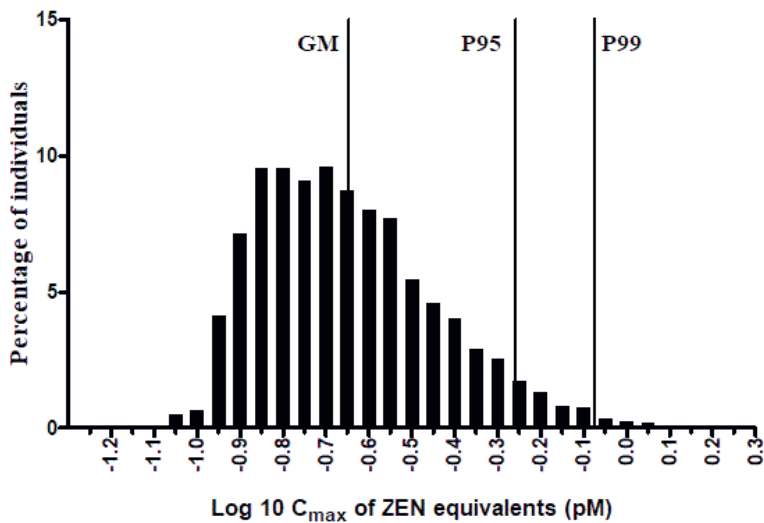


Figure 4.3. Frequency distribution for the C_{max} expressed in ZEN equivalents in 9879 individuals after a single oral dose of 0.25 $\mu\text{g}/\text{kg}$ bw obtained by Monte Carlo simulation including the variation in V_{max} and K_m for α -ZEL and β -ZEL formation from ZEN in liver

and microbiota. The GM, P95 and P99 representing the geometric mean, and the 95th and 99th percentile of the distribution are indicated.

Table 4.3. Geometric mean, GM, CV (%) and the fold difference between the minimum and maximum, the 5th and 95th or the 1st and 99th percentile of the C_{max} expressed in ZEN equivalents after exposure to an oral dose of 0.25 µg/kg bw of ZEN predicted by individual PBK models and by PBK modeling linked to Monte Carlo simulation.

	C _{max} of ZEN equivalents of 400 individual PBK models	C _{max} of ZEN equivalents of PBK model with MC simulation for liver and microbiota	
GM (pM)	0.2038	0.2252	
GM CV (%)	20	60	
Fold-variation	2.6 ^a	4.7 ^b	8.2 ^c

^a Fold variation of the predicted minimum and maximum C_{max} of ZEN equivalents by individual PBK models

^b Fold variation of the 5th and 95th percentile of the population for the predicted C_{max} of ZEN equivalents obtained from the PBK model coupled with Monte Carlo simulation

^c Fold variation of the 1st and 99th percentile of the population for the predicted C_{max} of ZEN equivalents obtained from the PBK model coupled with Monte Carlo simulation

4.4 Discussion

The present study aimed to assess the effect of interindividual variation in kinetics for conversion of ZEN to α-ZEL and β-ZEL by liver and intestinal microbiota for the blood concentration of ZEN plus α-ZEL expressed in ZEN equivalents. In this analysis α-ZEL was taken into account because this metabolite has been shown to be 60 fold more potent as an estrogen than ZEN itself, so the C_{max} was expressed in ZEN equivalents using a RPF for ZEN of 1.0 and for α-ZEL of 60 (EFSA, 2016). To quantify the interindividual variability, individual *in vitro* derived kinetics for liver and intestinal microbial formation of α-ZEL and β-ZEL from ZEN were included in a PBK model and results obtained were coupled with Monte Carlo simulations. A previous sensitivity analysis of this PBK model revealed liver conversion of ZEN to α-ZEL to be factors of major influence on the plasma levels of ZEN plus α-ZEL expressed in ZEN equivalents, with the influence of the conversion by the microbiota being relatively moderate (Chapter 4 this thesis). Nevertheless, interindividual differences in both these processes were included in the current analysis. To quantify

PBK and MC simulation to study interindividual differences in metabolism of ZEN

the interindividual differences in metabolism of ZEN and in the resulting plasma levels of ZEN plus α -ZEL expressed in ZEN equivalents, first, the kinetic parameters for the formation of α -ZEL and β -ZEL from ZEN were obtained from individual incubations with human liver S9 fractions and fecal samples, and used to build individual PBK models for ZEN. The 400 individual PBK models obtained were used to predict C_{\max} expressed in ZEN equivalents for 400 individuals. Secondly, the interindividual variation in a larger population was predicted by Monte Carlo simulation in connection with the PBK model for ZEN. The population distribution of C_{\max} expressed in ZEN equivalents from the Monte Carlo simulation was used for the prediction of CSAF values. The ratio of the GM and the 95th percentile resulted in a CSAF of 2.45 for a healthy population. Given that in risk assessment, the 95th percentile is generally considered to protect sensitive individuals in a population, the CSAF of 2.45 indicates that the default safety factor is adequately protective for the healthy population when compared to the default uncertainty factor of 3.16 (HK_{UF}) for inter-individual kinetic variation (IPCS, 2005). Whether this also holds for prepubertal individuals and children remains to be established, although it is expected that a potential increased sensitivity of this subgroups may rather be due to differences in toxicodynamics, such as interindividual differences in the number and sensitivity of ERs and the pathways following ER activation (Dänicke and Winkler, 2015; Fitzpatrick *et al.*, 1989; Kuiper *et al.*, 1998). In pigs, prepubertal individuals seem to be more sensitive to ZEN exposure, but the underlying mode of action and its relevance for human remains to be established (Andretta *et al.*, 2011; Bandera *et al.*, 2011; Döll *et al.*, 2004; Gajęcka *et al.*, 2012; Szuets *et al.*, 1997). Nevertheless, the inclusion of a subgroup including prepubertal individuals in defining the interindividual differences also for kinetics of ZEN remains of interest for future research. In the guideline of IPCS, it is established that a CSAF can be estimated for a bimodal population, selecting the 95th percentile of the sensitive subgroup to define the CSAF, dividing it by the GM of the general population (IPCS, 2005). This may result in a CSAF higher than 2.45 and perhaps more in line with the default value of 3.16 or the value obtained when using the 99th percentile of the distribution obtained in the present study amounting to 3.97.

The individual kinetic differences observed in liver may be ascribed to interindividual differences in the activity of the enzymes responsible for the aliphatic hydroxylation of ZEN, i.e. formation of α -ZEL and β -ZEL, 3α - and 3β -hydroxysteroid dehydrogenase (HSD) (Malekinejad *et al.*, 2005). These differences may relate to factors other than age or gender related variability; a previous study characterizing the activities of 3α -HSD and 3β -HSD in females and males reported

no significant variation between the two groups (Pirog and Collins, 1999). Dong *et al.* (2010) reported no significant gender differences based on an *in vitro* study assessing the formation of α -ZEL in hepatic tissue of goats. Similarly, no correlation was found between age (range 19 to 64 years) and the formation of α -ZEL and β -ZEL in the present study and also the mean catalytic efficiencies for α -ZEL and β -ZEL formation in males and females were comparable. The enzymes involved in the formation of α -ZEL and β -ZEL from ZEN by the intestinal microbiota have not yet been elucidated, but evidence suggests the presence of homologue proteins that resemble 3α -HSDs in steroid reduction activity (Kisiela *et al.*, 2012). Additionally, ZEN might act as terminal electron acceptor for anaerobic respiration in the gut (Spanogiannopoulos *et al.*, 2016), which might also explain the chemical reduction of ZEN to α -ZEL and β -ZEL.

Although no gender correlations were found in the present study, differences between individuals in the formation of α -ZEL, β -ZEL, and the ratio α -ZEL/ β -ZEL were found. This indicates that other factors may have an influence on the metabolism of ZEN. External factors, such as diet, could for example influence 3β -HSD expression in the liver (Rasmussen *et al.*, 2012) and intestinal microbial composition (Duncan *et al.*, 2007; Lewis *et al.*, 2015; Singh *et al.*, 2017). Genetic variation may also play a role. In humans 3α -HSD in the liver is encoded by the *AKR1C4* gene (NCBI, 2020). Single Nucleotide Polymorphisms (SNPs) in the *AKR1C4* gene may influence the biotransformation of exogenous and endogenous steroids (Rižner and Penning, 2014), and could therefore possibly influence the reduction pathway of ZEN. Furthermore, intestinal microbial composition is influenced by host genetics (Chen *et al.*, 2018; Goodrich *et al.*, 2014). Therefore, genetic and environmental factors may contribute to the interindividual variability in the metabolism of ZEN observed in the present study.

Overall, the variation in the human kinetics of ZEN and their influence in the C_{\max} values can be studied through PBK modelling linked to Monte Carlo simulation. The CSAF values estimated in this study of 2.45 for the 95th percentile and 3.97 for the 99th percentile of the adult population suggest the default HK_{UF} to be protective enough for the adult healthy population. Whether this also holds for children remains to be investigated, and could be done using a similar *in vitro-in silico* approach using PBK modelling in conjunction with Monte Carlo simulation for the estimation of health based guidance values defined using CSAF values for human interindividual variation.

Acknowledgements

This research was financially supported by the National Council of Science and Technology (CONACYT) through a scholarship awarded to Diana M. Mendez Catala (CVU 619449) for conducting her PhD in The Netherlands. Special thanks go to Katja van Dongen, Qianrui Wang and Chen Liu for their help with the collection of individual human fecal samples, and to Karsten Beekmann for critical reading of the manuscript.

4.5 References

- Andretta, I., Lovatto, P., Lanferdini, E., Lehnen, C., Rossi, C., Hauschild, L., Fraga, B., Garcia, G., Mallmann, C. Feeding of pre-pubertal gilts with diets containing aflatoxins or Zearalenone. *Arch. de Zootec.*, 60 (2011), 123-130. doi:
- Bandera, E.V., Chandran, U., Buckley, B., Lin, Y., Isukapalli, S., Marshall, I., King, M., Zarbl, H. Urinary mycoestrogens, body size and breast development in New Jersey girls. *Sci. Total Environ.*, 409 (2011), 5221-5227. doi: 10.1016/j.scitotenv.2011.09.029
- Chen, C., Huang, X., Fang, S., Yang, H., He, M., Zhao, Y., Huang, L. Contribution of Host Genetics to the Variation of Microbial Composition of Cecum Lumen and Feces in Pigs. *Front. Microbiol.*, 9 (2018). doi: 10.3389/fmicb.2018.02626
- Dänicke, S., Swiech, E., Buraczewska, L., Ueberschär, K.H. Kinetics and metabolism of zearalenone in young female pigs. *J. Anim. Physiol. Anim. Nutr. (Berl)*, 89 (2005), 268-276. doi: 10.1111/j.1439-0396.2005.00516.x
- Dänicke, S., Winkler, J. Invited review: Diagnosis of zearalenone (ZEN) exposure of farm animals and transfer of its residues into edible tissues (carry over). *Food Chem. Toxicol.*, 84 (2015), 225-249. doi: 10.1016/j.fct.2015.08.009
- Döll, S., Dänicke, S., Schnurrbusch, U. The effect of increasing concentrations of Fusarium toxins in piglet diets on histological parameters of the uterus and vagina. *Arch. Anim. Nutr.*, 58 (2004), 413-417. doi: 10.1080/00039420400004987
- Döll, S., Dänicke, S., Ueberschär, K.H., Valenta, H., Schnurrbusch, U., Ganter, M., Klobasa, F., Flachowsky, G. Effects of graded levels of Fusarium toxin contaminated maize in diets for female weaned piglets. *Arch. Anim. Nutr.*, 57 (2003), 311-334. doi: 10.1080/00039420310001607680
- Dong, M., Tulayakul, P., Li, J.Y., Dong, K.S., Manabe, N., Kumagai, S. Metabolic conversion of zearalenone to alpha-zearalenol by goat tissues. *J. Vet. Med. Sci.*, 72 (2010), 307-312. doi: 10.1292/jvms.09-0122
- Duncan, S.H., Belenguer, A., Holtrop, G., Johnstone, A.M., Flint, H.J., Lobley, G.E. Reduced dietary intake of carbohydrates by obese subjects results in decreased concentrations of butyrate and butyrate-producing bacteria in feces. *Appl. Environ. Microbiol.*, 73 (2007), 1073-1078. doi: 10.1128/aem.02340-06
- EFSA. Scientific Opinion on the risks for public health related to the presence of zearalenone in food. *EFSA J.*, 9 (2011), 2197. doi: 10.2903/j.efsa.2011.2197

- EFSA. Appropriateness to set a group health-based guidance value for zearalenone and its modified forms. *EFSA J.*, 14 (2016), e04425. doi: 10.2903/j.efsa.2016.4425
- Fitzpatrick, D.W., Arbuckle, L.D., Hassen, A.M. Zearalenone metabolism and excretion in the rat: effect of different doses. *J. Environ. Sci. Health B*, 23 (1988), 343-354. doi: 10.1080/03601238809372610
- Fitzpatrick, D.W., Picken, C.A., Murphy, L.C., Buhr, M.M. Measurement of the relative binding affinity of zearalenone, α -zearalenol and β -zearalenol for uterine and oviduct estrogen receptors in swine, rats and chickens: An indicator of estrogenic potencies. *Comp. Biochem. Physiol. C Comp. Pharmacol. Toxicol.*, 94 (1989), 691-694. doi: 10.1016/0742-8413(89)90133-3
- Gajęcka, M., Rybarczyk, L., Jakimiuk, E., Zielonka, Ł., Obremski, K., Zwierzchowski, W., Gajęcki, M. The effect of experimental long-term exposure to low-dose zearalenone on uterine histology in sexually immature gilts. *Exp. Toxicol. Pathol.*, 64 (2012), 537-542. doi:
- Goodrich, Julia K., Waters, Jillian L., Poole, Angela C., Sutter, Jessica L., Koren, O., et al. Human Genetics Shape the Gut Microbiome. *Cell*, 159 (2014), 789-799. doi: 10.1016/j.cell.2014.09.053
- IPCS, 2005. Chemical-specific adjustment factors for interspecies differences and human variability : guidance document for use of data in dose/concentration-response assessment. World Health Organization, Geneva, pp.
- Kisiela, M., Skarka, A., Ebert, B., Maser, E. Hydroxysteroid dehydrogenases (HSDs) in bacteria – A bioinformatic perspective. *J. Steroid Biochem. Mol. Biol.*, 129 (2012), 31-46. doi: 10.1016/j.jsbmb.2011.08.002
- Kuiper, G.G.J.M., Lemmen, J.G., Carlsson, B., Corton, J.C., Safe, S.H., van der Saag, P.T., van der Burg, B., Gustafsson, J.-A.k. Interaction of Estrogenic Chemicals and Phytoestrogens with Estrogen Receptor β . *Endocrinology*, 139 (1998), 4252-4263. doi: 10.1210/endo.139.10.6216
- Lewis, J.D., Chen, E.Z., Baldassano, R.N., Otley, A.R., Griffiths, A.M., et al. Inflammation, Antibiotics, and Diet as Environmental Stressors of the Gut Microbiome in Pediatric Crohn's Disease. *Cell host & microbe*, 18 (2015), 489-500. doi: 10.1016/j.chom.2015.09.008
- Liang, Z., Ren, Z., Gao, S., Chen, Y., Yang, Y., et al. Individual and combined effects of deoxynivalenol and zearalenone on mouse kidney. *Environ. Toxicol. Pharmacol.*, 40 (2015), 686-691. doi: 10.1016/j.etap.2015.08.029

- Malekinejad, H., Maas-Bakker, R., Fink-Gremmels, J. Species differences in the hepatic biotransformation of zearalenone. *Veterinary journal*, 172 (2006), 96-102. doi: 10.1016/j.tvjl.2005.03.004
- Malekinejad, H., Maas-Bakker, R.F., Fink-Gremmels, J. Bioactivation of zearalenone by porcine hepatic biotransformation. *Vet. Res.*, 36 (2005), 799-810. doi: 10.1051/vetres:2005034
- Mally, A., Solfrizzo, M., Degen, G.H. Biomonitoring of the mycotoxin Zearalenone: current state-of-the art and application to human exposure assessment. *Arch. Toxicol.*, 90 (2016), 1281-1292. doi: 10.1007/s00204-016-1704-0
- Mendez-Catala, D.M., Spenkelink, A., Rietjens, I.M.C.M., Beekmann, K. An in vitro model to quantify interspecies differences in kinetics for intestinal microbial bioactivation and detoxification of zearalenone. *Toxicol. Rep.*, 7 (2020), 938-946. doi: 10.1016/j.toxrep.2020.07.010
- Metzler, M., Pfeiffer, E., Hildebrand, A. Zearalenone and its metabolites as endocrine disrupting chemicals. *World Mycotoxin J.*, 3 (2010), 385-401. doi: 10.3920/WMJ2010.1244
- NCBI, 2020. AKR1C4 aldo-keto reductase family 1 member C4 [Homo sapiens (human)], pp.
- Ning, J., Rietjens, I., Strikwold, M. Integrating physiologically based kinetic (PBK) and Monte Carlo modelling to predict inter-individual and inter-ethnic variation in bioactivation and liver toxicity of lasiocarpine. *Arch. Toxicol.*, 93 (2019), 2943-2960. doi: 10.1007/s00204-019-02563-x
- Pirog, E.C., Collins, D.C. Metabolism of Dihydrotestosterone in Human Liver: Importance of 3 α - and 3 β -Hydroxysteroid Dehydrogenase1. *J. Clin. Endocrinol. Metab.*, 84 (1999), 3217-3221. doi: 10.1210/jcem.84.9.5963
- Rasmussen, M.K., Brunius, C., Zamaratskaia, G., Ekstrand, B. Feeding dried chicory root to pigs decrease androstenone accumulation in fat by increasing hepatic 3 β hydroxysteroid dehydrogenase expression. *J. Steroid Biochem. Mol. Biol.*, 130 (2012), 90-95. doi: 10.1016/j.jsbmb.2012.01.003
- Rižner, T.L., Penning, T.M. Role of aldo-keto reductase family 1 (AKR1) enzymes in human steroid metabolism. *Steroids*, 79 (2014), 49-63. doi: 10.1016/j.steroids.2013.10.012
- Singh, R.K., Chang, H.W., Yan, D., Lee, K.M., Ucmak, D., et al. Influence of diet on the gut microbiome and implications for human health. *J. Transl. Med.*, 15 (2017), 73. doi: 10.1186/s12967-017-1175-y

- Spanogiannopoulos, P., Bess, E.N., Carmody, R.N., Turnbaugh, P.J. The microbial pharmacists within us: a metagenomic view of xenobiotic metabolism. *Nat. Rev. Microbiol.*, 14 (2016), 273-287. doi: 10.1038/nrmicro.2016.17
- Strikwold, M., Spenkelink, B., Woutersen, R.A., Rietjens, I., Punt, A. Development of a Combined In Vitro Physiologically Based Kinetic (PBK) and Monte Carlo Modelling Approach to Predict Interindividual Human Variation in Phenol-Induced Developmental Toxicity. *Toxicol. Sci.*, 157 (2017), 365-376. doi: 10.1093/toxsci/kfx054
- Szuets, P., Mesterhazy, A., Falkay, G.Y., Bartok, T. Early Telarche Symptoms in Children and their Relations to Zearalenon Contamination in Foodstuffs. *Cereal Res. Commun.*, 25 (1997), 429-436. doi: 10.1007/BF03543747
- Takemura, H., Shim, J.Y., Sayama, K., Tsubura, A., Zhu, B.T., Shimoi, K. Characterization of the estrogenic activities of zearalenone and zeranol in vivo and in vitro. *J. Steroid Biochem. Mol. Biol.*, 103 (2007), 170-177. doi: 10.1016/j.jsbmb.2006.08.008
- Zhang, X., Tsang, A.M., Okino, M.S., Power, F.W., Knaak, J.B., Harrison, L.S., Dary, C.C. A Physiologically Based Pharmacokinetic/Pharmacodynamic Model for Carbofuran in Sprague-Dawley Rats Using the Exposure-Related Dose Estimating Model. *Toxicol. Sci.*, 100 (2007), 345-359. doi: 10.1093/toxsci/kfm232

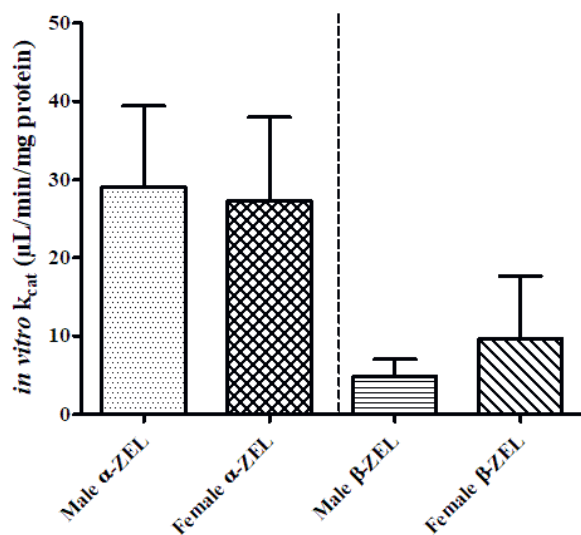
Supplementary Material

Supplementary Table 4.1. Information for individual liver S9 fractions from Corning (Woburn, MA, USA)

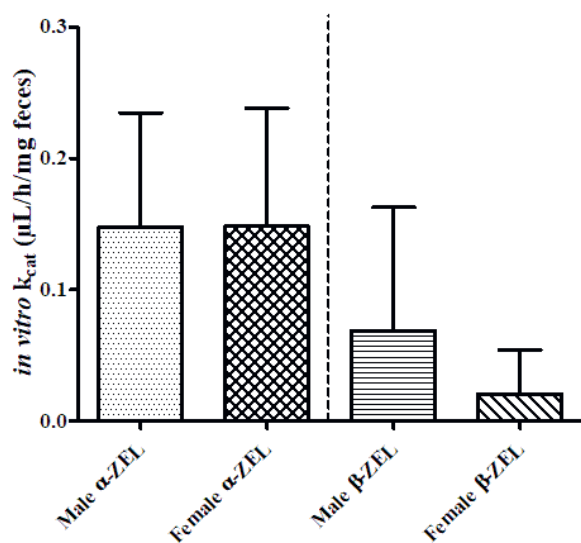
Individual code	Gender	Age
H0033	M	44
H0041	M	33
H0120	F	57
H0164	M	30
H0177	F	45
H0205	F	48
H0208	F	78
H0220	F	33
H0251	F	42
H0420	M	42
H0422	M	69
H0428	F	57
H0438	M	56
H0441	M	63
H0442	M	49
H0487	M	48
H0751	M	29
H0025	F	30
H0246	F	40

Supplementary Table 4.2. Information for the individual fecal samples collected in this study

Individual	Gender	Age
1	F	28
2	F	24
3	F	60
4	M	25
5	M	35
6	M	65
7	M	45
8	M	28
9	F	25
10	M	27
11	F	19
12	F	25
13	M	26
14	F	59
15	F	26
16	F	24
17	M	64
18	M	26
19	F	27
20	F	31



Supplementary Figure 4.1. Comparison of male and female *in vitro* k_{cat} values for α -ZEL and β -ZEL formation from incubations with human S9 fractions.



Supplementary Figure 4.2. Comparison of male and female *in vitro* k_{cat} values for α -ZEL and β -ZEL formation from incubations with human fecal slurries.

Chapter 5

Interspecies and human inter-individual differences in the intestinal microbial metabolism of zearalenone-14-glucoside (ZEN-14-G)

*Diana M. Mendez-Catala, Albertus Spengelink,
Karsten Beekmann & Ivonne M.C.M. Rietjens*

In preparation

Abstract

Zearalenone is a secondary metabolite from fungi (*Aspergillus* and *Fusarium*) infecting crops. In plants, ZEN is conjugated with glucose, to facilitate its storage in the vacuoles, with zearalenone-14-glucoside (ZEN-14-G) being the most prevalent form. The modified forms of ZEN were not considered to be of concern due to a low bioavailability, but in recent years it became clear that the intestinal microbiota can increase the bioavailability. In 2016 the European Food Safety Authority (EFSA), proposed a group health-based guidance value (HBGV) for ZEN and its modified forms, equal to 0.25 µg/ kg bw derived from estrogenic effects observed in immature gilts exposed to ZEN as critical effect. In the present study we used an *in vitro* model to study interspecies (rat, pig and human) and human interindividual differences in the hydrolysis of ZEN-14-G to ZEN by the intestinal microbiota derived from fecal samples. Substantial interspecies and interindividual differences were observed *in vitro*. An *in vivo* estimation indicated that all three species and all individuals are likely to fully hydrolyze ZEN-14-G in less than 0.01% of the total colonic transit time. These results suggest that ZEN-14-G will become bioavailable as ZEN by the action of the intestinal microbiota, and fully supports the inclusion of ZEN-14-G in the current group HBGV with equal potency to ZEN.

5.1 Introduction

Mycotoxins are secondary metabolites of fungi (e.g. *Aspergillus*, *Fusarium*, and *Penicillium*) infecting diverse crops and known to exert toxic effects in animals and humans. Zearalenone (ZEN) is a mycotoxin produced by *Fusarium* spp. mainly in crops of maize and wheat, that can be found in food and feed (EFSA, 2011). ZEN and its metabolites are known to cause reproductive disorders in animals and humans, and the group health-based guidance value (HBGV), i.e. the tolerable daily intake (TDI), proposed by the European Food Safety Authority (EFSA) was derived using the estrogenic effects observed in immature gilts exposed to ZEN as critical effect (EFSA, 2011; EFSA, 2016). The modified forms of ZEN are a result of plant metabolism, in which ZEN is conjugated with glucose and/or sulphates to increase its polarity and facilitate storage of the mycotoxin in the vacuoles (Broekaert *et al.*, 2015). Though ZEN has multiple sites for potential conjugation (Figure 5.1), most modifications occur at its hydroxyl moiety at C14 because conjugate formation at the hydroxyl moiety at C16 is hampered by formation of a hydrogen bond to the carbonyl at C1 of ZEN. Thus, ZEN-14-glucoside (ZEN-14-G) is known as the most prevalent conjugated (modified) form of ZEN. According to Berthiller *et al.* (2013) the presence of ZEN-14-G in food products could account for up to 30% of the total ZEN content.

Initially, the modified forms of ZEN were not considered to be of concern for human health due to their limited bioavailability related to a high molecular weight and poor absorption upon ingestion. However, it is now well recognized that the intestinal microbiota can mediate several metabolic reactions, one of them being deglycosylation (Sousa *et al.*, 2008), thereby affecting the bioavailability of ZEN-14-G. The metabolism of modified forms of ZEN has been studied *in vivo* in pigs (Binder *et al.*, 2017), and the potential of the human intestinal microbiota to hydrolyze the modified forms of ZEN has been shown *in vitro* using fecal samples (Dall’Erta *et al.*, 2013; Gratz *et al.*, 2017). This implies that the intestinal microbiota expands the host’s metabolic capacity for ZEN-14-G. However, overall differences in the intestinal microbial communities between species and individuals have been described (Krych *et al.*, 2013; Nguyen *et al.*, 2015), and may originate from differences in age, gender, diet, lifestyle and/or genetic background (Nicholson *et al.*, 2012).

The aim of the present study was to use an *in vitro* model based on the use of fecal samples derived from rats, pigs and humans to quantify the kinetic parameters for the hydrolysis of ZEN-14-G to ZEN by the intestinal microbiota. Additionally, interindividual differences in the formation of ZEN from ZEN-14-G by the human

intestinal microbiota were characterized. The kinetic data obtained were compared to intestinal residence time to get an insight in the efficiency of this metabolic conversion and the resulting bioavailability of ZEN from ZEN-14-G in the different species and for different individuals. The results obtained will elucidate possible species differences as well as human interindividual differences in microbial metabolism and the potential contribution of ZEN-14-G to ZEN exposure.

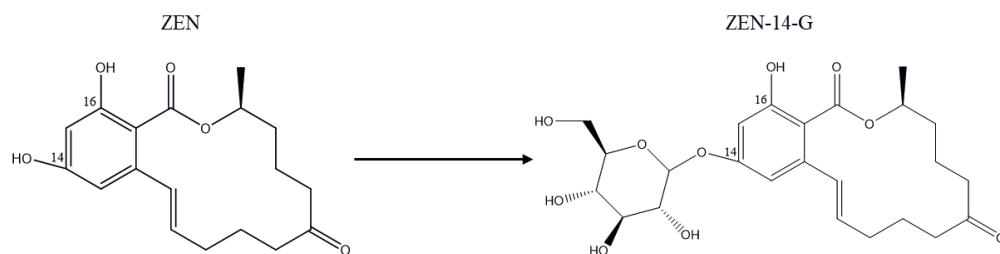


Figure 5.1. ZEN and its major modified form ZEN-14-G

5.2 Materials and methods

5.2.1 Materials

ZEN-14-β-D-glucoside (CAS 105088-14-0) was purchased from HPC standards GmbH (Cunnersdorf, Germany). ZEN (CAS 17924-92-4; ≥ 99.0%), was purchased from Sigma-Aldrich (Schnelldorf, Germany). Stock solutions of the test chemicals were prepared in dimethyl sulfoxide (DMSO) purchased from Merck (Darmstadt, Germany). Methanol (MeOH, UPLC/MS grade) and acetonitrile (ACN, UPLC/MS grade) were purchased from Biosolve (Valkenswaard, The Netherlands). Phosphate-buffered saline (PBS, pH 7.4), was obtained from Gibco (Paisley, UK).

5.2.2 Collection of fecal samples

Fecal samples of Wistar rats (10 male, 15 female) were kindly provided by BASF (Ludwigshafen, Germany). Fecal sample from piglets (5 females and 5 males) were kindly provided by Wageningen Livestock Research (Wageningen, The Netherlands) and collected during dissection of untreated control animals of an animal study for which permission (license number 2016.D0136.003) by the Animal Care and Use Committee of Wageningen University & Research (Wageningen, The Netherlands) was obtained. Fecal samples from human (7 females and 3 males) were donated by 10 healthy volunteers, aged 24-64 years. Volunteer donors did not consume antibiotics or visit tropical countries for 3 months prior to sample donation

and have no history of intestinal diseases. The research protocol for use of these human samples was evaluated by the Medical Ethical Reviewing Committee of Wageningen University (METC-WU) and judged not to require further evaluation within the scope of the Dutch Medical Research Involving Human Subjects Act. All samples were transferred into an anaerobic environment as soon as possible and at most within minutes after collection.

Briefly, fresh fecal samples were weighed and diluted in anaerobic solution of 10% glycerol in PBS to obtain a fecal slurry (20% w/v) under anaerobic conditions (85% N₂, 10% CO₂ and 5% H₂, in a Bactron EZ anaerobic chamber). The samples were manually homogenized with a sterile serological pipette and filtered using a woven sterile medical gauze dressing (HeltiQ) for rat and pig samples or SpinCon® (Meridian Bioscience Europe) centrifugal filters for human samples. The resulting filtrate was divided into aliquots and stored at -80°C until further use. Individual human samples were treated and stored separately. Prior to the experiment, a pool of 10 (human) individuals was prepared

5.2.3 *In vitro* incubation of ZEN-14-G with fecal samples

The *in vitro* incubations of ZEN-14-G with pooled fecal samples for rats, pigs and humans, as well as for the 10 individual humans, were performed under anaerobic conditions. To this end, a final incubation mixture of 100 µL was prepared in PBS (pH 7.4) containing 2 mg/mL (final concentration) of fecal slurry from rats, pigs, or humans and 1 - 200 µM ZEN-14-G (added from 100x concentrated stock solutions in DMSO). The reaction was started by the addition of ZEN-14-G after a 5-minute pre-incubation at 37 °C. The mixtures were incubated anaerobically at 37 °C for 5 minutes. Under these conditions, the hydrolysis of ZEN-14-G was linear in time and with the fecal concentration (see Supplementary Material). The reactions were terminated by the addition of 100 µl ice-cold MeOH, the samples were vortexed, and kept on ice for 10 minutes. Subsequently the samples were centrifuged at 21,500 \times g for 15 minutes at 4 °C, and the supernatants were kept for immediate liquid chromatography-tandem mass spectrometry (LC-MS/MS) analyses. Blank controls without fecal sample were included to assess the stability of ZEN-14-G during the incubation. Incubations with individual human fecal samples were performed in the same way. Three independent experiments for each species and for each (human) individual were done and data are presented as mean \pm standard deviation (SD).

5.2.4 Quantification of ZEN: LC-MS/MS analysis

The formation of ZEN from ZEN-14-G in incubations with rat, pig and human fecal slurry was quantified by LC-MS/MS. The analysis was performed on a Nexera XR LC-20ADXR UPLC system coupled to an LCMS 8045 mass spectrometer (Shimadzu Benelux, 's Hertogenbosch, The Netherlands). The UPLC system was equipped with a Kinetex® C18 column 1.7µm, 50 mm x 2.1 mm (Phenomenex) and operated at a flow rate of 0.3 ml/min at 40 °C. The mobile phases consisted of nanopure water containing 0.1% (v/v) formic acid (A) and ACN containing 0.1% (v/v) formic acid (B). The total run time was 14 minutes with the following gradient profile: 0-40% B (0 –1.3 min), 40-50% B (1.3 - 5.7 min), 50-100% B (5.7 - 6 min), 100 % B kept for 2 minutes and 100-0% B (8 - 8.1 min) and kept at 0% B for re-equilibration of the column. Per run, 1 µl of sample was injected. MS-MS analysis was performed in the LCMS 8045 triple quadrupole with electrospray ionization (ESI) interface. The analysis was operated in the negative ion mode and the MRM mode with a spray voltage of 4.5 KV. The transitions monitored were (*m/z*) 479.10 → 317.1 ZEN-14-G; and (*m/z*) 317.10 → 175.0, 317.10 → 273.10, 317.10 → 131.0 for ZEN. The Postrun Analysis function from the LabSolutions software (Shimadzu, Kyoto, Japan) was used to obtain the peak area of the total ion chromatogram (TIC) for each compound. For quantification, the areas were compared to standard curves made using commercially available standards.

5.2.5 Kinetic analysis

To derive the kinetic constants for the formation of ZEN from ZEN-14-G by rat, pig and human (pooled and individual) microbial metabolism, the amount of ZEN formed expressed per gram of feces and per unit of time (rate of formation) were calculated using Microsoft Excel (version 2016) and plotted against the substrate concentrations used. The curve for each metabolite was fitted in GraphPad Prism 5.04 (GraphPad software, San Diego California, U.S.A.) using a standard Michaelis-Menten regression (Equation 1) to obtain the *in vitro* kinetic constants, V_{\max} (nmol/min/mg of feces) and K_m (µM) for the microbial metabolism of ZEN-14-G.

$$V_{\text{ZEN}} = V_{\max} * [\text{ZEN-14-G}] / (K_m + [\text{ZEN-14-G}]) \quad \text{Equation 1}$$

5.2.6 Estimation of *in vivo* microbial metabolism of ZEN-14-G in rat, pigs and humans

The *in vitro* V_{\max} (nmol/min/mg feces) for the formation of ZEN in anaerobic incubations with fecal samples from rat, pig and (pooled and individual) human was scaled to an *in vivo* $V_{\max, \text{in vivo}}$ ($\mu\text{mol/h}$) using the reported average defecation masses of 4.1 g feces/day for rat (Kimura and Higaki, 2002), 1,360 g feces/day for pigs (Mariscal-Landin, 2007) and 128 g feces/day for humans (Rose *et al.*, 2015). The K_m values *in vitro* were assumed to be equal to the K_m values *in vivo*.

The kinetic parameters obtained were used to calculate the rate of formation of ZEN (V_{ZEN}) *in vivo* from a mean estimated intake of ZEN-14-G using equation 1, where the V_{\max} used was the estimated $V_{\max, \text{in vivo}}$ ($\mu\text{mol/h}$), K_m was assumed to be equal *in vivo* to *in vitro* and [ZEN-14-G] is the concentration of ZEN-14-G (nM) in the colon estimated as follows. The concentration of ZEN-14-G was assumed from an intestinal amount of ZEN-14-G resulting from an estimated daily intake (EDI) of 2.8 ng/kg bw/day calculated from the mean occurrence of ZEN-14-G of 39 $\mu\text{g/kg}$ reported in breakfast cereals (Boevre *et al.*, 2012) and a mean consumption for adults of 5 g cereal/day (EFSA, 2011). Firstly, the EDI was corrected for average body masses of 0.25 kg for rats (Brown *et al.*, 1997), 25 kg for pigs (Upton, 2008) and 70 kg for humans (Brown *et al.*, 1997). Secondly, the dose was converted to nmol using the molecular weight (MW) of 480.5 g/mol for ZEN-14-G. Finally the [ZEN-14-G] (nM) was calculated by dividing by the colonic volume assumed to be equal to the fecal defecation volume per day for rats, pigs and humans for this purpose to correct for differences in microbial density. The time (min) required to hydrolyze all ZEN-14-G at this dose could be estimated dividing ZEN-14-G (nmol) by the V_{ZEN} (nmol/h) obtained multiply by 60 for the conversion from hours to minutes. The times required for full hydrolysis of ZEN-14-G were compared to the fecal residence time reported in literature.

5.3 Results

5.3.1 *In vitro* and *in vivo* interspecies differences in intestinal microbial hydrolysis of ZEN-14-G

To study the hydrolysis of ZEN-14-G by the intestinal microbiota from rats, pigs and humans, the concentration-dependent conversion of ZEN-14-G to ZEN by pooled fecal samples under anaerobic conditions was quantified (Figure 5.2). The formation of ZEN from ZEN-14-G showed to be a rapid process. With the optimized conditions for linear metabolism of 2 mg/mL of fecal slurry and 5 minutes, the release of ZEN

from ZEN-14-G followed Michaelis-Menten behavior allowing the derivation of the *in vitro* kinetic constants V_{\max} and K_m . In the absence of the intestinal microbiota, ZEN-14-G was stable under the incubation conditions. The *in vitro* V_{\max} , K_m , and catalytic efficiency (k_{cat} calculated as V_{\max}/K_m) for the formation of ZEN are presented in Table 5.1. The comparison of the *in vitro* k_{cat} values of the three species, showed rat microbiota to intrinsically hydrolyze ZEN-14-G 3.2 times more efficiently than pigs and 3.6 times more efficiently than humans. The difference between human and pigs was smaller, with pig microbiota being only 1.3-fold more effective.

The *in vitro* parameters were used to estimate the time for a full conversion of ZEN-14-G by the intestinal microbiota *in vivo*. First, the *in vitro* parameter V_{\max} for the formation of ZEN from ZEN-14-G was scaled to the *in vivo* situation as described in the Materials and Methods section. Then, the *in vivo* V_{\max} and K_m (Table 5.1) were used to estimate the rate of the formation of ZEN (V_{ZEN}) *in vivo* at a concentration of ZEN-14-G that would result from an estimated daily intake of 2.8 ng/kg bw. The V_{ZEN} obtained was used to estimate the time required for the full hydrolysis of ZEN-14-G and was compared to the average colonic transit time reported in literature for each species. The results of these calculations are presented in Table 5.2 and show that full conversion of ZEN-14-G is expected to require 0.02, 0.05 and 0.06 min in rat, pigs and humans respectively, amounting to less than 0.01 % of the transit time in all species (Table 5.2). This indicates that during the transit through the colon full and efficient hydrolysis of ZEN-14-G will take place in all three species. The time needed for full hydrolysis of ZEN-14-G shows interspecies differences with a higher efficiency by rats, followed by pigs and finally humans, but overall fast hydrolysis of the dose is predicted.

Table 5.1. *In vitro* and *in vivo* kinetic parameters for the release of ZEN from ZEN-14-G by rat, pig and human intestinal microbiota.

Microbial	V_{\max} , <i>in vitro</i> ^a	K_m ^b	<i>in vitro</i> k_{cat} ^c	Scaled V_{\max} , <i>in vivo</i> ^d	<i>in vivo</i> k_{cat} ^e
Rat	2.67	45.1	58.9	654.4	58
Pig	1.36	73.2	18.6	1.1×10^5	61
Human	0.91	55.4	16.5	7×10^3	1.8

^a nmol/min/mg of feces

^b μM

^c $\mu\text{L}/\text{min}/\text{mg}$ feces

^d $\mu\text{mol}/\text{h}$

^e $\text{L}/\text{h}/\text{kg}$ bw

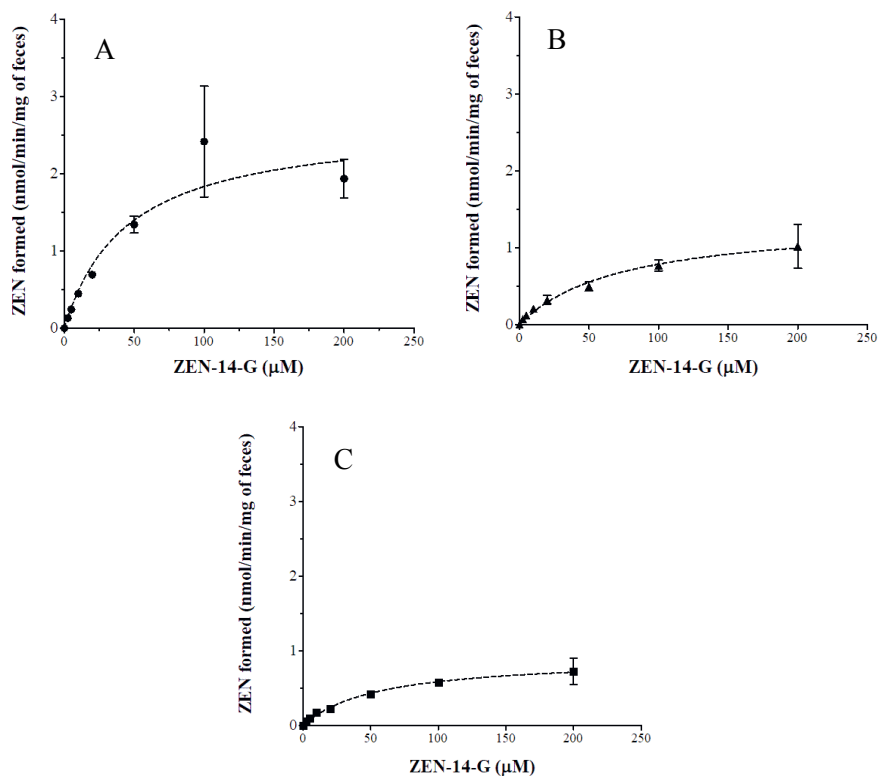


Figure 5.2. ZEN-14-G concentration-dependent formation of ZEN in incubations with pooled fecal samples of rat (A), pig (B) and human (C). Each data point represents the mean \pm SD of three independent experiments.

Table 5.2. *In vivo* estimation for the release of ZEN from a dose of 2.8 ng/kg bw/day of ZEN-14-G by rat, pig and human intestinal microbiota.

Species	[ZEN-14-G] ^a	V _{ZEN} ^b	Transformation time ^c	Reported colonic transit time ^e	% of transit time for full conversion
Rat	0.4	5	0.02	360 ^d	0.0047
Pig	0.1	162	0.05	2160 ^e	0.002
Human	3.2	401	0.06	1440 ^f	0.0042

^a nM; concentration of ZEN-14-G in colon estimated from and EDI of 2.8 ng kg bw⁻¹ [(EDI/480.5g mol⁻¹) *kg bw*volume of defecation per day)]

^b nmol/h; estimated rate of formation of ZEN from ZEN-14-G

^c min

^d de Zwart *et al.* (1999)

^e Musial *et al.* (1992)

^f Wilson (2000)

5.3.2 Human inter-individual differences in the intestinal microbial hydrolysis of ZEN-14-G

Besides the differences between humans and model animals such as rats and pigs, interindividual human differences in intestinal microbial metabolism were characterized. The kinetic parameters for the hydrolysis of ZEN-14-G were obtained from anaerobic incubations with fecal samples from 10 individuals. The release of ZEN for all individuals followed Michaelis-Menten kinetics. The individual kinetic parameters V_{max} and K_m obtained are presented in Table 5.3. The kinetic parameters were scaled to *in vivo* V_{max} values, and used to estimate the times for full hydrolysis of a dose of 2.8 ng/kg bw ZEN-14-G.

The average apparent *in vivo* V_{max} and K_m obtained from the individual incubations were 4,716 µmol/min and 37.6 µM, respectively. A 5.4-fold difference was observed between the highest and lowest *in vivo* V_{max} obtained for the 10 individuals, with a CV of 42.2%. The relatively high CV observed was caused by individuals 2 and 7 which have high apparent V_{max} values that are 4.1-5.4-fold higher than the mean V_{max}. The mean of the apparent *in vivo* k_{cat} (151 L/h) obtained from the individual incubations (Table 5.3) was in line with the apparent *in vivo* k_{cat} (126 L/h) obtained from the incubation with the pooled sample (Table 5.2). The estimation of the time required for full hydrolysis of ZEN-14-G shows that in all 10 individuals the hydrolysis will be complete within less than 0.16 min and thus less than 0.01% of the residence time.

Table 5.3. *In vitro* and *in vivo* kinetic parameters for the release of ZEN from ZEN-14-G derived from anaerobic incubations with 10 individual human fecal slurries. The *in vivo* scaling was done for a EDI = 2.8 ng kg bw⁻¹.

Individual	V_{\max} , <i>in vitro</i> ^a	K_m ^b	Scaled V_{\max} , <i>in vivo</i> ^c	<i>in vivo</i> k_{cat} ^d	V_{ZEN} ^e	Transformation time ^f	% of transit time for full conversion
1	0.26	40.1	1,975.3	49	156.1	0.16	0.0108
2	1.07	22.8	8,225.3	361	1,143.1	0.02	0.0015
3	0.57	39.4	4,365.3	111	351.1	0.07	0.0048
4	0.77	30.5	5,931.3	194	615.9	0.04	0.0027
5	0.38	41.3	2,888.4	70	221.6	0.11	0.0076
6	0.78	38.7	5,982.0	154	489.5	0.05	0.0035
7	0.83	29.3	6,338.3	216	685.6	0.04	0.0025
8	0.60	43.5	4,577.3	105	333.5	0.07	0.0051
9	0.20	66.4	1,530.6	23	73.1	0.33	0.0231
10	0.70	23.5	5,346.0	228	722.1	0.03	0.0023
Mean (μ_x) ^g	0.61	37.6	4,715.9	151	479.2	0.09	0.0064
SD ^h	0.3	11.9	1,989.1	96	305.7	0.1	0.0062
CV _x (%) ⁱ	42.2	31.8	42.2	64	63.8	96.9	96.9

^a nmol/min/mg feces

^b μ M

^c μ mol/h

^d L/h

^e nmol/h; estimated rate of formation of ZEN from ZEN-14-G

^f min

^g Mean of the kinetic constants for the ZEN release derived from 10 individuals

^h Standard deviation of the kinetic constants for the ZEN release derived from 10 individuals

ⁱ Coefficient of variation = SD/ μ_x *100

5.4 Discussion

The aim of this study was to assess the interspecies differences in the intestinal microbial hydrolysis of ZEN-14-G to ZEN using *in vitro* derived kinetics. Following the assessment of interspecies differences, we used this *in vitro* anaerobic incubation system to study inter-individual differences in the hydrolysis of ZEN-14-G in humans. ZEN-14-G is one of the major modified forms of ZEN present in food and feed, and due to the low absorption shown in *in vitro* studies (Gratz *et al.*, 2017), the exposure to ZEN-14-G *in vivo* may add to the overall ZEN exposure due to the capacity of the intestinal microbiota to hydrolyze ZEN-14-G to ZEN. The results obtained in the present study confirm that the intestinal microbiota can efficiently hydrolyze ZEN-14-G to ZEN in all three species. The hydrolysis of ZEN-14-G to ZEN by the intestinal microbiota is in line with results from *in vitro* studies showing the reaction to occur in incubations of ZEN-14-G with human fecal samples (Dall’Erta *et al.*, 2013; Gratz *et al.*, 2017).

The use of fecal samples offers a number of advantages for the study of intestinal microbial metabolism of ZEN-14-G, and other xenobiotics. Firstly, the use of fecal samples facilitates studies of interspecies and interindividual differences in metabolism. Secondly, the samples are obtained non-invasively with a high yield. Thirdly, these *in vitro* incubations enable quantification of kinetics for the metabolism of ZEN-14-G. While there are differences in microbial composition along the intestinal tract, the colon is the main site for bacterial fermentation, harboring 70% of the total bacteria present in the gut. Behr *et al.* (2018) reported the bacterial communities in feces and colon of rats to be highly comparable. Moreover, proofs of principle showing the adequacy of using anaerobic *in vitro* incubations using fecal samples for quantification of kinetics for intestinal microbial metabolism were reported (Mendez-Catala *et al.*, 2020; Wang *et al.*, 2020). As under the experimental conditions of the current study no lag phase was encountered, which allowed to establish linearity over time and concentration of fecal sample, kinetic studies were possible.

The comparison of *in vitro* k_{cat} values for the formation of ZEN from ZEN-14-G showed that of the three investigated species, the microbial communities of rats had the highest intrinsic efficiency, while humans had the lowest intrinsic efficiency. The scaling of the *in vitro* V_{max} to an *in vivo* V_{max} resulted in pigs having the highest efficiency followed by humans and rats, an outcome that is driven by the differences in defecation masses. The percentage of the colonic transit time required for the full hydrolysis of ZEN-14-G estimated from the *in vivo* kinetic parameters obtained at a

mean estimated intake of ZEN-14-G in humans of 2.8 ng/kg bw derived from occurrence data in breakfast cereals (Boevre *et al.*, 2012) showed the three species to hydrolyze the respective amount of ZEN-14-G quickly, in less than 1% of the colonic transit time. This observation is in line with results from *in vivo* studies in pigs showing that upon oral administration of ZEN-14-G, no ZEN-14-G was detected in plasma (Catteuw *et al.*, 2019), nor in feces or urine samples as reported by Binder *et al.* (2017), corroborating an efficient ZEN-14-G hydrolysis. Human inter-individual differences in hydrolysis of ZEN-14-G by intestinal microbiota were observed in this study with a CV of 42% *in vitro*. This seems to be in contrast with the study from Gratz *et al.* (2017) where no clear differences between 5 individuals were observed. However, this discrepancy may be due to the fact that in the report from Gratz *et al.* (2017) ZEN-14-G appeared to be completely hydrolyzed already at the first timepoint of sampling (i.e. 30 minutes) by all individuals, not reflecting the initial conditions of hydrolysis. The *in vivo* scaling of the individual intestinal microbial metabolism of ZEN-14-G pointed at full and efficient hydrolysis with the amount of ZEN-14-G ingested via the mean estimated intake from breakfast cereals being complete on average within 0.09 min amounting to 0.006 % of the colonic residence time.

ZEN-14-G is resistant to acidic conditions (Dall’Erta *et al.*, 2013), and therefore stomach hydrolysis in mammals is unlikely to occur. Gareis *et al.* (1990) suggested the hydrolysis of ZEN-14-G to be mediated by glycoside hydrolases such as β -glucosidase. The low absorption of ZEN-14-G shown from *in vitro* transfer studies with Caco-2 cells monolayers (Cirlini *et al.*, 2016; Gratz *et al.*, 2017) suggests a need for the involvement of microbial β -glucosidases in the release of ZEN from ZEN-14-G. Human β -glucosidases are expressed in tissues such as liver, gut, kidney and spleen and are known to be involved in the hydrolysis of plant glucosides such as glucosides of flavonoids, but their efficiency for hydrolysis is affected by the position of the glucose moiety and the chemical structure of the xenobiotic as observed when comparing for example the hydrolysis of quercetin-3-glucoside which is not hydrolyzed by human β -glucosidases, quercetin-3-glucoside is (Berrin *et al.*, 2002; Berthiller *et al.*, 2011). Additional to glucosidases encoded in the human genome, the microbial communities in the intestinal tract represent a significant source of glucosidases (Berthiller *et al.*, 2011; Gill *et al.*, 2006). The intestinal microbiota derived from fecal samples of rats, pigs and humans showed to fully and efficiently hydrolyze ZEN-14-G. This is different from the results reported by Berthiller *et al.* (2011) for deoxynivalenol-3- β -D-glucoside (DON-3-G), another modified mycotoxin glucoside, where cultures of individual bacteria derived from

the intestinal microbiota were not able to fully hydrolyze DON-3-G. Differences in experimental conditions, the use of only selected isolated bacterial strains, or an overall lower hydrolysis of DON-3-G could explain these differences in the extent of hydrolysis observed. While overall the human intestinal microbiota are considered to have a conserved metabolic capacity despite interindividual differences in composition (Koppel *et al.*, 2017), the observed differences in efficiency of hydrolysis of ZEN-14-G, i.e. the interindividual *in vivo* k_{cat} varying from 0.02 to 0.22 L/h, are likely due to interindividual differences in the expression of relevant hydrolytic enzymes, such as β -glucosidase (Cole *et al.*, 1985; Koppel *et al.*, 2017). The variation of intestinal microbial communities between species and individuals may also be associated with factors like gender, age and dietary habits. From the current analysis, due to the low number of subjects analyzed, such potential correlations could not be studied to a further extent.

To our knowledge, this is the first study to report interspecies and inter-individual differences in the kinetics for the hydrolysis for ZEN-14-G by the intestinal microbiome present in fecal samples. The results obtained reveal substantial interspecies and human inter-individual differences *in vitro* although for all species and individuals at estimated dietary levels of intake full hydrolysis of ZEN-14-G within the colonic transit time was estimated to occur *in vivo*. This suggests that ZEN-14-G could become bioavailable as ZEN by the action of the intestinal microbiota, and fully supports the inclusion of ZEN-14-G in the current group HBGV with a relative potency equal to that of free ZEN.

Acknowledgements

This research was financially supported by the National Council of Science and Technology (CONACYT) through a scholarship awarded to Diana M. Mendez Catala (CVU 619449) for conducting her PhD in The Netherlands. Special thank you to Katja van Dongen and Qianrui Wang in their collaboration for the collection of the fecal samples.

5.5 References

- Behr, C., Ramirez-Hincapie, S., Cameron, H.J., Strauss, V., Walk, T., Herold, M., Beekmann, K., Rietjens, I., van Ravenzwaay, B. Impact of lincosamides antibiotics on the composition of the rat gut microbiota and the metabolite profile of plasma and feces. *Toxicol. Lett.*, **296** (2018), 139-151. doi: 10.1016/j.toxlet.2018.08.002
- Berrin, J.G., McLauchlan, W.R., Needs, P., Williamson, G., Puigserver, A., Kroon, P.A., Juge, N. Functional expression of human liver cytosolic beta-glucosidase in *Pichia pastoris*. Insights into its role in the metabolism of dietary glucosides. *Eur. J. Biochem.*, **269** (2002), 249-258. doi: 10.1046/j.0014-2956.2001.02641.x
- Berthiller, F., Crews, C., Dall'Asta, C., Saeger, S.D., Haesaert, G., et al. Masked mycotoxins: A review. *Mol. Nutr. Food Res.*, **57** (2013), 165-186. doi: 10.1002/mnfr.201100764
- Berthiller, F., Krska, R., Domig, K.J., Kneifel, W., Juge, N., Schuhmacher, R., Adam, G. Hydrolytic fate of deoxynivalenol-3-glucoside during digestion. *Toxicol. Lett.*, **206** (2011), 264-267. doi: 10.1016/j.toxlet.2011.08.006
- Binder, S.B., Schwartz-Zimmermann, H.E., Varga, E., Bichl, G., Michlmayr, H., Adam, G., Berthiller, F. Metabolism of Zearalenone and Its Major Modified Forms in Pigs. *Toxins*, **9** (2017), 56. doi: 10.3390/toxins9020056
- Boevre, M.D., Mavungu, J.D.D., Landschoot, S., Audenaert, K., Eeckhout, M., Maene, P., Haesaert, G., Saeger, S.D. Natural occurrence of mycotoxins and their masked forms in food and feed products. *World Mycotoxin J.*, **5** (2012), 207-219. doi: 10.3920/wmj2012.1410
- Broekaert, N., Devreese, M., De Baere, S., De Backer, P., Croubels, S. Modified *Fusarium* mycotoxins unmasked: From occurrence in cereals to animal and human excretion. *Food Chem. Toxicol.*, **80** (2015), 17-31. doi: 10.1016/j.fct.2015.02.015
- Brown, R.P., Delp, M.D., Lindstedt, S.L., Rhomberg, L.R., Beliles, R.P. Physiological parameter values for physiologically based pharmacokinetic models. *Toxicol. Ind. Health*, **13** (1997), 407-484. doi: 10.1177/074823379701300401
- Catteuw, A., Broekaert, N., De Baere, S., Lauwers, M., Gasthuys, E., et al. Insights into In Vivo Absolute Oral Bioavailability, Biotransformation, and Toxicokinetics of Zearalenone, α -Zearalenol, β -Zearalenol, Zearalenone-14-glucoside, and Zearalenone-14-sulfate in Pigs. *J. Agric. Food. Chem.*, **67** (2019), 3448-3458. doi: 10.1021/acs.jafc.8b05838

- Cirlini, M., Barilli, A., Galaverna, G., Michlmayr, H., Adam, G., Berthiller, F., Dall'Asta, C. Study on the uptake and deglycosylation of the masked forms of zearalenone in human intestinal Caco-2 cells. *Food Chem. Toxicol.*, **98** (2016), 232-239. doi: 10.1016/j.fct.2016.11.003
- Cole, C.B., Fuller, R., Mallet, A.K., Rowland, I.R. The influence of the host on expression of intestinal microbial enzyme activities involved in metabolism of foreign compounds. *J. Appl. Bacteriol.*, **59** (1985), 549-553. doi: 10.1111/j.1365-2672.1985.tb03359.x
- Dall'Erta, A., Cirlini, M., Dall'Asta, M., Del Rio, D., Galaverna, G., Dall'Asta, C. Masked Mycotoxins Are Efficiently Hydrolyzed by Human Colonic Microbiota Releasing Their Aglycones. *Chem. Res. Toxicol.*, **26** (2013), 305-312. doi: 10.1021/tx300438c
- de Zwart, L., Rempelberg, C., Sips, A., Welink, J., van Engelen, J., 1999. Anatomical and physiological differences between various species used in studies on the pharmacokinetics and toxicology of xenobiotics. A review of literature. National Institute of Public Health and the Environment (RIVM), pp. 100.
- EFSA. Scientific Opinion on the risks for public health related to the presence of zearalenone in food. *EFSA J.*, **9** (2011), 2197. doi: 10.2903/j.efsa.2011.2197
- EFSA. Appropriateness to set a group health-based guidance value for zearalenone and its modified forms. *EFSA J.*, **14** (2016), e04425. doi: 10.2903/j.efsa.2016.4425
- Gareis, M., Bauer, J., Thiem, J., Plank, G., Grabley, S., Gedek, B. Cleavage of Zearalenone-Glycoside, a "Masked" Mycotoxin, during Digestion in Swine. *J. Vet. Med. Ser. B*, **37** (1990), 236-240. doi: 10.1111/j.1439-0450.1990.tb01052.x
- Gill, S.R., Pop, M., Deboy, R.T., Eckburg, P.B., Turnbaugh, P.J., et al. Metagenomic analysis of the human distal gut microbiome. *Science (New York, N.Y.)*, **312** (2006), 1355-1359. doi: 10.1126/science.1124234
- Gratz, S.W., Dinesh, R., Yoshinari, T., Holtrop, G., Richardson, A.J., Duncan, G., MacDonald, S., Lloyd, A., Tarbin, J. Masked trichothecene and zearalenone mycotoxins withstand digestion and absorption in the upper GI tract but are efficiently hydrolyzed by human gut microbiota *in vitro*. *Mol. Nutr. Food Res.*, **61** (2017), E1600680. doi: 10.1002/mnfr.201600680
- Kimura, T., Higaki, K. Gastrointestinal transit and drug absorption. *Biol. Pharm. Bull.*, **25** (2002), 149-164. doi: 10.1248/bpb.25.149

- Koppel, N., Maini Rekdal, V., Balskus, E.P. Chemical transformation of xenobiotics by the human gut microbiota. *Science*, **356** (2017), eaag2770. doi: 10.1126/science.aag2770
- Krych, L., Hansen, C.H.F., Hansen, A.K., van den Berg, F.W.J., Nielsen, D.S. Quantitatively Different, yet Qualitatively Alike: A Meta-Analysis of the Mouse Core Gut Microbiome with a View towards the Human Gut Microbiome. *PLoS One*, **8** (2013), e62578. doi: 10.1371/journal.pone.0062578
- Mariscal-Landin, G., 2007. Tratamiento excretas cerdos. Capítulo 7, Reporte de la Iniciativa de la Ganadería, el Medio Ambiente y el Desarrollo (LEAD)-Integración por Zonas de la Ganadería y de la Agricultura Especializadas (AWI)-Opciones para el Manejo de Efluentes de Granjas Porcícolas de la Zona Centro de México. FAO, pp.
- Mendez-Catala, D.M., Spenkelink, A., Rietjens, I.M.C.M., Beekmann, K. An in vitro model to quantify interspecies differences in kinetics for intestinal microbial bioactivation and detoxification of zearalenone. *Toxicol. Rep.*, **7** (2020), 938-946. doi: 10.1016/j.toxrep.2020.07.010
- Musial, F., Crowell, M.D., French, A.W., Guiv, N. Effect of prolonged, continuous rectal distention on mouth-to-cecum and colonic transit time in pigs. *Physiology & Behavior*, **52** (1992), 1021-1024. doi: 10.1016/0031-9384(92)90385-F
- Nguyen, T.L.A., Vieira-Silva, S., Liston, A., Raes, J. How informative is the mouse for human gut microbiota research? *Dis. Model Mech.*, **8** (2015), 1-16. doi: 10.1242/dmm.017400
- Nicholson, J.K., Holmes, E., Kinross, J., Burcelin, R., Gibson, G., Jia, W., Pettersson, S. Host-Gut Microbiota Metabolic Interactions. *Science*, **336** (2012), 1262-1267. doi: 10.1126/science.1223813
- Rose, C., Parker, A., Jefferson, B., Cartmell, E. The Characterization of Feces and Urine: A Review of the Literature to Inform Advanced Treatment Technology. *Crit. Rev. Environ. Sci. Technol.*, **45** (2015), 1827-1879. doi: 10.1080/10643389.2014.1000761
- Sousa, T., Paterson, R., Moore, V., Carlsson, A., Abrahamsson, B., Basit, A.W. The gastrointestinal microbiota as a site for the biotransformation of drugs. *Int. J. Pharm.*, **363** (2008), 1-25. doi: 10.1016/j.ijpharm.2008.07.009
- Upton, R.N. Organ weights and blood flows of sheep and pig for physiological pharmacokinetic modelling. *J. Pharmacol. Toxicol. Methods*, **58** (2008), 198-205. doi: 10.1016/j.vascn.2008.08.001



Chapter 6

General Discussion

6.1 Overview and main findings

Zearalenone (ZEN) is a mycotoxin present in food and feed. ZEN acts as an endocrine disrupting chemical (EDC) due to its structural similarity to the natural estrogen 17 β -estradiol (E2) and its ability to bind to and activate estrogen receptors (ERs). Observations in experimental animals have linked ZEN exposure to reproductive disorders. In mammals, ZEN is metabolized to α -ZEL and β -ZEL in liver and by the intestinal microbiota, with α -ZEL being on average 60-times more potent than ZEN as an estrogen active compound and β -ZEL being 5-times less potent than ZEN. Interspecies differences in the preference for α -ZEL and β -ZEL formation combined with interspecies differences in toxicodynamics have been associated with interspecies differences in sensitivity to ZEN exposure, with pigs being considered the most sensitive species in part due to their higher preference for α -ZEL formation. For humans, a TDI for ZEN of 0.25 $\mu\text{g/kg bw}$ was established based on a no observed effect level (NOEL) of 10.4 $\mu\text{g/kg bw}$ for the estrogenic effects of ZEN in young gilts (Döll *et al.*, 2004). Human kinetic studies on ZEN and its metabolism to α -ZEL and β -ZEL have not been reported. Therefore, the aim of this PhD project was to gain further insight into the metabolism of ZEN, including its metabolism in liver and intestinal microbiota of not only experimental animals but also human, and to include this information in physiologically based kinetic (PBK) models to enable evaluation of the role of metabolism of ZEN in its estrogenic activity.

In the present thesis, fecal samples from rats, pigs and humans were used in an *in vitro* model to assess and quantify the formation of α -ZEL and β -ZEL from ZEN by the intestinal microbiota (Chapter 2). The kinetics obtained were scaled to the *in vivo* situation and subsequently compared to the scaled *in vivo* liver metabolism of ZEN. The comparison of *in vivo* catalytic efficiencies (k_{cat}) of the intestinal microbial formation of α -ZEL and β -ZEL for the three species, based on defecation volumes per day and expressed per kg bw, revealed that the overall ZEN metabolism increased in the order human < rat < pig microbiota. The k_{cat} for liver metabolism, expressed per kg bw, in the three species surpassed the metabolism of the intestinal microbiota. While in pigs the formation of α -ZEL and β -ZEL from ZEN by the intestinal microbiota can be up to 36% of the activity of the liver, and might contribute to the bioactivation of ZEN in pigs, this contribution may be much less pronounced for humans due to the larger difference between the scaled k_{cat} of the liver and the microbiota for humans. The interspecies differences captured from the *in vitro* model for the intestinal microbial metabolism and the comparison to hepatic

metabolism highlight the importance of the development of human-specific models for the assessment of the kinetics of ZEN. To further study the role of the intestinal microbiota and liver in the overall metabolism of ZEN, PBK models for rats and humans were built for ZEN including a sub-model for α -ZEL (Chapter 3). The PBK model for rats was validated by comparing the predicted result for the maximum blood concentration (C_{\max}) of ZEN of 6.08 nM to a C_{\max} of 8.14 nM reported *in vivo* (Shin *et al.*, 2009) at an oral dose of 8 mg/kg bw, showing a 1.3-fold difference. The human model was evaluated with 24 h cumulative urinary levels of ZEN available for 2 (male) individuals exposed to 1.43 mg/kg bw (Mirocha *et al.*, 1981) and 0.143 μ g/kg bw (Warth *et al.*, 2013) of ZEN; resulting in predictions 1.8-fold lower and 2.1-fold higher than the *in vivo* reports, respectively. The integration of the intestinal microbiota in both PBK models indicated that the hepatic metabolism is dominant in the formation of α -ZEL. Additionally, the predicted C_{\max} for ZEN and α -ZEL in humans at a range of doses of 2.4-29 ng/kg bw, representing the estimated daily intake for the average adult population, were 3 orders of magnitude lower than the *in vitro* concentrations inducing estrogenic activity (EC_{10}) in *in vitro* bioassays for estrogenicity. Despite the higher estrogenicity of α -ZEL, the results of this study suggest that at normal dietary intake estrogenic effects are unlikely to occur. This is due to the efficient glucuronidation of ZEN and its metabolites, reducing the circulation of the biologically active aglycones. The study provided a proof-of-principle for inclusion of intestinal microbial metabolism in PBK models and how this offers a view into the role of the intestinal microbiota in the systemic concentrations of ZEN and its metabolite α -ZEL in the host. Despite the low concern at current exposures, interindividual differences in kinetics shown for piglets (Brezina *et al.*, 2016), which are most likely also present in humans, suggest the need for models to include interindividual toxicokinetic differences in the risk assessment of ZEN. In a further study of the present thesis (Chapter 4) human PBK models were developed using microbiota and tissue samples from individual donors and the outcomes of these models were combined with Monte Carlo simulation to obtain an insight into the interindividual differences in hepatic and intestinal microbial metabolism and bioactivation of ZEN, and the consequences for the interindividual differences in the C_{\max} of ZEN and α -ZEL. Initially, the kinetics for liver metabolism were determined using human liver S9 samples of 20 individuals, and kinetics for intestinal microbial metabolism were obtained using fecal samples from also 20 individuals following the *in vitro* approach developed in Chapter 2. The derived kinetic parameters provided the input for the definition of 400 individual PBK models from which the distribution of the C_{\max} for ZEN and α -ZEL in human plasma

could be predicted. Based on the characteristics of these distributions, the PBK model outcomes were combined with Monte Carlo simulations to simulate the distribution of C_{\max} for ZEN and α -ZEL for a larger population ($n = 9879$). The distribution of the predicted C_{\max} of ZEN and α -ZEL, presented in ZEN equivalents, was used to estimate a compound specific assessment factor (CSAF) for interindividual differences in kinetics of 2.45 for the 95th percentile of the adult population. This CSAF value suggests that the current default uncertainty factor for interindividual variation in kinetics (UF_{HK}) of 3.16 is sufficiently protective for the adult population. As some reports in mammals have suggested prepubertals to be possibly more sensitive to ZEN exposure, it remains to be investigated whether this also holds for humans and if so whether this can be ascribed to differences in toxicokinetics or is rather due to differences in toxicodynamics. This will indicate whether the inclusion of a sensitive subgroup of prepubertal individuals in the CSAF for interindividual differences in kinetics is required.

The strategy developed in Chapters 2- 4 provides a proof-of-principle for the *in vitro-in silico* study of ZEN kinetics and its interspecies and interindividual variability. Besides ZEN, zearalenone-14-glucoside (ZEN-14-G), a modified form of ZEN reported to occur frequently in food and feed in combination with ZEN can increase the exposure to ZEN. Despite the low bioavailability of ZEN-14-G, it may contribute to the systemic ZEN exposure because ZEN-14-G can be converted to ZEN by the action of the intestinal microbiota. Therefore, in further studies of the present thesis the *in vitro* model for quantification of metabolism by the intestinal microbiota was used to quantify the metabolism of ZEN-14-G in rats, pigs and humans (Chapter 5). Additionally, human interindividual differences in this metabolism were assessed. Substantial interspecies and interindividual differences for the hydrolysis of ZEN-14-G to ZEN by the intestinal microbiota were observed *in vitro*. The *in vitro* kinetic data were scaled to the *in vivo* situation and compared to the colonic residence time to obtain insight in whether *in vivo* full hydrolysis of ZEN-14-G would be likely to occur. The time for full hydrolysis of a realistic dietary dose of ZEN by the intestinal microbiota was estimated to amount to less than 0.01% of the reported total colonic residence time in all three species. This result indicates the importance of the intestinal microbiota upon exposure to ZEN-14-G and supports the inclusion of ZEN-14-G into the group health-based guidance value (HBGV), i.e. the TDI, of 0.25 $\mu\text{g}/\text{kg bw}$ (EFSA, 2016).

Though the study of the contribution of intestinal microbial metabolism to the overall host kinetics poses a number of challenges as addressed in later sections, the strategy

described and applied in this PhD thesis shows a proof-of-principle how the contribution of intestinal microbial metabolism can be considered.

6.2 General discussion and future perspectives

The *in vitro* model for intestinal microbial metabolism of ZEN and ZEN-14-G revealed interspecies and interindividual differences in metabolism. The inclusion of the kinetic parameters obtained for ZEN in PBK models enabled modeling of the contribution of the intestinal microbiota to the overall metabolism of ZEN in the host. This revealed that the conversion of ZEN by the intestinal microbiota is likely not as significant as the metabolism in the liver. Overall the results obtained offer several opportunities for further consideration and research which are discussed in some more detail in the following sections.

6.2.1 *In vitro* models to study the intestinal microbial metabolism

In toxicology, the consequences of metabolism by the intestinal microbiota have gathered increasing interest in part because of its wide array of metabolic enzymes, which is on average 100-fold larger than that of the host. Several *in vivo* and *in vitro* models have been developed to study intestinal microbial metabolism, each of them with its own limitations. However, there is a need for the development of suitable *in vitro* and *in silico* methods, given the request for reduction in the number of *in vivo* studies with experimental animals within the 3R (replacement, reduction, refinement) framework (Berg *et al.*, 2011; National Research Council, 2007). This development is also driven by the fact that results obtained with experimental animals may not adequately reflect the human situation. However, the use of *in vitro* models to study intestinal microbial metabolism poses several challenges. One of the main concerns is the source of the intestinal microbiota. The microbiota is known to vary along the gastrointestinal tract, with the highest concentration of microbiota found in the large intestine, a site with ideal conditions for the growth of communities of microbiota and for chemical reactions to take place. Fecal samples have shown to be representative of the colonic microbiota, as shown by the comparison performed for rats (Behr *et al.*, 2018) and humans (Visconti *et al.*, 2019; Zierer *et al.*, 2018). Although individual differences in the microbial composition of the intestinal microbiota are reported, many metabolic processes thereof have been shown to be comparable between individuals (Abubucker *et al.*, 2012). *In vitro* studies with fecal samples have been reported as initial inoculum for *in vitro* fermentation (Atkinson *et al.*, 2004; Gratz *et al.*, 2017) or for the preparation of fecalase (Tamura *et al.*, 1980), an extract of the microbial enzymes. In this PhD

thesis, fecal samples from three different species were obtained and used as a surrogate for the study of intestinal microbial metabolism of ZEN and ZEN-14-G. The proper preparation of these samples provided a suitable way for obtaining a high yield from a single sampling to be stored and used for further research (National Academies of Sciences and Medicine, 2018). Even though studies have used a similar approach, variation in the experimental conditions represent a major source for potential lack of reproducibility (Clarke *et al.*, 2019). The use of specific culture media to resemble the surroundings of the large intestine in *in vitro* fermentations may lead to selective growth of bacteria, and to the possible loss of other relevant bacteria (Mortelé *et al.*, 2019; Yousi *et al.*, 2019). In these circumstances, the metabolic potential arising from changes in the communities might affect the metabolic capacity. Continuous *in vitro* fermentation models derived from fecal samples, consisting of multiple connected compartments mimicking the intestinal microbiota in the different portions of the colon, have been developed (Nissen *et al.*, 2020). Examples of these models include the Simulator of the Human Intestinal Microbial Ecosystem (SHIME) (Van den Abbeele *et al.*, 2010) and the TNO *in vitro* model-2 (TIM-2) (Minekus *et al.*, 1999). The models allow for longer incubations, resulting in a stable composition due to a constant flow (refreshment) of nutrients, and in some cases removal of microbial metabolites; they offer the advantages of being able to mimic different sections of the intestinal tract to a certain extent, and allow to study perturbances of the intestinal microbiota. Despite this, the complexity of the models makes them costly, time and material consuming, and make that they do not offer any significant advantages over small batch static cultures for the purposes of the research described in this thesis. As an alternative to fecal samples used as inoculum, defined microbial populations which include bacterial species supposedly driving the metabolic activity observed *in vivo* were suggested (Schäpe *et al.*, 2019). While these well-defined populations can be useful for studying the interactions of the respective microorganisms with a compound of interest, the reduced complexity and representation of the actual intestinal microbiota, as compared to fecal samples used as inoculum, allowing to study interindividual and interspecies differences, is considered a disadvantage. The advantages and disadvantages of each model need to be considered when choosing an experimental system suitable for the objective of the study. In the development of the method described in the present thesis, compounds of interest were incubated with fecal samples in anaerobic PBS, which appeared to be a suitable medium for short-time incubations (< 24 hours). The incubations in PBS appeared to eliminate a lag time observed when incubations were performed in general growth media (data not

shown). Short incubations of these so called “static batch cultures” were reported to have an advantage over longer incubations because of possible changes in pH and redox potential at prolonged incubation times (Rumney and Rowland, 1992; Venema and van den Abbeele, 2013). As the culture is suggested to follow a typical bacterial growth curve, incubation times should be only as short as needed and not exceed 24 - 48 hours (Gibson and Wang, 1994; Sousa *et al.*, 2008). Overall, this method allowed to obtain kinetic parameter for the formation of α -ZEL and β -ZEL from ZEN (Chapter 2) as well as the kinetics for the hydrolysis of ZEN-14-G to ZEN (Chapter 5), by the intestinal microbiota present in the fecal samples of different species and individuals.

Obviously, the use of fecal samples for studies on the intestinal microbial metabolism still raises the question on the role of the intestinal microbiota in earlier portions of the intestine- i.e. duodenum and jejunum. Though the research to obtain samples from earlier portions of the intestine by less invasive techniques continues, including for example the application of swallowable devices to collect intestinal fluids, they still pose challenges connected to sample preservation after collection (Koziolek *et al.*, 2015; Rezaei Nejad *et al.*, 2019; Tang *et al.*, 2020). Until these techniques become more widely available and if the objective of the study does not point otherwise, fecal samples are expected to provide a suitable source for the study of microbial metabolism. It is concluded that anaerobic incubations with fecal samples represent a first-tier approach which can be further combined with other *in vitro* and *in silico* models, such as PBK modelling, offering the possibility for the analysis of the contribution of the intestinal microbiota to the overall metabolism in an organism. Combining the kinetics obtained in anaerobic fecal incubations with PBK modeling to obtain insight in the role of intestinal microbial metabolism in overall host metabolism has been shown valid also in a previous study on daidzein converted by the intestinal microbiota to *S*-equol (Wang *et al.*, 2020).

6.2.2 General contribution of the intestinal microbiota to host metabolism

The intestinal microbial metabolism of pharmaceuticals has been studied as part of an improvement of drug formulations for a better delivery and for the detection of metabolites that could result in a toxic congener. Although the drug-microbiome interactions are relatively well-understood, the contribution of the intestinal microbiota to the metabolism of xenobiotics entering through the food chain remains a topic for further research. Unlike the liver, where the metabolism is geared towards the elimination of xenobiotics (via introduction of functional groups followed by glucuronidation and sulfation), the intestinal microbiota has a wider metabolic

capacity, mainly through reduction and hydrolysis, that may add to the metabolism in liver or other extrahepatic tissues (Clarke *et al.*, 2019). The contribution of the intestinal microbial metabolism of the mycotoxin ZEN includes its conversion to α -ZEL and β -ZEL, which, when taking the same metabolic conversion in the liver into account, was shown to contribute up to 36% of the overall metabolism in pigs, while in humans the contribution of the intestinal microbiota appeared to be less than 0.1%. The inclusion of the *in vitro* kinetics in a human PBK model for ZEN, and the accompanying sensitivity analysis, revealed that the predicted blood concentrations of ZEN and α -ZEL in humans were predicted to be unaffected by the metabolism of ZEN by the intestinal microbiota, while the major contributions were provided by the glucuronidation in liver and intestinal tissue. The PBK models presented a proof-of-principle for the inclusion of intestinal microbial metabolism as part of the modelling strategy. A similar PBK model based approach by Wang *et al.* (2020) also quantified the role of metabolism of the intestinal microbiota for plasma concentrations of metabolites in the host. Wang *et al.* (2020) developed a model for daidzein which adequately predicted the plasma concentrations of *S*-equol, a metabolite uniquely formed by the intestinal microbiota. The actual contribution of the intestinal microbial metabolism to the host metabolism is dependent on the nature of the chemical. This is clearly illustrated for ZEN-14- G which was shown to be very rapidly and fully converted to ZEN by the intestinal microbiota. This is especially of interest given the limited transport of ZEN-14-G reported in *in vitro* studies with Caco-2 cell monolayers (Cirlini *et al.*, 2016), pointing at limited bioavailability. The efficient hydrolysis of ZEN-14-G by the intestinal microbiota observed from *in vitro* incubations for rats, pigs and humans, as well as that observed for other glucosides such as daidzin and genestin (Gaya *et al.*, 2016; Setchell *et al.*, 2002), supports the potential importance of the role of the intestinal microbiota and its inclusion in PBK models. Additionally, the intestinal microbiota can play an important role in the enterohepatic recirculation of xenobiotics. By deconjugating conjugated metabolites excreted via the bile into the intestine, the intestinal microbiota can make these molecules available for re-uptake. In the case of ZEN and its metabolites, it can be speculated that this process not only slows down the elimination of these compounds, but also increases the potential for metabolism of ZEN to α -ZEL and β -ZEL. In the future, these mechanisms (i.e. biliary excretion, microbial metabolism, and re-uptake) need to be combined and included in PBK models.

It is of importance to note that this inclusion of the intestinal microbial metabolism in PBK models via kinetic parameters obtained in fecal *in vitro* incubations requires

scaling of *in vitro* kinetics to the *in vivo* situation, which may not be straightforward. In the next section this will be discussed further.

6.2.3 *In vitro* to *in vivo* scaling factors for the study of intestinal microbial metabolism

The identification of metabolites formed from dietary constituents has been the main focus of *in vitro* studies on intestinal microbial metabolism (Bode *et al.*, 2013; Venema and van den Abbeele, 2013). In the present thesis the work focused on the *in vitro* quantification of the kinetics of the metabolic conversions by the intestinal microbiota and extrapolation of the results obtained to the *in vivo* situation. Such studies have been scarcely reported. To allow conversion of the *in vitro* kinetic data to the *in vivo* situation adequate scaling factors are required. Such scaling factors have so far not been reported in literature. In the present thesis, the scaling of *in vitro* intestinal microbial kinetics for ZEN and ZEN-14-G to the *in vivo* situation was done based on the average defecation mass per day under the assumption that the daily defecated microbial mass is equal to the microbial mass present in the intestine. This scaling converts the amount of fecal sample and corresponding microbiota to the whole organism, assuming that the microbial metabolic activity in the fecal mass reflects the total capacity of microbial metabolism that may occur in the intestine during a day, and that fecal metabolism reflects the major part of microbial metabolism in the intestinal tract. The fact that the predictions made appeared to adequately match available *in vivo* data supported the scaling applied. Nevertheless, other factors potentially affecting the scaling could also be considered in future studies, such as the factors discussed in some more detail hereafter.

The interindividual differences in defecation mass and the colonic transit time may need to be considered when refining the scaling factor. Defecation masses in humans vary greatly, for example, a range of 19 - 415 g/day in a population of 220 individuals in the United Kingdom was reported (Cummings *et al.*, 1992). In the present thesis the average defecation mass of 128 g/day (Rose *et al.*, 2015) was used, but the wide variation observed between individuals, along with the differences of microbial content represent a challenge for the QIVIVE of data obtained *in vitro* with intestinal microbiota to the *in vivo* situation. Alternatively, the fecal mass can be corrected for the microbial content (or microbial load) using e.g. quantitative PCR (qPCR) targeting 16S rRNA or flow cytometry. While these are promising tools the variability observed in the techniques needs further attention. For example, qPCR is a cost-effective technique for microbial load determination, but a number of uncertainties can be introduced through the preparation of the sample (extraction,

purification and amplification of DNA) (Bender *et al.*, 2018; Galazzo *et al.*, 2020). The colonic transit time is also known to vary between species and individuals, and so is composition of the intestinal microbiome, both factors which are also affected by host genetics and diet. The colonic transit time is an important aspect for the analysis as it will determine the time the compound of interest will be in contact with the microbiota and therefore affect the amount of metabolite formed. The inclusion of the colonic content (i.e. average defecation mass per day) and the colonic transit time in the estimation of the metabolite formation by the intestinal microbiome from deleobuvir showed the potential relevance of these variables on the scaling to an apparent *in vivo* situation for rats (McCabe *et al.*, 2015). In the same study, the formation of deleobuvir metabolites by the intestinal microbiota varied widely between the two volunteers included in the study, which indicates the role of variability in the intestinal microbiota and the intestinal transit time.

The research on incorporation of intestinal microbial metabolism in kinetic studies relevant for toxicology is still in an initial phase. Zimmermann *et al.* (2019) proposed and evaluated a model for brivudine, a drug for which microbiota and the host are involved in metabolism, indicating that assessing the contribution of each is important.

The model presented in Chapter 3 shows that including microbial metabolism in PBK models is a way forward to obtain insight into the relative importance of microbial metabolism and represents a proof-of-principle for the potential of the use of fecal samples in *in vitro* incubations to define relevant kinetic parameters. Extending the proofs-of-principle will also facilitate further refinement and validation of the scaling factors used to translate the *in vitro* kinetic data to the *in vivo* situation. Once refined scaling factors become available, the refinement of the PBK model for ZEN, in combination with the *in vitro* model for intestinal microbiota will allow an even better understanding on the impact of host and microbial metabolism.

6.2.4 Species differences in the kinetics and dynamics of ZEN

As previously mentioned, pigs, specifically young gilts, have been set as the most sensitive species for ZEN exposure, and the data available in young gilts have been used to define a health-based guidance value, a TDI, for humans. Though no direct evidence is currently available, it is possible that the higher sensitivity of pigs, compared to other livestock and laboratory animals is in part due to interspecies differences in toxicokinetics in addition to interspecies differences in toxicodynamics. It remains to be defined as well how the kinetics and dynamics of

ZEN in pigs relate to those in humans. In this section, the interspecies differences in metabolism and toxicity of ZEN will be discussed to a further extent.

Interspecies differences in metabolism of ZEN

The metabolic pathway of ZEN was already described in Chapter 1, and includes formation of α -ZEL and β -ZEL and the respective glucuronides as major metabolites. Species differences in the levels at which these metabolites are formed have been described and are mainly related to differences resulting from the liver metabolism. Studies in animals including pigs, rats, poultry and ruminants have shown a higher preference for the formation of α -ZEL in pigs in contrast to a preference for β -ZEL formation observed in the other animals (EFSA, 2017).

The formation of α -ZEL and β -ZEL from ZEN in the liver is mediated by 3α - and 3β -hydroxysteroid dehydrogenase (HSD), respectively, an enzyme with significant differences between animals and humans (Degtiar and Kushlinsky, 2001). In rats a single 3α -HSD is present, while in humans 4 isoenzymes exist, each of them with different activities (Dufort *et al.*, 2001; Matsuura *et al.*, 1998). The presence of a single form in rats suggests the regulatory mechanism(s) of the activity of 3α -HSD, to differ from those in human. The polysubstrate activity of 3α -HSD in humans, suggests a significant contribution to the metabolism of xenobiotics (activation or detoxification) (Cheng, 1992; Deyashiki *et al.*, 1992). The higher *in vitro* activity for the formation of α -ZEL by subcellular fractions reported for humans compared to rats (Chapter 2), suggests the differences in 3α -HSD to play a significant role. In pigs, the presence of isoforms of 3α -HSD is not reported in literature, but the higher sensitivity is also possibly due to a differential expression and activity of 3α -HSD in liver and extrahepatic organs of this species as compared to rats or human (Zheng *et al.*, 2019). The role of 3β -HSD is not yet fully understood, but a proof-of-principle shows that the expression of the enzyme is reduced in the presence of α -ZEL and β -ZEL (Rasmussen *et al.*, 2013; Tiemann *et al.*, 2003).

Conjugation of ZEN with glucuronic acid and sulfates in different species is reported. Based on *in vitro* (liver microsomes) and *in vivo* (urinary excretion) studies, glucuronidation appears to be the major pathway for ZEN metabolism (Malekinejad *et al.*, 2006; Pfeiffer *et al.*, 2010; Ueberschaer *et al.*, 2016; Yang *et al.*, 2017). Species differences in hepatic glucuronidation were described (Malekinejad *et al.*, 2006), reporting that after 30 minutes incubation the *in vitro* glucuronidation by liver S9 fractions with increasing concentrations of ZEN (10-250 μ M) is limited in rats and chickens (12-89%), while under the same *in vitro* conditions pig liver S9 samples showed a 90-100% glucuronidation at concentrations of 10-100 μ M. Pfeiffer *et al.*

(2010) reported species differences in rates of glucuronidation from incubations of ZEN (50-100 μ M) with liver microsomes from rats, pigs and humans. Despite both studies being performed at different incubations conditions, the rates of glucuronidation *in vitro* revealed that pigs display the highest glucuronidation capacity and intrinsic rate of glucuronidation in liver. A higher glucuronidation will result in a loss of estrogenic activity of ZEN, contrasting the notion that pig sensitivity is related the formation of more α -ZEL. In Chapter 3, the *in vitro* glucuronidation of ZEN and α -ZEL in incubations with liver S9 from rats and humans was efficient. The kinetics obtained showed that the *in vivo* k_{cat} for rats and humans were comparable, with rat being on average 1.1-fold more efficient than humans. A similar trend was observed by Pfeiffer *et al.* (2010) reporting that glucuronidation of ZEN and α -ZEL by rat liver samples were 1.6 and 1.5-fold higher, respectively, than that of human liver samples. Similar species differences in glucuronidation by the liver were also described for the mycotoxin deoxynivalenol (Lattanzio *et al.*, 2011; Schwartz-Zimmermann *et al.*, 2017), an observation that was suggested to be due to the influence of gender, age, diet and health status (Pestka *et al.*, 2017).

The intestinal tissue is also an important contributor to the glucuronidation of ZEN, acting as first-pass metabolism before ZEN is being transferred to the liver. In Chapter 3, the incubation of ZEN with rat intestinal fractions pointed at a higher *in vitro* catalytic efficiency than that obtained with rat liver fractions, and also at a 3-fold higher efficiency than what was observed for the human intestinal fraction. The high efficiency of the rat intestinal fractions for glucuronidation have been previously observed for other food-related compounds such as flavonoids (Boonpawa *et al.*, 2015; Brand *et al.*, 2010). The high glucuronidation of ZEN in rat intestinal tissue was indicated by the results from an *in vivo* study (Ieko *et al.*, 2020), where upon intestinal absorption of ZEN rapid glucuronidation occurred and low transport of unconjugated ZEN to the serosa portion was observed. This phenomenon reduces the amount of free ZEN reaching the liver to be potentially converted to α -ZEL. On the other hand, humans had lower glucuronidation efficiency than rats, indicating that a higher amount of ZEN may reach the liver and potentially be converted to α -ZEL. Building PBK models including the kinetics for all these processes for the different species will be a way forward to actually obtain better insight in these species dependent differences in ZEN metabolism.

ZEN has also been shown to activate the pregnane X receptor (PXR), a nuclear receptor involved in the regulation of a number of enzymes for xenobiotic metabolism such as cytochromes P450 (especially CYP3A4) and also UDP-

glucuronyl transferases (UGTs) (Ding *et al.*, 2006; Kast *et al.*, 2002). This may reduce the elimination rates for ZEN and its metabolites via glucuronidation due to a decrease in the activity of UGTs. It remains to be demonstrated how the glucuronidation pattern of ZEN and α -ZEL in pigs compares to that in humans or rats, but the higher yield of α -ZEL upon ZEN exposure suggests that the intestinal glucuronidation may not be as efficient as observed in rat and humans.

Interspecies differences in toxicity of ZEN and its metabolites

Sub-acute and sub-chronic toxicity studies in rodents suggest the exposure to ZEN and its metabolites to cause hematological alterations, hepatic lesion and estrogenic effects. In pigs, the most sensitive species, the reproductive toxicity upon ZEN exposure is suggested to be estrogen receptor (ER) mediated. ZEN and its reduced metabolites have shown to be full agonist to ER α and partial antagonist of ER β (Kuiper *et al.*, 1998). The study of the interaction of ZEN and its reduced metabolites with ERs has focused on ER α . In *in vitro* toxicity studies measuring the binding affinity to ER α , ER-mediated gene activation or cell proliferation showed α -ZEL to have a higher estrogenic potency than ZEN, while β -ZEL showed the lowest potency (Metzler *et al.*, 2010). This was confirmed in Chapter 2 with the U2OS ER α -CALUX assay, where the estrogenicity of α -ZEL was 55-fold higher than that of ZEN and the estrogenicity of β -ZEL was 25-fold lower than that of ZEN.

In addition to the species differences in ZEN metabolism to α -ZEL and β -ZEL, the variation in the susceptibility of different animal species and humans may also be related to differences in the number of ERs, as well as the ER binding affinities for ZEN or α -ZEL (Liu and Applegate, 2020). In mammals, the expression of ER α and ER β is tissue dependent; in reproductive organs ER α is mainly present in uterus, ovaries and mammary glands, while ER β is expressed in ovaries and to a lesser extent in mammary glands (Kerdivel *et al.*, 2013). The number of ERs in reproductive tissues during the developmental stages (Amenyogbe *et al.*, 2020; Meulen *et al.*, 1994), therefore the high sensitivity in young gilts suggests that differences in the number of ERs may play a role in species differences. This was observed by the comparison of available estrogen binding sites in pigs, rats and chickens showing that pigs and rats had a higher concentration of binding sites than chickens, as noted from the variance in the relative binding affinities of ZEN and α -ZEL (Fitzpatrick *et al.*, 1989; Harrison and Toft, 1975). Besides the number of ERs present, the affinity for binding of ZEN and its metabolites to the ligand-binding pockets of ERs should be considered (Dellafiora *et al.*, 2017; Ehrlich *et al.*, 2015; Kato *et al.*, 2018). Fitzpatrick *et al.* (1989) studied the relative binding affinities

(RBA) of ZEN, α -ZEL and β -ZEL to ERs derived from uterus in rats, pigs and chickens. Pigs had the highest RBAs, while rat and chickens had lower affinities. α -ZEL showed the highest RBA in the three species. This observation combined with the highest preference for α -ZEL formation by both the liver and intestinal microbiota in pigs and humans as observed in the present thesis (Chapter 2) provides a likely explanation for the relative higher sensitivity of pigs. This higher α -ZEL formation in both pigs and humans, combined with their physiological and anatomical similarities, also supports the extrapolation of data from pigs to humans, under the assumption that female humans will not be more sensitive than gilts (EFSA, 2011; EFSA, 2016). This assumed similarity in sensitivity towards the adverse effects of ZEN in pigs and human provided the basis for elimination of the default uncertainty factor of 2.5 for interspecies differences in dynamics in the establishment of the TDI. Whether also the default uncertainty factor of 4.0 for interspecies differences in kinetics can be modified awaits further studies on the differences in kinetic of ZEN in human and pigs. Clearly the results obtained so far in the present thesis do point to pigs being more efficient α -ZEL producers than humans. The human risk assessment of ZEN and its masked forms is discussed in some more detail in the next section.

6.2.5 Human risk assessment of ZEN and modified forms of ZEN

The risk assessment for ZEN in humans is hampered by a series of uncertainties including the uncertainties in interspecies and interindividual differences in toxicokinetics and toxicodynamics, the limited exposure data available for humans and the lack of insight in potential sensitive subpopulations. As part of the strategy to tackle the gaps in information, PBK modelling is being more widely recognized as a powerful tool for risk assessment, mainly when *in vivo* data are lacking (Paini *et al.*, 2019). In Chapters 2 - 4 the combination of *in vitro* models with PBK modelling as presented provided an insight in the impact of interspecies and interindividual differences in the kinetics of ZEN. In Chapter 3, the concentrations of ZEN and α -ZEL reaching the blood predicted by the PBK model resulted in 3-fold higher blood levels of α -ZEL in humans than rats. An initial assessment of the predicted concentration of ZEN and α -ZEL in blood from an exposure at the level of the current TDI revealed that these predicted blood concentrations were 3 orders of magnitude lower than the concentrations shown to elicit 10% of the estrogenic response (EC₁₀) *in vitro*. The predictions in this research are based on the exposure to ZEN and its metabolite α -ZEL. Future models could consider to also include exposure to the modified form of ZEN (ZEN-14-G) although based on the results of

the present thesis (Chapter 5) it is expected that ZEN-14-G will be completely hydrolyzed to ZEN by the intestinal microbiota. In pigs, *in vitro* studies with intestinal mucosa showed the presence of enzymes able to hydrolyze ZEN-14-G also in this tissue (Olsen *et al.*, 1987). If a similar phenomenon is present in humans, as shown for flavonoids (Németh *et al.*, 2003), the contribution of mucosal β -glucosidases to the hydrolysis of ZEN-14-G could be accounted for as well, although its contribution relative to that of the intestinal microbiota remains to be established.

Chemical-Specific Adjustments Factors (CSAF)

In human risk assessment of ZEN, the establishment of a TDI, or health-based guidance value (HBGV), of 0.25 $\mu\text{g/kg bw}$ is based on the NOEL derived from the pig study reported by Döll *et al.* (2004). The estimation of a TDI from animal studies includes default uncertainty factors (UF) for interspecies (10) and interindividual (10) differences in kinetics. The UF for ZEN includes UFs for human interindividual differences in kinetics and dynamics, and for the interspecies differences in kinetics with the default factor of 4, while the UF of 2.5 for interspecies differences in dynamics was discarded assuming that humans, specifically females, will not be more sensitive than young gilts. In cases where actual data are available, the default uncertainty factors can be replaced by so-called chemical-specific adjustment factors (CSAF). Use of such a CSAF was introduced to enable the incorporation of compound specific quantitative data for interspecies and interindividual differences into risk assessment (IPCS, 2005). The estimated CSAF value of 2.45 for interindividual differences in the metabolism of ZEN obtained in the present thesis (Chapter 4) shows that the default UF of 3.16 is protective enough for the healthy adult population. The identification of sensitive populations to ZEN exposure is still of interest as well as to what extent such increased sensitivity arises from differences in kinetics or rather from differences in dynamics. Age and reproductive status are reported to influence the sensitivity towards ZEN in pigs where prepubertal gilts are more sensitive, as shown from an increase in the size of the reproductive tract when exposed to ZEN (Döll *et al.*, 2004; Oliver *et al.*, 2012). When this increased sensitivity in part relates to interindividual differences in kinetics, this has to be considered in the CSAF for interindividual differences. To this end, kinetics of ZEN would need to be studied in young children. In humans, the presence in urine of ZEN and its metabolites has been studied in cases where precocious puberty in young girls (age 9-12) was reported (Bandera *et al.*, 2011). In the study, 78% of the samples (128 girls) were positive to the presence of mycotoxins, with ZEN having the highest incidence of detection (55% of the samples); yet, scarce epidemiological data for a

reference population are available which limits the conclusions that can be drawn from these findings. It is worth to mention that the sources of ZEN and/or its metabolites responsible for the exposure in this study were not established. For example, α -zearalanol (zearanol, α -ZAL) is a metabolite of ZEN with similar potency as α -ZEL (Leffers *et al.*, 2001), therefore is banned as a growth promotor in the European Union, while in the United States of America α -ZAL is still used and meat products may represent a source of exposure to α -ZAL. Though a direct link was not found, meat and popcorn were the most probable sources of mycoestrogens in diet (Bandera *et al.*, 2011). Whether the differences in ZEN sensitivity for different groups within a population can be attributed to toxicokinetics and/or toxicodynamics remains to be understood. The work in this thesis, alongside with earlier work on estragole (Punt *et al.*, 2016), phenol (Strikwold *et al.*, 2017) and lasiocarpine (Ning *et al.*, 2019), show the strength of the *in vitro-in silico* approach as a tool for the study of a larger population considering different sensitive subgroups and to study if the current uncertainty factors applied for ZEN risk assessment are protective enough.

Human biomonitoring data for the human risk assessment of ZEN and ZEN-14-G

The risk assessment of ZEN and its modified forms is hampered by the information gaps arising from the lack of exposure and biomonitoring data. Reports for the presence of ZEN in food products are scarce, a limitation raised by EFSA (EFSA, 2011; EFSA, 2016). Currently, Boevre *et al.* (2012) is the most complete study on the presence of ZEN and its modified forms in cereals from the Belgian market and has been used by a number of studies, including this thesis (Chapter 5), as a basis for the assessment of human exposure to ZEN-14-G. The limited data on the levels of ZEN and its modified forms in food products, along with the lack of kinetic studies in humans highlight the need of more comprehensive human biomonitoring data where the excreted biomarkers could provide a more complete overview of exposure to ZEN, accounting also for its modified forms.

Biomonitoring could include the measurement of concentrations of a compound or its effects (e.g. DNA-adduct formation, protein induction, etc.) as biomarkers in body fluids and/or tissues that could provide insight into the internal and related external exposure or the risk to a certain health effect (Tiesjema *et al.*, 2018). Based on the knowledge obtained from studies in pigs, excretion of ZEN and its modified forms is mainly through the urine, therefore urine has been a common source to study urinary levels of ZEN as a biomarker to assess the exposure. Biomonitoring of urine samples, or any other body fluids, still requires the use of other computational

methods such as PBK modelling as part of a reverse dosimetry approach to translate biomarker levels to actual exposure levels (Bahadori *et al.*, 2007).

An additional advantage of biomonitoring is that if the population is large enough, it may provide insight into sensitive subpopulations, an important aspect for the assessment of ZEN and its metabolites for which not only prepubertal girls might be at higher risk, but also pre- and postmenopausal women (Mauro *et al.*, 2018). The recent literature has focused on the effects of ZEN exposure in female populations, but the effects in a male population, and related gender specific toxicokinetics and/or toxicodynamics have not been fully elucidated and might be of interest for future work.

Proper study designs developed for the respective compounds to be studied by human biomonitoring, including the selection of the appropriate biomarkers and availability of sensitive analytical techniques, will provide a more comprehensive insight into exposure to compounds for which epidemiological and exposure data are limited.

6.2.6 Future perspectives

The role and contribution of the intestinal microbial metabolism of xenobiotics in toxicology gained attention in previous years leading to the need for the development and refinement of *in vitro* models, as well as the development of methods to translate the *in vitro* data to the *in vivo* situation. Though many advances have been made towards understanding the organisms of the gut microbiota, overall the high complexity of the microbial communities and their metabolic capacity still hampers a full understanding thereof, as well as the application of intestinal microbial metabolism data in toxicology. Future research needs to be done on the development of high throughput *in vitro* methods for the study of microbial metabolism of xenobiotics, which will contribute to a more comprehensive understanding of the role of the microbiome in toxicology. Furthermore, dysbiosis of the microbiome can lead to changes in its metabolic profile, such as changes production and metabolism of short-chain fatty acids, choline, amino acids and bile metabolites. Changes in, for example, the profile of bile acid metabolites may influence the host metabolism by changing expression patterns of phase I (CYP450) and phase II (glutathione-S-transferase and sulfotransferase) enzymes interfering with metabolic mechanisms for detoxification (Collins and Patterson, 2020). Additionally, changes in the metabolic profile of the microbiota have been linked to the development of diseases such as diabetes type 2 and inflammatory bowel disease (IBD) (Lavelle and Sokol, 2020; Velmurugan *et al.*, 2017). A combination of -omics technologies will allow a more

comprehensive understanding of the contribution of the intestinal microbiome to the co-metabolism and changes in toxicodynamics of xenobiotics, next to an understanding on the changes in metabolic profiles and the development of disease linked to intestinal microbiota. Moreover, the refinement of *in vitro* and/or *in silico* models for host-microbe interactions (von Martels *et al.*, 2017) should be encouraged.

Another area of interest is the refinement of the quantitative extrapolation of *in vitro* data to the *in vivo* situation (QIVIVE). The scaling of *in vitro* data to the *in vivo* situation requires the establishment and validation of appropriate scaling factors. Among others, the high diversity of the microbiota along the intestinal tract poses a challenge for deriving these scaling factors, for which the establishment of standardized (average) fecal masses varying from 19 - 415 g/day for humans or techniques for microbial load quantification and average colonic transit times are required. These scaling factors will also be important for the inclusion of *in vitro* intestinal microbial metabolic parameters in PBK models, and further refinement of the current models. Despite the development of PBK model descriptions moving towards simpler and generic models, the inclusion of intestinal microbial metabolism proved to be a potentially essential extension of these models to which also enterohepatic circulation needs to be added, as for many compounds their clearance from the body can be delayed due to excretion in bile and further hydrolytic activity of the microbiota followed by reuptake in the systemic circulation.

Risk assessments are moving at a fast pace towards the inclusion of *in vitro* and *in silico* data as part of the process. Currently, PBK models provide an essential tool for the prediction of levels of xenobiotics and their metabolites in host tissues or fluids, and to relate external to internal dose levels. For a number of xenobiotics, such as ZEN, the lack of human kinetic data limits the evaluation of PBK models that could be used for risk assessment. Future research for the risk assessment of ZEN and other xenobiotics with limited or no exposure data needs input from human biomonitoring studies to refine exposure data and to be combined with PBK models to further understand the kinetics of ZEN and other xenobiotics. Obtaining information on possible effects (toxicodynamics) of ZEN in humans, and how these effects compare to those observed in young guinea pigs on which the current TDI is based, might help to identify sensitive human subpopulations and possibly help to refine the current HBGV.

Finally, animal and human risk assessment is mainly based on single chemicals, but realistic exposure scenarios will need to include the study of chemical mixtures. The study of mixtures is challenged by the large number of chemicals present, the limited

information on toxicity and the different modes of action (Bopp *et al.*, 2019). For mycotoxins, this is an area that requires further development as the co-occurrence of mycotoxins is commonly reported, but the study of combinatorial effects hampered by the diverse toxic endpoints of the different types of mycotoxins (Dellafiora and Dall'Asta, 2017). To approach the challenges posed by mixtures there is a need for better exposure and kinetic data (e.g. biomonitoring data) as well as a better understanding on the toxicity of the chemicals, their mode of action, the toxicity endpoints and the potential for synergistic or antagonistic interactions.

6.3 Conclusion

In conclusion, the work presented in this thesis provides a proof-of-principle for the inclusion of *in vitro* kinetics for intestinal microbial metabolism, derived from incubations with fecal samples, together with host metabolism in PBK models to assess the contribution of intestinal microbial metabolism to the overall metabolism of ZEN. This work also gives insight into the human interindividual differences in the metabolism of ZEN enabling evaluation of the current uncertainty factor for interindividual differences in kinetics used in the risk assessment of ZEN. Finally, the capacity of the intestinal microbiota to fully hydrolyze ZEN-14-G supports the inclusion of this modified form in the group HBGV for the risk assessment of ZEN and its modified forms. Overall, the insight provided in this thesis opens a series of possibilities for further research including the identification of potential sensitive human subpopulations to ZEN exposure due to possible differences in toxicokinetics between individuals. The present thesis provides a way forward how to study this through the application of a combined effort of *in vitro*, and *in silico* studies.

6.4 References

- Abubucker, S., Segata, N., Goll, J., Schubert, A.M., Izard, J., et al. Metabolic Reconstruction for Metagenomic Data and Its Application to the Human Microbiome. *PLoS Comput. Biol.*, 8 (2012), e1002358. doi: 10.1371/journal.pcbi.1002358
- Amenyogbe, E., Chen, G., Wang, Z., Lu, X., Lin, M., Lin, A.Y. A Review on Sex Steroid Hormone Estrogen Receptors in Mammals and Fish. *Int. J. Endocrinol.*, 2020 (2020), 5386193. doi: 10.1155/2020/5386193
- Atkinson, C., Berman, S., Humbert, O., Lampe, J.W. In Vitro Incubation of Human Feces with Daidzein and Antibiotics Suggests Interindividual Differences in the Bacteria Responsible for Equol Production. *Nutr. J.*, 134 (2004), 596-599. doi: 10.1093/jn/134.3.596
- Bahadori, T., Phillips, R.D., Money, C.D., Quackenboss, J.J., Clewell, H.J., et al. Making sense of human biomonitoring data: Findings and recommendations of a workshop. *J. Exposure Sci. Environ. Epidemiol.*, 17 (2007), 308-313. doi: 10.1038/sj.jes.7500581
- Bandera, E.V., Chandran, U., Buckley, B., Lin, Y., Isukapalli, S., Marshall, I., King, M., Zarbl, H. Urinary mycoestrogens, body size and breast development in New Jersey girls. *Sci. Total Environ.*, 409 (2011), 5221-5227. doi: 10.1016/j.scitotenv.2011.09.029
- Behr, C., Ramirez-Hincapie, S., Cameron, H.J., Strauss, V., Walk, T., Herold, M., Beekmann, K., Rietjens, I., van Ravenzwaay, B. Impact of lincosamides antibiotics on the composition of the rat gut microbiota and the metabolite profile of plasma and feces. *Toxicol. Lett.*, 296 (2018), 139-151. doi: 10.1016/j.toxlet.2018.08.002
- Bender, J.M., Li, F., Adisetiyo, H., Lee, D., Zabih, S., et al. Quantification of variation and the impact of biomass in targeted 16S rRNA gene sequencing studies. *Microbiome*, 6 (2018), 155. doi: 10.1186/s40168-018-0543-z
- Berg, N., De Wever, B., Fuchs, H.W., Gaca, M., Krul, C., Roggen, E.L. Toxicology in the 21st century – Working our way towards a visionary reality. *Toxicol. In Vitro*, 25 (2011), 874-881. doi: 10.1016/j.tiv.2011.02.008
- Bode, L.M., Bunzel, D., Huch, M., Cho, G.-S., Ruhland, D., Bunzel, M., Bub, A., Franz, C.M.A.P., Kulling, S.E. In vivo and in vitro metabolism of trans-resveratrol by human gut microbiota. *Am J Clin Nutr*, 97 (2013), 295-309. doi: 10.3945/ajcn.112.049379
- Boevre, M.D., Mavungu, J.D.D., Landschoot, S., Audenaert, K., Eeckhout, M., Maene, P., Haesaert, G., Saeger, S.D. Natural occurrence of mycotoxins and

- their masked forms in food and feed products. *World Mycotoxin J.*, 5 (2012), 207-219. doi: 10.3920/wmj2012.1410
- Boonpawa, R., Moradi, N., Spenkelink, A., Rietjens, I.M.C.M., Punt, A. Use of physiologically based kinetic (PBK) modeling to study interindividual human variation and species differences in plasma concentrations of quercetin and its metabolites. *Biochem. Pharmacol.*, 98 (2015), 690-702. doi: 10.1016/j.bcp.2015.09.022
- Bopp, S.K., Kienzler, A., Richarz, A.-N., van der Linden, S.C., Paini, A., Parissis, N., Worth, A.P. Regulatory assessment and risk management of chemical mixtures: challenges and ways forward. *Crit. Rev. Toxicol.*, 49 (2019), 174-189. doi: 10.1080/10408444.2019.1579169
- Brand, W., Boersma, M.G., Bik, H., Hoek-van den Hil, E.F., Vervoort, J., et al. Phase II metabolism of hesperetin by individual UDP-glucuronosyltransferases and sulfotransferases and rat and human tissue samples. *Drug Metab. Dispos.*, 38 (2010), 617-625. doi: 10.1124/dmd.109.031047
- Brezina, U., Rempe, I., Kersten, S., Valenta, H., Humpf, H.-U., Dänicke, S. Determination of zearalenone, deoxynivalenol and metabolites in bile of piglets fed diets with graded levels of *Fusarium* toxin contaminated maize. *World Mycotoxin J.*, 9 (2016), 179-193. doi: 10.3920/wmj2015.1902
- Cheng, K.-C. Molecular cloning of rat liver 3 α -hydroxysteroid dehydrogenase and identification of structurally related proteins from rat lung and kidney. *J. Steroid Biochem. Mol. Biol.*, 43 (1992), 1083-1088. doi:
- Cirlini, M., Barilli, A., Galaverna, G., Michlmayr, H., Adam, G., Berthiller, F., Dall'Asta, C. Study on the uptake and deglycosylation of the masked forms of zearalenone in human intestinal Caco-2 cells. *Food Chem. Toxicol.*, 98 (2016), 232-239. doi: 10.1016/j.fct.2016.11.003
- Clarke, G., Sandhu, K.V., Griffin, B.T., Dinan, T.G., Cryan, J.F., Hyland, N.P. Gut Reactions: Breaking Down Xenobiotic–Microbiome Interactions. *Pharmacol. Rev.*, 71 (2019), 198-224. doi: 10.1124/pr.118.015768
- Collins, S.L., Patterson, A.D. The gut microbiome: an orchestrator of xenobiotic metabolism. *Acta Pharm. Sin. B.*, 10 (2020), 19-32. doi: 10.1016/j.apsb.2019.12.001
- Cummings, J.H., Bingham, S.A., Heaton, K.W., Eastwood, M.A. Fecal weight, colon cancer risk, and dietary intake of nonstarch polysaccharides (dietary fiber). *Gastroenterology*, 103 (1992), 1783-1789. doi: 10.1016/0016-5085(92)91435-7

- Degtiar, W.G., Kushlinsky, N.E. 3 α -Hydroxysteroid Dehydrogenase in Animal and Human Tissues. *Biochem. (Mosc.)*, 66 (2001), 256-266. doi: 10.1023/A:1010291527744
- Dellafiora, L., Dall'Asta, C. Forthcoming Challenges in Mycotoxins Toxicology Research for Safer Food-A Need for Multi-Omics Approach. *Toxins*, 9 (2017), 18. doi: 10.3390/toxins9010018
- Dellafiora, L., Ruotolo, R., Perotti, A., Cirlini, M., Galaverna, G., Cozzini, P., Buschini, A., Dall'Asta, C. Molecular insights on xenoestrogenic potential of zearalenone-14-glucoside through a mixed in vitro/in silico approach. *Food Chem. Toxicol.*, 108 (2017), 257-266. doi: 10.1016/j.fct.2017.07.062
- Deyashiki, Y., Taniguchi, H., Amano, T., Nakayama, T., Hara, A., Sawada, H. Structural and functional comparison of two human liver dihydrodiol dehydrogenases associated with 3 α -hydroxysteroid dehydrogenase activity. *Biochem. J.*, 282 (1992), 741-746. doi:
- Ding, X., Lichti, K., Staudinger, J.L. The mycoestrogen zearalenone induces CYP3A through activation of the pregnane X receptor. *Toxicol. Sci.*, 91 (2006), 448-455. doi: 10.1093/toxsci/kfj163
- Döll, S., Dänicke, S., Schnurrbusch, U. The effect of increasing concentrations of Fusarium toxins in piglet diets on histological parameters of the uterus and vagina. *Arch. Anim. Nutr.*, 58 (2004), 413-417. doi: 10.1080/00039420400004987
- Dufort, I., Labrie, F., Luu-The, V. Human Types 1 and 3 3 α -Hydroxysteroid Dehydrogenases: Differential Lability and Tissue Distribution1. *J. Clin. Endocrinol. Metab.*, 86 (2001), 841-846. doi: 10.1210/jcem.86.2.7216
- EFSA. Scientific Opinion on the risks for public health related to the presence of zearalenone in food. *EFSA J.*, 9 (2011), 2197. doi: 10.2903/j.efsa.2011.2197
- EFSA. Appropriateness to set a group health-based guidance value for zearalenone and its modified forms. *EFSA J.*, 14 (2016), e04425. doi: 10.2903/j.efsa.2016.4425
- EFSA. Risks for animal health related to the presence of zearalenone and its modified forms in feed. *EFSA J.*, 15 (2017), e04851. doi: 10.2903/j.efsa.2017.4851
- Ehrlich, V.A., Dellafiora, L., Mollergues, J., Dall'Asta, C., Serrant, P., Marin-Kuan, M., Lo Piparo, E., Schilter, B., Cozzini, P. Hazard assessment through hybrid in vitro / in silico approach: The case of zearalenone. *Altex*, 32 (2015), 275-286. doi: 10.14573/altex.1412232

- Fitzpatrick, D.W., Picken, C.A., Murphy, L.C., Buhr, M.M. Measurement of the relative binding affinity of zearalenone, α -zearalenol and β -zearalenol for uterine and oviduct estrogen receptors in swine, rats and chickens: An indicator of estrogenic potencies. *Comp. Biochem. Physiol. C Comp. Pharmacol. Toxicol.*, 94 (1989), 691-694. doi: 10.1016/0742-8413(89)90133-3
- Galazzo, G., van Best, N., Benedikter, B.J., Janssen, K., Bervoets, L., et al. How to Count Our Microbes? The Effect of Different Quantitative Microbiome Profiling Approaches. *Front. Cell. Infect. Microbiol.*, 10 (2020). doi: 10.3389/fcimb.2020.00403
- Gaya, P., Medina, M., Sánchez-Jiménez, A., Landete, J.M. Phytoestrogen Metabolism by Adult Human Gut Microbiota. *Molecules* (Basel, Switzerland), 21 (2016), 1034. doi:
- Gibson, G.R., Wang, X. Regulatory effects of bifidobacteria on the growth of other colonic bacteria. *J. Appl. Bacteriol.*, 77 (1994), 412-420. doi: 10.1111/j.1365-2672.1994.tb03443.x
- Gratz, S.W., Dinesh, R., Yoshinari, T., Holtrop, G., Richardson, A.J., Duncan, G., MacDonald, S., Lloyd, A., Tarbin, J. Masked trichothecene and zearalenone mycotoxins withstand digestion and absorption in the upper GI tract but are efficiently hydrolyzed by human gut microbiota in vitro. *Mol. Nutr. Food Res.*, 61 (2017), E1600680. doi: 10.1002/mnfr.201600680
- Harrison, R.W., Toft, D.O. Estrogen Receptors in the Chick Oviduct*. *Endocrinology*, 96 (1975), 199-205. doi: 10.1210/endo-96-1-199
- Ieko, T., Inoue, S., Inomata, Y., Inoue, H., Fujiki, J., Iwano, H. Glucuronidation as a metabolic barrier against zearalenone in rat everted intestine. *J. Vet. Med. Sci.*, 82 (2020), 153-161. doi: 10.1292/jvms.19-0570
- IPCS, 2005. Chemical-specific adjustment factors for interspecies differences and human variability : guidance document for use of data in dose/concentration-response assessment. World Health Organization, Geneva, pp.
- Kast, H.R., Goodwin, B., Tarr, P.T., Jones, S.A., Anisfeld, A.M., et al. Regulation of Multidrug Resistance-associated Protein 2 (ABCC2) by the Nuclear Receptors Pregnane X Receptor, Farnesoid X-activated Receptor, and Constitutive Androstane Receptor*. *J. Biol. Chem.*, 277 (2002), 2908-2915. doi: 10.1074/jbc.M109326200
- Kato, K., Fujii, K., Nakayoshi, T., Watanabe, Y., Fukuyoshi, S., et al. Structural differences between the ligand-binding pockets of estrogen receptors alpha

- and beta. *J. Phys. Conf. Ser.*, 1136 (2018), 012021. doi: 10.1088/1742-6596/1136/1/012021
- Kerdivel, G., Habauzit, D., Pakdel, F. Assessment and Molecular Actions of Endocrine-Disrupting Chemicals That Interfere with Estrogen Receptor Pathways. *Int. J. Endocrinol.*, 2013 (2013), 501851. doi: 10.1155/2013/501851
- Koziolek, M., Grimm, M., Becker, D., Iordanov, V., Zou, H., Shimizu, J., Wanke, C., Garbacz, G., Weitschies, W. Investigation of pH and Temperature Profiles in the GI Tract of Fasted Human Subjects Using the Intellicap® System. *J. Pharm. Sci.*, 104 (2015), 2855-2863. doi: 10.1002/jps.24274
- Kuiper, G.G.J.M., Lemmen, J.G., Carlsson, B., Corton, J.C., Safe, S.H., van der Saag, P.T., van der Burg, B., Gustafsson, J.-A.k. Interaction of Estrogenic Chemicals and Phytoestrogens with Estrogen Receptor β . *Endocrinology*, 139 (1998), 4252-4263. doi: 10.1210/endo.139.10.6216
- Lattanzio, V.M.T., Solfrizzo, M., De Girolamo, A., Chulze, S.N., Torres, A.M., Visconti, A. LC–MS/MS characterization of the urinary excretion profile of the mycotoxin deoxynivalenol in human and rat. *J. Chromatogr. B*, 879 (2011), 707-715. doi: 10.1016/j.jchromb.2011.01.029
- Lavelle, A., Sokol, H. Gut microbiota-derived metabolites as key actors in inflammatory bowel disease. *Nat. Rev. Gastroenterol. Hepatol.*, 17 (2020), 223-237. doi: 10.1038/s41575-019-0258-z
- Leffers, H., Næsby, M., Vendelbo, B., Skakkebæk, N.E., Jørgensen, M. Oestrogenic potencies of Zeranone, oestradiol, diethylstilboestrol, Bisphenol-A and genistein: implications for exposure assessment of potential endocrine disrupters. *Hum. Reprod.*, 16 (2001), 1037-1045. doi: 10.1093/humrep/16.5.1037
- Liu, J., Applegate, T. Zearalenone (ZEN) in Livestock and Poultry: Dose, Toxicokinetics, Toxicity and Estrogenicity. *Toxins (Basel)*, 12 (2020). doi: 10.3390/toxins12060377
- Malekinejad, H., Maas-Bakker, R., Fink-Gremmels, J. Species differences in the hepatic biotransformation of zearalenone. *Veterinary journal*, 172 (2006), 96-102. doi: 10.1016/j.tvjl.2005.03.004
- Matsuura, K., Shiraishi, H., Hara, A., Sato, K., Deyashiki, Y., Ninomiya, M., Sakait, S. Identification of a Principal mRNA Species for Human 3 α -Hydroxysteroid Dehydrogenase Isoform (AKR1C3) That Exhibits High Prostaglandin D₂ 11-Ketoreductase Activity. *J. Biochem. Tokyo*, 124 (1998), 940-946. doi:

- Mauro, T., Hao, L., Pop, L.C., Buckley, B., Schneider, S.H., Bandera, E.V., Shapses, S.A. Circulating zearalenone and its metabolites differ in women due to body mass index and food intake. *Food Chem. Toxicol.*, 116 (2018), 227-232. doi: 10.1016/j.fct.2018.04.027
- McCabe, M., Sane, R.S., Keith-Luzzi, M., Xu, J., King, I., Whitcher-Johnstone, A., Johnstone, N., Tweedie, D.J., Li, Y. Defining the Role of Gut Bacteria in the Metabolism of Deleobuvir: In Vitro and In Vivo Studies. *Drug Metab. Dispos.*, 43 (2015), 1612-1618. doi: 10.1124/dmd.115.064477
- Metzler, M., Pfeiffer, E., Hildebrand, A. Zearalenone and its metabolites as endocrine disrupting chemicals. *World Mycotoxin J.*, 3 (2010), 385-401. doi: 10.3920/WMJ2010.1244
- Meulen, J.v.d., Helmond, F.A., Oudenaarden, C.P.J. Oestrogen receptors in endometrial cytosol of gilts on days 10-13 of oestrous cycle and pregnancy. *NJAS*, 42 (1994), 217-223. doi:
- Minekus, M., Smeets-Peters, M., Bernalier, A., Marol-Bonnin, S., Havenaar, R., Marteau, P., Alric, M., Fonty, G., Huis in't Veld, J.H. A computer-controlled system to simulate conditions of the large intestine with peristaltic mixing, water absorption and absorption of fermentation products. *Appl. Microbiol. Biotechnol.*, 53 (1999), 108-114. doi: 10.1007/s002530051622
- Mirocha, C.J., Pathre, S.V., Robison, T.S. Comparative metabolism of zearalenone and transmission into bovine milk. *Food Cosmet. Toxicol.*, 19 (1981), 25-30. doi: 10.1016/0015-6264(81)90299-6
- Mortelé, O., Iturraspe, E., Breynaert, A., Verdickt, E., Xavier, B.B., et al. Optimization of an in vitro gut microbiome biotransformation platform with chlorogenic acid as model compound: From fecal sample to biotransformation product identification. *J. Pharm. Biomed. Anal.*, 175 (2019), 112768. doi: 10.1016/j.jpba.2019.07.016
- National Academies of Sciences, E., Medicine, 2018. Environmental Chemicals, the Human Microbiome, and Health Risk: A Research Strategy. The National Academies Press, Washington, DC.
- National Research Council, 2007. Toxicity Testing in the 21st Century: A Vision and a Strategy. The National Academies Press, Washington, DC, pp. 216.
- Németh, K., Plumb, G.W., Berrin, J.-G., Juge, N., Jacob, R., Naim, H.Y., Williamson, G., Swallow, D.M., Kroon, P.A. Deglycosylation by small intestinal epithelial cell β -glucosidases is a critical step in the absorption and metabolism of dietary flavonoid glycosides in humans. *Eur. J. Nutr.*, 42 (2003), 29-42. doi: 10.1007/s00394-003-0397-3

- Ning, J., Rietjens, I., Strikwold, M. Integrating physiologically based kinetic (PBK) and Monte Carlo modelling to predict inter-individual and inter-ethnic variation in bioactivation and liver toxicity of lasiocarpine. *Arch. Toxicol.*, 93 (2019), 2943-2960. doi: 10.1007/s00204-019-02563-x
- Nissen, L., Casciano, F., Gianotti, A. Intestinal fermentation in vitro models to study food-induced gut microbiota shift: an updated review. *FEMS Microbiol. Lett.*, 367 (2020). doi: 10.1093/femsle/fnaa097
- Oliver, W.T., Miles, J.R., Diaz, D.E., Dibner, J.J., Rottinghaus, G.E., Harrell, R.J. Zearalenone enhances reproductive tract development, but does not alter skeletal muscle signaling in prepubertal gilts. *Animal Feed Science and Technology*, 174 (2012), 79-85. doi: 10.1016/j.anifeedsci.2012.02.012
- Olsen, M., Pettersson, H., Sandholm, K., Visconti, A., Kiessling, K.H. Metabolism of zearalenone by sow intestinal mucosa in vitro. *Food Chem. Toxicol.*, 25 (1987), 681-683. doi: 10.1016/0278-6915(87)90101-3
- Paini, A., Leonard, J.A., Joossens, E., Bessems, J.G.M., Desalegn, A., et al. Next generation physiologically based kinetic (NG-PBK) models in support of regulatory decision making. *Comput. Toxicol.*, 9 (2019), 61-72. doi: 10.1016/j.comtox.2018.11.002
- Pestka, J.J., Clark, E.S., Schwartz-Zimmermann, H.E., Berthiller, F. Sex Is a Determinant for Deoxynivalenol Metabolism and Elimination in the Mouse. *Toxins*, 9 (2017), 240. doi:
- Pfeiffer, E., Hildebrand, A., Mikula, H., Metzler, M. Glucuronidation of zearalenone, zeranol and four metabolites in vitro: formation of glucuronides by various microsomes and human UDP-glucuronosyltransferase isoforms. *Mol. Nutr. Food Res.*, 54 (2010), 1468-1476. doi: 10.1002/mnfr.200900524
- Punt, A., Paini, A., Spenkelink, A., Scholz, G., Schilter, B., Van Bladeren, P.J., Rietjens, I.M.C.M. Evaluation of Interindividual Human Variation in Bioactivation and DNA Adduct Formation of Estragole in Liver Predicted by Physiologically Based Kinetic/Dynamic and Monte Carlo Modeling. *Chem. Res. Toxicol.*, 29 (2016), 659-668. doi: 10.1021/acs.chemrestox.5b00493
- Rasmussen, M.K., Ekstrand, B., Zamaratskaia, G. Regulation of 3β -hydroxysteroid dehydrogenase/ Δ^5 - Δ^4 isomerase: a review. *Int. J. Mol. Sci.*, 14 (2013), 17926-17942. doi: 10.3390/ijms140917926

- Rezaei Nejad, H., Oliveira, B.C.M., Sadeqi, A., Dehkharghani, A., Kondova, I., et al. Ingestible Osmotic Pill for In Vivo Sampling of Gut Microbiomes. *Adv. Intell. Syst.*, 1 (2019), 1900053. doi: 10.1002/aisy.201900053
- Rose, C., Parker, A., Jefferson, B., Cartmell, E. The Characterization of Feces and Urine: A Review of the Literature to Inform Advanced Treatment Technology. *Crit. Rev. Environ. Sci. Technol.*, 45 (2015), 1827-1879. doi: 10.1080/10643389.2014.1000761
- Rumney, C.J., Rowland, I.R. In vivo and in vitro models of the human colonic flora. *Crit. Rev. Food Sci. Nutr.*, 31 (1992), 299-331. doi: 10.1080/10408399209527575
- Schäpe, S.S., Krause, J.L., Engelmann, B., Fritz-Wallace, K., Schattenberg, F., et al. The Simplified Human Intestinal Microbiota (SIHUMIx) Shows High Structural and Functional Resistance against Changing Transit Times in In Vitro Bioreactors. *Microorganisms*, 7 (2019), 641. doi: 10.3390/microorganisms7120641
- Schwartz-Zimmermann, H.E., Hametner, C., Nagl, V., Fiby, I., Macheiner, L., et al. Glucuronidation of deoxynivalenol (DON) by different animal species: identification of iso-DON glucuronides and iso-deepoxy-DON glucuronides as novel DON metabolites in pigs, rats, mice, and cows. *Arch. Toxicol.*, 91 (2017), 3857-3872. doi: 10.1007/s00204-017-2012-z
- Setchell, K.D.R., Brown, N.M., Lydeking-Olsen, E. The clinical importance of the metabolite equol-a clue to the effectiveness of soy and its isoflavones. *J. Nutr.*, 132 (2002), 3577-3584. doi: 10.1093/jn/132.12.3577
- Shin, B.S., Hong, S.H., Bulitta, J.B., Hwang, S.W., Kim, H.J., et al. Disposition, oral bioavailability, and tissue distribution of zearalenone in rats at various dose levels. *J. Toxicol. Environ. Health A*, 72 (2009), 1406-1411. doi: 10.1080/15287390903212774
- Sousa, T., Paterson, R., Moore, V., Carlsson, A., Abrahamsson, B., Basit, A.W. The gastrointestinal microbiota as a site for the biotransformation of drugs. *Int. J. Pharm.*, 363 (2008), 1-25. doi: 10.1016/j.ijpharm.2008.07.009
- Strikwold, M., Spenkelink, B., Woutersen, R.A., Rietjens, I.M.C.M., Punt, A. Development of a combined in Vitro Physiologically Based Kinetic (PBK) and Monte Carlo modelling approach to predict interindividual human variation in phenol-induced developmental toxicity. *Toxicol. Sci.*, 157 (2017), 365-376. doi: 10.1093/toxsci/kfx054

- Tamura, G., Gold, C., Ferro-Luzzi, A., Ames, B.N. Fecalase: a model for activation of dietary glycosides to mutagens by intestinal flora. *Proc. Natl. Acad. Sci. U. S. A.*, 77 (1980), 4961-4965. doi: 10.1073/pnas.77.8.4961
- Tang, Q., Jin, G., Wang, G., Liu, T., Liu, X., Wang, B., Cao, H. Current Sampling Methods for Gut Microbiota: A Call for More Precise Devices. *Front. Cell. Infect. Microbiol.*, 10 (2020). doi: 10.3389/fcimb.2020.00151
- Tiemann, U., Tomek, W., Schneider, F., Vanselow, J. Effects of the mycotoxins α - and β -zearalenol on regulation of progesterone synthesis in cultured granulosa cells from porcine ovaries. *Reprod. Toxicol.*, 17 (2003), 673-681. doi: 10.1016/j.reprotox.2003.07.001
- Tiesjema, B., te Biesebeek, J.D., Mengelers, M., 2018. The use of epidemiologic studies for the biomonitoring of harmful substances. National Institute for Public Health and the Environment (RIVM), Bilthoven, The Netherlands, pp. 36.
- Ueberschaer, K.-H., Brezina, U., Dänicke, S. Zearalenone (ZEN) and ZEN metabolites in feed, urine and bile of sows: Analysis, determination of the metabolic profile and evaluation of the binding forms. *Landbauforschung Volkenrode*, 66 (2016), 21-28. doi: 10.3220/LBF1462863902000
- Van den Abbeele, P., Grootaert, C., Marzorati, M., Possemiers, S., Verstraete, W., et al. Microbial Community Development in a Dynamic Gut Model Is Reproducible, Colon Region Specific, and Selective for *Bacteroidetes* and *Clostridium* Cluster IX. *Appl. Environ. Microbiol.*, 76 (2010), 5237-5246. doi: 10.1128/aem.00759-10
- Velmurugan, G., Ramprasath, T., Gilles, M., Swaminathan, K., Ramasamy, S. Gut Microbiota, Endocrine-Disrupting Chemicals, and the Diabetes Epidemic. *Trends Endocrinol. Metab.*, 28 (2017), 612-625. doi: 10.1016/j.tem.2017.05.001
- Venema, K., van den Abbeele, P. Experimental models of the gut microbiome. *Best Pract. Res. Clin. Gastroenterol.*, 27 (2013), 115-126. doi: 10.1016/j.bpg.2013.03.002
- Visconti, A., Le Roy, C.I., Rosa, F., Rossi, N., Martin, T.C., et al. Interplay between the human gut microbiome and host metabolism. *Nat. Commun.*, 10 (2019), 4505. doi: 10.1038/s41467-019-12476-z
- von Martels, J.Z.H., Sadaghian Sadabad, M., Bourgonje, A.R., Blokzijl, T., Dijkstra, G., Faber, K.N., Harmsen, H.J.M. The role of gut microbiota in health and disease: In vitro modeling of host-microbe interactions at the aerobe-

- anaerobe interphase of the human gut. *Anaerobe*, 44 (2017), 3-12. doi: 10.1016/j.anaerobe.2017.01.001
- Wang, Q., Spenkelink, B., Boonpawa, R., Rietjens, I., Beekmann, K. Use of Physiologically Based Kinetic Modeling to Predict Rat Gut Microbial Metabolism of the Isoflavone Daidzein to S-Equol and Its Consequences for ER α Activation. *Mol. Nutr. Food Res.*, 64 (2020), e1900912. doi: 10.1002/mnfr.201900912
- Warth, B., Sulyok, M., Berthiller, F., Schuhmacher, R., Krska, R. New insights into the human metabolism of the Fusarium mycotoxins deoxynivalenol and zearalenone. *Toxicol. Lett.*, 220 (2013), 88-94. doi: 10.1016/j.toxlet.2013.04.012
- Yang, S., Zhang, H., Sun, F., De Ruyck, K., Zhang, J., et al. Metabolic Profile of Zearalenone in Liver Microsomes from Different Species and Its in Vivo Metabolism in Rats and Chickens Using Ultra High-Pressure Liquid Chromatography-Quadrupole/Time-of-Flight Mass Spectrometry. *J. Agric. Food Chem.*, 65 (2017), 11292-11303. doi: 10.1021/acs.jafc.7b04663
- Yousi, F., Kainan, C., Junnan, Z., Chuanxing, X., Lina, F., Bangzhou, Z., Jianlin, R., Baishan, F. Evaluation of the effects of four media on human intestinal microbiota culture in vitro. *AMB Express*, 9 (2019), 69. doi: 10.1186/s13568-019-0790-9
- Zheng, W., Feng, N., Wang, Y., Noll, L., Xu, S., et al. Effects of zearalenone and its derivatives on the synthesis and secretion of mammalian sex steroid hormones: A review. *Food Chem. Toxicol.*, 126 (2019), 262-276. doi: 10.1016/j.fct.2019.02.031
- Zierer, J., Jackson, M.A., Kastenmüller, G., Mangino, M., Long, T., et al. The fecal metabolome as a functional readout of the gut microbiome. *Nat. Genet.*, 50 (2018), 790-795. doi: 10.1038/s41588-018-0135-7
- Zimmermann, M., Zimmermann-Kogadeeva, M., Wegmann, R., Goodman, A.L. Separating host and microbiome contributions to drug pharmacokinetics and toxicity. *Science*, 363 (2019), eaat9931. doi: 10.1126/science.aat9931

Chapter 7

Summary

Zearalenone (ZEN) is a mycotoxin produced by *Fusarium spp.* present in food and feed. ZEN shows *in vivo* and *in vitro* endocrine disrupting potential via the activation of estrogen receptors (ERs). In mammals, liver and intestinal microbiota metabolize ZEN to α -ZEL and β -ZEL, with the estrogenic potency of α -ZEL being 60-times higher than that of ZEN and β -ZEL being 5-times less potent than ZEN. The species differences in sensitivity to ZEN exposure, with pigs being the most sensitive species, might be ascribed to interspecies differences in the formation of α -ZEL and β -ZEL in combination with possible interspecies differences in toxicodynamics. EFSA proposed in 2016 a group health-based guidance value (HBGV), i.e. a tolerable daily intake (TDI) for ZEN and its modified forms, of 0.25 $\mu\text{g}/\text{kg}$ bw based on the no observed effect level (NOEL) of 10.4 $\mu\text{g}/\text{kg}$ bw for estrogenic effects of ZEN in young gilts. Considering the uncertainty around the effects of ZEN in humans, the aim of this PhD project was to gain further insight into the metabolism of ZEN, including its metabolism in liver and intestinal microbiota of not only experimental animals but also human, and to include this information in physiologically-based kinetic (PBK) models to enable evaluation of the role of metabolism of ZEN in its estrogenic activity. To this end, intestinal microbial metabolism of ZEN was studied *in vitro* using anaerobic incubations of fecal samples from rats, pigs and humans, and scaled to the *in vivo* situation to enable comparison to metabolism in the liver. The apparent *in vivo* catalytic efficiencies (k_{cat}) for the formation of α -ZEL and β -ZEL in the three species showed that overall metabolism was higher in pigs, followed by rats and humans. The comparison to liver metabolism showed that the intestinal microbiota of pigs contributes up to 36% to the overall formation of α -ZEL from ZEN, and might thus contribute to the bioactivation of ZEN. For rats, this contribution amounted to 27%, while in humans this was less than 0.1%. These interspecies differences highlighted the importance for the development of human specific models to assess the kinetics of ZEN. In further studies of the present thesis the kinetic constants for the metabolism of ZEN by liver and intestinal microbiota were included in newly developed physiologically-based kinetic (PBK) models for ZEN and its bioactive metabolite α -ZEL, for rats and humans. These models enabled prediction of the maximum blood concentrations of ZEN and α -ZEL, as well as a comparison of these concentrations to concentrations known to induce estrogenicity in *in vitro* bioassays like the estrogen receptor α -mediated reporter gene (ER α -CALUX) assay and cell proliferation assays. The results obtained revealed that at a range of doses of 2.4-29 ng/kg bw of ZEN, representing the estimated daily intake in Europe for the average adult population, the maximum levels reaching the blood circulation in humans are 3 orders of

magnitude below the concentrations of ZEN and α -ZEL known to be active in *in vitro* studies for estrogenicity of these compounds (EC₁₀). Additionally, the human PBK model was used to study interindividual differences in toxicokinetics of ZEN. To this end *in vitro* derived kinetic constants for conversion of ZEN by individual liver and intestinal microbiota samples were combined to define 400 individual PBK models enabling the prediction of a distribution of the maximum blood concentrations (C_{max}) for ZEN and α -ZEL. Subsequently the PBK model outcomes were combined with Monte Carlo simulation to obtain a distribution for a larger population (n=9,879). The distribution of the C_{max} at a dose equivalent to the current TDI of 0.25 μ g/ kg bw was used to estimate a chemical-specific assessment factor (CSAF) for human interindividual differences in toxicokinetics of 2.45 for the 95th percentile of the adult population. The estimated CSAF obtained for the simulated population indicated that the current default uncertainty factor for interindividual differences in kinetics of 3.16 is sufficiently protective. Age and reproductive status are reported to influence the sensitivity towards ZEN. In pigs, prepubertal gilts seem to be more sensitive to ZEN exposure. In humans, the presence of ZEN in urine of young girls with cases of precocious puberty was suggested to have a causal relation, while this could not be proven. It remains of interest for future studies to characterize if the CSAF also adequately covers the interindividual differences for sensitive groups and whether the relatively high sensitivity in younger populations is in part also related to differences in toxicokinetics or solely due to differences in toxicodynamics. Overall, the work of this thesis presents a proof-of-principle for the inclusion of *in vitro* kinetics for intestinal microbial and host metabolism in PBK models. Additionally, combining the PBK model with Monte Carlo simulations was shown to provide a strong *in vitro-in silico* tool for the study of interindividual differences in metabolism and to evaluate the default uncertainty factors used in the current risk assessment. Furthermore, the rapid hydrolysis by the intestinal microbiota *in vitro* of zearalenone-14-glucoside (ZEN-14-G) to release ZEN indicates the importance of the intestinal microbiota upon exposure to ZEN-14-G and supports the inclusion of ZEN-14-G into the group HBGV (EFSA, 2016) of 0.25 μ g/ kg bw.

In conclusion, the insights provided in this PhD thesis open a series of possibilities for further research including the identification of potential sensitive human subpopulations to ZEN exposure due to possible differences in toxicokinetics between individuals. The present thesis provides a way forward how to study this through the application of a combined approach of *in vitro*, and *in silico* studies.



Annex

Acknowledgements

Curriculum Vitae

*Overview of completed training
activities*

ACKNOWLEDGEMENTS

The road to finishing my PhD was bumpy, and besides growing as a researcher, my personal growth is something I will take with me. I am grateful to every person that followed me these 4 years, as well as those that with their short stay soothed the bumpy journey.

First I would like to thank Karsten and Ivonne for giving me the opportunity to pursue this PhD. Through your guidance and knowledge I was able to tackle the challenging topic. I am grateful that considering a number of changes along the way including the definition of the direction for this research, your support and critical input guided me to finalize this project. Despite the pandemic posing a new challenge last year, thank you Ivonne and Karsten for your help to tackle one of the most critical and difficult moments of a PhD project. I would also like to thank the PhD thesis committee Prof. Kersten, Dr. Louise, Prof. Dall'asta and Dr. Mengelers for your critical review on this PhD thesis.

To everyone at TOX, thank you for the great time! Nico and Hans B. thank you for all your constructive remarks and for bringing fresh topics to the department. Lidy, thank you so much for all your help since my Master until your last day at TOX (including the PhD trip). Carla and Gerda, thank you so much also for all your help with all administrative matters. Big hurrray to all our amazing technician team (Bert, Hans, Laura, Sebas and Wouter), without you we wouldn't have such a nice place to work. Also thank you for all your understanding and teaching. Bert, I want to thank you for everything, I remember you since I joined TOX during my Master time as a Grandpa always willing to help and to have a nice chat. I hope now you are truly enjoying your retirement. Hans, though by now you will also be enjoying your retirement, big thanks for all your help with the collection of samples.

To all the *Intoxicated PhDs* (old and new), I am so happy and grateful to have shared this time with you (birthdays, Sinterklaas, dinners, BBQs, etc): Biyao, Diego, Menno, Shensheng, Aziza, Jin Jing, Suparmi, Gogo, Tessa, Nina, Jingxuan, Aafke, Veronique, Katja, Akanksha, Yiming, Nacho, Marta, Lenny, Felicia, Edith, Jing, Bohan, Isaac, Danlei, Annelies and Maartje. Mengying, Diego, Marta and Lenny thank you for inviting me to join the committee, despite all I have to say "we did it!". I wish you all to have a wonderful time and for those who already finished, all the success in the future! To my students Matthijs, Aïsha, Foteini, Elisa, Yuqing, Desiree, Maura, Loïs and Ifigeneia thank you so much for all your hard work and for allowing me to learn much more from you.

Special thanks to the "poep" group Karsten, Bert, Katja, Qianrui and Chen, it was a lot of work but we managed in the end. Katja, Qianrui and Chen I will always

remember that despite the long hours of work, we grew as friends lightening our days of hard work. To my officemates Shuo, Miaoying, Weijia, Merel and Qiuhui I really had a great time with all of you. Shuo and Miaoying I want to thank you for all the heartfelt talks. Ixchel, Mengying, Biyao, Annelies and Katja I do not know how to start to thank you for everything. I think you were a great support during these four years, we laughed and we cried but we always kept each other strong. I am really happy to have met you!

My dear Pomonians, Mariana, Arely, Loo Wee, Jane, Chihiro, Ivette, Vera, Sofi, Varsha, Tibo and Iris I am so grateful to had such an amazing housemates and friends. You became my family away from home and we always celebrated every small milestone. Despite we've gone different ways, I wish you all the best!

Ixchel, Pau, Iván, Sam, Vicky, Estela, Karla y Mariam (Mexican crew in Wageningen) thanks so much for everything. I joined a bit late the crew, but I enjoyed every single laugh and moment we had. The constant support we gave to each other was important. Now for everyone: *¡Si se puede!*

Lucy, Aide, Ale, Ame, Isa, JK, Isael, Pau (flor), Mirni, Jess y Verito *muchas gracias por todas esas pláticas y risas a pesar de la distancia es como si el tiempo no hubiera pasado.*

Finally, the most important to me, my family: Mom, Dad, Fabi and Renecito thank you so much for all your support. *¡Gracias papi y mami! Los quiero mucho y los extraño. No fue sencillo dejar México por tanto años, pero su apoyo constante a lo largo de mi carrera me dio la fuerza para continuar.* I couldn't have done all this without you! Felix, we lived together some of the most critical times (finishing our PhDs) and your constant love and support was important and gave me much of the energy to finish.

A mis tías, tíos, primos, primas, sobrinos y sobrinas muchas gracias por tanta alegría compartida, a pesar de los momento difíciles, cada año me entusiasmaba poder verlos. Tía To y tía Chayito, me hubiera gustado haber compartido esto en persona con ustedes, siempre estarán presentes.



CURRICULUM VITAE

Diana Marisol Méndez Catalá was born on 4 December 1990 in Mexico City, Mexico. She studied Biotechnology Engineering at the Institute of Technology and Higher Education of Monterrey with focus in molecular biology. After obtaining her BSc, in 2014 she obtained a scholarship from the National Council of Science and Technology (CONACYT) of Mexico to pursue her MSc studies in Food Safety at Wageningen University and Research. By the end of 2016, she obtained a second scholarship from CONACYT to continue with her PhD research at the Division of Toxicology under the supervision of Prof. Ivonne Rietjens and Dr. Karsten Beekmann. The results of the research program are presented in this dissertation. During her PhD she followed a postgraduate education as part of the training required for the registration as European Toxicologist. Diana is currently working as part of the Regulatory Affairs team at Byondis.

OVERVIEW OF COMPLETED TRAINING ACTIVITIES

Discipline specific courses

Molecular toxicology	Postdoctoral Education in Toxicology (PET), 2017
Laboratory of animal science	PET, 2017
Toxicogenomics	PET, 2017
Environmental toxicology	Wageningen University & Research (WUR), 2017
Cell Toxicology	PET, 2018
Organ Toxicology	PET, 2018
Epidemiology	PET, 2018
Immunotoxicology	PET, 2018
General toxicology	WUR, 2018
Pathobiology	PET, 2019

Meetings

Annual meeting of the Dutch society of Toxicology (NVT)	Hilversum, 2018
Annual NVT meeting	Ede, 2019
55th congress of the European Societies of Toxicology	Helsinki, 2019

General Courses

VLAG PhD week	WUR, 2017
Project and time management	WUR, 2017
Scientific Publishing	WUR, 2017
The Essentials of Scientific Writing and Presenting	WUR, 2017
PhD Peer Consultation - a powerful tool to tackle PhD challenges	WUR, 2017

Optional

Preparation of research proposal	WUR, 2017
PhD trip to Japan (organizing committee)	Division of Toxicology, WUR, 2018
Weekly group meetings	Division of Toxicology, WUR, 2016-2021

Approved by VLAG graduate school

The research described in this thesis was financially supported by the National Council of Science and Technology (CONACYT) from Mexico through a scholarship awarded to Diana Marisol Mendez Catala (CVU 619449) in 2016.

Financial support from Wageningen University and Research for printing this thesis is gratefully acknowledged.

